

Functional characterisation
of the mitochondrial Hsp70 cochaperone
Zim17

Dissertation

zur
Erlangung des Doktorgrades (Dr. rer. nat.)
der
Mathematisch-Naturwissenschaftlichen Fakultät
der
Rheinischen Friedrich-Wilhelms-Universität Bonn

vorgelegt von

Ilka Lewrenz

aus

Lippstadt

Bonn, 06. Mai 2013

Angefertigt mit Genehmigung der Mathematisch-Naturwissenschaftlichen Fakultät
der Rheinischen Friedrich-Whilhelms-Universität Bonn

1. Gutachter: Prof. Dr. Wolfgang Voos

2. Gutachter: Prof. Dr. Dieter O. Fürst

Tag der Promotion: 12. September 2013

Erscheinungsjahr: 2013

*Success is not final, failure is not fatal:
It is the courage to continue that counts*

Winston Churchill

Acknowledgements

First and foremost I would like to thank Prof. Dr. Wolfgang Voos for giving me the opportunity to work in his laboratory and the excellent supervision of my phd thesis. I would like to express my gratitude for his guidance and constructive advice. His scientific experience and the interest he showed on my project largely contributed to the progress of this work and his patience and kindness created a pleasant working atmosphere.

I am grateful to my colleagues in the laboratory of Prof. Dr. Voos for their great teamwork, help and support. I thank Dr. Dorothea Becker and Dr. Tom Bender for the excellent introductions into the techniques used in the mitochondrial field and for their very helpful discussions and advice. To Ursula Gerken a big thank you for professional technical assistance and for her help in stressfull times. Especially, I would like to express my gratitude to Ursula Seibold - her advice in technical and experimental problems and her presence and support in difficult moments have been invaluable and always encouraged me to carry on.

I wish to thank my friends and my family, especially my parents, who have accompanied and supported me during my studies and my doctorate. To my friends Katharina Klein and Jan Schürings many thanks for critically reading this thesis. My special gratitude is adressed to Adrian Bradshaw for his unyielding support, patience and understanding during the work on my PhD.

Finally, I would like to thank the members of the Institute of Biochemnistry and Molecular Biology for the open and friendly working atmosphere which made my time here a great experience.

Abstract

The mitochondrial zinc finger protein Zim17 belongs to a newly identified class of cochaperones that maintain the function of Hsp70 proteins in mitochondria and plastides of eukaryotic cells, presumably by preventing the aggregation of their respective chaperone partners. However, while its aggregation-preventive function is well demonstrated *in vitro*, little is known about the influence of the Zim17 interaction on the chaperone activity of mitochondrial Hsp70s (mtHsp70s) and its concurrent effects in the cellular context.

Due to the aggregation-protective character of Zim17, recombinant co-expression with the zinc finger protein allowed the purification of the main yeast mtHsp70 Ssc1 from *E.coli* cells under native conditions. The purified proteins were used to analyse the influence of Zim17 on the solubility of Ssc1 as well as the character and stability of its binding to the chaperone. Zim17 interacted with Ssc1 as a single molecule but tended to form dimers in the absence of the Hsp70 chaperone. Though the presence of Zim17 improved the solubility of recombinant Ssc1 in *E.coli* cells, substantial amounts of the Hsp70 chaperone still aggregated, even when Zim17 was expressed in saturated amounts.

To study the effects of a loss of Zim17 function in the cellular environment, novel conditional mutations within the *ZIM17* gene of the model organism *Saccharomyces cerevisiae* were generated. Yeast cells carrying these mutations showed a temperature-sensitive growth phenotype and a tendency to develop respiratory deficits. On fermentable growth media, the mutant cells were prone to lose their respiratory competence and were inviable at elevated temperatures. In these cells, a strong aggregation of the mitochondrial Hsp70 Ssc1 together with a concomitant defect in Fe/S protein biogenesis was observed. In contrast, under respiring conditions, the mitochondrial Hsp70s Ssc1 and Ssq1 exhibited only a partial aggregation. The induction of the *zim17* mutant phenotype by subjection to a high temperature

treatment lead to a strong import defect for Ssc1-dependent matrix-targeted precursor proteins that correlated with a significantly reduced binding of newly imported substrate proteins to Ssc1. Both *in vitro* and *in vivo* approaches point to the conclusion that Zim17 is not primarily required for the maintenance of mtHsp70 solubility. Instead, a functional analysis of the chaperone cycles of Ssc1 and Ssq1 shows that Zim17 directly assists the functional interaction of mtHsp70 with substrate proteins in a J-protein cochaperone-dependent manner.

Contents

List of Figures	xii
List of Tables	xiii
Acronyms	xv
1 Introduction	1
1.1 Mitochondria	1
1.1.1 Mitochondrial protein import	2
1.1.1.1 TIM23-mediated import pathways for matrix- and inner membrane proteins	2
1.1.1.2 Tim23-independent import pathways	4
1.1.1.2.1 Import into the inner and outer mitochondrial membrane	4
1.1.1.2.2 Import into the intermembrane space	6
1.1.2 Mitochondrial protein homoeostasis	6
1.1.3 The mitochondrial Fe/S cluster assembly machinery	9
1.2 Hsp70 proteins and their cochaperones	12
1.2.1 Mitochondrial Hsp70 proteins	15
1.2.1.1 The role of Ssc1 in the import and folding of preproteins	15
1.2.1.2 The role of Ssq1 in the biogenesis of mitochondrial Fe/S cluster proteins	17
1.3 Zinc finger proteins and cellular zinc	17
1.4 Zim17, a newly identified mtHsp70 cochaperone	18
1.5 Research objectives	22
2 Materials and Methods	23
2.1 Yeast and <i>E.coli</i> strains	23
2.2 Plasmids	26
2.3 Growth media	27

2.4	Molecular biological methods	28
2.4.1	Polymerase chain reaction	28
2.4.1.1	Phusion-polymerase system	28
2.4.1.2	<i>In vitro</i> mutagenesis by overlap-extension PCR	28
2.4.2	Agarose-gelelectrophoresis	29
2.4.3	Restriction digest of DNA	29
2.4.3.1	Analytical restriction digest	29
2.4.3.2	Preparative restriction digest	29
2.4.4	Ligation	30
2.4.5	Transformation of competent bacteria	30
2.4.6	DNA isolation from <i>E.coli</i>	31
2.4.7	Expression of recombinant proteins in <i>E.coli</i>	31
2.4.8	Transformation of <i>S. cerevisiae</i>	31
2.4.9	DNA isolation from yeast	32
2.4.9.1	Quick isolation of plasmid and genomic DNA	32
2.4.9.2	Small scale isolation of genomic DNA for PCR and sequencing	32
2.4.10	Whole cell yeast extracts for Western blot	32
2.4.11	Subcellular fractionation of yeast cells	33
2.4.12	Isolation of mitochondria from <i>S. cerevisiae</i>	33
2.4.13	Genomic integration	34
2.4.14	Random spore analysis	35
2.5	Protein-biochemical and immunological methods	36
2.5.1	SDS-polyacrylamid-gelelectrophoresis (SDS-PAGE)	36
2.5.2	Western blot	37
2.5.3	Immunodetection of immobilized proteins	38
2.5.4	Precipitation of proteins with trichloroacetic acid (TCA)	38
2.5.5	Purification of recombinant proteins via affinity tags	38
2.5.5.1	Purification under native conditions via a deka-histidine-tag	38
2.5.5.2	Purification under native conditions via a <i>Strep</i> -tag	39
2.5.6	Fast protein liquid chromatography (FPLC)	39
2.5.6.1	Calibration of the Sephadex 75 column	40
2.6	Biochemical <i>in-vitro</i> and <i>in-organello</i> assays	41
2.6.1	<i>In-vitro</i> translation of radiolabelled proteins in reticulocyte lysate	41
2.6.2	<i>In-organello</i> import of radiolabelled precursor proteins	41
2.6.2.1	Import into respiratory-competent mitochondria	41

2.6.2.2	Import into respiratory-deficient mitochondria	42
2.6.3	Assessment of an inward-directed translocation force ('pulling')	43
2.6.4	Assessment of the Ssc1 folding activity	43
2.6.5	Analysis of protein-interactions by pulldown experiments	44
2.6.5.1	Ssc1-pulldown with immobilised Zim17	44
2.6.5.2	Ssc1-His pulldown via Ni-NTA	44
2.6.6	<i>In vitro</i> -analysis of Ssc1 substrate and nucleotide-binding properties	45
2.6.6.1	Binding of Ssc1 to immobilized ATP	45
2.6.6.1.1	Binding of purified Ssc1 to ATP-Agarose	45
2.6.6.1.2	Binding of Ssc1 from isolated mitochondria to ATP-Agarose	45
2.6.6.2	Binding of Ssc1 to immobilized model substrate	45
2.6.6.2.1	Preparation of reduced carboxy-methylated α -lactalbumin (RCMLA)	45
2.6.6.2.2	Coupling of RCMLA to Cyanogen bromide (CNBr)-activated Sepharose	46
2.6.6.2.3	Binding of Ssc1 from isolated mitochondria to RCMLA-Sepharose	46
2.6.7	Aggregation assay	46
2.6.8	Assessment of Aconitase activity	47
2.6.9	Assessment of the mitochondrial inner membrane potential $\Delta\Psi$	47
2.7	List of primers and oligonucleotides	48
2.8	List of antisera	49
2.9	List of chemicals	50
2.10	List of kits	51
2.11	List of laboratory instruments	52
2.12	List of software	53
3	Results	55
3.1	Co-purification and <i>in vitro</i> analysis of recombinant Ssc1 and Zim17	55
3.1.1	Co-expression of Ssc1-His and Zim17-Strep in <i>E. coli</i>	55
3.1.1.1	Generation of the expression vectors pIL1 and pIL2	55
3.1.1.2	Limited Ssc1 solubility in <i>E. coli</i> in the presence of Zim17	56
3.1.2	Purification and FPLC analysis of Ssc1-His in the presence of Zim17	57
3.1.2.1	FPLC analysis in presence of high Zim17 amounts	58
3.1.2.2	FPLC analysis in presence of low Zim17 amounts	58
3.1.2.3	ATP-binding properties of FPLC-purified Ssc1	59
3.1.3	Purification and FPLC analysis of Zim17-Strep	60
3.1.4	Nucleotid-dependency of the Zim17-Ssc1 interaction	62

3.1.4.1	Ssc1 interacts with immobilized Zim17 preferably in the absence of ATP	62
3.1.4.2	Ssc1 interacts with Zim17 <i>in organello</i> in the absence of ATP	63
3.2	Role of the zinc-chelating cysteine residues in Zim17	65
3.2.1	Generation of the zinc finger mutants <i>zim17-C78S</i> and <i>zim17-C100S</i>	65
3.2.2	Solubility of Zim17 zinc finger mutants in <i>E. coli</i>	65
3.2.3	<i>Zim17</i> zinc finger mutants are soluble after import into isolated yeast mitochondria	66
3.2.3.1	Generation of the preforms of the zinc finger mutants for <i>in vitro</i> translation	66
3.2.3.2	<i>In organello</i> import and solubility test of Zim17 zinc finger mutants . .	66
3.3	Analysis of the temperature-sensitive mutants <i>zim17-2</i> , <i>zim17-3</i> and <i>zim17-4</i>	68
3.3.1	Expression of Zim17-2, -3 and -4 from plasmids in a <i>zim17</i> Δ genetic background . .	68
3.3.2	Sequence analysis of <i>zim17-2</i> , -3 and -4	69
3.3.3	Generation of a corresponding wild type plasmid	70
3.3.4	Growth phenotype of <i>ZIM17-corrWT</i> , <i>zim17-3</i> and <i>zim17-4</i>	71
3.3.5	Aggregation of Ssc1 in <i>zim17-3</i> and <i>zim17-4</i>	71
3.4	Novel conditional <i>zim17</i> mutants	74
3.4.1	Generation of the mutants <i>zim17-3a</i> and <i>zim17-3b</i>	74
3.4.2	Genomic integration of the mutated <i>ZIM17</i> genes	75
3.4.3	Random spore analysis of <i>zim17-3a</i> and <i>zim17-3b</i> integrants	75
3.4.4	<i>Zim17</i> mutant integrants show a temperature-sensitive respiratory instable phenotype	79
3.4.4.1	Growth phenotype of <i>zim17-3a</i> and -3b	79
3.4.4.2	Temperature sensitivity of <i>zim17-3a</i> and -3b	80
3.4.4.3	Respiratory competence of <i>zim17-3a</i> and -3b	80
3.4.4.3.1	Effect of heat treatment	80
3.4.4.3.2	Effect of carbon sources	81
3.4.5	Differentiation between respiratory-competent (<i>zim17_{rc}</i>) and incompetent (<i>zim17_{ri}</i>) mitochondria isolated from mutant integrants	81
3.5	Biochemical analysis of genomic <i>Zim17</i> conditional mutants	83
3.5.1	Aggregation of Hsp70 chaperones	83
3.5.1.1	Aggregation in respiratory-deficient <i>zim17</i> integrants	83
3.5.1.2	Aggregation in respiratory-competent <i>zim17</i> integrants	83
3.5.1.2.1	Aggregation of mature Ssc1	83
3.5.1.2.2	Aggregation of newly imported Ssc1	84
3.5.2	Relative abundance of mtHsp70s and their cochaperones in <i>zim17</i> mutant cells . .	84
3.5.2.1	Expression levels of mutant Zim17s in <i>zim17</i> integrants	84

3.5.2.2	Expression levels of mtHsp70 proteins and their cochaperones in respiratory-competent <i>zim17</i> integrants	86
3.5.2.3	Expression levels of mtHsp70 proteins and their cochaperones in respiratory-deficient <i>zim17</i> integrants	86
3.5.3	Interaction of mutant Zim17 with Ssc1	88
3.5.4	Analysis of Ssq1-related processes in <i>zim17</i> conditional mutants	90
3.5.4.1	Expression levels of the Fe/S cluster protein aconitase in <i>zim17</i> mutants	90
3.5.4.2	Expression levels of citrate cycle and respiratory chain proteins	90
3.5.4.3	Diminishment of aconitase activity in respiratory-competent <i>zim17</i> mutants	91
3.5.5	Analysis of Ssc1-related processes in <i>zim17</i> conditional mutants	94
3.5.5.1	Preprotein import into respiratory-deficient <i>zim17</i> mitochondria	94
3.5.5.2	Preprotein import in respiratory-competent <i>zim17</i> mitochondria	94
3.5.5.3	Preprotein import into wt, <i>zim17-3a</i> and <i>zim17-3b</i> mitochondria <i>in vivo</i>	95
3.5.5.4	Analysis of import-related functions of Ssc1 in respiratory-competent <i>zim17</i> mitochondria	97
3.5.5.4.1	ATP-binding properties of Ssc1	97
3.5.5.4.2	<i>Zim17</i> mutants show an intact inward directed translocation force	98
3.5.5.4.3	<i>Zim17</i> mutants show a diminished Ssc1-interaction with newly imported substrate proteins	99
3.5.5.5	Analysis of matrix functions of Ssc1 in respiratory-competent <i>zim17</i> mitochondria	101
3.5.5.5.1	Binding of Ssc1 to immobilized model substrates	101
3.5.5.5.2	<i>Zim17</i> mutants show an intact folding activity of Ssc1	101
4	Discussion	103
4.1	Co-expression with Zim17 is a suitable method to purify functional recombinant Ssc1.	103
4.2	Recombinant Zim17 tends to form dimers in solution but interacts with Ssc1 as a monomer	105
4.3	Dependence of the Zim17-interaction on the nucleotide-binding state of Ssc1	107
4.4	Expression of Zim17 conditional mutants in a <i>zim17</i> Δ genetic background is not suitable for the direct analysis of Zim17 functions	108
4.5	Two novel genomic integrated <i>zim17</i> mutants show a temperature-sensitive phenotype combined with an instable respiratory deficiency	110

4.6	The respiratory instable phenotype of conditional <i>zim17</i> mutants derives from a deficient mitochondrial Fe/S cluster biogenesis as a consequence of mtHsp70 loss of function	111
4.7	Zim17 exerts a direct supportive function on Hsp70 activities independent of its aggregation-protective role	113
4.8	Does the zinc finger domain of Zim17 play a role in exerting its Hsp70-supporting function?	117
4.9	Is the prevention of Hsp70 aggregation a primary Zim17 function?	118
5	Bibliography	119
A	Appendix	133
A.1	Sequences	134
A.1.1	pIL1 and pIL2	134
A.1.2	pFL-Zim17-ts2,3,4-CEN, pFL-Zim17-corrWT-CEN	143
A.1.3	<i>ZIM17::LEU2</i> -insert for genomic integration	149
A.2	Vector maps	153
A.2.1	pDB10	153
A.2.2	pIL1	154
A.2.3	pIL2	155
A.2.4	pIL4	156
A.2.5	pIL6/ pIL7	157
A.2.6	pRS415	158
A.2.7	pFL-zim17-ts-CEN	159
A.2.8	pFL39	160

List of Figures

1.1	Tim23-mediated import pathways	5
1.2	Tim23-independent import pathways	7
1.3	The mitochondrial protein quality control system	10
1.4	The mitochondrial Fe/S protein biogenesis system	13
2.1	<i>In vitro</i> mutagenesis of <i>ZIM17</i>	36
2.2	Calibration of Sephadex 75	40
3.1	Expression levels of Ssc1-His and Zim17-Strep in <i>E. coli</i>	57
3.2	FPLC analysis of Ssc1 in the presence of high Zim17 amounts	59
3.3	FPLC analysis of Ssc1 in the presence of low Zim17 amounts	60
3.4	ATP-Agarose assay with purified Ssc1	60
3.5	FPLC analysis of Zim17	61
3.6	Binding of Ssc1 to immobilized Zim17	63
3.7	Interaction of Zim17 with Ssc1-His	64
3.8	Expression levels and solubility of Zim17-C78S and Zim17-C100S in <i>E. coli</i>	65
3.9	Import and solubility of Zim17-C78S and C100S in yeast mitochondria	67
3.10	Subcellular fractionation of <i>zim17-2,-3 and -4</i> mutant cells	69
3.11	Sequence alignment of wt and mutant Zim17 proteins	70
3.12	Growth phenotype of <i>zim17-corrWT,-3 and -4</i> mutants	72
3.13	Aggregation of Ssc1 in <i>zim17-3, -4</i> and wt mitochondria	73
3.14	Generation of conditional <i>zim17</i> -mutants	74
3.15	Colony-PCRs of wt, <i>zim17-3a, -3b</i> and <i>-4</i> integrants	76
3.16	Random spore analysis of wt, <i>zim17-3a</i> and <i>zim17-3b</i> integrants	77
3.17	Colony-PCRs of wt, <i>zim17-3a</i> and <i>zim17-3b</i> tetrads.	78
3.18	Growth phenotype of respiratory-competent wt, <i>zim17-3a</i> and <i>zim17-3b</i> mutant integrants	79

3.19	Temperature sensitivity of respiratory-competent wt, <i>zim17-3a</i> and <i>zim17-3b</i> integrants	80
3.20	Respiratory competence of wt, <i>zim17-3a</i> and <i>zim17-3b</i> integrants	82
3.21	Aggregation of mtHsp70s in <i>zim17_{ri}</i> and <i>zim17_{rc}</i>	85
3.22	Expression of Zim17-wt, -3a and 3b in <i>zim17_{ri}</i> and <i>zim17_{ri}</i> mitochondria	85
3.23	Relative abundance of mtHsp70 proteins and their cochaperones in <i>zim17_{rc}</i> mutant integrants	87
3.24	Abundance of mtHsp70 proteins and their cochaperones in <i>zim17_{ri}</i> mutant integrants	88
3.25	Interaction of wt and mutant Zim17s with mtHsp70s	89
3.26	Aconitase levels in <i>zim17_{rc}</i> mutant integrants	91
3.27	Loss of enzymes of the citric acid cycle and respiratory chain in <i>zim17_{ri}</i> mitochondria	92
3.28	Aconitase activity and aggregation in <i>zim17_{rc}</i> mitochondria	93
3.29	Import phenotype of <i>zim17_{ri}</i> mitochondria	95
3.30	Import phenotype of <i>zim17_{rc}</i> mitochondria	96
3.31	<i>In-vivo</i> import phenotype of <i>zim17</i> mutant integrants	97
3.32	Ssc1 nucleotide-binding and 'pulling' activity in <i>zim17_{rc}</i> mitochondria	99
3.33	Interaction of Ssc1 from <i>zim17_{rc}</i> mitochondria with newly imported substrate proteins	100
3.34	Ssc1 substrate-binding and 'folding' activity in <i>zim17_{rc}</i> mitochondria	101

List of Tables

2.1	<i>E.coli</i> strains	23
2.2	Yeast strains I	24
2.3	Yeast strains II	25
2.4	Plasmids	26
2.5	Growth media	27
2.6	Cycle conditions for PCR	28
2.7	Polyacrylamid gels for SDS-PAGE	37
2.8	Primer and Oligonucleotides	48
2.9	Antisera	49
3.1	Growth phenotypes of wt, <i>zim17-3a</i> and <i>-3b</i> tetrades	77

Acronyms

Aco1	Aconitase 1
ATP	Adenosine-5'-triphosphate
BSA	Bovine serum albumin
bp	Basepairs
Cit1	Citrate synthase 1
CoxIV	Cytochrome C oxidase IV
DHFR	Dihydrofolate reductase
DNA	Desoxyribonucleic acid
DTT	Dithiothreitol
E. coli	Escherichia coli
EDTA	Ethylenediaminetetraacetic acid
FPLC	Fluid phase liquid chromatography
His	Histidine
Hsp	Heat shock protein
IPTG	Isopropyl β -D-1-thiogalactopyranoside
Iso1	Iron-sulfur cluster scaffold homolog 1
Jac1	J-type accessory chaperone 1
kb	Kilo basepairs

kDa	Kilo Dalton
m	mature; the mature form of an imported protein
MCS	multiple cloning site
Mdh1	Malate dehydrogenase 1
Mdj1	mitochondrial DnaJ
Mge1	Mitochondrial GrpE, nucleotide exchange factor for mtHsp70s
MIA	mitochondrial intermembrane space assembly
MrpL40	Mitochondrial ribosomal protein, Large subunit 40
mtHsp70	mitochondrial heat shock protein of 70 kDa
MTX	Methotrexate
NAD(H)	Nicotinamide adenine dinucleotide
NBD	Nucleotide-binding domain
Ni-NTA	Nickel-nitrilotriacetic acid
OD	optical density
p	pre; the precursor form of a mitochondrial-destined protein
PAM	Presequence-translocase associated motor
PCR	Polymerase chain reaction
PK	Proteinase K
PVDF	Polyvinylidene difluoride
RCMLA	Reduced carboxy-methylated α -lactalbumin
Rip1	Rieske iron-sulfur protein 1
RNA	Ribonucleic acid
SBD	Substrate-binding domain
SAM	Sorting and assembly machinery
S. cerevisiae	Saccharomyces cerevisiae
SDS	Sodium dodecyl sulfate
SDS-PAGE	SDS-polyacrylamid gelelectrophoresis
Sod2	Superoxide dismutase 2
Ssc1	Stress-seventy subfamily C
Ssq1	Stess-seventy subfamily Q
Strep	Streptacin

TCA	Trichloroacetic acid
TIM	Translocase of the inner membrane
TOM	Translocase of the outer membrane
ts	temperature-sensitive
wt	wild type
YPD	Yeast Extract Peptone Dextrose
YPG	Yeast Extract Peptone Glycerol
Zim17	Zinc finger motif protein of 17 kDa
$\Delta\Psi$	mitochondrial inner membrane potential

1. Introduction

1.1. Mitochondria

Mitochondria are ubiquitous eukaryotic cell organelles that play crucial roles in many cellular functions including respiration and energy production, Fe/S cluster assembly, metabolism of amino acids and lipids and apoptosis.

Mitochondria origin from an endosymbiotic event that occurred over 1.5 billion years ago and most likely derive from an α -prokaryotic ancestor that was assimilated by a host cell of eukaryotic or prokaryotic origin (Dyall, Brown and Johnson 2004; Gray, Burger and Lang 2001). As a result of a symbiotic relationship between the two organisms, a conversion of the proto-mitochondrion to an organelle took place. During this evolutionary process, the genome of mitochondria was reduced and genes were transferred to the nuclear genome of the host cell (Adams and Palmer 2003; Gabaldón and Huynen 2004). A machinery for the transport of proteins from the cytosol to the organelle and presequences to target the mitochondrial precursor proteins to their destination developed co-evolutionary (Adams and Palmer 2003; Dyall, Brown and Johnson 2004). The mitochondrial proteome of yeast and other organisms thus mainly consists of two sets of proteins: those that are of prokaryotic origin and have bacterial homologues and those that occur only in eukaryotes (Gray, Burger and Lang 2001).

Though mitochondria are not sustainable outside the cellular environment, they are considered autonomous organelles that have kept the ability to self-replicate and to synthesise a subset of their proteins. Moreover, mitochondria constitute an intra-organellar environment isolated from the cytosol. Protein homeostasis in mitochondria thus has to be strictly maintained and is autonomously controlled by i) a regulated import machinery that guides nuclear-encoded precursors to their

subcompartmental destination, ii) an autonomous protein quality control system that consists of a set of molecular chaperones and proteases.

1.1.1. Mitochondrial protein import

As most mitochondrial proteins are encoded in the nucleus and synthesised as precursor forms in the cytosol, they must be imported into the organelle. Almost all precursor proteins enter the mitochondria through the translocase of the outer membrane (TOM). Mitochondrial precursor proteins carry a signal peptide at their N-terminus that consists of 15-80 amino acids (Neupert and Herrmann 2007; Roise and Schatz 1988). The signal peptide forms an amphipathic α -helix with one hydrophobic and one positively charged face and is recognized by the receptor protein Tom20 at the cytosolic side of the outer mitochondrial membrane (Abe 2000; Saitoh 2007). Tom20 forms a complex with Tom22 that connects it to the central translocation pore, which consists of the channel protein Tom40 and a number of small Tom proteins (Tom 4,5 and 6, figure 1.1) (Neupert and Herrmann 2007; Schmidt, Pfanner and Meisinger 2010). In the special case of hydrophobic membrane destined precursor proteins, an additional TOM-component, Tom70 interacts with Hsp70 and Hsp90 chaperones that are bound to the precursor to protect it from aggregation in the hydrophilic environment of the cytosol (Young, Hoogenraad and Hartl 2003). The interaction of Tom70 with the presequence and the bound chaperones makes sure that the protein is immediately transferred to the Tom20-Tom22 receptor and inserted into the Tom40 channel (Schmidt, Pfanner and Meisinger 2010). After passing the TOM complex, the precursor proteins are distributed to the mitochondrial subcompartments (the intermembrane space, the inner and outer membrane and the matrix) via different pathways.

1.1.1.1. TIM23-mediated import pathways for matrix- and inner membrane proteins

Matrix-destined preproteins are imported via the translocase of the inner membrane (TIM) in a membrane potential ($\Delta\Psi$) -dependent manner. The positive charge of its N-terminal signal peptide directs the preprotein along the proton gradient over the inner mitochondrial membrane through the TIM23 channel into the matrix compartment (Martin, Mahlke and Pfanner 1991; Roise and Schatz 1988).

The TIM23 complex is composed of the channel proteins Tim23 and Tim17 (figure 1.1). A third component, Tim50, consists of a transmembrane segment and a domain

that reaches into the intermembrane space where it is able to interact with the TOM-complex and transmit the information about the entrance of a preprotein from TOM to TIM (Geissler 2002). The Tim50-mediated transient interaction between the two complexes induces the closure of the Tim23 channel to prevent a leakage of ions across the inner membrane (Meinecke 2006). On the matrix-side the presequence translocase associated import motor (PAM), consisting of the proteins Pam16, Pam17 and Pam18, and a mitochondrial Hsp70 protein assist in completion of the import into the matrix compartment by exerting an ATP-dependent reaction (section 1.2.1.1). In this composition, the TIM complex is also called TIM23^{PAM} or TIM23^{MOTOR} (Laan, Hutu and Rehling 2010). When the precursor has reached the matrix, its presequence is cleaved off by proteases. The main protease of the mitochondrial matrix is the matrix processing peptidase (MPP) that removes the targeting sequence of almost all entering precursors. Besides, the proteases Icp55 and Oct1 are found in the mitochondrial matrix. While Icp55 is thought to remove single amino acid residues as a component of the 'N-end-rule' pathway, the functional significance of Oct1, that removes segments of 8 amino acids, is unknown (Gakh, Cavadini and Isaya 2002; Mossmann, Meisinger and Vögtle 2012).

Mitochondrial inner membrane proteins can be inserted into the membrane via the TIM23-complex, the TIM22-complex or the OXA-complex. Inner membrane proteins that are imported via the Tim23 complex carry an N-terminal target signal followed by a hydrophobic sorting sequence that induces an arrest of the import. Subsequently, the protein is released into the inner membrane via an unknown mechanism. Recent studies suggest that during this so-called sorting pathway, the TIM23 complex seems to be free of the PAM module but includes an additional Tim-protein, Tim21. According to its function, this form of the complex has been termed Tim23^{SORT} (Chacinska 2005, 2010; Laan 2007). Tim21 interacts with the TOM-complex via Tom22 in the intermembrane space (Mokranjac 2005). Additionally, it seems to be connected with the respiratory chain, most likely via complex III (cytochrome bc1 complex) and complex IV (cytochrome C oxidase, Laan 2006). This interaction is thought to contribute to the $\Delta\Psi$ -dependent process of the inner membrane sorting. However, its precise role remains to be elucidated. Furthermore, the existence of two functionally fully separated TIM23 modules is still discussed (Mokranjac and Neupert 2010; Popov-Celeketić 2008). Recent studies indicate that TIM23 is found in the Tim23^{SORT} form at the initial phase of the import of matrix-destined precursors before it switches to the PAM-attached TIM23^{MOTOR} complex during the import

process and are thus in a dynamic interaction with each other (Chacinska 2010; Wiedemann 2007).

1.1.1.2. Tim23-independent import pathways

1.1.1.2.1. Import into the inner and outer mitochondrial membrane

Mitochondrial inner membrane proteins are either encoded by the mitochondrial genome or by nuclear genes. Proteins encoded by the mitochondrial genome are translated on ribosomes in the mitochondrial matrix and are integrated into the inner membrane via the OXA-complex (Stuart 2002, figure 1.2). Though some nuclear encoded inner membrane proteins can also use the OXA-pathway their majority is integrated into the inner mitochondrial membrane by the TIM23 complex (section 1.1.1.1) or the TIM22 complexes. Proteins that are imported via the TIM22 complex are recognized by the receptor Tom70 as described above (section 1.1.1.1) and enter the intermembrane space via the TOM-complex. In the intermembrane space (IMS), the precursor proteins are bound by the small Tim-proteins TIM9 and Tim10. Tim9 and Tim10 form hexameric complexes in the intermembrane space (Lu 2004; Webb 2006) and transfer the incoming precursor proteins to TIM22. The TIM22 complex consists of the inner membrane proteins Tim22, Tim18 and Tim54. Part of Tim54 is exposed to the IMS and probably provides an interaction site for the small Tim proteins (Wagner 2008).

Similarly, β -barrel precursors of the outer membrane are guided by the small Tim-proteins Tim9-Tim10 and the homologous proteins Tim8-Tim13 to the sorting and assembly machinery (SAM) complex. The SAM complex consists of the outer membrane proteins Sam35, Sam37 and Sam50. Sam35 interacts with a C-terminal signal of the precursor protein and initializes its membrane insertion by the channel-forming Sam50 in a process that is not fully understood (Kutik 2008). The insertion of complex-forming outer membrane proteins like Tom40 is additionally promoted by the protein Mdm10 (mitochondrial distribution and morphology), a component the MDM complex (Meisinger 2004). The MDM complex is also found at junctions between the outer mitochondrial membrane and the ER and seems to play a role in the transport of lipids and Ca^{2+} . For proteins with α -helical transmembrane segments a second mechanism for the insertion of outer membrane proteins exists. This poorly characterized pathway involves the outer membrane protein Mim1 (mitochondrial import1) (Schmidt, Pfanner and Meisinger 2010).

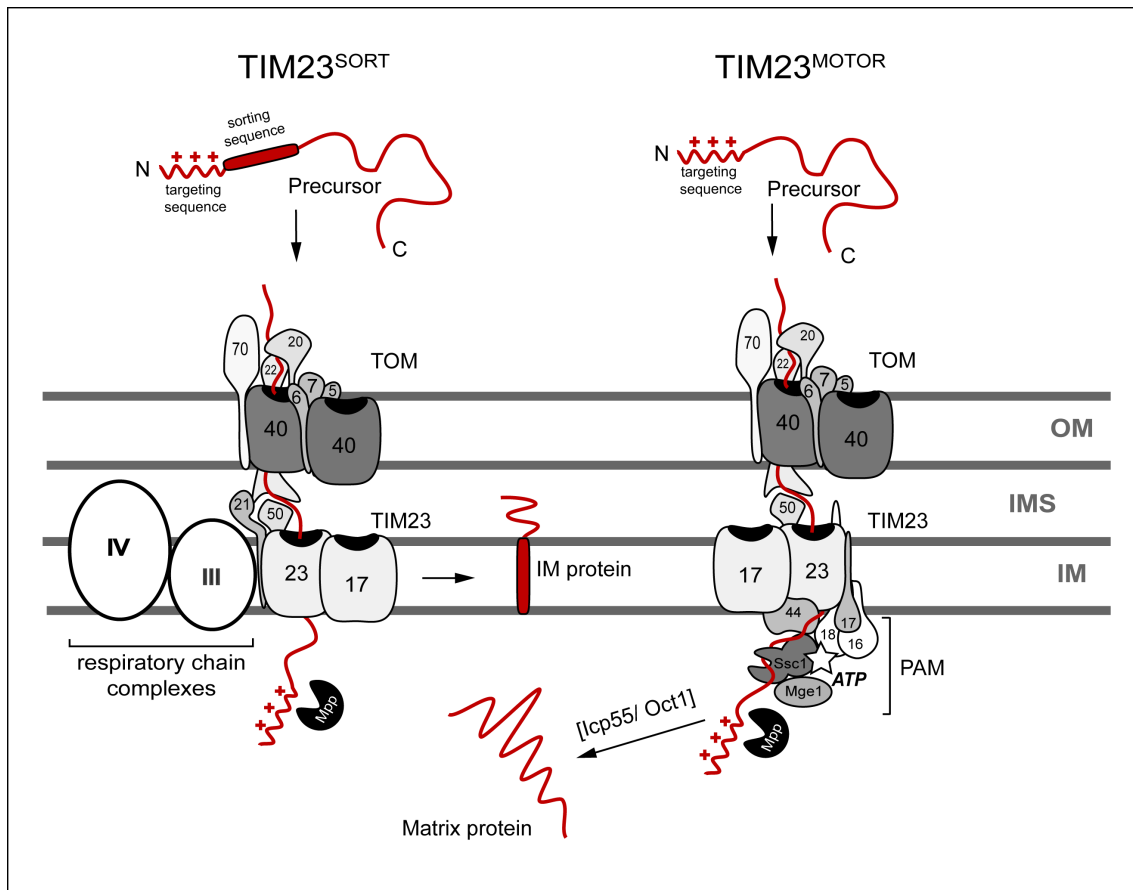


Figure 1.1.: Tim23-mediated import pathways, adapted from Schmidt (2010). Precursor proteins with an N-terminal mitochondrial targeting sequence are recognized by Tom20 and Tom22 and imported by the translocase of the outer membrane (TOM) complex. After passing the outer membrane, the precursors are further imported by two modules of the translocase of the inner membrane (TIM) complex. TIM23^{SORT} mediates the release of precursors with an additional sorting sequence into the inner membrane and comprises Tim23, Tim17, Tim50 and Tim21. Tim21 interacts with the TOM complex and transiently binds to complexes of the respiratory chain. TIM23^{MOTOR} lacks Tim21 but interacts with Tim44 and the presequence-translocase associated motor (PAM) that assists in the import of matrix-destined proteins. Precursor-import into the matrix is powered by the membrane potential ($\Delta\Psi$) and an ATP-driven reaction of mtHsp70 that is recruited to the translocase by Tim44. After reaching the matrix compartment, the presequence is cleaved off by the mitochondrial processing peptidase (MPP). Some proteins are further processed by the peptidases Lcp55 or Oct1 before they are folded into their final conformation. OM, outer membrane; IM, inner membrane; IMS, intermembrane space.

1.1.1.2.2. *Import into the intermembrane space*

Proteins of the intermembrane space can be imported via the Tim23 sorting pathway if they contain a bipartite signal sequence composed of an N-terminal matrix signal followed by a hydrophobic sorting sequence. Import is arrested and the protein is inserted into the inner membrane as described above (section 1.1.1.1). After import, the matrix-targeting signal and the sorting sequence are removed by proteolytic cleavage and the protein is released into the IMS (Neupert and Herrmann 2007). Another way for the import of proteins into the IMS is provided by a specialised system applying the inner membrane protein Mia40 (mitochondrial intermembrane space assembly 40) (Chacinska 2004). This special import pathway applies to a group of small IMS proteins that have no cleavable presequences but contain cysteine residues as a common characteristic (Longen 2009). After passage into the intermembrane space via the TOM-complex, the newly imported proteins need to be folded into their functional state. Despite of the reducing environment, cysteine-containing proteins in the IMS generally occur in their oxidized form. Mia40 functions as an oxidoreductase that induces disulfide bonds between cysteine residues by forming a transient disulfide bridge with its client proteins. The disulfide bond is then transferred to the target protein, while Mia40 itself becomes reduced. After release of the target protein, Mia is probably re-oxidized by its interaction partner Erv1, a sulphhydryl-oxidase that also plays a role in the biogenesis of iron sulphur cluster proteins. According to the role of Mia40, this import pathway was named the 'disulfid relay' (Hell 2008; Mesecke 2005). The small Tim proteins Tim9 and Tim10 are examples for proteins that are imported via the Mia40 pathway (Müller 2008).

1.1.2. Mitochondrial protein homoeostasis

Protein homoeostasis in mitochondria is controlled via a network of proteases and chaperones (Voos 2013, figure 1.3). Briefly, chaperones of the mitochondrial matrix fulfil two important tasks: the *de novo* folding of newly imported precursors and the recognition and refolding of misfolded proteins. Chaperones of the Hsp70 class play a key role in these processes. Hsp70 proteins consist of a peptide binding domain (PBD) and a nucleotide-binding domain (NBD) and interact with substrate proteins in a nucleotide-dependent manner. Their function is based on their intrinsic ATPase activity that confers conformational changes from the NBD to the PBD and thus allows the chaperone to work on its substrate. Mitochondrial Hsp70 chaperones

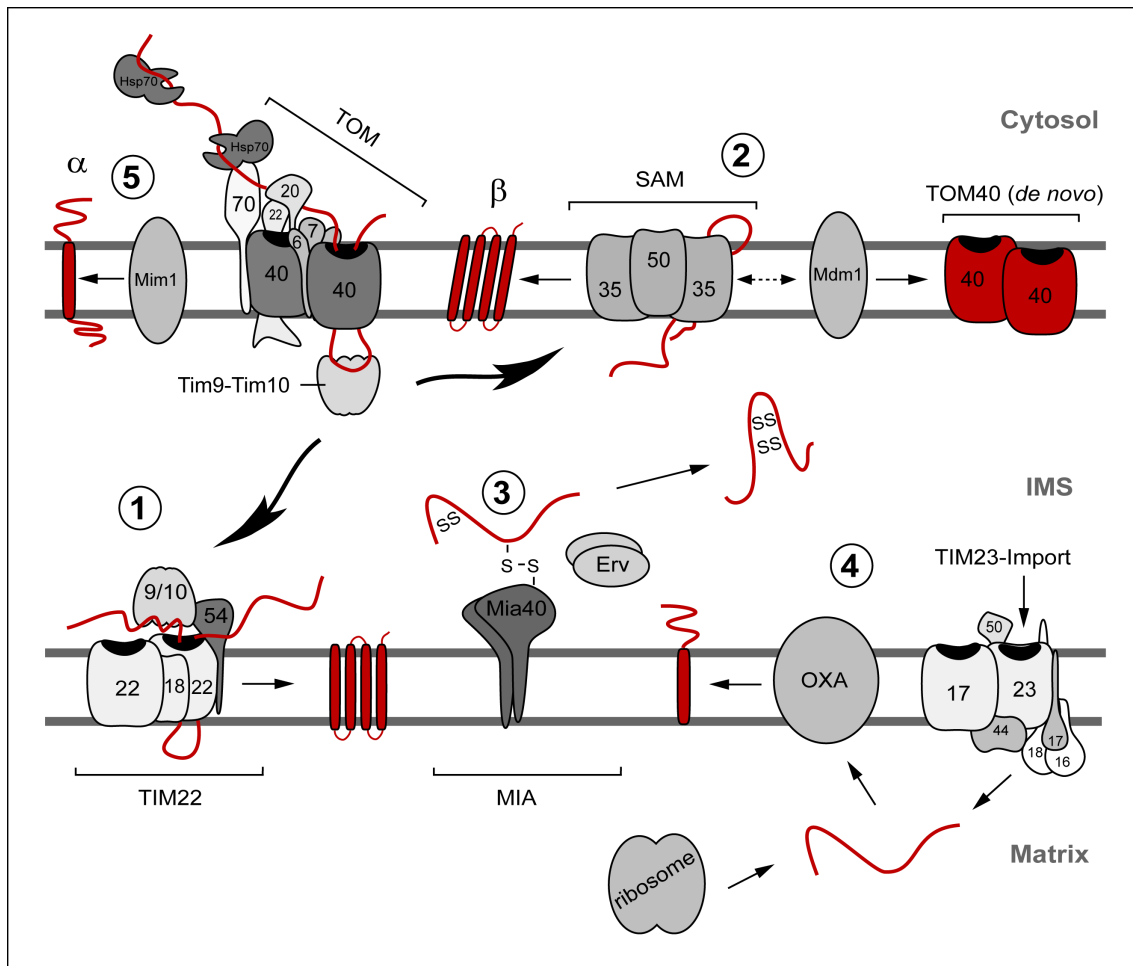


Figure 1.2.: Tim23-independent import pathways. After passage through the TOM-complex, proteins that lack an N-terminal matrix-targeting signal can use different sorting pathways. The Tim9-Tim10 complex transfers hydrophobic precursor proteins through the IMS to either the TIM22 complex in the inner membrane (1) or the sorting and assembly machinery (SAM) in the outer membrane (2), that mediates the release of β -barrel proteins and the assembly of the Tom40 channel with the help of Mdm1. The mitochondrial intermembrane space assembly machinery (MIA) drives the import of many IMS proteins by mediating an oxidative folding process that also involves the sulphhydryl-oxidase Erv1 (3). Inner membrane proteins that are synthesised on mitochondrial ribosomes and a few proteins that enter the mitochondrial matrix via the TIM23 complex are integrated into the inner membrane by the OXA-complex (4). The precursors of α -helical outer membrane proteins are not imported via the TOM complex but are inserted into the outer membrane by alternative pathways involving the newly identified mitochondrial import 1 (Mim1)(5).

interact with incoming precursor proteins at the import channel and assist in the import reaction itself. After import, the Hsp70 chaperone stays attached to the precursor and promotes the folding into its final conformation. Similarly, it stabilises misfolded polypeptides in the mitochondrial matrix and assists in their refolding. In yeast mitochondria, the main Hsp70 chaperone that assists in both import and folding processes is called Ssc1 (Stress-Seventy subfamily C1, Kang 1990; Rowley 1994). Ssc1 interacts with exposed hydrophobic segments of the unfolded precursor protein. A second mitochondrial Hsp70 protein, Ssq1, fulfils a more specialised function in the biogenesis of mitochondrial iron-sulphur-cluster (Fe/S)-proteins (see section below). While the functions of Ssc1 and Ssq1 are well characterized, the role of the third yeast mitochondrial Hsp70 chaperone Ecm10 (Ssc3) remains to be determined.

Hsp70 proteins are not the only chaperones that assist in the folding and refolding of proteins in the mitochondrial matrix. A second class of chaperones that promote the folding of newly imported proteins are Hsp60 proteins (Cheng 1989). The yeast mitochondrial Hsp60 chaperone is an orthologue of the *E.coli* protease GroEL. Chaperones of the Hsp60 class form large complexes consisting of 14 monomers that oligomerize into two heptameric rings with a hydrophobic substrate-binding cavity in their center. Hsp60 interacts with unfolded polypeptides to a size of 50 kDa. The cofactor Hsp10 covers the cavity and allows the substrate protein to fold into a native conformation. The isolation of the substrate during the folding process protects it from aggregation through interaction with other unfolded proteins (Walter 2002). Hsp60-assisted folding is promoted by ATP hydrolyses. The induced conformational change renders the interface of substrate-binding cavity more hydrophilic and forces the protein to fold into a soluble state. Mitochondrial Hsp60 acts chronologically after Hsp70 in the folding of newly imported matrix proteins (Heyrovská 1998) and is probably also involved in the refolding of endogenous proteins (Bender 2011).

Besides the folding-promoting chaperones of the Hsp60 and Hsp70 classes, the protein quality control system of the mitochondrial matrix contains a set of proteins which resolubilize aggregated proteins or remove polypeptides that are irreparably damaged. In yeast mitochondria, Hsp78, a chaperone of the Hsp100 or Clp (Caseinolytic peptidase protein homolog) class that belongs to the AAA+ protein family (ATPases associated with diverse cellular activities), plays an important role in the disaggregation and degradation of misfolded proteins (Janowsky 2006; Rottgers 2002). Hsp78, like its *E.coli* homologue ClpB, forms large oligomeric ring-complexes and act

together with Hsp70 chaperones in the refolding of substrates (Germaniuk, Liberek and Marszalek 2002; Leidhold 2006). Hsp78/ClpB chaperones exist in bacteria and yeast mitochondria but are not found in higher eukaryotes, where their roles are probably taken over by proteins of the Hsp70 class.

In yeast mitochondria, the removal of irreparably damaged proteins as a last instance is finally taken over by the Pim (proteolysis in mitochondria)/LON protease (Major 2006; Van Dyck, Pearce and Sherman 1994). LON proteases are serine peptidases that consist of a catalytical domain, an ATPase domain and an N-terminal domain that is involved in the binding of substrates.

In bacteria, a second protease, ClpP, forms a ring-shaped hexameric complex that degrades polypeptides with certain signal sequences. ClpP can interact with the cofactors ClpA, ClpX or ClpC that perform substrate-recruiting functions (Voos 2013). In yeast mitochondria, a ClpP protease-system does not exist. However, mitochondria contain the protein Mcx1 (Dyck 1998), a ClpX-homologue of unknown function and with no identified binding partner.

For the proteolysis of membrane-integrated substrate proteins, two mitochondrial proteases have been identified. Both consist of a zinc metallo-protease of the AAA-family and an integral membrane domain. The m-AAA-protease consists of the two subunits Yta10 and Yta12 with its ATPase domain pointing to the mitochondrial matrix. The protease domain of the i-AAA-protease Yme1 is exposed to the IMS and represents the only known protease in the intermembrane space of yeast mitochondria so far. Its functional significance for the degradation of soluble IMS proteins still has to be determined. In higher eukaryotes a soluble IMS protease, Htr2A, has been identified. However, its function remains unknown.

1.1.3. The mitochondrial Fe/S cluster assembly machinery

The mitochondrial Fe/S (ISC) cluster assembly machinery is an essential process of particular importance as it affects the biogenesis of cytosolic Fe/S cluster-containing proteins and thus draws a direct connection between mitochondrial and cytoplasmatic processes (Lill 2012). Fe/S cluster proteins occur throughout the cell and fulfill important roles in electron transfer, enzyme catalysis and regulatory processes (Lill 2006). The general importance of an intact iron-sulphur cluster assembly machinery is mirrored by the fact that defects in this process lead to diseases like Friedreichs ataxia or different forms of myopathies (reviewed in Sheftel, Stehling and Lill 2010). A key component for the biogenesis of Fe/S cluster-containing proteins is the mitochondrial

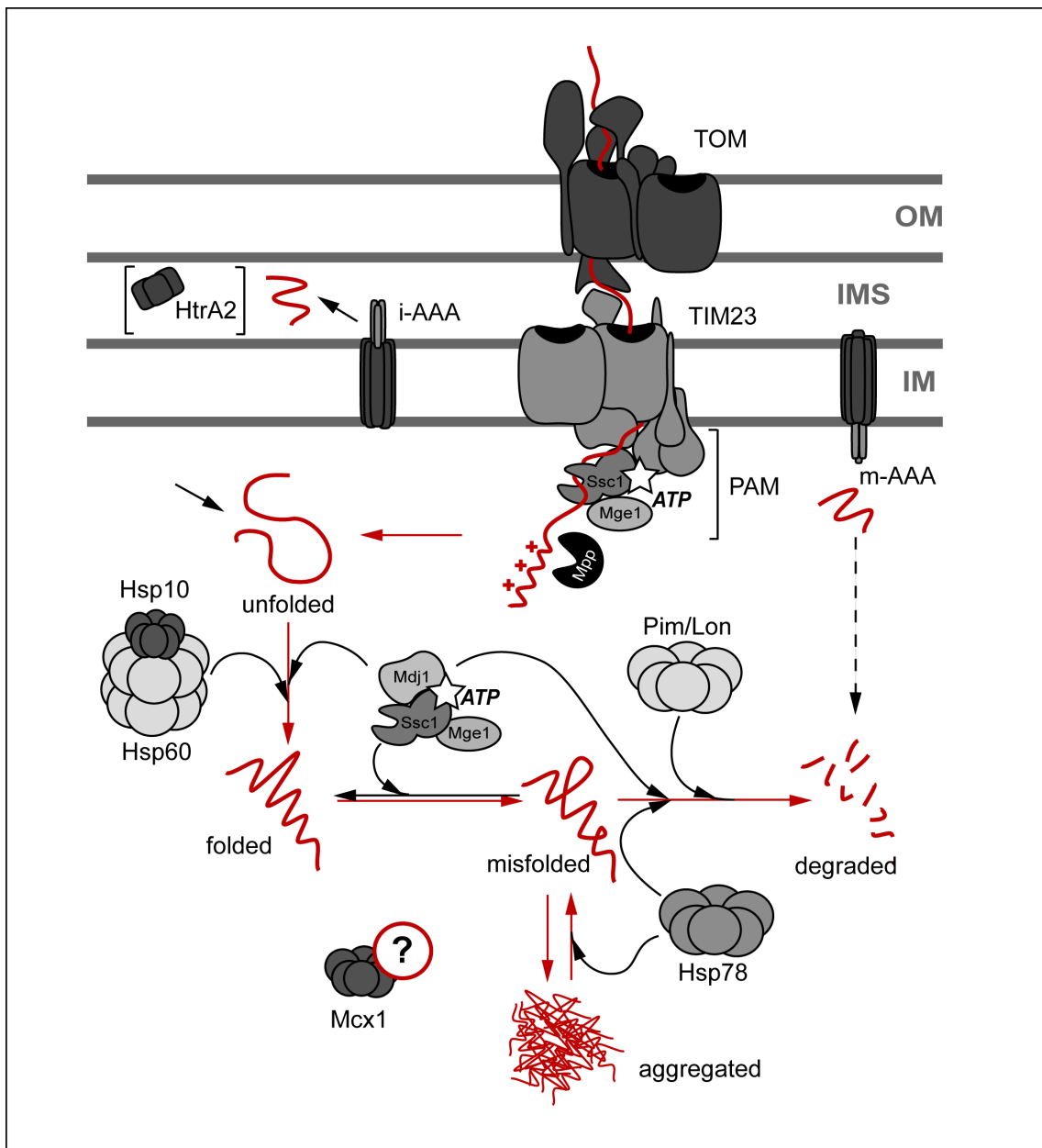


Figure 1.3.: The mitochondrial protein quality control system, adapted from Voos (2013). After import via the TIM23 complex, matrix proteins are folded by the mitochondrial Hsp70 and Hsp60 systems. Misfolded proteins are degraded with the help of Hsp78, a protein of the Hsp100 class of chaperones or the Pim/LON-protease. Hsp78 also assists in the solubilisation and degradation of aggregated proteins, a process that also involves the mtHsp70 chaperone system. The role of Mcx1, a homologue of the bacterial ClpXP protease-component ClpX, is unknown. The m-AAA and i-AAA proteases assist in the degradation of membrane-integrated substrate proteins. A homologue of Htr2A, a protease of unknown function in the IMS of higher eukaryotes has not been identified in yeast yet. OM, outer membrane, IM, inner membrane, IMS, intermembrane space.

protein Isu1, on which the Fe/S cluster is built up before it is transferred to its apoprotein (Knieszner 2005). For the synthesis of the [2Fe-2S]-cluster on Isu1, iron is transported from the cytosol into the mitochondrial matrix via the carriers Mrs3 and Mrs4 that use the pH gradient over the inner membrane as a driving force (Froschauer, Schweyen and Wiesenberger 2009, figure 1.4). During the assembly of Fe/S clusters on Isu1, the protein Nfs1 serves as a sulphur donor. Nfs1 is part of the cysteine desulfurase Nfs1-Isd11 (Adam 2006; Wiedemann 2006) that releases a sulphur from free cysteine and transfers it to Isu1 (Lill 2006, 2012). Iron is integrated into the complex with the help of frataxin (Yfh1 in yeast) that probably serves as an iron donor (Gerber, Mühlhoff and Lill 2003; Mühlhoff 2003). Besides Nfs1-Isd11 and frataxin, an electron transfer chain composed of ferredoxin (Yah1), ferredoxin reductase (Arh1) and NAD(P)H plays an important, yet unresolved role in the assembly of the Fe/S cluster on Isu1. Ferredoxin is an Fe/S protein that requires the mitochondrial Fe/S assembly machinery for its own biogenesis and is essential in yeast (Lill 2012). Upon its assembly on the scaffold protein Isu1, the Fe/S cluster is transferred to its apo-protein, a process that involves the Hsp70 protein Ssq1, the J-protein Jac1 and the monothiol glutaredoxin Grx5 in yeast. Ssq1 and Jac1 are thought to destabilise the binding of the Fe/S cluster to Isu1, thereby facilitating its transfer (Dutkiewicz 2006). Grx5 might assist in the transfer by transiently binding the Fe/S cluster, however, its precise role remains elusive (Rodríguez-Manzanique 2002). While the previously described steps are common for the biogenesis of all mitochondrial Fe/S cluster proteins, further steps are dependent on the individual target protein. In yeast mitochondria, the proteins Isa1, Isa2 and Iba57 are involved in the assembly of [4Fe-4S]-cluster proteins, for example aconitase (Mühlhoff 2007, 2011). Further, specialised components of the ISC assembly machinery assist in the biogenesis of individual proteins. Nfu1 transiently binds to the [4Fe-4S]-cluster and is involved in its transfer to lipoate synthase and respiratory chain complex II (SDH) (Navarro-Sastre 2011). Another [4Fe-4S]-interacting protein, Ind1 is involved in the biogenesis of complex I (Lill 2012).

As depletion of components of the mitochondrial Fe/S cluster machinery, for example Nfs1 or ferredoxin, also compromises the cytosolic Fe/S cluster assembly machinery (CIA), the two processes must be connected to each other. Presumably, a yet unidentified component synthesised in the mitochondria is exported to the cytosol where it is utilized in the CIA machinery. The ABC transporter Atm1 of the inner mitochondrial membrane seems to be involved in the export. Interestingly, the

function of Atm1 is probably dependent on the sulphhydryl oxidase Erv1 that is also involved in the Mia40-dependent import of IMS proteins (Lill 2012).

In mitochondria, proteins of respiratory metabolism like components of the respiratory chain complexes I and II as well as the citric acid cycle protein aconitase carry Fe/S clusters. Besides, Fe/S cluster proteins take part in the biogenesis of amino acids and cofactors and play important roles in the mitochondrial and cytosolic Fe/S cluster assembly machineries themselves (Lill 2006). It has been reported that yeast cells with defects in the ISC assembly machinery show a substantial downregulation of proteins of the respiratory chain and the citric acid cycle (Foury and Talibi 2001; Hausmann 2008; Lill 2012). The downregulation of iron-responsive genes could be part of a transcriptional response that resembles the response to iron starvation and is achieved by constitutive activation of the transcription factors Aft1 and Aft2. Aft1 and 2 activate the transcription of the iron regulon, a set of genes that are involved in cellular iron uptake and intracellular iron distribution. This process also leads to the transcriptional regulation of iron-responsive genes, for instance by the degradation of mRNA (Lill 2012). In the cytosol and nucleus, Fe/S cluster proteins play important roles in nucleotide metabolism, protein translation and tRNA modification. Nuclear Fe/S cluster proteins are involved in the synthesis and repair of DNA and in the assembly of ribosomes (Lill and Mühlenhoff 2008). Hence, defects in the cytosolic and mitochondrial ISC assembly machinery can lead to nuclear genome instability (Netz 2012; Veatch 2009). This link between mitochondrial function and nuclear DNA and RNA metabolism may contribute to the essentiality of mitochondria for most eukaryotic cells (Lill 2012).

1.2. Hsp70 proteins and their cochaperones

Hsp70 (heat shock protein of 70 kDa) proteins are important members of the mitochondrial protein quality control system and compose an ubiquitous family of chaperones whose members occur throughout all species (except archae). The main function of Hsp70 proteins is the stabilization and aggregation prevention of misfolded or unfolded substrate proteins via an interaction with exposed hydrophobic residues (Frydman 2001). Due to this property, Hsp70s are involved in a multitude of cellular processes. These include the folding of newly synthesised proteins, the assistance in intercellular protein sorting, but also the refolding of denatured polypeptides, a characteristic that becomes especially important under stress conditions (Bukau,

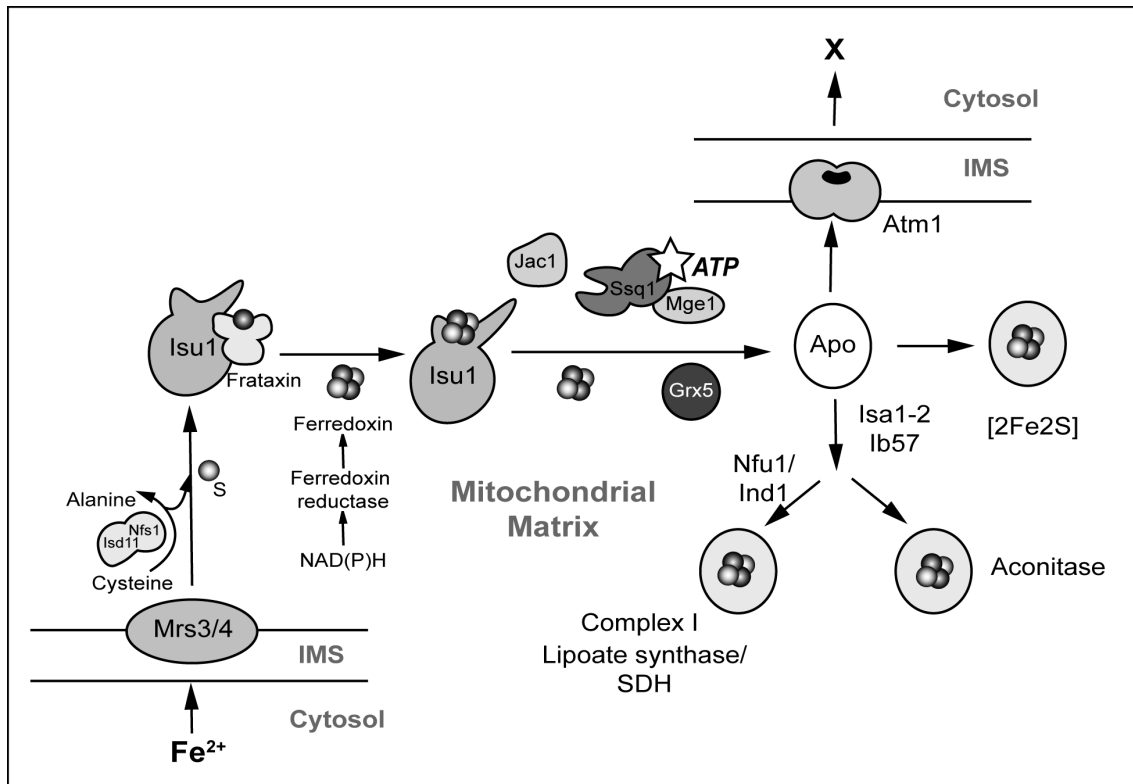


Figure 1.4.: The mitochondrial Fe/S protein biogenesis system, adapted from Lill (2012). Iron is transported over the mitochondrial inner membrane via the transporter Mrs3/4. The Fe/S cluster in the mitochondrial matrix is built up on the scaffold protein Isu1, a process involving frataxin as a potential iron donor and the desulfurase complex Nfs1-Isd11 as a sulphur donor. Additionally, an electron transfer chain consisting of NAD(P)H, ferredoxin reductase (Arh1) and ferredoxin (Yah1) plays a role in the cluster assembly. Upon assembly on Isu1, the Fe/S cluster is labilized and transferred to its apoprotein with the help of the monothiol glutaredoxin Grx5. Labilization of the Fe/S cluster in yeast involves a Hsp70 chaperone system consisting of the Hsp70 protein Ssq1, the J-protein Jac1 and the nucleotide exchange factor Mge1. While these steps are common for all mitochondrial Fe/S cluster proteins, specialised components involving the proteins Isa1, Isa2 and Iba57 catalyse the generation of [4Fe-4S]-clusters. The assembly of lipoate synthase and complex II of the respiratory chain (SDH) involve the protein Nfu1 while Ind1 assists the assembly of complex I. The connection between the mitochondrial and the cytosolic Fe/S assembly machineries is established by the export of an unidentified component via the transporter Atm1 in the inner mitochondrial membrane.

Weissman and Horwich 2006; Frydman 2001; Hartl, Bracher and Hayer-Hartl 2011; Mayer and Bukau 2005; Voos and Röttgers 2002; Young 2004). The biochemical activity of Hsp70 proteins is based on their ATPase-activity that determines the affinity for its client proteins. The initial interaction with substrate polypeptides occurs in the ATP-state, where the overall substrate affinity of the chaperone is low and its conformation is characterized by an opened substrate-interaction site exhibiting high on-off binding rates. After ATP hydrolysis, intramolecular conformational changes allow a closure of the SDB and the chaperone shows a high substrate-affinity. Only after exchange of the bound ADP to ATP, the client protein is released and a new substrate can bind (Mayer and Bukau 2005; Saibil 2008).

This apparently simple mechanism, however, needs to be carefully adjusted for each individual member of the Hsp70 family. For this reason, Hsp70 proteins interact with numerous specific protein factors, termed cochaperones. In many cases the cochaperones determine the specific cellular function of their cognate Hsp70 chaperone. There are two main groups of cochaperones that influence the activity of Hsp70 proteins. Firstly, almost all Hsp70 proteins need nucleotide-exchange factors (NEFs) that destabilise the binding to ADP and allow the interaction with fresh nucleotides after ATP hydrolysis and the folding of the client protein have occurred. In yeast mitochondria, Mge1 (mitochondrial GrpE homolog1) serves as a nucleotide exchange factor for the two main Hsp70s Ssc1 and Ssq1 (Miao, Davis and Craig 1997; Schmidt, Pfanner and Meisinger 2010). Mge1 is named after GrpE, the nucleotide exchange factor of the *E.coli* Hsp70 protein DnaK.

Secondly, all Hsp70s depend on the activity of J-proteins. J-proteins are a diverse class of Hsp70 cofactors. The common feature of all J-proteins is their ability to stimulate the ATPase activity of substrate-bound Hsp70s and thus facilitate the folding of the client protein. This function is exerted by interaction of the J-protein with the ATPase domain of Hsp70s through a conserved motif consisting of a His-Pro-Asp tripeptide (HPD) that is located in the N-terminal part of the J-protein, called J-domain. While the J-domain is a mutual element of all J-proteins, additional domains and motifs divide the J-proteins into three classes. The J-domain of class I J-proteins is followed by a flexible Gly-Phe-rich region and a C-terminal extension. The C-terminus of class I J-proteins contains a cysteine-rich domain forming two zinc-binding motifs (zinc center I and II) and a hydrophobic substrate-binding pocket. The namesake of the J-protein family is the *E.coli* DnaJ, a typical class I J-protein. Class II J-proteins lack the zinc-binding regions and do not interact with substrate

proteins. Moreover, some members of classes I and II of the J-protein family are known to dimerize via a poorly conserved domain at their C-terminus (Kampinga and Craig 2010; Langer 1992). *E.coli* DnaJ and the yeast cytosolic J-proteins Ydj1 (class I) and Sis1 (class II) belong to the dimeric J-proteins. Residues that are involved in the dimer formation have been identified for *E.coli* DnaJ and for the yeast cytosolic class II J-proteins Ydj1 and Sis1 (Sha, Lee and Cyr 2000; Wu 2005). For Ydj1, the yeast DnaJ homologue, a crystal structure of the substrate-bound dimer is available (Li, Qian and Sha 2003). The class III J-proteins, a third group of DnaJ-like cochaperones, does not resemble class I or class II except for the J-domain. However, class III J-proteins can contain additional motifs that differ from the classic J-protein components (Kampinga and Craig 2010; Kelley 1999; Walsh 2004). The intrinsic substrate-binding activity of class I J-proteins is thought to keep unfolded or misfolded Hsp70 client proteins soluble and deliver them to the chaperone, where the J-protein eventually assists the Hsp70 chaperone by stimulating its ATPase activity. There are hints that the two zinc centers of the C-terminal domain are probably involved in the interaction with Hsp70 substrates (Linke 2003; Lu and Cyr 1998; Szabo 1996). While only class I J-proteins contain zinc-binding motifs, the ability to interact with substrates is not restricted to this group. Some class II and many class III J-proteins have substrate-binding domains that strongly differ from those of the class I J-proteins but have the same importance for their function. Those proteins can show selective binding properties for single distinct substrates or substrate-groups or promiscuous client binding like class I J-proteins (reviewed in Kampinga and Craig 2010).

1.2.1. Mitochondrial Hsp70 proteins

1.2.1.1. The role of Ssc1 in the import and folding of preproteins

During the import of proteins into the mitochondrial matrix, the negatively charged presequence of the precursor protein enters the preprotein translocase and is directed into the matrix by the electric potential ($\Delta\Psi$) across the inner mitochondrial membrane. ATP-bound Ssc1 is recruited to the import channel by the scaffold protein Tim44, a component of the Tim23-translocase of the inner mitochondrial membrane where it interacts with the incoming precursor and the J-protein complex consisting of the proteins Pam16 and Pam18 (D'Silva 2003; D'Silva 2005; Frazier 2004; Truscott 2003). While Pam18 consists of a C-terminal transmembrane domain and a J-domain

that is facing the mitochondrial matrix, Pam16 contains a J-like domain but lacks the characteristic HPD motif. The ATPase-enhancing function of Pam18 is thought to be negatively regulated by Pam16 (D'Silva 2008; Li 2004). Pam17, a recently discovered component of the PAM complex, might induce the interaction of Pam18 with Pam16 and stabilise their binding to the translocase (Van Der Laan 2005). Upon binding to the incoming precursor protein, Pam18 induces ATP hydrolysis and Ssc1 is released from Tim44 simultaneously. The binding of the nucleotide exchange factor Mge1 induces exchange of the bound ADP with a fresh ATP. Upon ATP-binding, Mge1 is released from the chaperone followed by dissociation of the precursor and a concomitant dissociation of Ssc1 from Pam18 and the import channel. While the binding of Mge1 is transient, the interaction of J-proteins with mtHsp70 proteins is relatively stable. FRET-based *in vitro* experiments with purified components of the Ssc1 chaperone system, showed that the dissociation of Mge1 from the chaperone occurred in milliseconds, while Mdj1, the J-protein of Ssc1 in the mitochondrial matrix, was released only after seconds (Mapa 2010).

The precise role of Hsp70 proteins in the import reaction has been discussed extensively. It is widely believed that the conformational changes caused by ATP-hydrolysis exert an inward directed force ('pulling') on the incoming substrate and thus facilitate its translocation through the import channel (Lim 2001; Voisine 1999; Voos 1996). On the other hand, it is also possible that binding of the Hsp70 protein fulfils only a passive trapping function and simply prevents the precursor from sliding backwards through the import channel (Neupert and Herrmann 2007). However, as precursor proteins have to enter the TIM23-channel in an unfolded conformation, the 'pulling' activity of Hsp70 is of particular importance during the import of long substrates that are probably partially folded in the cytosol while it is dispensable for the import of short, unfolded preproteins (Glick 1993; Krayl 2007; Voos 1993). Besides its function during the import reaction, Ssc1 assists in folding and refolding of unfolded or denatured substrates in the mitochondrial matrix. The interaction partners of Ssc1 during the folding reaction are Mge1 and the class I J-protein Mdj1 (Rowley 1994; Westermann 1996). Like all class I J-proteins, Mdj1 is able to bind to client proteins and delivers them to Ssc1. Furthermore, Mdj1 appears to possess an intrinsic chaperone function independent of Ssc1 (Duchniewicz 1999).

1.2.1.2. The role of Ssq1 in the biogenesis of mitochondrial Fe/S cluster proteins

The second, less abundant mtHsp70 protein, Ssq1, fulfils a highly specialised task in the mitochondrial Fe/S cluster assembly machinery (Dutkiewicz 2003; Knight 1998). The only known substrate of Ssq1 is Isu1, the scaffold protein on which the Fe/S cluster is built up before it is transferred to its apo-protein. Ssq1 is believed to facilitate this transfer by inducing conformational changes on Isu1 (Dutkiewicz 2006). Upon its assembly on Isu1, the [2Fe-2S]-cluster is transferred to its apo-protein with the help of Ssq1 and its partner protein Jac1. Jac1 belongs to the class III of J-proteins that lack the typical class I substrate interaction site. Instead, the J-protein specifically binds to holo-Isu1 through a region in its C-terminal domain and delivers it to the chaperone (Ciesielski 2012). Ssq1 interacts with Isu1 through a conserved LPPVK motif. A conformational change induced by ATP hydrolysis stimulated by Jac1 may weaken the binding of Isu1 to the Fe/S cluster and induces the transfer of the Fe/S cluster to its apo-protein. Concomitantly, the binding between Ssq1 and Isu1 is stabilised. The specialised Ssq1-system only exists in *S. cerevisiae* and a few other fungi, while in higher eukaryotes, a single mtHsp70 chaperone takes over both Ssc1 and Ssq1 functions. Jac1, the specialised J-protein partner of Ssq1 has co-evolved with the chaperone (Puksza 2010). The binding of Ssq1 to Isu1 via a defined interaction site is far more specific than the more general substrate interaction of Ssc1. Moreover, as also Jac1 selectively interacts with Isu1, it strongly contributes to this specificity. Notably, the nucleotide exchange factor for Ssq1, Mge1, is the same as for the Ssc1 chaperone system, underlining the importance of J-proteins for the Hsp70-substrate interaction.

1.3. Zinc finger proteins and cellular zinc

The first zinc-binding protein motif was identified in the transcription factor TFIIIA from *Xenopus laevis* and belonged to the classical C_2H_2 family of DNA-binding zinc fingers (Miller, McLachlan and Klug 1985). Today, over 20 classes of zinc fingers with a high structural and functional diversity are known (Krishna, Majumdar and Grishin 2003). Besides their classical functions in transcriptional regulation by recognition of specific DNA sequences, zinc finger motifs can play important roles in structural stabilization or serve as protein-recognition motifs (Gamsjaeger 2007; Namuswe and Berg 2012). Roughly, the major role of the bound zinc ion

can be catalytic, cocatalytic or structural (McCall, Huang and Fierke 2000). In catalytic zinc sites, that often contain histidine, glutamic acid and aspartic acid as zinc-chelating ligands, the zinc atom is directly involved in the enzymatic reaction and binds at least one water molecule. The zinc atom in structural zinc-binding sites, is usually chelated by four cysteines. The stabilising properties of zinc ions derive from secondary interactions of the chelating ligands with other groups in the protein via hydrogen bonds that support its structure (Namuswe and Berg 2012). Moreover, structural zinc sites contain no water molecule, a characteristic that is diagnostic for catalytic zinc-binding motifs (McCall, Huang and Fierke 2000).

Zinc binding proteins occur throughout the cell. As many zinc finger proteins fulfil classical roles in transcriptional regulation, they play important roles in processes involved in stress tolerance. For instance, the transcription factors Atf1 and Atf2 that induce the expression of genes of the iron regulon, contain zinc-binding motifs. Other zinc finger proteins that are involved in yeast stress tolerance are the transcription factors Msn2 and Msn4 (Multicopy suppressor of SNF1 mutation 2 and 4) that bind to the stress-responsive element (SRE) in *S. cerevisiae*. Also zinc finger proteins that are not involved in the transcriptional regulation, for instance members of the J-protein family, have functions that are crucial for cellular survival. In mitochondria, zinc finger proteins are involved in several metabolic functions, such as alcohol oxidation (Adh3, Adh4), respiration (CoxIV) or leucine biosynthesis (Leu9). Furthermore, they include a series of zinc-binding metalloproteases such as Yta10, Yta1 and Yme1. The small Tim-proteins Tim9 and Tim10 that are involved in the import of proteins by the Tim22 import pathway are able to bind zinc ions (Pierrel, Cobine and Winge 2007). Furthermore, the homodimeric IMS protein Sod1 that plays an important role in the cellular defense against oxidative stress is stabilised by the binding of a copper and a zinc ion (Ding and Dokholyan 2008; Zhao and Bai 2012). Finally, some J-proteins, important cofactors of Hsp70 chaperones, carry zinc finger motifs, among them the yeast mitochondrial J-protein Mdj1. Recently, the zinc-chelating mtHsp70 interacting protein Zim17 has been discovered (Burri 2004).

1.4. Zim17, a newly identified mtHsp70 cochaperone

The yeast mitochondrial zinc finger protein Zim17 (Zinc finger motif protein of 17 kDa) belongs to a newly identified class of mtHsp70 cochaperones that are characterized

by a central zinc ribbon domain (Krishna, Majumdar and Grishin 2003) consisting of two CXXC motifs flanked by several β -sheets (Momose 2007). Homologues of Zim17 have been identified in chloroplasts and mitochondria of fungi as well as plants and higher eukaryotes (Kluth 2012). However, there are no Zim17 proteins known in bacteria or archaea. Zim17 has also been termed Tim15 (Translocase of the inner mitochondrial membrane 15) and Hep1 (Hsp70 escort protein 1). The name Hep1 refers to the ability of Zim17 to prevent the aggregation of Hsp70 chaperones in mitochondria of eukaryotic cells (Sichting 2005) while the name Tim15 derives from an observed import defect in Zim17-depletant cells (Yamamoto 2005). However, as it has been shown that Zim17 is not a part of the inner membrane translocase (Sanjuán Szklarz 2005; Sichting 2005) it does not belong to the Tim proteins.

Cells lacking Zim17 (*zim17* Δ) show severe phenotypic defects like the inability to grow at elevated temperatures. Furthermore, it was observed that the loss of Zim17 leads to a respiratory-deficient phenotype (Sichting 2005). However, a tetrad analysis of a newly generated *zim17* Δ strain yielded spores that were respiratory-competent initially but showed a high frequency to generate a petite phenotype (Sanjuán Szklarz 2005). Zim17 is known to interact with both Ssc1 and Ssq1 in the mitochondrial matrix of *S. cerevisiae* and its binding site is most likely located in the mtHsp70 ATPase domain (Blamowska 2010; Zhai 2008). The binding of Zim17 seems to be ATP-dependent and occurs preferably in the absence of nucleotides (Sichting 2005). It has been demonstrated that the human and chloroplast Zim17 orthologues Hep1 and HEP2 are able to interact with their mtHsp70 partners also in the presence of ATP, however, the binding under ATP-free conditions was much stronger (Goswami, Chittoor and D'Silva 2010; Willmund 2008; Zhai 2008). Moreover, it was shown that the human Zim17 orthologue Hep1 is able to enhance the ATPase activity of Hsp70 proteins (Goswami, Chittoor and D'Silva 2010; Zhai 2008) a function that was not observed for yeast Zim17 (Blamowska 2010; Sichting 2005). Though the Hsp70-interaction site of human Hep1 has been confined to the region around a highly conserved Asp-Asn-Leu (D111 N112 L113) motif close to the zinc-binding residues, the exact nature of its interaction with Hsp70s is still unclear (Momose 2007; Zhai 2011). It has been reported, that the conserved aspartate at position 111 (D111) and a histidine residue at position 107 (H107) are probably part of the Hsp70 binding site (Momose 2007; Zhai 2011). In particular, H107 has been shown to be essential for the ATPase-stimulating function of human Hep1 (Zhai 2011).

Because the highly conserved DNL motif is in close proximity to the zinc-binding

residues, the cysteine rich region of Zim17 has been classified as DNLZ-type zinc finger (Zhai 2011). The relevance of the zinc finger domain for the function of Zim17 remains to be determined. It was shown that binding of the zinc atom has a stabilising role in both yeast Zim17 and human Hep1. Yeast cells expressing Zim17 mutants that are deficient in the binding of zinc were inviable (Yamamoto 2005). Furthermore, recombinantly expressed Zim17 zinc finger mutants formed insoluble aggregates (inclusion bodies) in *E.coli* cells (Momose 2007). A recent study showed that the binding of the zinc atom promotes stabilising effects through the coordinating cysteine residues C75 and C110 that particularly influence the region around the residues R106, H107 and D111 (Fraga 2012). Furthermore, purified Zim17 seems to tend to form oligomers in solution that are, like the monomeric protein, stabilised in the presence of zinc (Dores-Silva 2013). Dimeric forms of the chloroplast Zim17-orthologue HEP2, as well as dimers of human Hep1 were observed before (Willmund 2008; Zhai 2008), however, their functional significance remains to be clarified.

In organello-experiments revealed that loss of Zim17 results in aggregation of the two main mitochondrial Hsp70 chaperones Ssc1 and Ssq1 (Momose 2007; Sichtung 2005). An aggregation-preventive function has also been observed for the human Zim17 orthologue Hep1. It was thus suggested that the nucleotide-free form of mtHsp70 is prone to aggregation and that the primary function of Zim17 is to maintain its solubility (Blamowska 2010). In support of this thesis, further studies indicated that Zim17 participates in the *de novo* folding of the main yeast mitochondrial Hsp70 chaperone Ssc1 while components of the mitochondrial protein quality control system (Hsp60, Hsp78 and Hsp70 itself) did not seem to be involved in this process. Furthermore, Zim17 was able to promote the re-folding of Ssc1 *in vitro* (Blamowska, Neupert and Hell 2012). Conclusively, the aggregation-preventive character of Zim17 has been claimed to be its primary function (Blamowska, Neupert and Hell 2012; Sanjuán Szklarz 2005). The aggregation of mtHsp70 proteins presumably leads to other observed defects in *zim17* Δ cells, for instance an impaired import of matrix destined preproteins (Burri 2004; Yamamoto 2005) and a loss of Fe/S enzymes such as aconitase (Sichtung 2005). These defects would consequently result in an enrichment of dysfunctional mitochondria and an instable respiratory competence (Sanjuán Szklarz 2005). As a long-term consequence a nuclear genome instability of *zim17* Δ cells that is possibly induced by the functional loss of the mitochondrial Fe/S assembly machinery has been reported (Díaz de la Loza 2011). However, it has

also been observed that other Hsp70 cochaperones can have stabilising effects as well (Momose 2007). Furthermore, Zim17 orthologues from other species show functions that differ from a simple aggregation prevention mechanism. While recombinant Ssc1 tends to aggregate in the absence of Zim17, its orthologue in chloroplasts of *Chlamydomonas reinhardtii*, HEP2, is rather needed to keep the chaperone HSP70B in an active state (Willmund 2008). The human Zim17 orthologue Hep1, prevents the aggregation of mtHsp70. However, Hep1 also shows the propensity to enhance the ATPase activity of its chaperone partner (Zhai 2008). This data raises the question if the prevention of mtHsp70 aggregation is the primary function of Zim17.

1.5. Research objectives

The aim of this thesis was to gain further insight into the functional cooperation of Zim17 with its Hsp70 binding partners. Recent studies suggest that the main function of Zim17 is given by its aggregation-preventive influence on mtHsp70 proteins. Phenotypic effects like a defect in the mitochondrial iron sulphur cluster assembly machinery (Sichting 2005) or the import of preproteins into the mitochondrial matrix (Burri 2004; Sichting 2005) were considered to derive secondarily due to a loss of soluble Hsp70 chaperones. However, as the aggregation of mitochondrial Hsp70 chaperones in Zim17 deficient yeast cells is not complete (Sichting 2005) and other Hsp70 cochaperones seem to have a similar aggregation-preventive effect (Momose 2007), the question arises if the aggregation of mtHsp70 proteins alone can lead to the prominent effects listed above.

One objective of this work was to study the role of the aggregation-preventive function of Zim17 and its interaction mechanism with Ssc1 in a biochemical approach. In particular, the influence of Zim17 on the solubility of Ssc1 as well as the character and stability of its binding to the chaperone were intended to be analysed. As the zinc ligand of Zim17 was suggested to have a stabilizing character (Momose 2007), recombinant Zim17 mutants that were unable to chelate the zinc ligand should further be generated and analysed with regard to their effect on the solubility of Zim17.

A second aim was the classification of the precise cochaperone function of Zim17 and its effects in a cellular context *in vivo*. A deletion of ZIM17 in *S.cerevisiae* leads to a pleiotropic phenotype that makes it difficult to define the primary effects of a Zim17 loss. To avoid the accumulation of secondary effects, conditional Zim17 mutants with a temperature-sensitive behaviour were intended to be generated. To clarify if the prevention of mtHsp70 aggregation is the main function of Zim17, its influence on mtHsp70 solubility and on mtHsp70-dependent processes should be examined. Specifically, the Ssc1-dependent import of precursor proteins into the mitochondrial matrix and the Ssq1-dependent biogenesis of Fe/S cluster-containing proteins were destined to be analysed in detail to identify possible direct effects of the Zim17 loss of function on the mtHsp70 chaperone activity.

2. Materials and Methods

2.1. Yeast and *E.coli* strains

Table 2.1.: *E.coli* strains

strain	genotype	origin
NEB-5 α	fhuA2 Δ (argF-lacZ)U169 phoA glnV44 Φ 80 Δ (lacZ) M15 gyrA96 recA1 relA1 endA1 thi-1 hsdR17	New England Biolabs
BL21 Codon plus [®] (DE3)-RP	B F _B ⁻ ompT hsdS(r _B ⁻ m _B ⁻) dcm ⁺ Tet ^r gal λ (DE3) endA Hte [argU proL Cam ^r]	Stratagene

Table 2.2.: Yeast strains I

strain	genotype	origin
YPH 499	MAT a, <i>ura3-52, lys2-801, ade2-101, trp1-Δ63, his3-Δ200, leu2-Δ1</i>	EUROSCARF
BY 4742	MAT alpha, <i>his3Δ1, leu2Δ0, lys2Δ0, ura3Δ0</i>	EUROSCARF
PK 82	<i>Mat alpha, his4-713 lys2 ura3-52 leu2-3,112 trp1</i>	Kang1990
PK 81 (<i>ssc1-2</i>)	Mat alpha, <i>ade2-101 lys2 ura3-52 leu2-3,112 trp1, ssc1-2(LEU2)</i>	Kang1990
BGY-Fomp3-20-2 (<i>zim17-2</i>)	Mat a, <i>ade2-101, his3-Δ200, leu2-Δ1, ura3-52, trp1-Δ63, lys2-801 zim17::ADE2</i> pFLzim17-Ts2-CEN	S. Szklarz 2005
BGY-Fomp3-C1 (<i>zim17-3</i>)	Mat a, <i>ade2-101, his3-Δ200, leu2-Δ1, ura3-52, trp1-Δ63, lys2-801 zim17::ADE2</i> pFLzim17-Ts3-CEN	S. Szklarz 2005
BGY-Fomp3-6-4 (<i>zim17-4</i>)	Mat a, <i>ade2-101, his3-Δ200, leu2-Δ1, ura3-52, trp1-Δ63, lys2-801 zim17::ADE2</i> pFLzim17-Ts4-CEN	S. Szklarz 2005
yBGΔ-Fomp3-2 (<i>zim17Δ</i>)	Mat a, <i>ade2-101, his3-Δ200, leu2-Δ1, ura3-52, trp1-Δ63, lys2-801 zim17::ADE2</i>	S. Szklarz 2005

Table 2.3.: Yeast strains II - strains generated in this study

strain	genotype	origin
ILY01	MAT a, <i>ura3-52, lys2-801, ade2-101, trp1-Δ63, his3-Δ200, leu2-Δ1</i> pFLzim17-corrWT-CEN	this work
ILY02	MAT a, <i>ura3-52, lys2-801, ade2-101 trp1-Δ63, his3-Δ200, leu2-Δ1 ZIM17Δ :: ADE2</i> pFLzim17-corrWT-CEN	this work
ILY08	MAT a, <i>ura3-52, lys2-801, ade2-101, trp1-Δ63, his3-Δ200, leu2-Δ, ZIM17-wt (LEU2)</i>	this work
ILY09	MAT a, <i>ura3-52, lys2-801, ade2-101, trp1-Δ63, his3-Δ200, leu2-Δ, ZIM17-3a (LEU2)</i> , respiratory incompetent	this work
ILY10	MAT a, <i>ura3-52, lys2-801, ade2-101, trp1-Δ63, his3-Δ200, leu2-Δ, ZIM17-3b (LEU2)</i> , respiratory incompetent	this work
ILY20	MAT a/alpha <i>leu2Δ0/leu2Δ, lys2-801/lys2-Δ0, URA3/ura3-Δ0, ade2-101/ADE2, trp1-Δ63/TRP1, his3-Δ200/HIS3, zim17::LEU2/ZIM17</i>	this work
ILY21	MAT a/alpha <i>leu2Δ0/leu2Δ, lys2-801/lys2-Δ0, URA3/ura3-Δ0, ade2-101/ADE2, trp1-Δ63/TRP1, his3-Δ200/HIS3, zim17-3a::LEU2/ZIM17</i>	this work
ILY22	MAT a/alpha <i>leu2Δ0/leu2Δ, lys2-801/lys2-Δ0, URA3/ura3-Δ0, ade2-101/ADE2, trp1-Δ63/TRP1, his3-Δ200/HIS3, zim17-3b::LEU2/ZIM17</i>	this work
ILY24	<i>leu2, trp1-Δ63, ZIM17::LEU2</i> , respiratory-competent	this work
ILY27	<i>leu2, trp1-Δ63, zim17-3a::LEU2</i> , respiratory-competent	this work
ILY28	<i>leu2, trp1-Δ63, zim17-3b::LEU2</i> , respiratory-competent	this work

2.2. Plasmids

Table 2.4.: Plasmids used in this work

Vector	purpose	origin
pCR bluntII TOPO	blunt end cloning	Invitrogen
pGEM-4z	Cloning of proteins for <i>in vitro</i> translation, SP6 and T7 promotor, Ampicillin resistance	Promega
pETDuet	Procaryotic expression of proteins (<i>E.coli</i>), T7-promotor, Ampicillin resistance	Novagen
pET28	Procaryotic expression of proteins (<i>E.coli</i>), T7-promotor, Kanamycin resistance	Novagen
pDB10	Procaryotic co-expression of Ssc1 and Zim17 in pETDuet	D. Becker, unpublished results
pIL1/ pIL2	Procaryotic co-expression of Ssc1 and Zim17 in pETDuet	this work
pIL4	Procaryotic expression of Zim17 in pETDuet	this work
pIL1/ pIL2	Procaryotic expression of Ssc1 in pET28	this work
pIL6/ pIL7	Procaryotic expression of Zim17 zinc finger mutants in pETDuet	this work
pIL8, pIL9, pIL10	Cloning of pre-Zim17 wt and zinc finger mutants in pCR bluntII TOPO for <i>in vitro</i> translation	this work
pFL39	Eukaryotic protein expression (<i>S.cerevisiae</i>), modified pUC19	Bonneaud 1991
pFL-Zim17-ts2-CEN, pFL-Zim17-ts3-CEN, pFL-Zim17-ts4-CEN	Eukaryotic expression of Zim17-2, -3, and -4 in pFL39	S.Szklarz 2005
pFL-Zim17-corrWT-CEN	Eukaryotic expression of Zim17-wt	this work
pRS415	Amplification of <i>LEU2</i>	Sikorski 1989

2.3. Growth media

Table 2.5.: Growth media

Medium	composition
YEAST	
YPD	10 g/l yeast extract, 20 g/l bacto peptone, 2% glucose, pH 5.0
YPG	10 g/l yeast extract, 20 g/l bacto peptone, 3% glycerol, pH 5.0
SD	6.7 g/l yeast nitrogen base w/o amino acids (Roth), addition of amino acid supplements (CSM -Trp/ -Leu/ -LeuTrp or CSM -URA), MP bio
presporulation medium	0.8% yeast extract, 0.3% bacto peptone, 10% glucose
sporulation medium	0.1% yeast extract, 1% Kaliumacetat, CSM complete supplement mix (MP bio, Eschwege)
SOS	50% YPD, 1 M sorbitol, 6.5 mM CaCl ₂
BACTERIA	
LB	5 g/l yeast extract, 10 g/l tryptone, 10 g/l NaCl

2.4. Molecular biological methods

2.4.1. Polymerase chain reaction

2.4.1.1. Phusion-polymerase system

The polymerase chain reaction (PCR, Saiki 1985) was used to amplify DNA-fragments from yeast genomic or plasmid DNA with the Phusion High-Fidelity DNA Polymerase system (Thermo Scientific). PCR reaction mixes with a total volume of 50 μ l were composed according to the instructions of the supplier and generally contained 1-fold concentrated PHUSION-HF-buffer, 0.02 U/ μ l polymerase, 200 μ M dNTP, 25 pmol of each oligonucleotide and 1-5 ng of plasmid DNA or 50-100 ng of genomic yeast DNA respectively. Cycle conditions are shown in table 2.6. Melting temperatures for the annealing part of the applied oligonucleotides were calculated using the formular

$$T_m = 69.3\text{ }^{\circ}\text{C} + (0.41\text{ }^{\circ}\text{C} * (G + C)\%) - 650/bp \quad (2.1)$$

Generally, an annealing temperature 3-5 $^{\circ}$ C above the lower calculated melting temperature was used.

Table 2.6.: Cycling conditions for PCR

Step	Temperature	Duration	
Initial denaturation	98 $^{\circ}$ C	60 s	
Denaturation	98 $^{\circ}$ C	10 s	
Annealing	$T_m + 3\text{ }^{\circ}\text{C}$	15 s	35 cycles
Extending	72 $^{\circ}$ C	30 s per kb	
Final Extending	72 $^{\circ}$ C	10 min per kb	

2.4.1.2. *In vitro* mutagenesis by overlap-extension PCR

The overlap extension PCR method (Higuchi, Krummel and Saiki 1988; Ho 1989) was used to insert point mutations into DNA fragments. In a first step, two PCR reactions were carried out to induce the desired mutation into the target sequence. The first PCR applied a flanking forward primer in combination with an internal reverse primer that contained the mismatched base pairs. For the second PCR, an

internal forward primer and a flanking reverse primer were used. As the two inner primers are reverse complementary to each other, two overlapping PCR fragments were amplified. The PCR fragments act as primers for each other and thus were combined via a primer extension reaction in a third PCR applying the two flanking primers from step one.

2.4.2. Agarose-gelelectrophoresis

Depending on the size of the analysed DNA fragments, 1-2% agarose in TAE buffer with 1 µg/µl Ethidiumbromid was used for the preparation of agarose gels. 1-10 µl DNA samples were mixed with loading dye (10 mM Tris/HCl, pH 7.6, 60% glycerol, 60 mM EDTA, 0.03% Xylene Cyanol FF, 0.03% bromphenolblue) before loading on the gel. Adequate markers from New England Biolabs (e.g. Quick load™1kb ladder or Quick load™100bp ladder) were used as size standards. DNA fragments were separated by applying an electric tension of 120-200 V depending on the size of the gel. Gels were analysed with the Bio doc analyze Biometra system (Analytik Jena). To isolate DNA from a gel, bands were cut out under UV-light with a scalpel and DNA was purified via a column using the innu PREP Gel extraction Kit (Analytik Jena).

2.4.3. Restriction digest of DNA

For cloning of PCR fragments into plasmids, restriction sites were added via the applied oligonucleotides. For restriction digests, enzymes and buffers from Fermentas were used (Fermentas/ Thermo Scientific).

2.4.3.1. Analytical restriction digest

For a standard restriction digest for control purposes and analysis of vectors and PCR fragments, 1 µl DNA (between 200 ng and 1 µg) was mixed with 1 U enzyme, 1 µl of the appropriate 10 x buffer and H₂O in a total volume of 10 µl. Samples were incubated for 1 h at 37 °C and subsequently analysed by agarose gelelectrophoresis.

2.4.3.2. Preparative restriction digest

To extract PCR products or cloned DNA fragments, approximately 10 µg DNA were digested with 5 U of the appropriate restriction enzymes as described above and

incubated at 37°C for several hours or over night. After gelelectrophoresis, DNA fragments were extracted from the agarose gel as described in section 2.4.2.

2.4.4. Ligation

DNA fragments prepared by restriction digest were cloned into plasmids that were cut with the same restriction enzymes (cloning via cohesive ends). Ligations were performed using the Rapid DNA dephos. and ligation kit (Roche). For a 10 µl ligation reaction, 50-100 ng vector DNA were mixed with 1 µl dilution buffer (Roche) and water. The amount of insert was calculated using the formular

$$ng\ insert = \frac{ng\ vector * kb\ insert}{kb\ vector} \quad (2.2)$$

1 µl T4 Ligase (Roche) was added and samples were incubated 20-25 min at 25°C. 5 µl of the ligation preparation was used for the transformation of 50 µl competent *E.coli* cells (section 2.4.5).

2.4.5. Transformation of competent bacteria

Transformation of *E.coli* cells with plasmid DNA was performed using the strain BL21cp for the expression of recombinant proteins (section 2.4.7). *E. coli* cells from the strain NEB 5α (New England Biolabs) were used for cloning and replication of plasmid DNA. 50 µl of frozen competent *E.coli* cells were mixed with 10-100 ng plasmid DNA. Cells were incubated 30 min on ice, subjected to an 80 s heat shock at 42°C in a water bath and directly transferred to ice for 5 min. 1 ml of room temperature LB medium was added and cells were incubated for 1 h at 37°C. 100 µl of each sample were plated directly on solid LB medium containing the appropriate antibiotics to select successfully transformed cells. If the transformation efficiency was low, the sample volume was reduced by collecting the cells with a 5 min centrifugation step at 4500 rpm. Cell pellets were resuspended in 100 µl LB medium and the whole amount of transformed cells was distributed to selective LB medium. The plates were incubated over night at 37°C. Single colonies were picked and incubated in liquid medium for further analysis.

2.4.6. DNA isolation from *E.coli*

To isolate small amounts of plasmid DNA (for sequencing and control digests) or large amounts of plasmid DNA (for instance for the transformation of yeast cells) the GeneJET® Plasmid Miniprep or Midiprep Kits (Fermentas/ Thermo Scientific) were used. DNA was isolated according to the manufacturers specifications and resuspended in water (for sequencing) or in TE buffer (10 mM Tris/HCl, 1 mM EDTA, pH 8.0). The purity and concentration of DNA was determined photometrically by measuring the absorption at 260 nm and 280 nm with a BioPhotometer plus (Eppendorf). DNA has an absorption maximum at 260 nm with an extinction $E_{260} = 1$ at a concentration of 50 $\mu\text{g}/\mu\text{l}$ double strand DNA. Measurement of the absorption at 280 nm allows an estimation of the of contaminating proteins. A solution containing pure DNA displays an E_{260}/E_{280} ratio of 1.9.

2.4.7. Expression of recombinant proteins in *E.coli*

For the recombinant expression of proteins, the vector pETDuet from Novagen was used. Transformed *E.coli* BL21cp were grown over night at 37 °C in 5 ml LB-medium containing the appropriate antibiotics. On the next day, the culture was transferred into 50 ml fresh medium and further incubated at 37 °C till an OD_{600} of 0.6-0.8 was reached. Protein expression was induced after 1 h by addition of 0.1 M Isopropyl β -D-1-thiogalactopyranoside (IPTG). After 3-5 h, the cells were harvested by centrifugation at 4500 rpm. Cell pellets were stored at -20 °C. Samples were taken before and after the induction of protein expression and analysed by SDS-PAGE (section 2.5.1) and Western blot (section 2.5.2).

2.4.8. Transformation of *S. cerevisiae*

For the transformation of yeast, cells were grown in YPD medium to an OD_{600} of 0.6-0.8. Cells were harvested by centrifugation at room temperature for 5 min at 4000 rpm, washed and resuspended in 1 ml LiTE buffer (100 mM LiOAc, 10 mM Tris/HCl, pH 7.4, 1 mM EDTA, 1.2 M Sorbitol). After 1 h incubation at 37 °C, 2-10 μg plasmid DNA were added to 100 μl of cell suspension. After addition of 235 μl of 50% PEG-4000, the cells were subjected to a 15 min heat shock at 42 °C. After the heat treatment, the cells were spun down, resuspended in 500 μl SOS medium (table 2.5) and incubated at 30 °C for 15 min. 200 μl of the cell suspension were distributed on

selective medium lacking the appropriate amino acid to select successfully transformed cells.

2.4.9. DNA isolation from yeast

2.4.9.1. Quick isolation of plasmid and genomic DNA

A method according to Hoffman and Winston (1987) was used to isolate plasmid DNA from yeast cells, e.g. for subsequent *E.coli* transformations. The same method was used for yeast colony screening after *in vitro* mutagenesis. 5 ml cultures were spun down and resuspended in 400 µl TSTES (2% Triton-X-100, 1% SDS, 10 mM Tris/HCl pH 8.0, 100 mM NaCl, 1 mM EDTA). 200 µl glass beads and 200 µl phenol/chloroform were added and the mixture was vortexed in short intervals for 5-10 min. After centrifugation for 10 min at 14 000 rpm, the aqueous phase was transferred to a fresh tube and DNA was extracted two times with chloroform. 2.5 Vol. ethanol were added and precipitates were spun down 10 min at 14 000 rpm. After two washing steps with 70% ethanol, DNA-pellets were dried and resuspended in 50 µl aqua bidest.

2.4.9.2. Small scale isolation of genomic DNA for PCR and sequencing

To isolate genomic DNA from yeast for subsequent PCR and sequencing, cells were grown in 1 ml YPD to an OD₆₀₀ of 0.5-0.7. Cells were harvested by centrifugation at room temperature and 4 500 rpm for 5 min. Cell pellets were put on ice and resuspended in 150 µl solution A (50 mM Tris/HCl pH 7.5, 10 mM EDTA, 0.3% β-mercaptoethanol, 0.5 mg/ml Zymolase). After incubation at 37 °C for 1 h, 20 µl 10% SDS and 100 µl ammoniumacetate were added to precipitate proteins. The mixture was vortexed and incubated at -20 °C for 15 min. After a 15 min clarifying spin at 14 000 rpm and 4 °C, 180 µl of the supernatant fraction were mixed with 120 µl isopropanol. After a second centrifugation step, the DNA pellet was washed with 70% ethanol, dried and resuspended in 20-30 µl TE buffer. 2 µl of isolated genomic DNA were used in a PCR reaction.

2.4.10. Whole cell yeast extracts for Western blot

To prepare protein extracts from yeast, 1 OD of cells was spun down 5 min at 4 000 rpm and resuspended in 1 ml water. After addition of 148 µl 2 M NaOH and 12 µl β-mercaptoethanol, cells were vortexed and incubated for 10 min on ice. 160 µl

50% trichloroacetic acid (TCA) were added and cells were incubated for another 10 min. Precipitates were spun down 10 min at 14 000 rpm and 4 °C and resuspended in 35 µl 2x Laemmli. 15 µl 1 M Tris/HCl pH 8.0 were added to neutralize residual TCA. 5-10 µl of the cell extracts were analysed by SDS-Page and Western blot.

2.4.11. Subcellular fractionation of yeast cells

To separate mitochondria from the cytosolic fraction of yeast cells for Western blot analysis, 1 ml cultures of yeast cells were grown to an OD₆₀₀ of 0.8-1.0. 1 OD of cells was harvested and resuspended in 1 ml TEB-buffer (200 mM Tris/HCl pH 8.0, 20 mM EDTA, 1% β-mercaptoethanol). Cell suspensions were shaken for 10 min at room temperature, spun down for 5 min at 4 000 rpm and resuspended in 1 ml SPM-buffer (1.2 mM sorbitol, 50 mM KPi, pH 7.3, 1 mM MgCl₂). 150 µl of 10 mg/ml Zymolase dissolved in SPM buffer were added and cells were incubated for 60 min at 37 °C. Cells were spun down 5 min at 4 000 rpm, 4 °C, washed 3x with SPM-buffer and put on ice. Cell lysis was performed in SET-buffer (50 mM Tris/HCl pH 7.5, 200 mM Sorbitol, 1 mM EDTA, 1x PI) by pipetting up and down 20 times with a yellow tip. After a clarifying spin for 5 min at 500 x g and 4 °C, 1/10 of the supernatants was taken as a total sample and mixed with 50 µl 2x Laemmli. Mitochondria were separated from the cytosolic fraction by a 10 min centrifugation at 13 000 x g, 4 °C. 1/10 of the supernatant fraction containing cytosolic proteins was taken and mixed with 50 µl 2x Laemmli. The mitochondria pellet was resuspended in 100 µl 1x Laemmli. 10-20 µl of all fractions were analysed by SDS-PAGE and Western blot.

2.4.12. Isolation of mitochondria from *S. cerevisiae*

To gain high culture volumes of *S. cerevisiae* for a preparative isolation of mitochondria, yeast cells were initially grown in 5 ml of the appropriate growth medium (YPD, YPG or in some cases selective medium) at 25 or 30 °C. After 3-5 days, the whole culture volume was transferred into 200 ml fresh medium and further incubated for 2-4 days. In case of slow growing yeast strains, the cells were grown in 50 ml fresh medium for 2-3 days before the whole culture was transferred to 200 ml fresh medium. Depending on the growth rate of the individual yeast strains, 21 cultures were inoculated to an OD₆₀₀ of 1.5-2.0 after growth over night. For wild type yeast cells a doubling time of approximately 5 h in YPG and 4 h in YPD was assumed. However, the doubling times can differ largely depending on growth medium, temperature or

mutations and thus must be determined individually for each yeast strain. After an OD₆₀₀ of 1.5 was reached, cells were harvested by a 5 min centrifugation step at 4 000 rpm in weighed centrifuge tubes at room temperature. Cell pellets were washed with water and wet weight of the pellets was determined. After resuspension in 2 ml DTT-buffer (100 mM Tris/H₂SO₄ pH 9.4, 10 mM Dithiothreitol (DTT)) per g wet pellet weight, the cell suspensions were gently shaken at 25 or 30 °C for 20 min. Cells were harvested by 5 min centrifugation at 4 000 rpm, washed with 100 ml prewarmed zymolase-buffer (20 mM K_p_i pH 7.4, 1.2 M sorbitol) and resuspended in 7 ml zymolase buffer per g wet pellet weight. 4 mg/ml Zymolase were added and the cell suspension was incubated for 1 h at 30 °C or for 2 h at 25 °C respectively. The cells were spun down, washed 1 x with zymolase buffer and were resuspended in homogenization buffer (0.6 M sorbitol, 4 mM Tris/ HCl pH 7.4, 1 mM EDTA, 0.2% BSA). Cells were put on ice immediately and disrupted in a homogenisator ('potter'). Lysates were centrifuged 3 min at 1 500 rpm directly followed by 4 min at 3 000 rpm and 4 °C to precipitate cellular debris. Supernatants were centrifuged at 4 000 rpm for 5 min and subjected to a 15 min centrifugation step at 12 000 rpm. Mitochondria pellets were resuspended in SEM-buffer (200 mM sucrose, 1 mM EDTA, 10 mM MOPS/KOH pH 7.2) and subjected to another centrifugation step at 4 000 rpm. Supernatants were collected and spun down 15 min at 12 000 rpm. Pellets were resuspended in SEM buffer, frozen in liquid nitrogen and stored at -80 °C.

2.4.13. Genomic integration

Zim17-mutants were inserted into the genome of *S.cerevisiae* through replacement of the endogenous *ZIM17* gene by homologous recombination. Mutant and wild type (wt) *ZIM17* genes were amplified from pFLzim17-Ts3-CEN and pFLzim17-Ts4 (obtained from the yeast strains BGY-Fomp3-C1 and BGY-Fomp3-6-4) and the corresponding wild-type plasmid. For *zim17-3a*, *zim17-4* and the corresponding wt a forward primer annealing 88 nucleotides downstream the *ZIM17* start codon was chosen (A1-fw, table 2.8). To exclude the mutation at residue 79, a second forward primer with an annealing sequence at position 217 in the *ZIM17* ORF was used to amplify the *zim17-3b* fragment (A1b-fw). The reverse primer for all constructs, A2-rev, has an annealing side 115 bp downstream of the *ZIM17* ORF. The *LEU2* gene was amplified from the vector pRS415 (Sikorski and Hieter 1989) using the antisense-primer B2-rev and the sense-primer B1-fw that has a 20 nucleotide extension complementary to the *zim17* reverse primer sequence. Annealing parts of

the oligonucleotides for amplification of the *LEU2* marker were chosen as suggested by Brachmann (1998). The *LEU2* marker was fused to the mutant and wt *ZIM17* fragments by overlap extension PCR (section 2.4.1.2) employing the forward primers A1-fw and A1b-fw and the antisense oligonucleotide C-rev that contains a 55-bp extension reverse complementary to a region of the 3'UTR of the *ZIM17* gene. PCR products were preserved by cloning into the vector pSC-B using the pSC-B blunt cloning Kit (Stratagene). For insertion into the genome of *S.cerevisiae*, freshly prepared PCR-products were transformed into YPH499 yeast cells containing a 2 μ URA3-containing plasmid Yep352 with the *ZIM17* open reading frame between the MET25 promoter and the CYC1 terminator (pGB8233, provided by Dr. Bernard Guiard, Centre de Génétique Moléculaire, Université Pierre et Marie Curie, Gif-sur-Yvette, France). Integrants were grown on minimal dropout medium lacking leucine and uracil and subsequently replica-plated to the same medium containing 1 g/l 5-FOA to allow loss of the Yep-*ZIM17* plasmid.

2.4.14. Random spore analysis

Genomic integrants were crossed with the wild-type strain BY4742 and diploid cells were selected by growth on minimal dropout medium without leucine and tryptophane. Diploid cells were grown on presporulation medium (table 2.5) and sporulation was induced by subsequent subjection to sporulation medium. Sporulation was carried out at 25 °C for 5-10 days until a sporulation rate of 50 % or higher was reached. Tetrades were treated with 50 mg/ml zymolase at 30 °C. Asci and remaining diploid cells were disrupted with glass beads and the remaining spores were plated out on YPD medium. A random spore analysis was carried out by replica plating to drop-out media lacking Leucine, Tryptophane or both. Temperature sensitivity and respiratory competence of spores carrying the mutant *zim17* alleles were assayed by subjection to non-permissive temperature on both fermentable (YPD) and non-fermentable (YPG) conditions. An overview of the yeast strains generated in this work is listed in table 2.3.

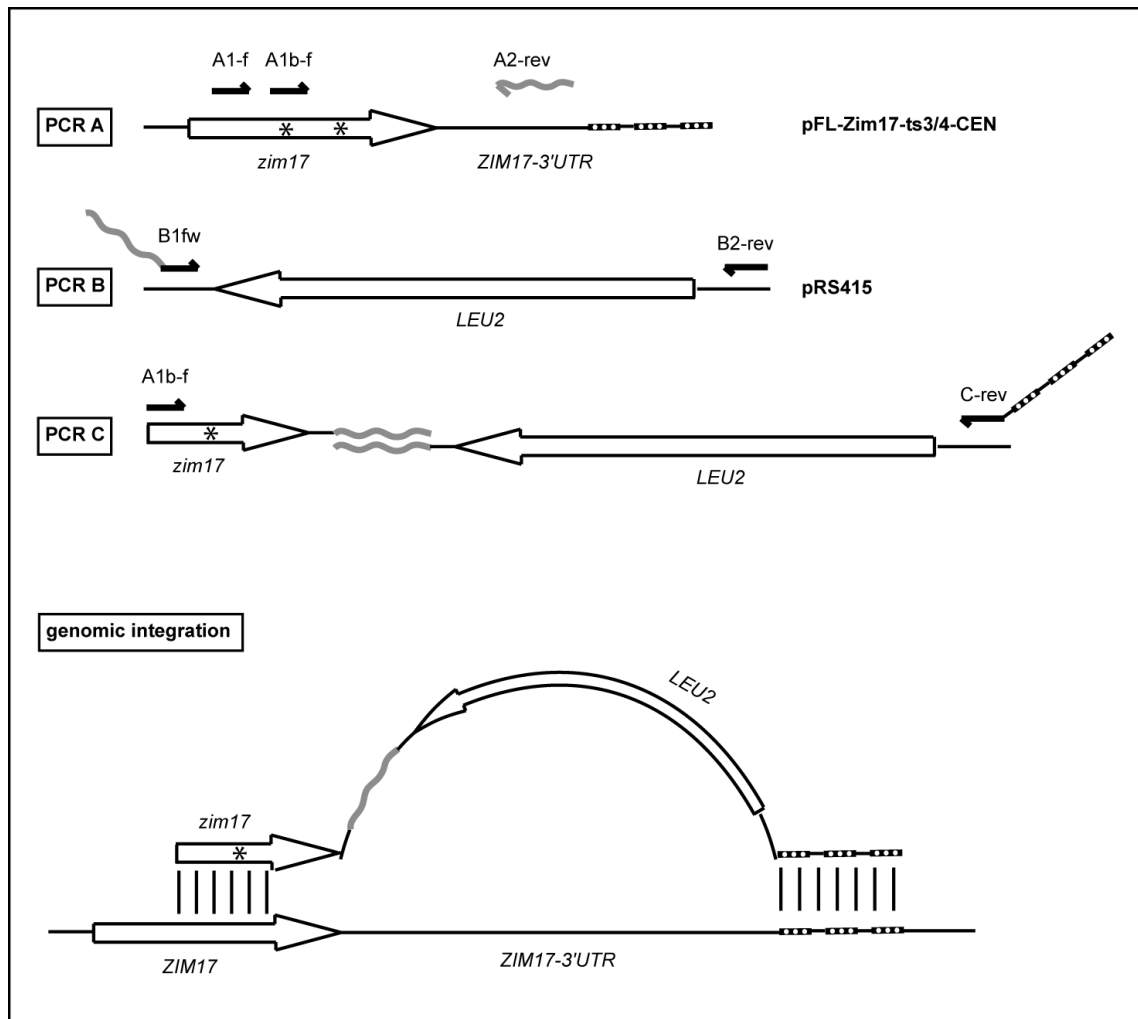


Figure 2.1.: *In vitro* mutagenesis of *ZIM17*. Mutant and wt *zim17* alleles were amplified from the plasmids pFL-Zim17-ts3-CEN and pFL-Zim17-ts4-CEN (**PCR A**). *LEU2* gene was amplified from the vector pRS415 (**PCR B**). The products of PCR A and PCR B were fused via overlap-extension PCR (**PCR C**) and inserted into the genome of *S.cerevisiae* via homologous recombination (**genomic integration**).

2.5. Protein-biochemical and immunological methods

2.5.1. SDS-polyacrylamid-gelelectrophoresis (SDS-PAGE)

Proteins were separated by discontinuous SDS-polyacrylamid-gelelectrophoresis as initially described by Laemmli (1970). Depending on the sizes of the proteins of interest, 8-16% polyacrylamid (Rotiphorese® Gel30 (37.5:1), Roth) were used for the preparation of gel mixtures according to table 2.7. The running buffer

was composed of 50 mM Tris/HCl pH 8.3, 384 mM Glycin and 0.1% SDS. As not otherwise stated, samples were resuspended in 20 μ l 1 x Laemmli buffer (2% SDS, 5% β -mercaptoethanol 10% v/v Glycerin, 60 mM Tris/HCl pH 6.8 and 0.02% w/v Bromphenol blue) and boiled for 5 min at 37 °C. Large gels (125 x 140 x 1 mm) were subjected to an electric current of 20-35 mA. For minigels (Biorad) a constant electric tension of 200 V was used. Gels were further analysed by Western blot (section 2.5.2) and immunodetection (section 2.5.3) or stained and dried with a Model 543 geldrier (Biorad, Munich). For staining, gels were incubated for 30 min with Coomassie stainer (10% v/v acetic acid, 30% v/v methanol, 0.1% w/v Coomassie brilliant blue R-250) destained for 2-3 h in 10% v/v acetic acid and 30% v/v methanol. Radioactively labelled proteins were detected by digital autoradiographie using the FLA-5100 imaging system (FUJIFILM Life Science). Signals were quantified using the programme Multi Gauge Version 3.2 (FUJIFILM Life Science).

Table 2.7.: Composition of polyacrylamid gels for SDS-PAGE

Component	Resolving gel				Stacking Gel
	16	12.5	10	8	
% Polyacrylamid					
Rotiphorese® Gel30 (37.5:1) [ml]	9	6.9	5.7	4.6	0.83
1.857 M Tris pH 8.8 [ml]	3.5	3.5	3.5	3.5	
0.6 M Tris pH 6.8 [ml]					0.5
10% SDS [μ l]	170	170	170	170	50
aqua bidest [ml]	4.2	6.3	7.5	8.6	3.55
TEMED [μ l]	100	100	100	100	50
10% APS [μ l]	10	10	10	10	10
total Vol.[ml]		17			5

2.5.2. Western blot

For analysis via immunological methods, proteins were immobilized on polyvinylidene difluoride (PVDF) membranes. Proteins separated by SDS-PAGE were transferred to the membrane via semi-dry Western blot (Renart, Reiser and Stark 1979). Gels were applied onto the PVDF membranes between several layers of Whatmann paper (Rotilabo® blotting paper 1 mm, Roth) that was soaked in blotting buffer (20 mM

Tris, 150 mM Glycin, 0.02% SDS, 20% methanol) and proteins were transferred by applying a constant electric current of 1 mA/cm^2 for 90 min. After the transfer, the membranes were stained with Coomassie stainer (section 2.5.1) and analysed by immunodetection.

2.5.3. Immunodetection of immobilized proteins

For immunodetection, the PVDF membranes with immobilized proteins were blocked 45 min in 5% milk powder that was dissolved in DEKO-SALT (50 mM Tris, 150 mM NaCl, 0.05% Tween). Incubation with primary antibodies diluted 1 : 500-1 : 10 000 in DEKO-SALT was carried out for 1 h at room temperature or over night at 4°C . To remove excess antibodies, the membranes were washed three times for 10 min in DEKO-SALT. Incubation with the secondary antibody (peroxidase-coupled anti-rabbit) was carried out for 45 min. After three further washing steps, bound antibodies were detected via a chemiluminescence reaction using the Lumi light^{PLUS} reagent (Roche) according to the manufacturers specifications. Signals were detected by applying a Super RX Medical X-Ray film (FUJIFILM Life Science) or with the LAS-4000 Mini system (FUJIFILM Life Science).

2.5.4. Precipitation of proteins with trichloroacetic acid (TCA)

For the precipitation of proteins in a sample, 1/5 volumes 72% TCA were added to the samples and incubated for 30 min at 4°C . Precipitates were spun down 30 min at 14 000 rpm and 4°C and washed with acetone. After a second 15 min centrifugation step, pellets were dried and resuspended in 1 x Laemmli buffer for SDS-PAGE and Western blot analysis.

2.5.5. Purification of recombinant proteins via affinity tags

2.5.5.1. Purification under native conditions via a deka-histidine-tag

Recombinant proteins that were expressed in *E.coli* cells from pET-plasmids (section 2.4.7) were purified via their histidine or *Strep*-tags respectively. All purification steps were carried out on ice or at 4°C respectively.

Histidine-tagged proteins were purified via Nitrilo-Tri-Acetic-Acid (NTA)-Agarose. Frozen bacteria pellets from 100 ml *E.coli* cultures (section 2.4.7) were thawed 15 min on ice and resuspended in 2 ml lysis-buffer (50 mM Tris/HCl pH 7.4, 100 mM KCl, 5%

Glycerol, 2 mM ATP, 5 mM MgCl₂, 1 mM DTT, 1 x cOmplete EDTA-free Protease Inhibitor Cocktail (Roche) 10 mM imidazole, 1 mg/ml Lysozyme) per gram wet pellet. Cells were lysed for 30 min and sonicated 5-10 times for 10 s on ice with a 10 s cooling period between each burst. Lysates were centrifuged for 20 min at 10 000 x g and supernatants were subjected to Ni-NTA columns using 0.5 ml 50% Ni-NTA slurry in washing buffer (50 mM Tris/HCl pH 7.4, 100 mM KCl, 5% Glycerol, 5 mM MgCl₂, 1 mM DTT, 1 x protease-inhibitor cocktail, 20 mM imidazole) per 1 ml cleared lysate. The columns were incubated for at least 1 h at 4 °C on an end-over-end shaker. After three washing steps with 3 x 2 column volumes washing-buffer, bound proteins were eluted from the column with 4 column volumes elution buffer (50 mM Tris/HCl pH 7.4, 100 mM KCl, 5% Glycerol, 5 mM MgCl₂, 1 mM DTT, 1 x protease-inhibitor cocktail, 20 mM imidazole). Eluates were collected in 500 µl fractions and analysed by SDS-PAGE and Western blot. Fractions with the highest amounts of purified proteins were combined, desalted by centrifugation at 6 000 rpm using centricons (10 000 NMWL, Millipore) and further analysed by FPLC (section 2.5.6).

2.5.5.2. Purification under native conditions via a *Strep*-tag

For the purification of *Strep*-tagged proteins, pellets from 100 ml *E.coli* cultures were resuspended in 5 ml of a buffer composed of 50 mM NaH₂PO₄ pH 8.0, 300 mM NaCl, 5% Glycerol, 5 mM DTT, 1 mg/ml Lysozyme and protease-inhibitors. After 30 min incubation on ice, cells were sonicated 5-10 times for 10 s and subjected to a clarifying centrifugation step as described above. Lysates were applied to a 5 ml Streptactin-Sepharose column and incubated at least 1 h at 4 °C on an end-over-end shaker. Unbound material was removed by rinsing the column with 20 ml washing buffer (50 mM NaH₂PO₄ pH 8.0 300 mM NaCl, 5% Glycerol, 5 mM DTT) and elution was carried out by applying 5 ml washing buffer containing 2.5 mM desthiobiotin. Eluates were collected and desalted as described above and subjected to FPLC analysis.

2.5.6. Fast protein liquid chromatography (FPLC)

Proteins that were purified from *E.coli* cells via Ni-NTA or Streptactin-Sepharose were subjected to size exclusion chromatography. FPLC was carried out with the ÄKTATM FPLCTM system (Amersham/ GE healthcare) using a Sephadex 75 column with 24 ml total volume (V_t). A buffer composed of 30 mM Tris/HCl, pH 7.4,

50 mM KCl, 5% Glycerol and 1 mM DTT was used as running buffer. For FPLC analysis of Zim17 30 μ M ZnSO₄ was added to the buffer. Chromatography runs were programmed and analysed with the UNICORN softwarepackage (GE Healthcare), Version 5.0.

2.5.6.1. Calibration of the Sephadex 75 column

Calibration of the Sephadex 75 column (figure 2.2) was done with the low molecular weight gel filtration calibration kit (GE healthcare) consisting of conalbumin (75 kDa), carbonic anhydrase (29 kDa) ribonuclease A (13.7 kDa) and apronitin (6.5 kDa). The mobile phase volume (void volume) of the column was determined by applying dextran blue, a substance that is not retained by the column material. The k_D value of each protein was calculated using the formular .

$$K_D = V_E - V_0 / V_t - V_0 \quad (2.3)$$

in which V_E , V_t and V_0 are defined as the elution volume, the total bed volume and the void volume of the column. The K_D values of each standard protein were plotted against the logarithm of its molecular weight and the equation of the resulting regression line was used to determine the molecular weight of proteins or protein complexes of unknown size.

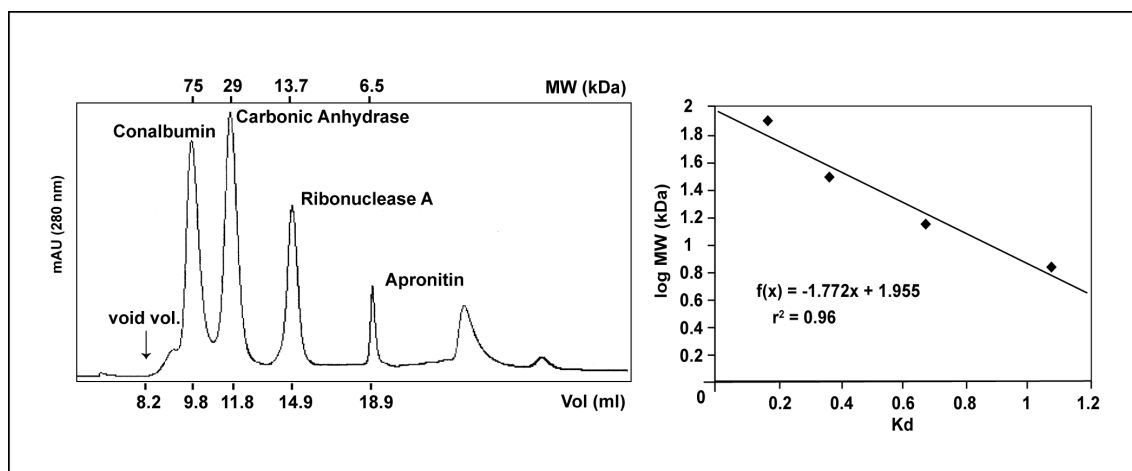


Figure 2.2.: Calibration of the Sephadex 75 column.

2.6. Biochemical *in-vitro* and *in-organello* assays

Biochemical *in-vitro* and *in-organello* assays were intended to analyse specific functions and interactions of proteins with substrates, nucleotides or binding partners in an environment resembling the conditions in a living cell. As not otherwise stated, all experiments were done at 4 °C. Analytical reagent grade chemicals (p.A) and ultrapure water (Millipore quality) were used for all following experiments.

2.6.1. *In-vitro* translation of radiolabelled proteins in reticulocyte lysate

Radioactive labelling of proteins for *in organello* import assays was done with the TNT[®]-coupled reticulocyte lysate systems (Promega). Proteins of interest were either cloned into the Vector pGEM-4Z or directly translated from PCR products by applying primers with a T7-promotorsequence. For a 50 µl translation reaction applying Vector DNA as a template, 25 µl TNT[®] rabbit reticulocyte lysate (Promega, # 4610) were mixed with 2 µl TNT[®] reaction buffer, 2 µl amino acid mixture minus methionine, 1.5 µl 40 U/µl RNAsin and 1 µg circular template DNA. 2 µl [³⁵S]-methionine (EXPRE³⁵S³⁵S Protein Labelling Mix, 2mCi, 74MBq, Perkin Elmer) and 2 µl TNT[®] RNA polymerase (SP6 or T7) were added and the reaction mixture was filled up with RNase-free water to a total volume of 50 µl. For a translation reaction applying PCR products as a template, 40 µl TNT[®] PCR Quick Master Mix were added to 2.5 µl unpurified PCR product and 2 µl [³⁵S]-methionine. RNase-free water was added to a total volume of 50 µl. All reaction mixtures were incubated 90 min at 30 °C for transcription and translation of the precursor proteins. Ribosomes and aggregates in the samples were spun down by a 30 min centrifugation step at 45 000 rpm. Supernatants were mixed with 12.5 µl 2.5% sucrose and analysed by SDS-PAGE and digital autoradiographie. Samples were frozen in liquid nitrogen and stored at -80 °C.

2.6.2. *In-organello* import of radiolabelled precursor proteins

2.6.2.1. Import into respiratory-competent mitochondria

To asses the import efficiency of different mutants, isolated yeast mitochondria were incubated with radiolabelled preproteins in a time-course experiment. As not otherwise stated, the artificial protein Su9(86)-DHFR, that consists of the N-terminal pre-sequence and the first 20 mature residues of the F_o subunit9 of the F₁F_o-

ATPase from *Neurospora crassa* fused to the entire mouse dihydrofolate reductase (DHFR) molecule was used as a model precursor. 50 μg isolated mitochondria per sample were taken and resuspended in p80 import buffer (250 mM sucrose, 10 mM MOPS/KOH pH 7.2, 80 mM KCl, 5 mM MgCl_2) containing 3% w/v BSA (p80_{3%}) to a concentration of 0.25 $\mu\text{g}/\mu\text{l}$. 20 mM Kp_i , 2 mM ATP, 2 mM NADH and 5 mM MOPS/Met (0.2 M MOPS/KOH pH 7.2, 0.1 M methionine) were added. One sample containing 1% (v/v) AVO-Mix (50 μM valinomycin, 800 μM antimycin, 2 mM oligomycin) to disrupt the inner membrane potential was pipetted for control purposes. Depending on the individual translation efficiency, 1-10 μl lysate containing radiolabelled preproteins (section 2.6.1) was added and import reactions were carried out for 20-40 min depending on the experiment. As not otherwise stated, samples containing 50 μg mitochondria were taken at different time points and the import reaction was stopped by addition of 0.5 μM Valinomycin. Samples were put back on ice, divided into halves and subjected to a 15 min treatment with 100 $\mu\text{g}/\mu\text{l}$ proteinase K (PK). The PK reaction was stopped by addition of 100 mM PMSF. Mitochondria were spun down 10 min at 14 000 rpm and washed 1 x with SEM-PMSF (250 mM sucrose, 1 mM EDTA, 10 mM MOPS/KOH pH 7.2). Mitochondrial pellets were resuspended in 20 μl 1 x Laemmli and analysed by SDS-PAGE and digital autoradiography.

2.6.2.2. Import into respiratory-deficient mitochondria

As the membrane potential ($\Delta\Psi$) of respiratory-deficient mitochondria is generally low due to a lack of H^+ ions deriving from oxidative phosphorylation, excess ATP was added to the import reaction to generate an artificial membrane potential. At low levels of protons and high levels of ATP, the $\Delta\Psi$ -dependent ATP-generating reaction that is catalysed by the F_1F_o -ATPase can be reversed by using ATP to generate a proton gradient over the inner mitochondrial membrane. 5 mM ATP, 10 mM CP (creatine phosphate) and 10 $\mu\text{g}/\mu\text{l}$ CK (creatine kinase) were added to the import buffer (section 2.6.2.1). As the proton gradient generated by the reverse ATPase reaction is usually not as strong as the gradient generated by the electron transport reactions of the respiratory chain, the preproteins were denatured in a buffer containing 7 M urea, 30 mM MOPS/KOH pH 7.2 and 1 mM DTT to facilitate the import. Preproteins were added to isolated mitochondria to a final urea-concentration of 2-4% and import reactions were carried out as described above.

2.6.3. Assessment of an inward-directed translocation force ('pulling')

To test the pulling activity of Ssc1, another standard preprotein, $b_2(167)_{\Delta}$ DHFR, was imported into *Zim17_{rc}* mitochondria in the presence of the DHFR ligand methotrexate (MTX). $b_2(167)_{\Delta}$ DHFR consists of the pre-sequence and the first 89 N-terminal residues of the mature cytochrome b_2 fused to the entire mouse DHFR molecule. In contrast to wild type cytochrome b_2 , the fusion protein $b_2(167)_{\Delta}$ DHFR is targeted to the mitochondrial matrix due to a deletion of the intermembrane space sorting signal (amino acids 49 to 65). MTX binds to the DHFR domain of $b_2(167)_{\Delta}$ -DHFR, thereby stabilising its folding state and arresting the preprotein in the import channel. The amino-terminal segment of the preprotein can reach the matrix compartment and interacts with the translocation machinery. When Ssc1 is able to generate an intact inward-directed force ('pulling'), the MTX-stabilised DHFR domain is pulled tightly to the surface of the outer mitochondrial membrane and remains largely resistant to externally added proteases. 25 μ l $b_2(167)_{\Delta}$ DHFR were incubated with 5 μ M MTX for 5 min at 25 °C prior to the import reaction. Import was carried out for 20 min. After the import reaction was stopped by addition of valinomycin, all samples were treated with proteinase K as described above (section 2.6.2.1). To assess the total import rate, one sample omitting the PK treatment was assayed for each mutant. Samples were analysed by SDS-PAGE and digital autoradiography.

2.6.4. Assessment of the Ssc1 folding activity

To estimate the folding capacity of Ssc1, the propensity of the DHFR domain to assume a tightly folded form inside the mitochondrial matrix was utilized in a special assay applying proteinase K. The DHFR domain of Su9(86)DHFR becomes resistant against low amounts of the protease after it has acquired its native conformation in the matrix compartment. Thus, the amount of protease-resistant DHFR domain after import into mitochondria is directly proportional to the folding activity of Ssc1. Radiolabelled Su9(86)DHFR was denatured with 7 M urea as described above (section 2.6.2.2) and imported into isolated *zim17_{rc}* mitochondria at 25 °C. After the import reaction was stopped, mitochondria were washed with SEM-PMSF and lysed in a buffer composed of 0.5% Triton x-100, 30 mM Tris pH 7.4 and 200 mM KCl and 5 mM EDTA with or without 180 μ g/ml proteinase K. Protease resistant proteins were detected by SDS-PAGE and digital autoradiography, quantified and set in relation to the overall amount of imported protein as described in section 2.6.3.

2.6.5. Analysis of protein-interactions by pulldown experiments

2.6.5.1. Ssc1-pulldown with immobilised Zim17

To analyse the interaction of Ssc1 from mitochondrial lysates with immobilized Zim17, 25 µg FPLC-purified Zim17-Strep (section 2.5.5.2 and section 2.5.6) was immobilized on 50 µl 50% Streptactin-Sepharose in solubilization buffer (30 mM Tris/HCl, pH7.4, 50 mM KCl, 5% glycerol, 5 mM MgCl₂, 1 mM Zn-acetate, 1 mM PMSF and 1 x cOmplete EDTA-free Protease Inhibitor Cocktail, Roche) for 1 h at 4 °C. The column was washed 3 times in solubilization buffer, sealed and set aside. 320 µg isolated mitochondria were spun down 10 min at 14 000 rpm and resuspended in a buffer composed of 5 mM MgCl₂ and 20 mM K_pi in p80 buffer containing 0.1% BSA. To create ATP-regenerating conditions, 2 mM ATP, 4 mM NADH and an ATP-regenerating system consisting of creatine phosphate (10 mM CP) and creatine kinase (10 µg/µl CK) that transfers the phosphate group from creatine phosphate to ADP, were added to the reaction. To deplete ATP from the samples, the uncoupler Oligomycin (20 µM) and 0.1 u/µl apyrase, an enzyme that catalyses the hydrolysis of ATP, were used. Samples were incubated for 15 min at 25 °C. Mitochondria were spun down, washed with SEM-PMSF and lysed under native conditions in 300 µl lysis buffer (0.03% Triton-X-100 in solubilisation buffer) with or without 2 mM ATP by pipetting 20 x up and down with a yellow tip. Mitochondrial lysates were incubated 1 h at 25 °C with the prepared Zim17-Sepharose or with empty Streptactin Sepharose as a control. Samples were spun down 2 min at 1 000 x g. The supernatants were removed and the columns were washed 5 times with 100 µl solubilization buffer. Bound proteins were eluted with 25 µl 2 x Laemmli and samples were analysed by SDS-PAGE and Western blot.

2.6.5.2. Ssc1-His pulldown via Ni-NTA

To analyse the binding of Zim17 to Ssc1 in its native environment, pull down His-tagged Ssc1 from mitochondrial lysates were precipitated via Ni-NTA. 200 µg mitochondria were resuspended in p80 buffer containing 0.1% BSA to a concentration of 1 µg/µl. To generate nucleotide-free conditions, Apyrase and Oligomycin were added to the samples in the concentrations described in section 2.6.5.1. Mitochondria were incubated for 15 min at 25 °C, spun down and lysed in 50 µl of a buffer composed of 1% Triton-x-100, 30 mM Tris/HCl, pH7.4, 50 mM KCl, 10% glycerol, 2 mM MgCl₂, 0.5 mM Zn-acetate, 50 mM imidazole, 1 mM PMSF and 1 x cOmplete EDTA-free

Protease Inhibitor Cocktail (Roche). ATP and NADH or Apyrase and Oligomycin were added as described above. Samples were filled up to a volume of 200 μ l with the same buffer and transferred to a 50 μ l Ni-NTA column. After 1 h incubation at 4 °C on an end-over-end-shaker, samples were spun down 2 min at 3 000 rpm and washed 3 times with 100 μ l ATP-free buffer. Bound proteins were eluted from the column with 200 μ l of the same buffer containing 250 mM imidazole. Proteins in the samples were TCA-precipitated and analysed by SDS-PAGE and Western blot.

2.6.6. *In vitro*-analysis of Ssc1 substrate and nucleotide-binding properties

2.6.6.1. Binding of Ssc1 to immobilized ATP

2.6.6.1.1. *Binding of purified Ssc1 to ATP-Agarose*

To assess the ability of the purified Ssc1-His to bind and release nucleotides, 1 μ g protein was diluted 1:10 in a buffer composed of 30 mM Tris/HCl, pH7.4, 50 mM KP_i , pH7.4, 200 mM KCl, 5 mM $MgCl_2$, 5% glycerol, 1 mM PMSF and 1 x cComplete EDTA-free Protease Inhibitor Cocktail, Roche. The protein suspension was subjected to 25 μ l ATP-Agarose (Sigma) and incubated for 90 min at room temperature on an end-over-end shaker. Samples were spun down for 1.5 min at 7 000 rpm and washed 3 times with 200 μ l buffer. Bound proteins were eluted by a 30 min incubation at room-temperature in the same buffer containing 2 mM ATP followed by a second elution step with 25 μ l 2 x Laemmli. All fractions were collected, TCA-precipitated and analysed by SDS-PAGE and western blotting.

2.6.6.1.2. *Binding of Ssc1 from isolated mitochondria to ATP-Agarose*

To test the nucleotide-binding properties of native Ssc1, 50 μ g mitochondria were spun down and resuspended in lysis buffer (100 mM KCl, 100 mM NaCl, 50 mM KP_i , pH7.4, 5 mM $MgCl_2$, 0.1% Trito-X-100, 5% glycerol, 1 mM PMSF and 1 x cComplete EDTA-free Protease Inhibitor Cocktail). Samples were subjected to ATP-Agarose and incubated 90 min at room-temperature followed by 3 washing steps applying the same buffer. Bound proteins were eluted with 2 x Laemmli.

2.6.6.2. Binding of Ssc1 to immobilized model substrate

2.6.6.2.1. *Preparation of reduced carboxy-methylated α -lactalbumin (RCMLA)*

To generate the permanently unfolded Ssc1 model substrate reduced carboxy-methylated α -lactalbumin (RCMLA), 10.5 mg (1.3 mM α -lactalbumin were incu-

bated in 1 ml reducing buffer (200 mM Tris/HCL, pH 8.7, 7 M guanidinium-chloride, 20 mM DTT, 2 mM EDTA for 90 min at room temperature. Iodoacetic acid was added to a final concentration of 100 mM and the protein was further incubated for 20 min under dark room conditions. The reaction was quenched with an excess of reduced glutathione (0.2 M reduced glutathione in 200 mM 0,2 M Tris, pH 7.5). The sample was dialysed against 20 mM KP_i , pH 7.5 using a SpectraPor Dialysis Membrane (MWCO 8000, Spectrum Labs) and applied to cyanogenbromide-activated sepharose.

2.6.6.2.2. Coupling of RCMLA to Cyanogen bromide (CNBr)-activated Sepharose

0.5 g activated Sepharose (Cyanogen bromide-activated-Sepharose[®] 4B, Sigma) were suspended in 1 mM HCl on a glass filter. Sepharose was washed by repeated rinsing with a total volume of 100 ml 1 mM HCl and transferred into a fresh 15 ml Falcon tube. 10 mg RCMLA were added in a volume of 2.5 ml coupling buffer (0.1 mM $NaHCO_3$, pH 8.3, 0.5 M NaCl) and incubated 2 h at room temperature in an end-over-end shaker. Sepharose beads were washed 1 x with coupling buffer and residual active sites were blocked by 2 h incubation at room temperature in 0.1 M Tris/HCl pH 8.0. Beads were washed three times in 0.1 M sodium acetate, pH 4.0 and subsequently three times in a buffer composed of 0.1 M Tris/HCl pH 8.0 and 0.5 M NaCl. The RCMLA-Sepharose was stored in 0.1% sodium azide.

2.6.6.2.3. Binding of Ssc1 from isolated mitochondria to RCMLA-Sepharose

To analyse the binding of Ssc1 to RCMLA-sepharose, isolated mitochondria were activated by a 15 min incubation in a buffer consisting of 20 mM Kp_i pH 7.4, 3 mM ATP and 3 mM NADH in p80 buffer containing 3% BSA. Mitochondria were collected by 10 min centrifugation at 14 000 rpm for 10 min and immediately resuspended in lysis buffer (section 2.6.6.1.2). Samples were incubated with 50 μ l 1:3 RCMLA-Sepharose in lysis buffer for 60 min at room temperature, washed 3 times and eluted with 3 mM ATP in the same buffer. Total and elution fractions were TCA-precipitated and analysed by SDS-PAGE and Western blot.

2.6.7. Aggregation assay

Mitochondria were centrifuged and lysed with 1 μ l of a buffer composed of 30 mM Tris, pH 7.5, 200 mM KCl, 5 mM EDTA; 0.5% Triton; 5 mM PMSF and 1 x cOmplete EDTA-free Protease Inhibitor Cocktail per μ g mitochondria. A 25 μ l total-sample

was taken and the remaining lysate was subjected to a high-velocity spin at 125 000 x g for 30 min at 4 °C. Supernatants were removed and 25 µl were taken as a sample for SDS-PAGE. The pellets were re-extracted by vigorous shaking with 100 µl lysis buffer and then centrifuged again at 125 000 x g for 30 min at 4 °C. The supernatants were discarded. Total, supernatant, and pellet samples were analysed by SDS-PAGE, Western blot and incubation with specific antibodies. To assess the aggregation of newly imported mtHsp70s, radiolabelled Ssc1 was imported into isolated mitochondria. The import reaction was stopped after 15 min by addition of valinomycin. Mitochondria were re-isolated, treated with proteinase K as described in section 2.6.2.1 and subjected to the aggregation assay as described above. Samples were analysed by SDS-PAGE and digital autoradiography.

2.6.8. Assessment of Aconitase activity

To determine enzymatic activity of aconitase in mitochondrial lysates, isolated mitochondria were centrifuged and lysed in homogenisation buffer (50 mM Tris pH 7.4 and 0.2% laurylmaltoside). Mitochondrial lysates were then added to 1.4 ml quartz cuvettes containing 1 ml of pre-warmed (30 °C) reaction buffer (50 mM Tris pH 7.4 5 mM sodium citrate; 0.6 mM MnCl₂, 0.2 mM NADP⁺) followed by thorough mixing. After addition of 0.1 mg/ml isocitrate dehydrogenase, the aconitase activity was measured in a GeneSys 10s UV-Vis Spectrophotometer (Thermo Scientific) by following the increase in NADPH.

2.6.9. Assessment of the mitochondrial inner membrane potential $\Delta\Psi$

The electric membrane potential ($\Delta\Psi$) of isolated mitochondria was assessed by use of the potential-sensitive fluorescent dye 3,3'-dipropylthiadicarbocyanine iodide (diSC₃(5)) as described Waggoner (1976). Measurements were performed with a fluorescence spectrometer (Aminco-Bowman) at 25 °C (excitation at 622 nm, emission at 670 nm) in a buffer composed of 0.6 M sorbitol, 0.1% (w/v) bovine serum albumin, 10 mM MgCl₂; 20 mM KP_i, pH 7.4; 5 mM malate; 10 mM glutamate.

2.7. List of primers and oligonucleotides

Table 2.8.: List of primers and oligonucleotides used in this work

oligonucleotide	sequence
pDB10-IL1-f	5'-CTG TTG CCG GTT CTT CTG GT-3'
pDB10-IL1-r+rbs	5'-TTT CAT ATG ATA CCT CCT GGA TTA TGC GGC CGT GTA CAA-3'
pDB10-IL2-r	5'-TTT CAT ATG CGC AAG CTT AGT GAT GAT GA-3'
pIL4-C78S-f	5'-GCA AGA AAT CTA ACA CCC GAT CGT CAC ACA-3'
pIL4-C78S-r	5'-TGT GTG ACG ATC GGG TGT TAG ATT TCT TGC-3'
pIL4-C100S-f	5'-GAA AGG TAC CGT CTT GAT CTC TTC TCC GCA CTG-3'
pIL4-C100S-r	5'-CAG TGC GGA GAA GAG ATC AAG ACG GTA CCT TTC-3'
pIL4-Zim17-f	5'-GGG AAT TGT GAG CGG ATA AC-3'
pIL4-Zim17-r	5'-TAA AGC TGC GCT AGT AGA CG-3'
gen-Zim17-f	5'-GGC GCC ACC ATG ATT CCG AGG ACT AGA AC-3'
gen-Zim17-r	5'-TCA TTT CTG GGA AAG GGT GAA GG-3'
Zim17-corrWT-f	5'-TAG CAG AAG CCC TGC GAG TA-5'
Zim17-corrWT-r	5'-GCG AAG CTT AGC ACA GCC CTC TTC CTC TT-3'
A1-fw	5'-ACG-TGT-GCC GTA CTC TAC CC-3'
A1b-fw	5'-TCA CCT GCA AGA AAT GTA ACA CC-3'
A2-rev	5'-AAT CTT CTG CTG GTT ATC GC-3'
B1-fw	5'-GCG ATA ACC AGC AGA AGA TTA GAT TGT ACT GAG AGT GCA C-3'
B2-rev	5'-CTG TGC GGT ATT TCA CAC CG-3'
C-rev	5'-TGC GGT TCA ACT TTT CAT ATC TAG CAG TGG CTC ATC TTT ATG TAC TCT AGT CCT ACT GTG CGG TAT TTC ACA CCG-3'
K-fw	5'-ATG ATT CCG AGG ACT AGA ACA-3'
K-rev	5'-GGT TGA CCC TAT CGC CAC TA-3'

2.8. List of antisera

Table 2.9.: Antisera used in this study

Antiserum	internal number	dilution	origin
AcoI	945	1:20 000	G
Cit1	208	1:1 000	F
CoxIV	577	1:500	G/F
GroEL	80322	1:1 000	M
Isu1	724	1:500	G
Jac1	228	1:500	F
Mge1	23210	1:1 000	W
Mdh1	1088	1:1 000	G
Mdj1	121	1:1 000	F
mrpL40	-	1:500	K
Pam18	752	1:500	G/F
Rip1	543	1:1 000	G/F
Sod2	1051	1:1 000	G
Ssc1	41756	1:5 000	M
Ssq1	213	1:1 000	F
Tim23	133	1:1 000	F
Tim44	128	1:1 000	F
Tom40	168	1:1 000	F
Zim17	554	1:500	G/F

Antisera were kindly provided by:

F = AG Pfanner, University of Freiburg, Germany; M = AG Neupert, Ludwig Maximilians-University, Munich, Germany; W = E. Craig, University of Wisconsin-Madison, Wisconsin, USA; K = S. Gruschke, University of Kaiserslautern, Germany

G = Antisera purchased from Gramsch Laboratories, Schwabhausen, Germany

2.9. List of chemicals

AMS BIO, ABINGDON, UK

zymolyase 20T

FUJIFILM LIFE SCIENCE, DÜSSELDORF

Super RX Medical X-Ray film

MP BIO, ESCHWEGE

CSM -Leu, CSM -Leu/-Trp, CSM -URA

QIAGEN, HILDEN

Ni-NTA-Agarose, Strep-Tactin Superflow

ROCHE, MANNHEIM

adenosine triphosphate (ATP), cOmplete EDTA-free Protease Inhibitor Cocktail, creatine kinase, creatine phosphate, Lumi Light^{PLUS} Western blotting substrate

ROTH, KARLSRUHE

acetic acid, ammonium acetate, ammonium persulfate (APS), bacto peptone, bovine serum albumine, bromophenol blue, calcium chloride, Coomassie brilliant blue R-250, dextrose (glucose), dipotassium phosphate, dithiothreitol, dodecyl- β -D-maltoside (laurylmaltoside), ethylenediaminetetraacetic acid (EDTA), ethanol, L-glutamic acid (glutamate), glycerol, guanidinium chloride, hydrogen chloride, imidazole, iodoacetic acid, isopropyl- β -D-1-thiogalactopyranoside (IPTG), lysozyme, magnesium chloride, DL-malic acid (malate), manganese(II) chloride, methanol, β -mercaptoethanol, 3-(N-morpholino)propanesulfonic acid (MOPS), nicotinamide adenine dinucleotide phosphate (NADPH and NADP⁺), PEG-4000, potassium acetate, potassium chloride, potassium dihydrogen phosphate, 2-propanol, Rotilabo[®] blotting paper 1 mm, Rotiphorese[®] Gel30, Roti[®]-phenol/ chloroform/ isoamylalcohol, Roti[®]-PVDF, sodium acetate, sodium azide, sodium chloride, sodium citrate, sodium dihydrogen phosphate, sodium dodecyl sulfate, sodium hydrogen carbonate, sodium hydroxide, sorbitol, dialysis membrane SpectraPor 7 MWCO 8000, sucrose, sulfuric acid, trichloroacetic acid, Tris, Triton-X-100, tryptone, Tween-20, xylene cyanol, yeast

extract, yeast nitrogen base, zinc acetate, zinc sulfate

SIGMA, ST. LOUIS, MISSOURI, USA

antimycin A, apyrase from potato, 5'ATP-Agarose 4B, Cyanogen bromide-activated-Sephrose[®] 4B, D-desthiobiotin, 3,3'-dipropylthiadicarbocyanine iodide, glutathione, oligomycin, peroxidase conjugate-goat anti-rabbit IgG, valinomycin

THERMO SCIENTIFIC, WALTHAM, MASSACHUSETTS, USA

Phusion High-Fidelity DNA Polymerase

2.10. List of kits

ANALYTIK JENA, JENA

innu PREP Gel Extraction Kit

GE HEALTHCARE, MUNICH

Low molecular weight Gel filtration calibration Kit

PROMEGA, MANNHEIM

TNT[®]-coupled Reticulocyte Lysate System

ROCHE, MANNHEIM

Rapid DNA Dephos & Ligation Kit

STRATAGENE, LA JOLLA, CALIFORNIA, USA

StrataClone blunt PCR cloning Kit

THERMO SCIENTIFIC, WALTHAM, MASSACHUSETTS, USA

Fermentas GeneJET[®] Plasmid Mini and Midiprep Kits, PHUSION high fidelity PCR Kit

2.11. List of laboratory instruments

ANALYTIK JENA, JENA

Bio doc analyze Biometra System and associated software, Thermomixer TMix

BECKMAN COULTER, KREFELD

Avanti[®] J-E centrifuge; Rotors: JA-10, JA-25.50

BIOMETRA, GÖTTINGEN

Thermocycler (Trioblock)

BIORAD, MUNICH

Model 534 Gel drier

EPPENDORF, HAMBURG

BioPhotometer plus, Centrifuge 5417-R, Centrifuge 5804-R; Rotors: A-4-44, F-34-6-38, New Brunswick Scientific innova[®] Incubator shaker series, Thermomixer comfort series

FUJIFILM LIFE SCIENCE, DÜSSELDORF

FLA-5100 imaging system and associated software, LAS-4000 Mini system and associated software

GE HEALTHCARE, MUNICH

Amersham ÄKTATM FPLCTM system and Sephadex 75 column

THERMO SCIENTIFIC, WALTHAM, MASSACHUSETTS, USA

Aminco-Bowman fluorescence spectrometer, GeneSys 10s UV-Vis Spectrophotometer, Varioklav[®] steam sterilizer

2.12. List of software

ADOBE, SAN JOSE, CALIFORNIA, USA

Adobe Illustrator CS2 and CS3, Adobe Photoshop CS6

APPLE, CUPERTINO, CALIFORNIA, USA

MAC OS X 10.6 Snow Leopard

FUJIFILM LIFE SCIENCE, DÜSSELDORF

Multi Gauge Version 3.2

GE HEALTHCARE, MUNICH

UNICORN softwarepackage; Version 5.0

GRAPHPAD SOFTWARE, INC., LA JOLLA, CALIFORNIA, USA

GraphPad Prism; Version 5

MICROSOFT, REDMOND, WASHINGTON, USA

Microsoft Office 2010, Windows 7 Home Premium

FREE AND OPEN SOURCE SOFTWARE

BioEdit Sequence alignment editor, Gimp Version 2.0, Libre Office 3.5.7.2, Linux (Fedora 17 and 18), Mendeley Desktop Version 1.7.1, Serial Cloner Version 2.5, LaTeX (TeX Live pdfTEX Version 3.14)

3. Results

3.1. Co-purification and *in vitro* analysis of recombinant Ssc1 and Zim17

Zim17 is known to maintain the function of Hsp70 chaperones in mitochondria of *S. cerevisiae*, most likely by preventing their aggregation in the mitochondrial matrix. Deletion of *ZIM17* in yeast cells leads to severe growth defects such as temperature-sensitivity and respiratory deficiency, underlining its importance for the functional integrity of mitochondrial Hsp70 systems. Because of the innate tendency of mtHsp70 proteins to aggregate (Blamowska 2010), Ssc1, the main Hsp70 chaperone in the matrix of yeast mitochondria, is prone to form inclusion bodies upon its recombinant expression in *E. coli* cells. As the aggregation is impeding its purification under native conditions, recombinant Ssc1 has to be purified from yeast mitochondria - a time consuming process with generally low yields of protein. Due to its aggregation-preventive character, Zim17 was co-expressed with Ssc1 in *E. coli* cells to allow a more efficient purification of the fully functional chaperone.

3.1.1. Co-expression of Ssc1-His and Zim17-Strep in *E. coli*

3.1.1.1. Generation of the expression vectors pLL1 and pLL2

The plasmid pDB10 (D. Becker, unpublished results) was used for the recombinant expression of Ssc1 and Zim17 in *E. coli* cells. pDB10 derives from the vector pETDuet-1 (Novagen). The original pETDuet-1 plasmid contains two multiple cloning sites (MCS1 and MCS2) for the co-expression of proteins in *E. coli* cells (section A.2.1). In case of pDB10, a copy of the *SSC1* gene with a C-terminal 10-histidine tag and a copy of the *ZIM17* gene with a C-terminal Strep tag were cloned into MCS1 and MCS2 via the NcoI/HindIII (MCS1, *SSC1*) and NdeI/XhoI (MCS2, *ZIM17*) restriction sites respectively (section A.1.1). Expression of Ssc1-His and Zim17-Strep from pDB10 in the *E. coli* strain BL21cp resulted in a high overexpression of Zim17-Strep while

the expression levels of Ssc1-His were low (figure 3.1, lane 2). In attempt to gain comparable amounts of Ssc1 and Zim17, the original pDB10 plasmid was altered to reduce the amounts of expressed Zim17. MCS1 and MCS2 of the pETDuet-1 vector contains two separate T7 promoters, each followed by a ribosome binding site. The T7-promotor of MCS2 was removed by a restriction digest employing the enzymes MfeI and NdeI to generate a single mRNA encoding both the *SSC1* and the *ZIM17* genes. The MfeI restriction site is located in the *SSC1* coding sequence 311 nucleotides upstream of the stop codon while the NdeI restriction site lies at the 5'end of the *ZIM17* insert. The 311 nucleotides at the 3'end of *SSC1*-His that were removed by the digest were amplified using the primer pair pDB10-IL1-f and pDB10-IL1+rbs-r (table 2.8). The PCR product was digested with MfeI and NdeI and re-inserted into the plasmid (section A.1.1). A new ribosome binding site upstream of the *ZIM17*-gene was added via the reverse primer pDB10-IL1+rbs-r that contains a Shine Dalgarno sequence (5'-AGGAGG-3'). In a second approach, the reverse primer pDB10-IL2-r without the Shine Dalgarno sequence was used, resulting in the plasmid pIL2 that lacks both the T7 promoter and the ribosome binding site of MCS2. pIL1 and pIL2 were transformed into *E. coli* BL21cp cells and protein expression was induced by IPTG. A Western blot analysis of *E. coli* cell lysates showed that in case of pIL1 the expression levels of Zim17-Strep were similar to its expression levels when the plasmid pDB10 was used. In case of pIL2 the expression levels of Zim17-Strep were considerably reduced and comparable to the levels of Ssc1-His (figure 3.1, lanes 6 and 10). However, a third translation product with a size of approximately 21 kDa (Zim17*) occurred during the expression from pIL2. Zim17* is translated from an additional ATG close to the 3'end of the *SSC1* gene that is in frame with the *ZIM17* insert. Zim17* thus represents a Zim17 protein with a 25 amino acid extension at its N-terminus (see section A.1.1). A solubility test showed that 100% of the Zim17*-artefact was found in a nonsoluble, aggregated form (figure 3.1, lanes 11 and 12). It therefore can be assumed that Zim17* is most likely non-functional and does not interfere with Zim17 or Ssc1 in the *E. coli* cell.

3.1.1.2. Limited Ssc1 solubility in *E. coli* in the presence of Zim17

To assess the aggregation behaviour of the co-expressed proteins in the cytosol of *E. coli*, cells were collected, lysed and inclusion bodies were separated from soluble proteins by centrifugation at 14 000 rpm as described in section 2.6.7. Samples were analysed via SDS-PAGE and Western blot followed by immunodecoration with

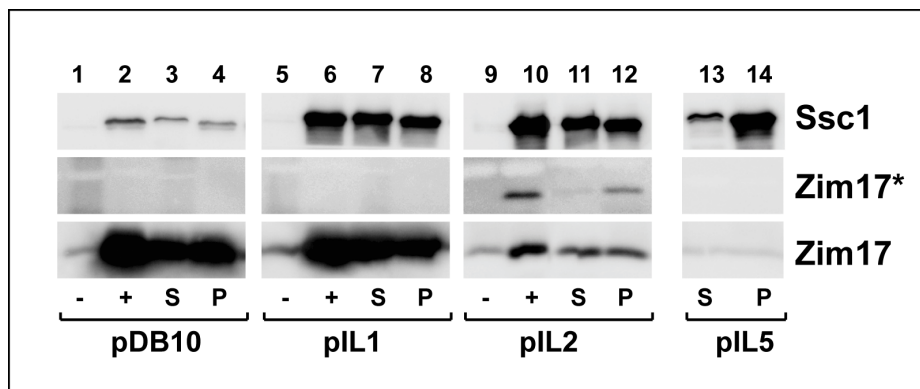


Figure 3.1.: Expression levels of Ssc1-His and Zim17-Strep in *E. coli*. Zim17-Strep and Ssc1-His were expressed in *E. coli* cells from the vectors pDB10, pIL1, pIL2 and pIL5. Cells were lysed and soluble material was separated from insoluble inclusion bodies by a high velocity centrifugation step. Cell extracts before (-) and after (+) induction of protein expression with IPTG, supernatant (S) and pellet (P) fractions were analysed via SDS-PAGE, Western blot and decoration with antibodies against the indicated proteins. **Zim17*** = Zim17-artefact derived from an additional ATG in the SSC1-His gene (see text).

specific antibodies against Zim17 and Ssc1. To compare the aggregation behaviour of Ssc1 in the presence of Zim17 to its aggregation behaviour in the absence of Zim17, the plasmid pIL5 that was generated by cloning Ssc1 into the vector pET28 (Novagen) was used as a control. Upon expression in *E. coli* BL21cp from pIL5, almost 100% of the soluble fraction of Ssc1 was found in insoluble inclusion bodies (figure 3.1, pIL5, lane 13 and 14). Approximately 50% of the recombinant Ssc1 aggregated in all three *E. coli* strains that were co-expressing Ssc1-His and Zim17-Strep (figure 3.1, pIL1, pIL2 and pDB10, lanes 4, 8, 12), even in the presence of saturating amounts of Zim17 (pIL2, figure 3.1, lanes 3, 4, 7, 8, 11, 12). Similarly, about 50% of Zim17-Strep was found in the form of insoluble aggregates (inclusion bodies). In summary, only a part of the total Ssc1 amount was efficiently protected from aggregation upon its co-expression with Zim17 in the cytosol of *E. coli* cells.

3.1.2. Purification and FPLC analysis of Ssc1-His in the presence of Zim17

To examine the interaction between Ssc1 and Zim17 more closely and to gain highly purified proteins for further *in vitro* assays, Ssc1-His was purified and analysed via FPLC (section 2.5.6). After co-expression from pIL1 and pIL2 in *E. coli* BL21cp, cells were lysed and applied to Ni-NTA-Agarose. Subsequent FPLC analysis of the purified Ssc1-His using a Sephadex75 column was performed by W. Tomberg at the Institute for Biochemistry and Molecular Biology in Bonn.

3.1.2.1. FPLC analysis in presence of high Zim17 amounts

When expressed from pIL1, Ssc1 and Zim17 eluted at volumes corresponding to molecular weights of approximately 90.3 and 30.6 kDa (figure 3.2 A). A Western blot analysis showed that the fraction that eluted at a volume corresponding to a molecular weight of 90.3 kDa contained a mixture of Ssc1 and Zim17 (figure 3.2 B, lanes 1-3). Zim17, together with small amounts of remaining Ssc1, was detected in the fractions containing a protein species of 30.6 kDa (figure 3.2 B., lanes 4-6). As this molecular weight represents the mass of approximately two Zim17 molecules, the results strongly suggest that Zim17 might occur as a dimer during its interaction cycle with Ssc1. In support of this idea, decoration with the Zim17 antibody showed a second Zim17 signal at a size of approximately 36 kDa in all Ssc1-containing fractions, probably representing remaining dimers in the samples that were not solubilized by the SDS in the Laemmi buffer. However, the calculated molecular weight of 90.3 kDa in the Ssc1-containing fractions corresponds to the molecular weight of an Ssc1 molecule with only a single Zim17 molecule attached, implying that Zim17 interacts with Ssc1 in its monomeric form. A third peak at a molecular weight of 8.3 kDa (figure 3.2 B, lanes 7-10) most likely represents the translation-product deriving from one of the in-frame ATG codons in the Zim17 sequence (section A.1.1). Monomeric Zim17 was also detected in these fractions, probably due to an overload of the column.

3.1.2.2. FPLC analysis in presence of low Zim17 amounts

In case of pIL2, the expression levels of Zim17 are much lower than in case of pIL1 and thus more likely to resemble the *in vivo* situation in yeast mitochondria. When expressed from pIL2, two main peaks corresponding to molecular weights of 92.6 and 7.6 kDa were observed in the FPLC (figure 3.3 A). In a Western blot analysis, both Ssc1 and Zim17 were detected in the fractions that eluted at a volume corresponding to a molecular weight of 92,6 kDa (figure 3.3 B, lanes 1-6) while hardly any Zim17 remained in the fractions containing a protein species of 7.6 kDa. These results are in consistence with the observations made for pIL1. A third peak, that eluted at a volume corresponding to a molecular weight 29 kDa and thus most likely represents a dimeric form of Zim17 (section 3.1.2) was hardly visible. In a Western blot analysis of the appendant fractions, Zim17 and remaining Ssc1 were detected (figure 3.3 B, lanes 7-10). While the Ssc1 signal most likely derives from a column overload, the low

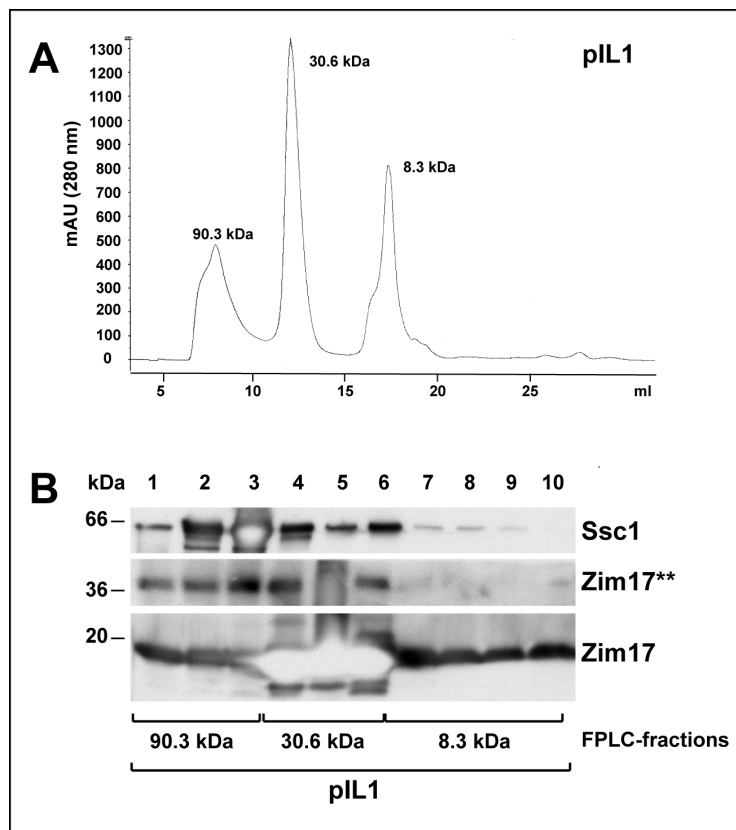


Figure 3.2.: FPLC analysis of Ssc1 in the presence of high Zim17 amounts. FPLC analysis of Ssc1-His purified from pIL1. **(A)** FPLC result **(B)** Western blot analysis of the FPLC fractions. 1 μ g protein from protein-containing FPLC fractions were applied on a 15% SDS-Gel and analysed via Western blot and incubation with antibodies against Zim17 and Ssc1. Due to an overexposure, parts of the Zim17 signal appear as a white area. ** putative Zim17-dimer.

abundance of dimeric Zim17 supports the theory that the cochaperone interacts with Ssc1 in its monomeric form while it tends to form dimers in solution. In contrast to pIL1, where Zim17 was expressed in saturated amounts and a large moiety of its unbound form remained, almost all Zim17 was associated with Ssc1 molecules when the proteins are co-expressed from pIL2.

3.1.2.3. ATP-binding properties of FPLC-purified Ssc1

To test the functionality of the purified recombinant Ssc1, its ability to interact with ATP was determined. FPLC-purified Ssc1 expressed from pIL1 was taken and bound to immobilized ATP as described in section 2.6.6.1.1. Bound protein was washed from the column with excess ATP followed by a second elution step with Laemmli buffer to remove all remaining proteins from the column. Samples were analysed via SDS-PAGE, Western blot and subsequent incubation with antibodies against Ssc1. Approximately 50% of the total amount of applied Ssc1 was bound to the immobilized ATP confirming that its general ability to interact with nucleotides remained (figure 3.4). However, while Ssc1 could be eluted from the column with

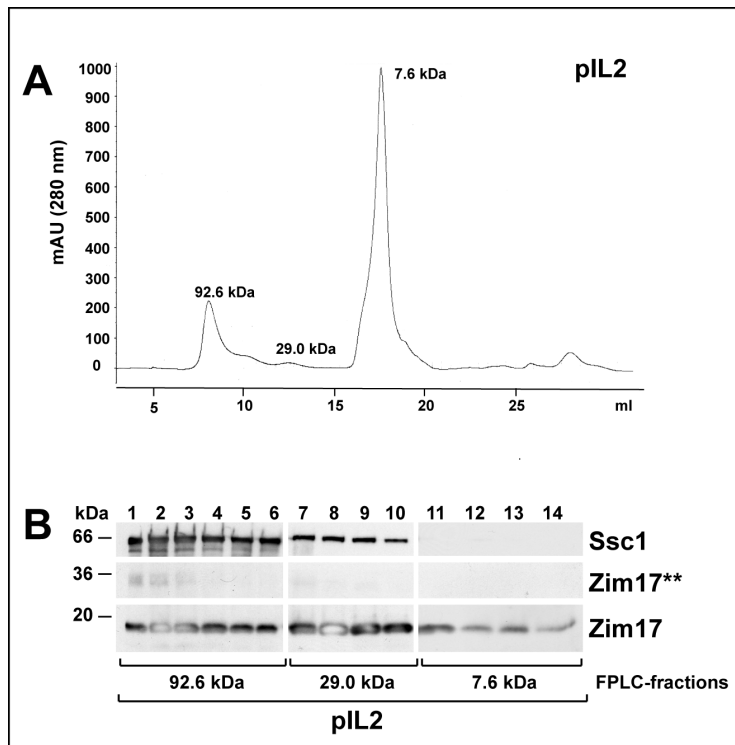


Figure 3.3.: FPLC analysis of Ssc1 in the presence of low Zim17 amounts. FPLC analysis of Ssc1-His purified from pLL1. **(A)** FPLC result **(B)** Western blot analysis of FPLC fractions. 1 μ g protein from protein-containing FPLC fractions was applied on a 15% SDS-Gel and analysed via immunoblotting with antibodies against Zim17 and Ssc1.

Laemmli buffer, the chaperone kept stably associated with the immobilized nucleotides when an elution step with excess ATP was performed, indicating a diminished ability to hydrolyse ATP or to release ADP from its nucleotide binding pocket after hydrolysis. Furthermore, it was noted that a subset of the copurified Zim17 stayed attached to the Hsp70 chaperone during its interaction with the immobilized nucleotides.

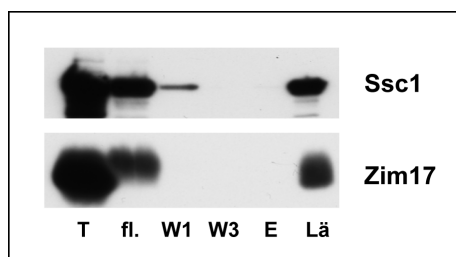


Figure 3.4.: ATP-agarose assay with purified Ssc1 Ssc1 was expressed in *E. coli* from pLL1 and purified via Ni-NTA and FPLC. 1 μ g total protein taken from FPLC-fraction A6 (figure 3.1) was bound to 100 μ l immobilized ATP. **T** Total, **fl.** flow through, **W1/W3** washing steps 1 and 3, **E** elution with excess ATP, **Lä** elution with Laemmli

3.1.3. Purification and FPLC analysis of Zim17-Strep

Even after a purification via FPLC, Zim17 and Ssc1 could not be totally separated from each other. To obtain highly purified Zim17, an *E. coli* expression vector that solely carried the *ZIM17* gene was generated. *ZIM17*-Strep was taken from pDB10

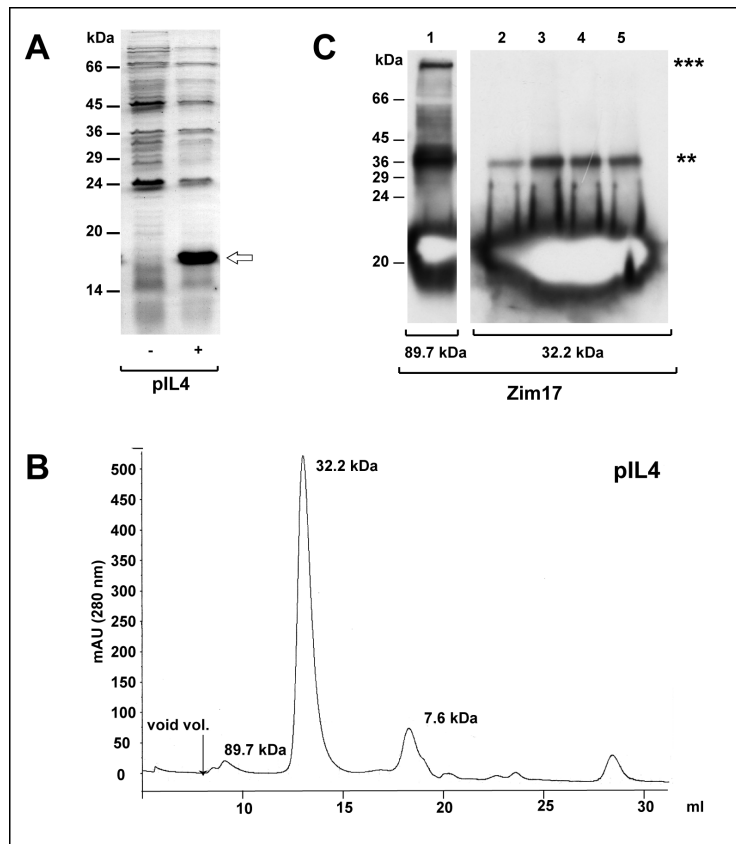


Figure 3.5.: FPLC analysis of Zim17. FPLC analysis of Zim17-Strep purified from pIL4. **(A)** Coomassie-stain of *E. coli* BL21cp-cell extracts before (-) and after (+) induction of protein expression from pIL4 with IPTG. Overexpressed Zim17-Strep is indicated by an arrow. **(B)** FPLC result **(C)** Western blot analysis of FPLC fractions. 1 μ g protein from protein-containing FPLC fractions was applied on a 15% SDS-Gel and analysed via immunoblotting with an antibody against Zim17. ** putative Zim17-dimers *** putative Zim17-multimers.

and cloned into MCS1 of the empty pETDuet plasmid via the NdeI/XhoI restriction sites resulting in the plasmid pIL4. After expression in the *E. coli* strain BL21cp (figure 3.5 A) Zim17 was purified via StrepTactin-Sepharose and an FPLC analysis was performed as described above. In consistence with the observations described above (section 3.1.2.1) Zim17 eluted as a dimer at a volume corresponding to a molecular weight of 32.2 kDa. Additionally, two small peaks corresponding to 89.7 and 7.6 kDa were detected (figure 3.5 B). Western blot analysis and incubation with a Zim17 specific antibody showed signals at the size of its monomeric (17 kDa) and dimeric form (34 kDa) in the elution fractions that contained a protein species of approximately 32.2 kDa (figure 3.5 B, lanes 2-5). The elution of a protein species with an approximate molecular weight of 89.7 kDa probably derives from an interaction of Zim17 with the *E. coli* Hsp70 protein DnaK. In a Western blot analysis of these fractions, monomers, dimers and potential multimers with a molecular weight >100 kDa were detected by the Zim17 antibody, the latter probably representing an aggregated form of the protein.

3.1.4. Nucleotid-dependency of the Zim17-Ssc1 interaction

The interaction of Hsp70 proteins with most of their cochaperone binding partners is dependent on their nucleotide binding state. It has been shown that Zim17 interacts with Ssc1 most likely in its nucleotide-free form (Sichting 2005). However, when purified Ssc1 was applied to ATP agarose, Zim17 was found in the elution fractions, indicating that it is also able to interact with Ssc1 in the presence of nucleotides (figure 3.4, section 3.1.2.3). To assess the dependence of the Zim17 interaction on the ATP binding state of Ssc1 in more detail, two different approaches of binding experiments with native Ssc1 obtained directly from mitochondrial lysates were performed.

3.1.4.1. Ssc1 interacts with immobilized Zim17 preferably in the absence of ATP

Ssc1-free Zim17-Strep that was purified upon expression from pIL4 was immobilized on a Streptacin sepharose column. 300 µg mitochondria isolated from the wild type yeast strain PK 82 were incubated for 20 min at 37 °C under ATP-depleting or ATP-regenerating conditions. To deplete ATP from the samples the uncoupler oligomycin and the enzyme apyrase were added. ATP regenerating conditions were provided by addition of creatine kinase and its substrate creatine phosphate (section 2.6.5.1). Mitochondrial lysates were prepared under native conditions in a Triton-X100 containing buffer as described in section 2.6.5.1 and subjected to the immobilized Zim17. Proteins in the total and elution fractions were TCA precipitated and analysed via SDS-PAGE, Western blot and incubation with specific antibodies as shown in figure 3.6 lane 5. Ssc1 seemed to interact with Zim17 preferably at ATP-free conditions, while the binding to Zim17 in the presence of ATP was indistinguishable from its binding to an empty Streptactin column (lanes 3 and 6). However, the possibility that Ssc1 interacts with the immobilized Zim17 in a substrate-like manner, cannot be excluded.

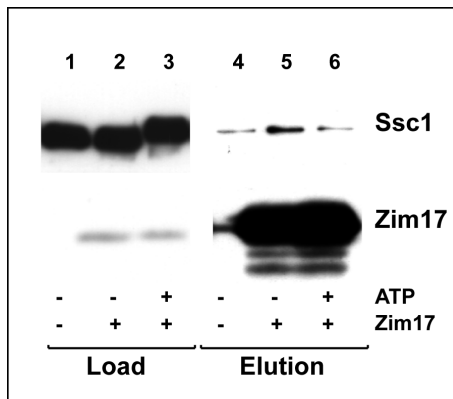


Figure 3.6.: Binding of Ssc1 to immobilized Zim17. 25 μ g FPLC-purified Zim17-Strep (figure 3.5) were immobilized on 50 μ l Streptacin sepharose. The binding of Ssc1 from mitochondrial lysates was assayed in the presence (lanes 2 and 5) and absence (lanes 3 and 6) of nucleotides. Proteins were eluted from the column with Laemmli buffer and analysed via immunoblotting with antibodies against Zim17 and Ssc1. Zim17-free Streptactin was used as a control (lanes 1 and 4).

3.1.4.2. Ssc1 interacts with Zim17 *in organello* in the absence of ATP

To assess the interaction of Ssc1 with native amounts of Zim17 *in organello*, isolated mitochondria of an *S. cerevisiae* strain carrying a copy of the *SSC1* gene with a C-terminal histidine tag were subjected to a Ni-NTA column as described in section 2.5.5.1. Before lysis, all mitochondria were pretreated 15 min at 25 °C under ATP-depleting or ATP-regenerating conditions as described above. As the zinc-binding properties of Zim17 make it prone to interact with the Ni-NTA itself, high concentrations of imidazole (50 mM) were used in the washing steps to elute unspecifically bound protein from the column. As a control, mitochondria of the *S. cerevisiae* PK 82 wild type strain were used to exclude an unspecific binding of Zim17 to the Ni-NTA matrix. Proteins in the elution fractions were precipitated with TCA and subjected to SDS-PAGE and Western blot analysis followed by incubation with specific antibodies against Ssc1 and Zim17. Immunoblotting with antibodies against the Ssc1 cochaperones Mdj1 and Mge1 was carried out as positive controls. While the binding of Ssc1 to the nucleotide exchange factor Mge1 is known to be diminished by the addition of nucleotides (Miao, Davis and Craig 1997), its interaction with the J-protein Mdj1 should be stable in the presence of ATP. Binding of Ssc1 to the Ni-NTA matrix occurred in the samples containing the histidine-tagged protein while no signal was detectable in the elution fractions of the control samples containing wild type Ssc1. As expected, Mdj1 coeluted with Ssc1-His in the presence of ATP (figure 3.7, lane 8) while Mge1 eluted in the absence of nucleotides (figure 3.7, lane 6). Though the interaction of Zim17 with the Ni-NTA matrix is quite strong, almost all background signals could be removed due to the stringent washing

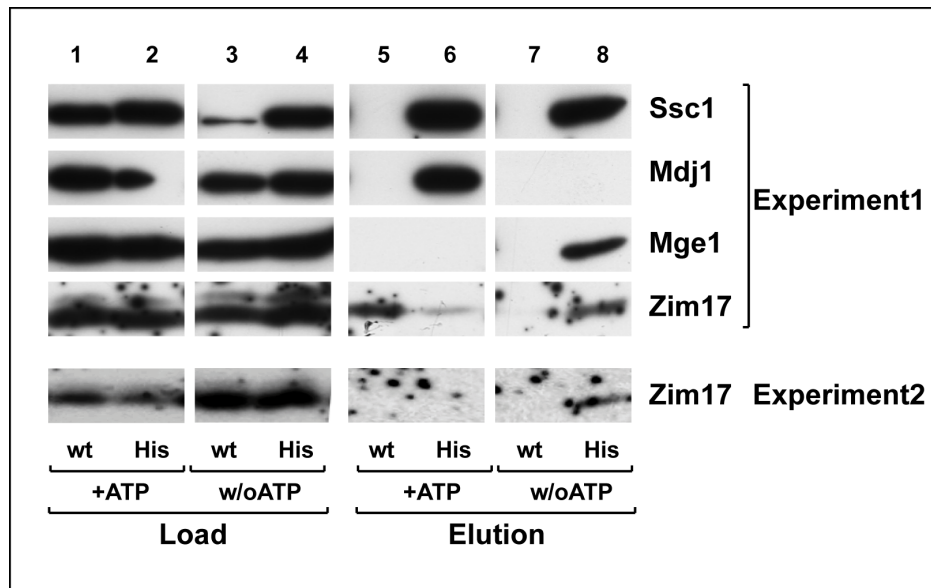


Figure 3.7.: Interaction of Zim17 with Ssc1-His. 200 μ g mitochondrial lysates from an *ssc1-his*-yeast strain were subjected to 50 μ l Ni-NTA in the presence and absence of nucleotides. Proteins were eluted from the column with 250 mM imidazole and analysed via Western blot and incubation with antibodies against the indicated proteins. Wild type mitochondria from the *S. cerevisiae* strain PK 82 were used as a control.

conditions. As it was observed before (Sichting 2005), Zim17, similar to Mge1, was coeluted with Ssc1 only under nucleotide-free conditions (figure 3.7, lane 8).

3.2. Role of the zinc-chelating cysteine residues in Zim17

3.2.1. Generation of the zinc finger mutants *zim17-C78S* and *zim17-C100S*

The zinc-chelating residues in Zim17 are believed to be essential for the protein to gain and maintain its native structure (Momose 2007). However, little is known about the importance of the zinc-binding domain for the cochaperone function of Zim17. In attempt to assess if a diminished binding of the zinc atom affects the Zim17 interaction with Ssc1, two zinc finger mutants were created by an exchange of the cysteine residues at positions 78 and 100 with serines. The mutations were inserted into the mature form of *ZIM17* by overlap extension PCR (section 2.4.1.2) via the internal primers pIL4-C78S-f/r and pIL4-C100S-f/r respectively. The plasmid pIL4 (section 3.1.3) was used as a template. The subsequent fusion PCR was performed using the flanking primers pIL4-Zim17-f and pIL4-Zim17-r that anneal at the 5'- and 3'-end of *ZIM17*, omitting the residues of the presequence. The PCR products were inserted into the empty pETDuet vector via the NdeI and XhoI restriction sites of MCS2 resulting in the plasmids pIL6 (C78S) and pIL7 (C100S).

3.2.2. Solubility of Zim17 zinc finger mutants in *E. coli*

Protein expression from pIL6 and pIL7 was induced in *E. coli* BL21 cp cells and a solubility test followed by SDS-PAGE and Western blot analysis was performed. As already observed by Momose (2007), both Zim17-C78S and Zim17-C100S were detected as insoluble aggregates in the *E. coli* cell lysates (figure 3.8). As the zinc finger mutants were not able to achieve a native folding state, no further purification or co-expression assays were performed in *E. coli*.

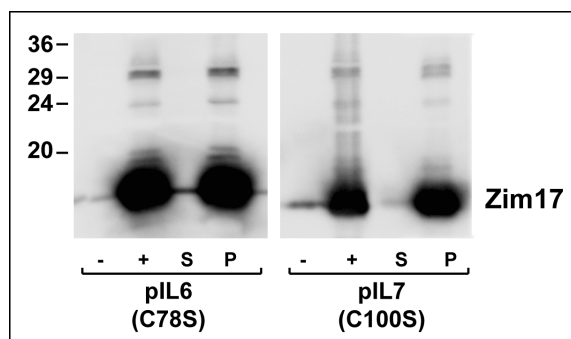


Figure 3.8.: Expression levels and solubility of Zim17-C78S and Zim17-C100S in *E. coli*. Zim17-C78S and C100S were expressed in *E. coli* cells from the vectors pIL6 and pIL7. Cells were lysed and soluble material was separated from insoluble inclusion bodies as described in section 3.1.1.2. - cell extracts before induction of protein expression. + protein expression from plasmids induced with IPTG. **S** Supernatant, soluble proteins **P** Pellet, insoluble proteins (inclusion bodies).

3.2.3. *Zim17* zinc finger mutants are soluble after import into isolated yeast mitochondria

3.2.3.1. Generation of the preforms of the zinc finger mutants for *in vitro* translation

As the cytosol of *E. coli* cells provides a non-natural environment for the expression of yeast proteins, the formation of insoluble aggregates may occur to a less severe extent in the matrix compartment of yeast mitochondria. To estimate the solubility of the zinc finger mutants in the mitochondrial matrix, precursor forms of the zinc finger mutant proteins were generated and imported into isolated mitochondria of the *S. cerevisiae* YPH499 wild type strain. The mutations were inserted into the *ZIM17* gene by overlap extension PCR, using the internal primers pIL4-C78S-f/r and pIL4-C100S-f/r in combination with the flanking primers gen-Zim17-r and gen-Zim17-f that anneal at the 5'- and 3'-ends of the *ZIM17* ORF. For control purposes, the precursor form of the wild type *ZIM17* gene was amplified additionally. Genomic DNA of the yeast strain BY4741 was used as a template. The forward primer gen-Zim17-f that was used for the fusion PCR contains a KOZAK sequence at its 5'-end, that provides a ribosome binding site. The PCR products were inserted into the pCR-BluntII-TOPO vector (Invitrogen) via blunt end cloning, resulting in the plasmids pIL8 (pre-*ZIM17*), pIL9 (pre-*zim17-C78S*) and pIL10 (pre-*zim17-C100S*). Radioactively labelled proteins were generated by *in vitro* translation (section 2.6.1) using the SP6-promotor of pCR-BluntII-TOPO.

3.2.3.2. *In organello* import and solubility test of *Zim17* zinc finger mutants

The radioactively labelled *Zim17* wild type and zinc finger mutant proteins were imported to isolated mitochondria as described in section 2.6.2.1. Samples were taken at the time points indicated in figure 3.9 A, treated with proteinase K and analysed via SDS-PAGE and digital autoradiography. All three proteins were imported efficiently to a protease-protected location. The precursor forms of the different *Zim17* proteins were not degraded by the externally added protease, indicating a slow processing probably due to the short length of *Zim17*.

To assess the solubility of the imported zinc finger mutants, an aggregation test was performed after a 30 min import reaction. Mitochondrial lysates were prepared directly after the import reaction and subjected to a high velocity centrifugation step as described in section 2.6.7. In contrast to their aggregation behaviour in *E. coli* cells, both zinc finger mutants were 100% soluble in the mitochondrial matrix (figure 3.9 B),

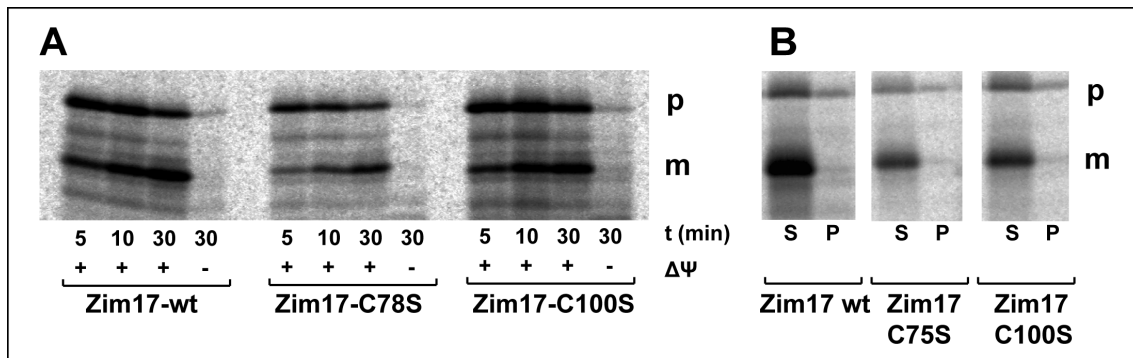


Figure 3.9.: Import and solubility of Zim17-C78S and C100S in yeast mitochondria. (A) Radiolabeled Zim17-wt, -C78S and -C100S were imported into isolated YPH499 wild type mitochondria for 30 min. **(B)** Aggregation assay after 30 min of import. Mitochondria were lysed in a Triton-X-100 containing buffer and subjected to an ultracentrifugation step at 45 0000 rpm as described in section 2.6.7. Samples were taken at the time points indicated, treated with proteinase K and analysed via SDS-PAGE and digital autoradiography. **S** Supernatant **P** Pellet.

suggesting that the structural role of the zinc finger domain is less important than it has been assumed on the basis of experiments applying recombinantly expressed proteins (Momose 2007, this study).

3.3. Analysis of the temperature-sensitive mutants *zim17-2*, *zim17-3* and *zim17-4*

3.3.1. Expression of Zim17-2, -3 and -4 from plasmids in a *zim17* Δ genetic background

Zim17 is known to interact with mitochondrial Hsp70 chaperones. *In vitro* assays using proteins that were overexpressed in *E. coli* could confirm that the interaction of Zim17 with Ssc1 occurs in the absence of nucleotides in mitochondrial lysates (section 3.1.4). Moreover, binding of purified Ssc1 to immobilized ATP seemed to occur while Zim17 was still associated with the chaperone under *in vitro* conditions (section 3.1.2.3). Zim17 also appears to be able to dimerize, most likely when it is not bound to a Hsp70 molecule (section 3.1.2).

To study the functional interaction of Zim17 with mtHsp70s in its natural environment, deletion mutants have been used in a number of studies in the past years (Blamowska, Neupert and Hell 2012; Blamowska 2010; Díaz de la Loza 2011; Sanjuán Szklarz 2005; Sichting 2005). However, *zim17* Δ strains seem to display a strong tendency to develop a respiratory-deficient phenotype (Sanjuán Szklarz 2005). Thus, it is likely that a deletion of the *ZIM17* gene leads to an accumulation of secondary, indirect effects over time. To study the direct, short-term consequences of a Zim17 loss of function on the main mtHsp70s Ssc1 and Ssq1 in their natural environment, a set of *zim17* mutants was generated by error-prone PCR in the laboratory of Professor Dr. N. Pfanner at the University of Freiburg with the aim to gain conditional mutations within the *ZIM17* gene. The amplified mutant alleles together with approximately 600 bp of the *ZIM17* 3'UTR and 300 bp of the *ZIM17* 5'UTR were cloned into the vector pFL39 (Bonneaud 1991), allowing the expression of the mutant Zim17s under the control of their own promoter (Sanjuán Szklarz 2005). Plasmids carrying the mutations were named pFLzim17-tsx-CEN with x referring to the number of the individual mutant and transformed into *zim17* Δ yeast cells (Sanjuán Szklarz 2005).

Transformants were screened for a temperature-sensitive growth phenotype. In this work, the mutants that showed the most severe temperature-sensitive phenotype (referred to as *zim17-2* and *zim17-3* and *zim17-4* respectively) were selected for further analysis. A subcellular fractionation (section 2.4.11) that was carried out to confirm the expression and distribution of the mutant Zim17 proteins. Zim17-3 and Zim17-4 were located to the mitochondrial compartment of the yeast cells (figure 3.10 A). However, Zim17-3 was strongly overexpressed, while Zim17-4 seemed to be expressed

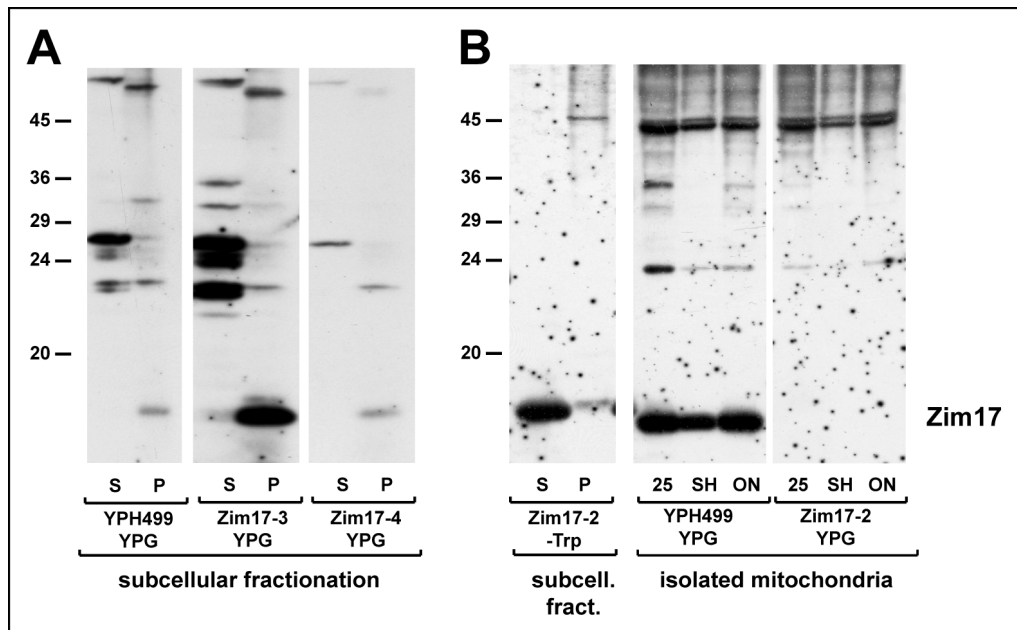


Figure 3.10.: Subcellular fractionation of *zim17-2,-3* and *-4* mutant cells. (A) Subcellular fractionation of *zim17-3* and *-4*. Cells were grown for 5 days in YPG or selective medium as indicated. Cells were lysed and subcellular fractionations were performed as described in section 2.4.11. **(B)** Subcellular fractionation and mitochondrial isolation of *zim17-2* mutants. Mitochondria were isolated after growth at 25 °C (**25**), a 4h heat treatment at 37 °C (**SH**) or after a 16h heat treatment at 37 °C (**ON**). **S** supernatant (cytosolic fraction), **P** pellet (mitochondrial fraction)

in low amounts. Unexpectedly, the mutant protein Zim17-2, that has been used in a previous study on the function of Zim17, (Sanjuán Szklarz 2005) seemed to remain in the cytosolic fraction of the cells (figure 3.10 B).

3.3.2. Sequence analysis of *zim17-2*, *-3* and *-4*

To identify the mutated residues in *zim17-2*, *-3* and *-4*, a sequence analysis was performed (figure 3.11). *Zim17-2* showed mutations at residues 40, 59 and 107 of its amino acid sequence. At positions 40 and 59, two leucine residues were exchanged with serines. At position 107, a histidine was replaced by a proline. As the leucine at position 40 lies inside the predicted Zim17 pre-sequence, this mutation potentially impairs its import to the mitochondrial matrix, leading to extremely low mitochondrial levels of the mutant protein.

Sequencing of *zim17-3* revealed a mutation at residue 111 where the aspartic acid in the highly conserved DHL-motif was replaced by a neutral glycine. An additional mutation was found at the less conserved residue 79 where an asparagine was replaced with a serine.

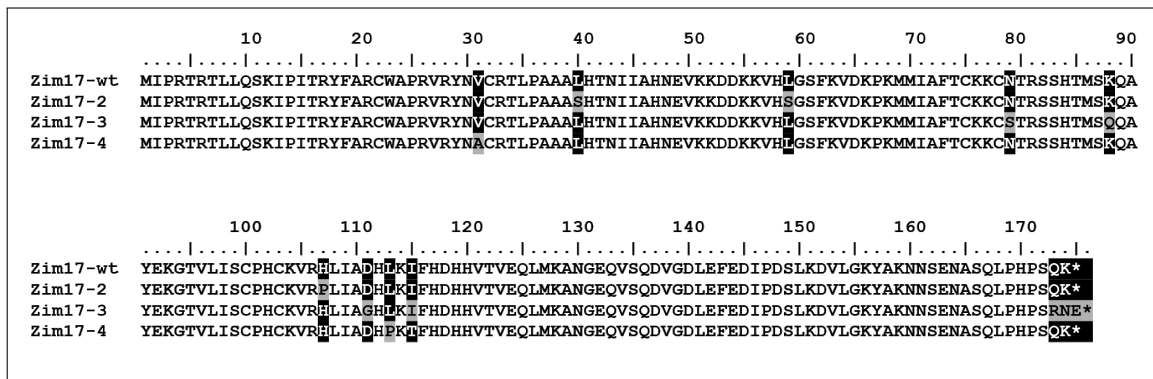


Figure 3.11.: Sequence alignment of wt and mutant Zim17 proteins. The positions of mutations in one of the proteins are indicated by black bars. Mutated residues are indicated in gray.

In *zim17-4* mutations were found at positions 113 and 115 where the hydrophobic leucin and isoleucin were replaced with a heterocyclic proline and a neutral threonine. A third mutation was found at residue 31 where valine was exchanged to alanine. The mutation at position 31 in Zim17-4 also lies in the pre-sequence of Zim17 and thus might explain its low mitochondrial levels in comparison to Zim17-3. In addition to the mutations described above, all three mutants carried a number of silent mutations and mutations in the 3'- and 5'UTRs of the mutants indicated in section A.1.2. Of all three mutants, *zim17-4* carried the largest number of silent mutations.

3.3.3. Generation of a corresponding wild type plasmid

As the mutant Zim17 proteins were expressed in a *zim17* Δ genetic background, a corresponding wild type plasmid was generated for control purposes. The plasmid pFLzim17-ts3-CEN carrying the *Zim17-3* allele was digested with the restriction enzyme HindIII (restriction sites indicated in section A.1.2) to remove all mutated residues. One HindIII restriction site is found at position -332 upstream the *ZIM17* ATG sequence. The second HindIII site belongs to the multiple cloning site of the pFL39 vector and lies at the 3'end of the *zim17*-insert. A PCR applying yeast genomic DNA obtained from the BY4741 wild type strain as template was performed using the primer pair Zim17-corrWT-f and Zim17-corrWT-r (table 2.8). The PCR product was inserted into the empty pFLzim17-ts3-CEN vector via the HindIII restriction sites, resulting in the new plasmid pFLzim17-corrWT-CEN.

3.3.4. Growth phenotype of *ZIM17-corrWT*, *zim17-3* and *zim17-4*

To analyse the growth phenotype of *zim17-3* and *zim17-4*, serial drop dilution tests at different temperatures were performed on growth media with two kinds of carbon sources. YPD medium that contains glucose as a carbon source, allows the yeast cells to switch from respiratory to fermentative metabolism if needed. On YPG medium with non-fermentable glycerol as a single carbon source, the yeast cells are restricted to respiratory metabolism and thus are unable to grow in case of a respiratory deficiency.

Zim17-3, *zim17-4* and corresponding wt cells were grown on YPD or YPG respectively. After log phase was reached, the cells were spotted onto solid medium that contained the same carbon source as the medium that was used for the precultures. All three *zim17*-strains were able to grow on both YPD and YPG medium, though the cells that were grown on YPG grew slower than cells that were cultivated on YPD (figure 3.12 A). At 37 °C, *zim17-3* displayed a strongly diminished growth on both carbon sources while *zim17-4* was not able to grow at all.

As both mutant and corresponding wild type cells grew poorly under non-fermentable conditions, a second experiment was performed to assess the stability of their respiratory competence. Precultures were grown in YPD until log phase and then spotted onto YPG medium (figure 3.12 B). After the shift from glucose to glycerol, *zim17-4* cells were not able to grow even at a permissive temperature of 25 °C while *zim17-3* cells formed few, slowly growing colonies. Surprisingly, the corresponding wild type strain, like *zim17-4*, was not able to grow on a non-fermentable carbon source at all after incubation in fermentable medium suggesting that the expression of the wt plasmid was not able to completely restore a wild type-like growth phenotype in *zim17Δ* cells.

3.3.5. Aggregation of Ssc1 in *zim17-3* and *zim17-4*

MtHsp70 proteins are known to have the tendency to aggregate in the mitochondrial matrix of yeast cells lacking Zim17 (Burri 2004). To measure the propensity of the mutant Zim17s to keep mtHsp70s soluble, an aggregation analysis was performed. *Zim17-3*, *-4* and the corresponding wt cells were grown at a permissive temperature of 25 °C to an OD_{600} of approximately 1.0. All cultures were grown in selective medium lacking tryptophan in attempt to ensure maximal expression levels of the mutated Zim17 proteins. As the mutant cells grew very slowly on selective medium

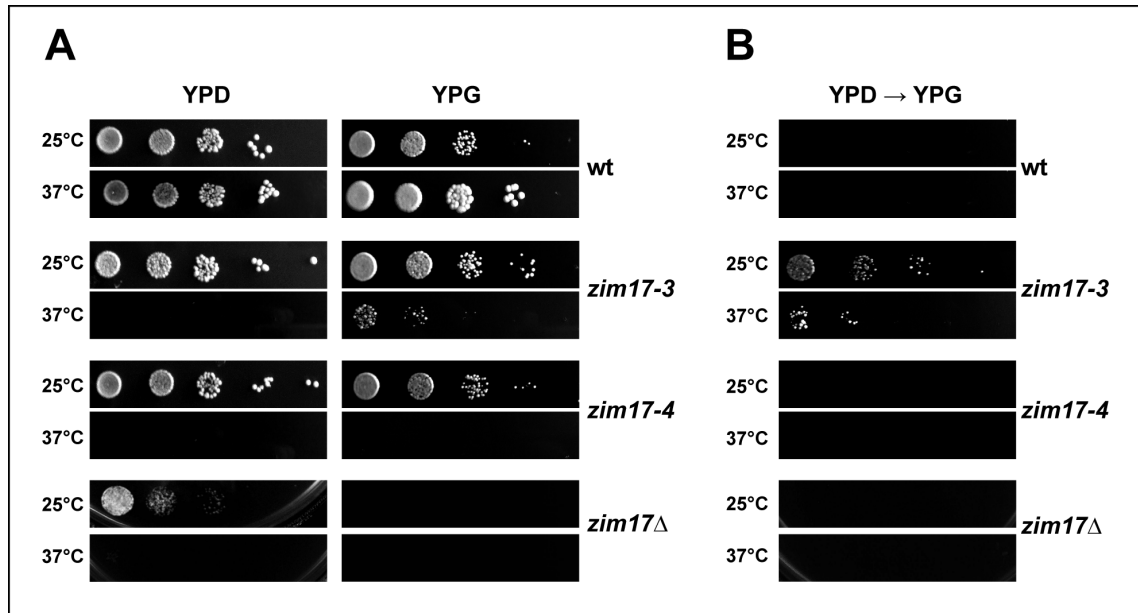


Figure 3.12.: Growth phenotype of *zim17-3* and *-4* mutants in comparison to wt and *zim17Δ*. (A) Serial dilution droptests on fermentable (YPD) or non-fermentable (YPG) medium. (B) Switch from fermentable conditions to non-fermentable conditions. Serial dilution drop test on YPG after growth to log phase in liquid YPD.

containing glycerol as the sole carbon source, 2% glucose was added to the medium. To distinguish between long term and short term effects of a heat treatment, one third of the cultures was subjected to a short-term heat shock of 4 h at 37°C (SH) while another third was treated for 16 h at 37°C (ON) as suggested in Szklarz (2005). The remaining culture was kept at a permissive temperature of 25°C. Mitochondria were isolated, lysed and subjected to an aggregation test (section 2.6.7). Total and pellet fractions were analysed via SDS-PAGE, Western blot and incubation with the antibodies indicated in figure 3.13. Despite of the wild type-like growth of both mutants at permissive temperature, Ssc1 in *zim17-3* mitochondria aggregated already at a permissive temperature of 25°C (figure 3.13, lanes 15). *Zim17-4* mutant mitochondria showed a less severe Ssc1 aggregation at permissive temperature and after a short-term heat shock. The amounts of aggregated Ssc1 in *zim17-4* after a long term heat treatment were similar to the amounts in the *zim17-3* mutant (figure 3.13, lanes 16, 20, 24). Surprisingly, the corresponding wild type mitochondria displayed the most severe Ssc1 aggregation phenotype (figure 3.13, lanes 14, 18, 22) while a YPH499 wt strain carrying the *zim17-corrWT* plasmid that was used as a control showed no Ssc1 aggregation at all (figure 3.13, lanes 13, 17, 21). Decoration with the Zim17 antibody showed that Zim17 was strongly overexpressed in the wt

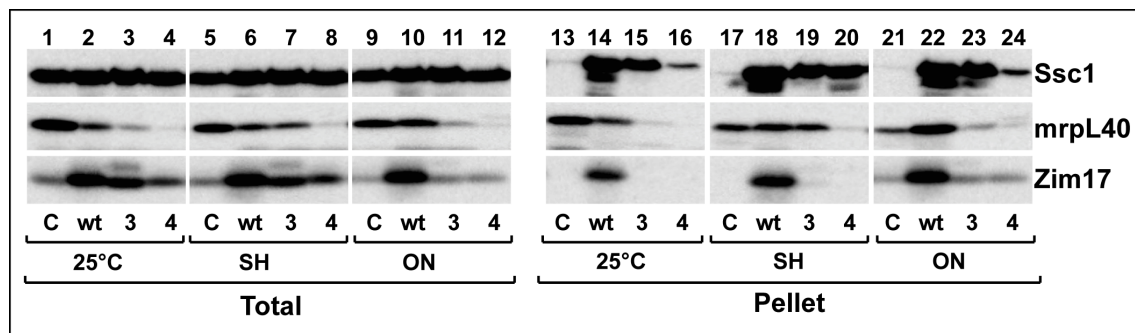


Figure 3.13.: Aggregation of Ssc1 in *zim17-3*, *-4* and wt mitochondria. Isolated mitochondria from heat-treated or non-heat-treated cells were lysed under native conditions in a buffer containing 0.5% Triton-X100. To separate soluble proteins from insoluble aggregates, the lysates were subjected to a high velocity spin. 25 °C, growth at 25 °C, **SH**, 4 h heat treatment at 37 °C **ON**, 16 h heat treatment at 37 °C. **C**, control; expression of *zim17-corr-wt* in *S. cerevisiae* YPH499, **wt/3/4**, expression of *zim17-corrWT*, *-3* and *4* in *zim17Δ*.

and the *zim17-3* strain (figure 3.13, lanes 2, 3, 6, 7, 10, 11), correlating with the high Ssc1 aggregation in these samples. It was also noted that the levels of mrpL40, that was used as an aggregation control, were diminished in all strains with a *zim17Δ* genetic background (figure 3.13, lanes 1-12).

Taken together, the *zim17* mutants showed a mixture of phenotypic effects differing from wild type like growth defects and aggregation of mitochondrial Hsp70s that could derive from the mutated Zim17 protein or from its previous lack in the *zim17Δ* host strain.

3.4. Novel conditional *zim17* mutants

3.4.1. Generation of the mutants *zim17-3a* and *zim17-3b*

Expression of plasmid-encoded Zim17 wild type and mutant proteins in yeast cells with a *zim17* Δ genetic background leads to a mixture of phenotypes that make it impossible to distinguish between direct effects of the *zim17* mutations and secondary effects that derive from the previous lack of Zim17 in the cells. To overcome this problem, the mutant proteins and their corresponding wild type were integrated into the genome of *S. cerevisiae*.

The mutation at position 111 in the peptide sequence of *zim17-3* (D111G) was previously shown to lead to a reduced interaction between Zim17 and Ssc1 *in vitro*, suggesting that the DHL-motif might be part of a potential Ssc1 binding site (Momose 2007). To distinguish between the effects derived solely from the D111G mutation and those derived from the combination of both D111G and N79S, a second mutant carrying only the mutation at position D111 was created in addition to the original *zim17-3*. In the following, the two new *zim17-3* mutants will be referred to *zim17-3a* (D111G/N79S) and *zim17-3b* (D111G) (figure 3.14).

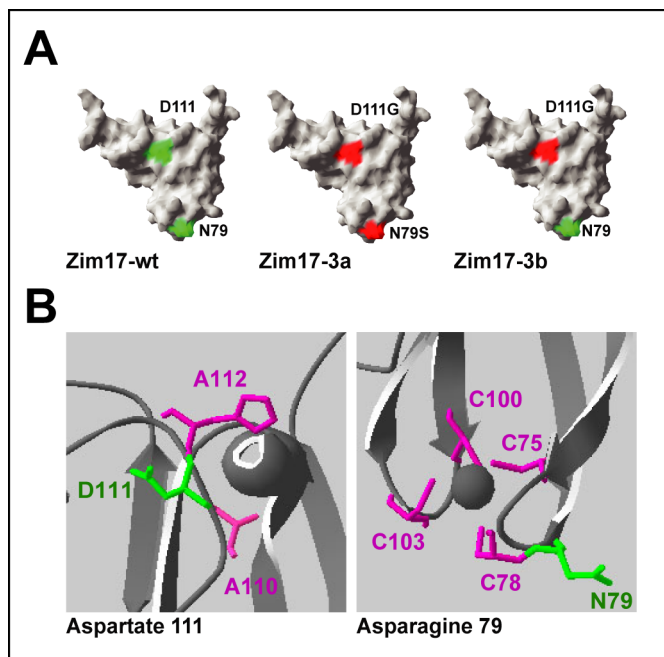


Figure 3.14.: Generation of conditional *zim17*-mutants (A) Surface representation of the Zim17 structure. The locations of the amino acid changes present in the *zim17-3a* and *zim17-3b* mutants are indicated. The mutated residues are indicated in red. **(B)** Magnification into the molecular environment of the amino acids D111 and N79 in the three-dimensional structure of Zim17 (Protein Data Bank code 2E2Z (Momose 2007)). N79 and D111 are indicated in green, neighbouring residues and the four cysteines binding the zinc atom (sphere) are indicated in purple. Structures were visualized using the program Swiss-PdbViewer.

3.4.2. Genomic integration of the mutated *ZIM17* genes

ZIM17-wt, *zim17-3a*, *-3b* and *zim17-4* were inserted into the genome of *S. cerevisiae* under the addition of a *LEU2* marker by PCR-mediated gene disruption (Baudin 1993; Lorenz 1995, section A.1.3, section 2.4.13). Colonies derived from cells that were able to grow on leucine-free medium and thus likely to contain the integrated *zim17*-alleles were screened for a temperature-sensitive phenotype. While a large number of wt, *zim17-3a* and *3b* cells were able to grow in the absence of leucine, only 5 *zim17-4* colonies survived on the selective medium. *Zim17-3a*, *-3b* and *-4* colonies that showed a temperature-sensitive behaviour and were unable to grow at 37°C were picked and tested for successful integration of the mutant *zim17* alleles by colony PCRs applying the primer pair k-fw and k-rev (figure 3.15 A). The antisense-primer k-rev anneals inside the *LEU2* gene. The sense-primer k-fw has an annealing site in the part of the *ZIM17* gene that is not replaced by the integrated PCR fragment. The resulting PCR product of 1663 bp can only be amplified when the insert was integrated into the genomic DNA successfully and at the right position. The DNA of positive wt, *zim17-3a* and *zim17-3b* clones was sequenced to confirm the presence of the appropriate mutations. While D111G/N79S and the D111G were present in *zim17-3a* and *zim17-3b*, the two positive *zim17-4* colonies (figure 3.15 B, *zim17-4* #1 and #3) carried an insert containing the wild type *ZIM17* gene. All sequenced wt, *zim17-3a* and *zim17-3b* clones were tested for respiratory competence by subjection to a non-fermentable carbon source. While wt cells were able to grow on both fermentable and non-fermentable carbon sources, the original *zim-3a* and *-3b* integrants were respiratory incompetent. The clones wt #5, *zim17-3a* #14 and *zim17-3b* #15 (figure 3.15 B) were preserved in glycerol stocks and used for further experiments.

3.4.3. Random spore analysis of *zim17-3a* and *zim17-3b* integrants

An instable respiratory phenotype was observed in *zim17-3a* and *-3b* genomic integrants as well as in *zim17*Δ cells (Sanjuán Szklarz 2005) and in the plasmid-originated *zim17-3* and *zim17-4* mutants (section 3.3.4). Therefore, wt *zim17-3a* and *zim17-3b* integrants were subjected to a random spore analysis (section 2.4.14) to assess if the respiratory deficiency and the temperature-sensitivity were both directly related to the mutations in the *ZIM17* gene. *Zim17* integrants were crossed with *S. cerevisiae* BY4742 wild type cells. After sporulation and disruption of the tetrads, haploid

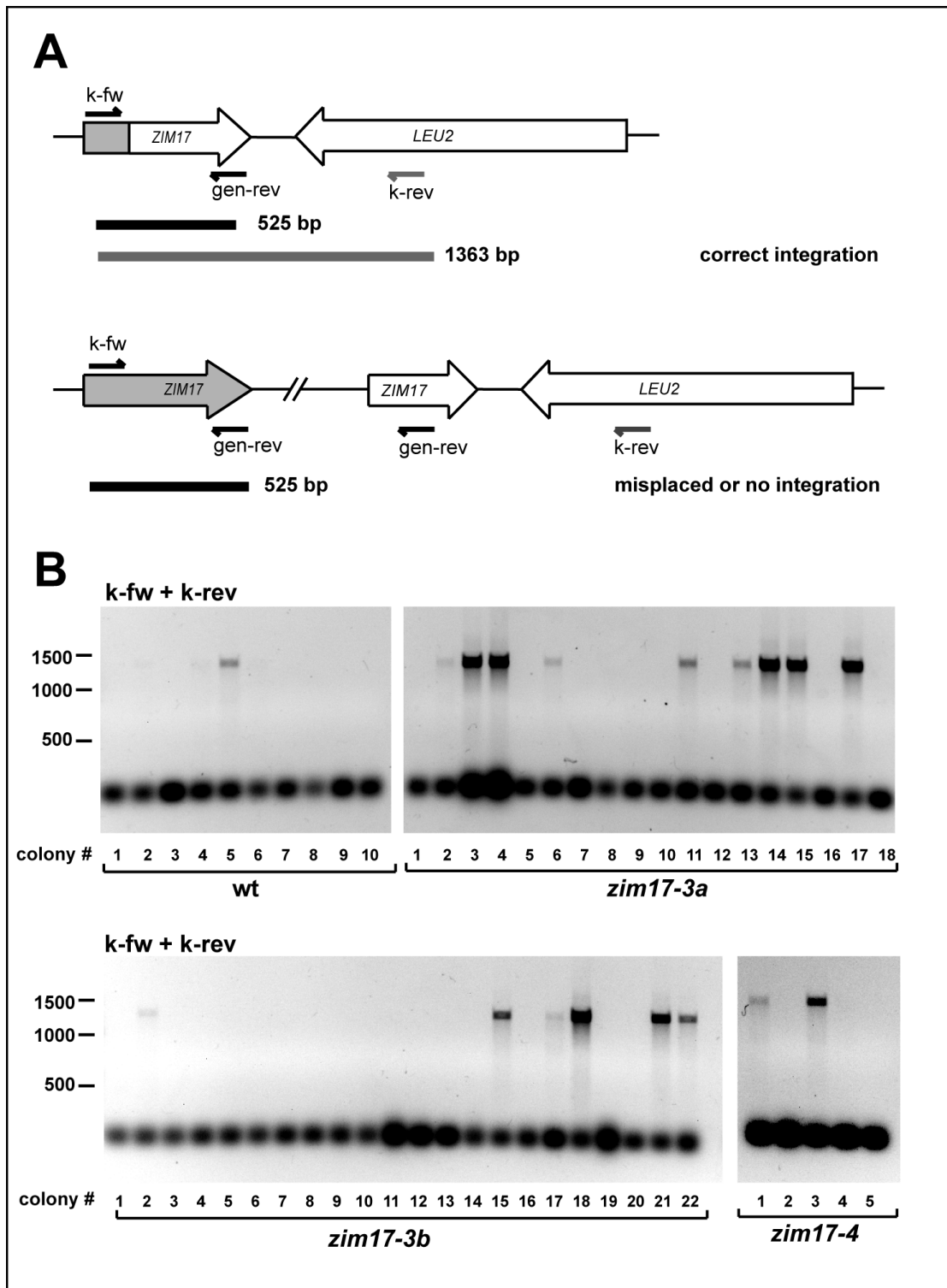


Figure 3.15.: Colony-PCRs of wt, *zim17-3a*, *-3b* and *-4* integrants. (A) Schematic illustration of control PCRs used to identify positive mutant integrants. **(B)** DNA was isolated from cells that showed a temperature-sensitive growth behaviour and were able to grow on leucine. The primers k-fw and k-rev were used for control PCRs.

Table 3.1.: Growth phenotypes of wt, *zim17-3a* and *zim17-3b* tetrades

tetrad	wt				<i>zim17-3a</i>				<i>zim17-3b</i>			
	CFUs	%petites	%ts	%rho-	CFUs	%petites	%ts	%rho-	CFUs	%petites	%ts	%rho-
total	138				205				226			
SD -Trp	25	0	0	0	36	8.3	0	0	55	1.8	0	0
SD -Leu	41	0	0	0	41	95.1	100	36.6	54	98.1	98.1	74.0
SD -Leu/-Trp	38	nd	nd	nd	78	nd	nd	nd	62	nd	nd	nd
only YPG	34	nd	nd	nd	49	nd	nd	nd	55	nd	nd	nd

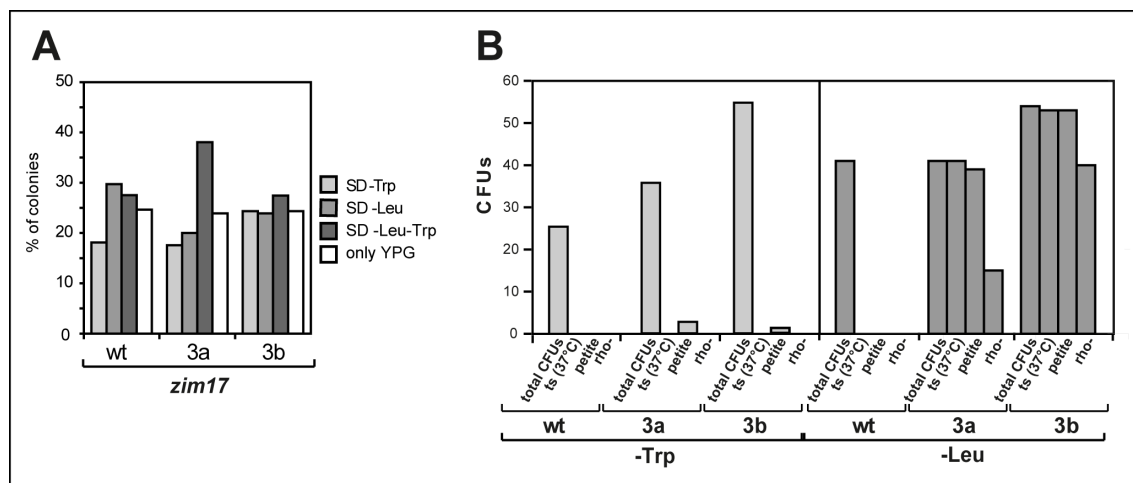


Figure 3.16.: Random spore analysis of wt, *zim17-3a* and *zim17-3b* integrants. **(A)** Growth of tetrades on single and double dropout media. Bars show the percentage of total counted colony forming units (CFUs). **(B)** Growth phenotype of wild type and *zim17* mutant tetrades. Bars represent the absolute numbers of counted CFUs.

cells deriving from single spores were grown on the appropriate single and double dropout media (see table 3.1, figure 3.16 A). As the *TRP1* gene from BY4742 and the *LEU2* gene from the *zim17* integrants are encoded on different chromosomes and are thus completely unlinked, the ratio between cells that were able to grow only on full medium or on dropout media lacking leucine, tryptophan or both was equal (figure 3.16 A). In case of *zim17-3a* the amount of cells that were able to grow on -Leu/-Trp double dropout medium was slightly enhanced, probably due to diploid cells remaining after the tetrad disruption.

As the integrated *zim17* alleles are linked to the *LEU2* gene, the phenotype of cells that are only able to grow on leucine-free medium can be directly related to the appropriate *zim17* mutant. Therefore, all tetrades were tested for temperature-sensitivity and respiratory deficiency (figure 3.16 A). Over 95% of the *zim17-3a* and *zim17-3b* integrants showed a temperature-sensitive phenotype, confirming that the temperature-sensitivity derives from defects directly related to the *zim17* mutations

(table 3.1, figure 3.16 B, right panel). In contrast, only 36.6% of *zim17-3a* integrants and 74% of the *zim17-3b* integrants displayed a tendency to lose their respiratory competence and hence were not viable when subjected to non-fermentable medium, revealing that the loss of respiration is not a direct consequence of the loss of Zim17 function. As expected, all cells deriving from spores that were able to grow only on -Trp dropout medium and thus carrying the BY4742 *ZIM17* gene were able to grow at elevated temperatures and showed a respiratory-competent phenotype (table 3.1, figure 3.16 B, left panel). Single colonies of respiratory-competent wt, *zim17-3a*, and *zim17-3b* spores were selected and stored as glycerol stocks. DNA of the respiratory-competent spores was isolated and tested for the presence of the integrated sequences by PCR applying the primer pair k-fw/ k-rev (figure 3.15 A). A PCR with the primers k-fw and gen-zim17-rev (figure 3.15 A) that amplify the 3'end of *ZIM17* was performed as a control. Genomic DNA from BY4742 yeast cells and from the wt integrant #5 (section 2.4.13) was used as a negative and a positive control respectively. As shown in figure 3.17 all respiratory competent spores contained the *zim17/LEU2* inserts. The presence of the *zim-3a* and *zim17-3b* mutations was confirmed by sequencing of the PCR products.

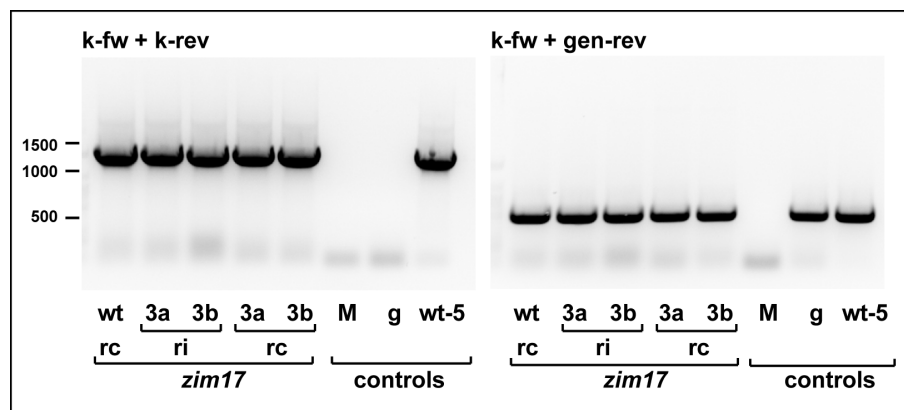


Figure 3.17.: Colony-PCRs of wt, *zim17-3a* and *zim17-3b* tetrads. Respiratory competent (rc) and respiratory incompetent (ri) tetrads were grown on selective media (-leu) and cell extracts were prepared as described in section 2.4.9.2. PCRs were carried out using the primers k-fw, k-rev and gen-rev as described in figure 3.15 A, section 3.4.2. A mock sample without DNA (M), genomic yeast DNA (g) and DNA of the original genomic wt integrant #5 (wt-5, see figure 3.15) were used as controls.

3.4.4. *Zim17* mutant integrants show a temperature-sensitive respiratory instable phenotype

3.4.4.1. Growth phenotype of *zim17-3a* and *-3b*

Spores carrying the mutated *zim17* alleles were generally able to respire, however, part of the populations seemed to lose their respiratory competence over time. To study this instable respiratory-competent phenotype in more detail, the ability of *zim17* integrants to grow on different carbon sources was examined under specified conditions. To examine the growth phenotype of the respiratory-competent spores, serial dilution drop tests at 25 °C and 37 °C were performed. Cells derived from respiratory-competent spores were grown in liquid cultures of fermentable (YPD) or non-fermentable (YPG) medium 25 °C to an OD₆₀₀ of 0.8-1.0 and subsequently spotted on solid medium containing the same carbon source (figure 3.18). On YPG the growth phenotype of *zim17-3a* and *-3b* was indistinguishable from the growth of the wt at a permissive temperature of 25 °C. At 37 °C both *zim17-3a* and *zim17-3b* showed a slow and diminished growth in comparison to wt. On YPD, both *zim17* mutant integrants formed small, slow growing colonies at permissive temperature that strongly resembled the petite phenotype and thus most likely display a reduced ability to respire (Sanjuán Szklarz 2005). At an elevated temperature of 37 °C *zim17-3a* and *zim17-3b* were not able to grow at all. Wt cells grew normally on YPD under all examined conditions. To study the effects of a heat treatment and of the carbon source on the respiratory competence of the *zim17* mutants in more detail, further growth experiments were performed.

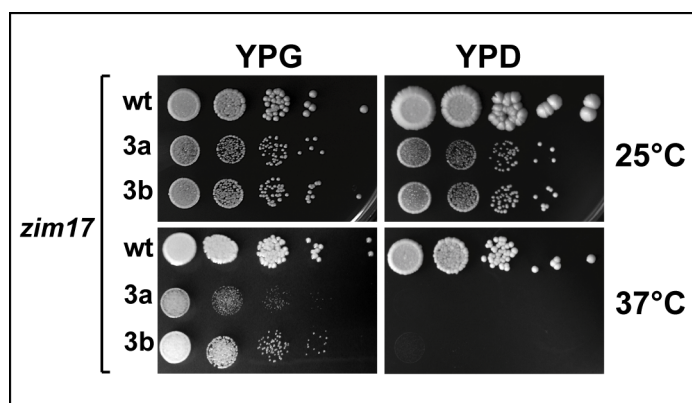


Figure 3.18.: Growth phenotype of respiratory-competent wt, *zim17-3a* and *zim17-3b* mutant integrants. Tenfold serial dilutions of cells grown in liquid precultures of YPD or YPG were spotted onto solid medium, followed by incubation at the indicated temperatures for 4 d.

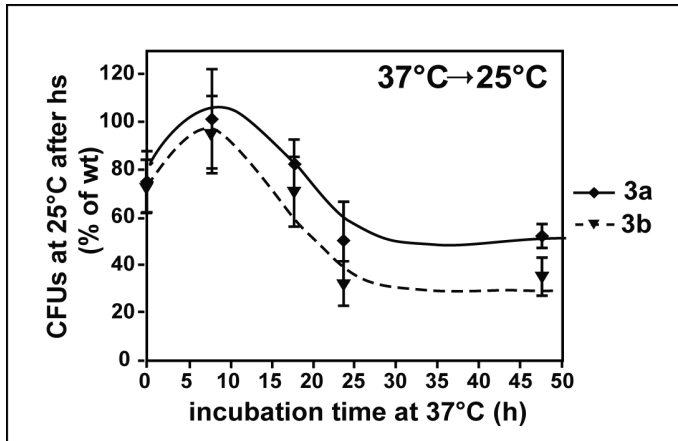


Figure 3.19.: Temperature sensitivity of respiratory-competent wt, *zim17-3a* and *zim17-3b* integrants. Wt, *zim17-3a* and *zim17-3b* cells were grown in liquid YPG medium at 25 °C and subjected to non-permissive temperature (37 °C) for 48 h. At the indicated time points, samples were taken, plated on solid YPG and incubated for 5 days at 25 °C. CFUs were counted and the viability of *zim17-3a* and *zim17-3b* in relation to the wt was determined. Cells were kept at the logarithmic growth phase (OD_{600} 0.6 – 0.8) throughout the experiment. Values shown are means \pm SEM of 4 independent experiments.

3.4.4.2. Temperature sensitivity of *zim17-3a* and *-3b*

To measure the general effect of a heat treatment on the survival of *zim17* mutant cells, a time course experiment was performed. Respiratory competent *zim17* integrants were grown in liquid non-fermentable medium at 25 °C. After an OD_{600} of 0.8-1.0 was reached, cells were subjected to a heat treatment at 37 °C for 48h. Equal amounts of cells were taken at the time points indicated in figure 3.19. and distributed onto solid non-fermentable medium at 25 °C. Colony forming units (CFUs) were counted and the number of wt cells was set to 100%. After a heat treatment of approximately 12 h the survival rate of *zim17-3a* and *-3b* cells began to drop rapidly in comparison to the wt. After a 24 h heat treatment, the number of CFUs *zim17-3a* and *-3b* was reduced to 40% and 60% of the wt respectively. In conclusion, the primary effects of a 37 °C heat shock take place between 12 and 24 h of heat treatment.

3.4.4.3. Respiratory competence of *zim17-3a* and *-3b*

3.4.4.3.1. Effect of heat treatment

To examine if a heat treatment also influences the respiratory competence of *zim17* mutant cells, respiratory-competent *zim17* integrants were grown in liquid YPG and subjected to a 48h heat treatment as described above. Equal amounts of cells were taken at the time points indicated in figure 3.20 A and spread out on solid YPD and YPG at 25 °C. Colony forming units (CFUs) on both media were counted and the number of CFUs that grew on YPD was set to 100%. The relative amount of CFUs on YPD was determined to measure the respiratory competence of the cells.

As shown in figure 3.20 A, all *zim17* integrants showed a similar growth on both carbon sources after the heat-treatment. Thus, even though both mutants exhibited a temperature-sensitive behaviour, their respiratory competence was not affected by the heat treatment under non-fermentable conditions.

3.4.4.3.2. Effect of carbon sources

To test the effect of different carbon sources on the respiratory competence of *zim17-3a* and *zim17-3b* cells, precultures of respiratory competent *zim17* mutant integrants were grown in liquid YPG as described above. Cells were harvested, resuspended in YPD and further incubated for 48 h at a constant temperature of 25 °C. Samples were taken at the time points indicated in figure 3.20 B. Equal amounts of cells were washed with water and spread on fermentable and nonfermentable medium respectively. The relative amount of respiratory-competent cells was determined as described above. While the wt cells were able to keep their respiratory competence, the number of *zim17-3a* and *-3b* integrants that were able to grow on YPG began to decrease rapidly after 6h growth on YPD. After an incubation time of 25h only about 50% of the *zim17* mutant integrants remained to be able to respire. After 48h the number of cells that were able to form colonies on YPG was less than 10% of those on YPD.

3.4.5. Differentiation between respiratory-competent (*zim17_{rc}*) and incompetent (*zim17_{ri}*) mitochondria isolated from mutant integrants

As the respiratory competence of *zim17* mutant integrants is dependent on the carbon source, further experiments distinguished between respiratory incompetent and respiratory-competent mitochondria. To isolate respiratory-competent mitochondria, *zim17* integrants were grown on YPG at 25 °C to an OD_{600} of approximately 1.0. Cultures grown in YPG were divided in two halves and further grown at 25 °C and 37 °C respectively. According to figure 3.19 in section 3.4.4.2, a 16 h heat treatment was chosen for all further experiments.

To generate respiratory incompetent mitochondria, *zim17* integrants were grown on YPD at 25 °C. As a temperature of 37 °C was lethal for *zim17-3a* and *zim17-3b* cells under those conditions (figure 3.18), the heat treatment was not performed.

Mitochondrial isolations were performed as described in section 2.4.12. In the following, *zim17* mutants will be referred to as *zim17_{rc}* for respiratory-competent mi-

tochondria isolated from cells grown on YPG and *Zim17_{ri}* for respiratory incompetent mitochondria isolated from cells grown on YPD.

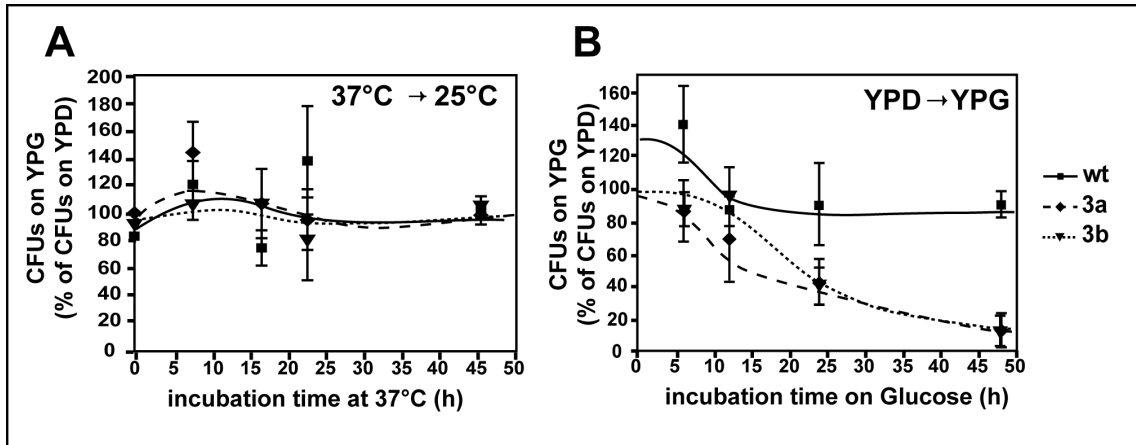


Figure 3.20.: Respiratory competence of wt, *zim17-3a* and *zim17-3b* mutant integrants. (A) Influence of heat treatment on respiratory competence. **(B)** Influence of a fermentable carbon source on respiratory competence. Respiratory competent wt, *zim17-3a* and *zim17-3b* yeasts were grown in liquid precultures in glycerol-containing medium (YPG) at 25 °C to an OD₆₀₀ of 1. Cells were washed, diluted with water to an OD₆₀₀ of 0.6 and further incubated in glycerol-containing medium at 37 °C **(A)** or in glucose-rich medium at 25 °C **(B)** for 48 h. At the indicated time points, samples were taken and equal amounts of cells were plated on YPD and YPG solid medium. After a 5 d incubation at 25 °C, colony forming units (CFUs) were counted and the ratio of CFUs on YPG compared to CFUs on YPD was determined. Cells were kept at the logarithmic growth phase (OD 0.6 – 0.8) throughout the time courses of both experiments. Values shown are means ±SEM of 4 independent experiments.

3.5. Biochemical analysis of genomic *Zim17* conditional mutants

3.5.1. Aggregation of Hsp70 chaperones

As it is known that a loss of *Zim17* results in the aggregation of mitochondrial Hsp70s, *zim17* mutant integrants were tested for aggregation of the two main yeast mtHsp70 chaperones Ssc1 and Ssq1. *Zim17_{ri}* and *Zim17_{rc}* mitochondria were isolated and lysed in a buffer containing 0.5% Triton-X100. Soluble proteins were separated from insoluble aggregates by a high velocity centrifugation step. Samples of total mitochondrial lysates, supernatants and pellets were analysed via SDS page and immunoblotting with specific antibodies as indicated in figure 3.21. To exclude an unspecific aggregation behaviour, the soluble matrix protein Sod2 was probed as a control.

3.5.1.1. Aggregation in respiratory-deficient *zim17* integrants

In respiratory-incompetent *Zim17_{ri}* mitochondria, both mtHsp70s were aggregating at a permissive temperature of 25 °C (figure 3.21 A). While Ssq1 showed an aggregation between 70% and 100%, the aggregation of Ssc1 was 50% or higher in both mutants. To differentiate between effects due to respiratory deficiency and effects due to the *zim17*-mutations, mitochondria obtained from a respiratory-deficient variant of the *S. cerevisiae* YPH499 strain lacking mitochondrial DNA (rho-) were used as a control. Ssc1 and Ssq1 were soluble in both YPH499 wt (rho+) and YPH499 rho- cells, suggesting the mtHsp70 aggregation as a consequence of the loss of *Zim17*. It also has to be noted that the levels of the control protein Sod2 were diminished in *zim17_{ri}-3a* and *zim17_{ri}-3b* (figure 3.21, lanes 4 and 5).

3.5.1.2. Aggregation in respiratory-competent *zim17* integrants

3.5.1.2.1. Aggregation of mature *Ssc1*

Concerning respiratory-competent *zim17_{rc}* mitochondria, both mtHsp70 proteins were soluble at a permissive temperature of 25 °C (figure 3.21 B, lanes 8 and 9). After a 37 °C heat treatment, Ssc1 and Ssq1 were detected in the pellet fractions of *zim17_{rc}-3a* and *zim17_{rc}-3b* (figure 3.21 B, lanes 11 and 12). Additionally, the total amounts of the less abundant mtHsp70 protein Ssq1 were decreased in both *Zim17_{rc}-3a* and *Zim17_{rc}-3b* mitochondria (figure 3.21 B, lanes 2, 3, 5, 6). Quantification of the signals obtained from three independent experiments showed that 30% of total Ssc1

and 70% of total Ssq1 were found in the aggregate pellet of *Zim17_{rc}-3a* mitochondria. In *Zim17_{rc}-3b* mitochondria 13% of total Ssc1 and 6% of total Ssq1 were detected in the pellet. However, considerable amounts of both heat shock proteins were not affected by aggregation and remained in the supernatants.

3.5.1.2.2. Aggregation of newly imported Ssc1

To examine the effect of a loss of Zim17 function on the *de novo* folding of mtHsp70, radiolabelled Ssc1 was generated by *in vitro* translation and imported into heat-treated and non-heat-treated isolated *Zim17_{rc}* mitochondria for 20 min. Before lysis, mitochondria were treated with proteinase K to remove unimported precursor proteins. After a washing step, mitochondrial lysates were subjected to a high velocity centrifugation step as described above and samples were analysed via SDS-PAGE, Western blot and digital autoradiography. In contrast to mature mtHsp70s, less than 1% of newly imported Ssc1 was detected in the pellet fractions of heat-treated *zim17* mutant mitochondria (figure 3.21 B), pointing to the conclusion that the formation of aggregates does not occur during the general biogenesis of mtHsp70s in the *zim17-3a* and *-3b* mutants.

3.5.2. Relative abundance of mtHsp70s and their cochaperones in *zim17* mutant cells

3.5.2.1. Expression levels of mutant Zim17s in *zim17* integrants

Mutant and wild type Zim17 proteins showed a high overexpression when they were encoded on plasmid DNA in a *zim17* Δ genomic background, probably as a reaction to the previous lack of the protein in the mitochondrial matrix of those cells. To assess the expression levels of Zim17 in *zim17_{rc}* and *zim17_{ri}* mitochondria, a Western blot membrane with mitochondrial lysates was incubated with a Zim17 specific antibody (figure 3.22). In comparison to YPH499 and YPH499 rho-, Zim17-3a and -3b levels were elevated in *zim17_{ri}* mutants while Zim17-wt was expressed normally. In *zim17_{rc}* mutant integrants the amounts of Zim17-3a were strongly reduced in comparison to Zim17-wt. Zim17-3b showed a higher expression than Zim17-3a, however, it was still expressed in lesser amounts than the wt protein.

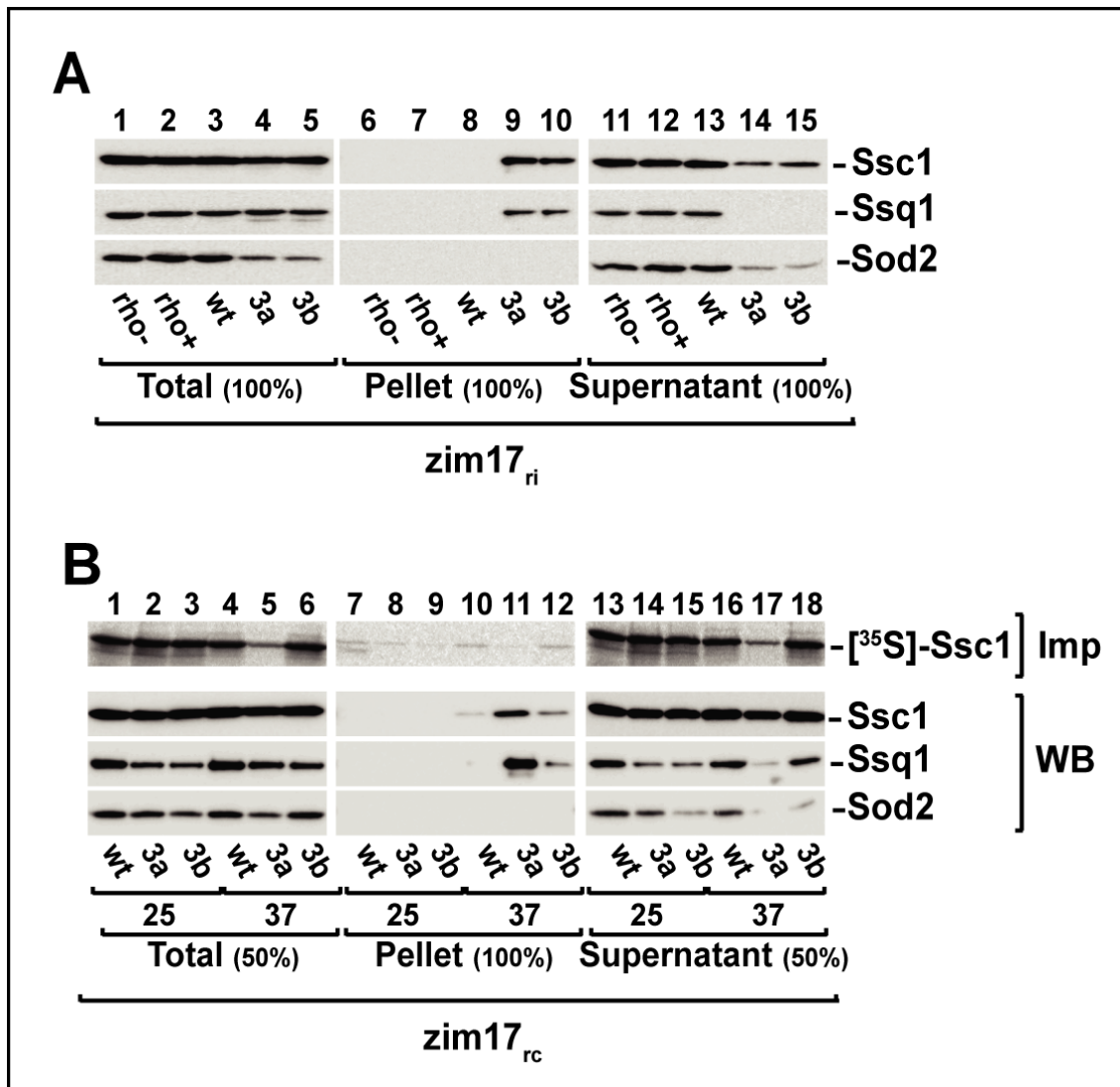


Figure 3.21.: Aggregation of mtHsp70s in *zim17_{ri}* and *zim17_{rc}* under fermentative and non-fermentative conditions. Lysates of mitochondria isolated from yeast cells grown on YPD (*zim17_{ri}*), (A) and YPG (*zim17_{rc}*), (B) were centrifuged at high velocity (45 000 rpm, 30 min) and analysed via SDS-PAGE and immunoblotting with specific antisera against the indicated proteins.

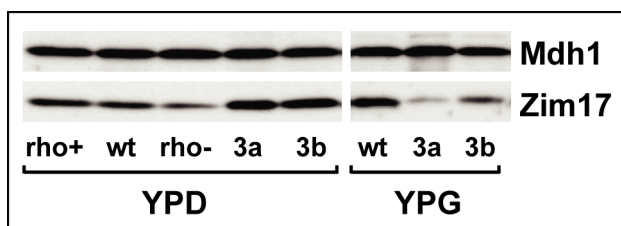


Figure 3.22.: Expression of Zim17-wt, -3a and 3b in *zim17_{ri}* and *zim17_{rc}* mitochondria. 25 µg of mitochondria were lysed in Laemmli buffer and analysed via SDS-PAGE followed by Western blot and incubation with specific antibodies

3.5.2.2. Expression levels of mtHsp70 proteins and their cochaperones in respiratory-competent *zim17* integrants

The levels of Zim17 were diminished in both *zim17_{rc}-3a* and *zim17_{rc}-3b* mitochondria. To examine if the expression levels of other key proteins of the two matrix chaperone systems were affected as well, a Western blot analysis of *zim17_{rc}* mitochondria was performed. Equal amounts of mitochondria were lysed in Laemmli buffer and subjected to SDS-PAGE. Proteins of interest were detected using specific antibodies. The amounts of each protein were quantified and normalized to the citrate cycle protein Mdh1. The protein amounts determined for wt mitochondria were set to 100% for each experiment. Figure 3.23 shows the results of at least 5 independent experiments for each measured protein.

The levels of the main Hsp70 protein Ssc1 were slightly diminished in *zim17_{rc}-wt*, *-3a* and *-3b* mitochondria at a permissive temperature of 25 °C. After a 16h heat treatment at 37 °C, Ssc1 showed a heat-stress induced upregulation that was stronger in the mutants than in wt mitochondria. The J-protein partner of Ssc1 in the mitochondrial matrix, Mdj1, showed a significant reduction in both mutants already at 25 °C. At 37 °C the Mdj1 levels in *zim17_{rc}-3a* and *-3b* were indistinguishable from its levels in wt mitochondria. As Mdj1 is a heatshock protein itself, its levels were probably restored by temperature-induced overproduction. The inner membrane J-protein Pam18 that assists Ssc1 in fulfilling its function during the import reaction, showed stable, wild type-like levels before and after the heat treatment.

As already observed in section 3.5.2.1, the levels of the second matrix Hsp70 Ssq1 were severely downregulated to less than 50% of wild type levels in *zim17_{rc}-3a* and *zim17_{rc}-3b* mitochondria. An overproduction of Ssq1 after a 37 °C heat treatment could not restore its amounts back to normal levels. Jac1, the J-protein partner of Ssq1, showed consistent expression levels at 25 °C. However, after heat treatment, its amounts were enhanced about 3-fold in both *zim17* mutants. Similar to Jac1, the levels of the Ssq1-interacting scaffold protein Isu1 remained constant at 25 °C but were strongly elevated, in this case almost 10-fold, at 37 °C.

3.5.2.3. Expression levels of mtHsp70 proteins and their cochaperones in respiratory-deficient *zim17* integrants

As respiratory-competent *zim17* mutants showed alterations in the expression levels of mtHsp70 proteins and some of their key-interaction partners, the levels of mito-

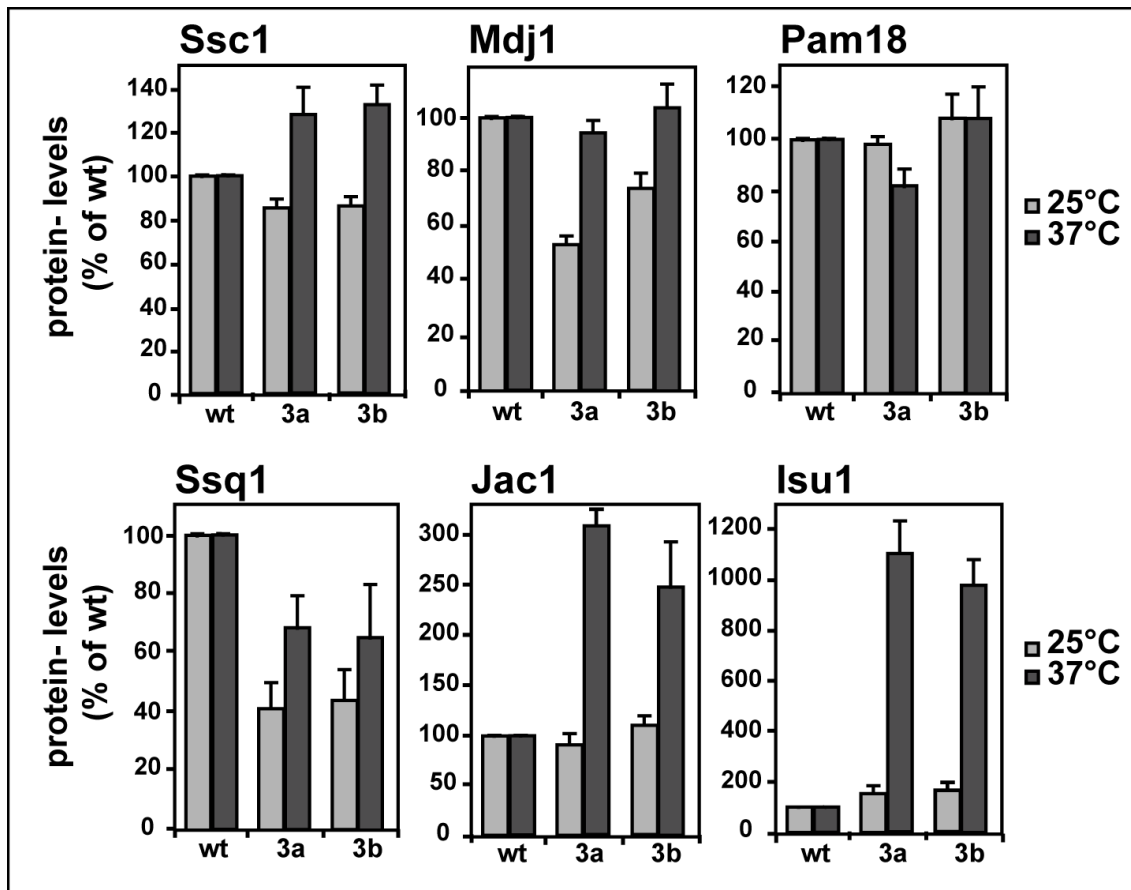


Figure 3.23.: Relative abundance of mtHsp70 proteins and their cochaperones in *zim17_{rc}* mutant integrants. Mitochondria isolated from respiratory-competent yeast cells grown on YPG were lysed and assayed by SDS-PAGE, Western blot and incubation with antisera against the indicated proteins. Values shown are means \pm standard error of protein amounts in *zim17_{rc}-3a* and *-3b* relative to wt mitochondria of at least 5 independent experiments. All values were normalized to the amounts of Mdh1.

chondrial proteins isolated from respiratory-incompetent *zim17* cells were examined as a comparison. As described above, equal amounts of *zim17_{ri}* mitochondria were subjected to SDS-PAGE and Western blot and analysed via incubation with antibodies as indicated in figure 3.24. Tim23 was decorated as a quantity control. As already described in section 3.5.1.1 YPH499rho- and YPH499 mitochondria were used as respiratory-deficient and respiratory-competent control wild type strains. The levels of Ssc1 and its J-proteins Mdj1 and Pam18 remained stable in *zim17_{ri}-3a* and *-3b* mitochondria. In contrast to *zim17_{rc}* mitochondria, the Ssq1-levels in the *zim17_{ri}-3a* and *-3b* mutants were indistinguishable from its levels in in the wt. Also the Ssq1 cochaperone Jac1 displayed constant levels in the mutants and in the wt. As an exception, the levels of Isu1 were upregulated in *zim17_{ri}* mitochondria already at a permissive temperature of 25 °C.

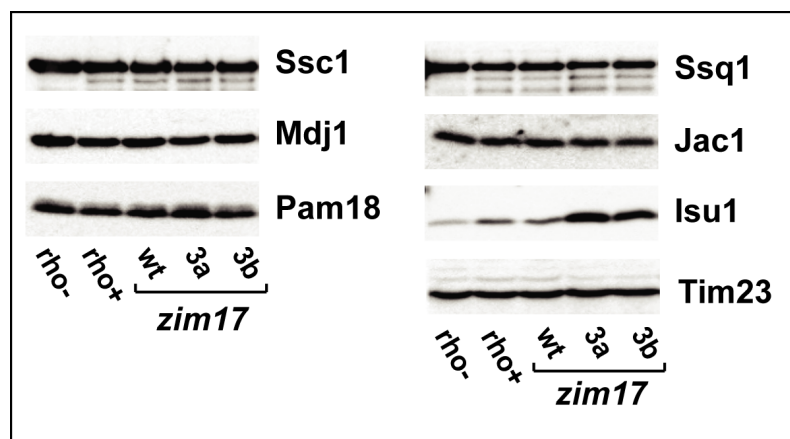


Figure 3.24.: Abundance of mtHsp70 proteins and their cochaperones in *zim17_{ri}* mutant integrants. Mitochondria isolated from respiratory-competent yeast cells grown on YPD were lysed and assayed by SDS-PAGE and immunoblotting with antisera against the indicated proteins.

3.5.3. Interaction of mutant Zim17 with Ssc1

The mutation D111G that is present in both *zim17* mutants, was suggested to play a role in the interaction of Ssc1 and Zim17. To test if the mutant Zim17 proteins were still able to interact with mtHsp70s in the mitochondrial matrix, a co-fractionation experiment was performed. To assay the interaction under true *in organello* conditions and avoid a bias due to aggregated or misfolded Ssc1 caused by *in vivo* expression of the Zim17 mutations, co-immunoprecipitation experiments with radiolabelled prepro-

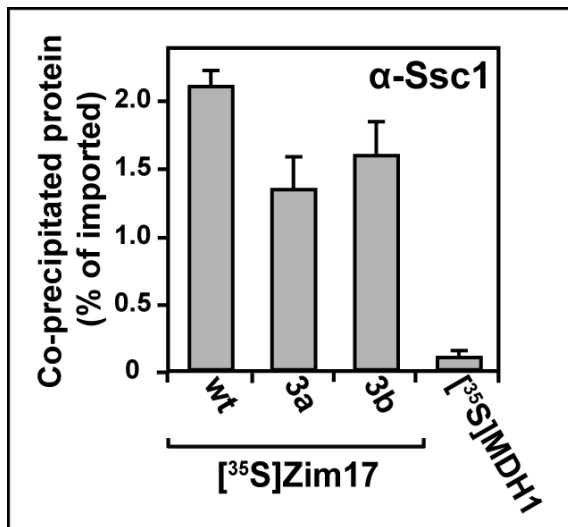


Figure 3.25.: Interaction of wt and mutant Zim17s with mtHsp70s. Radiolabeled preproteins (Zim17-wt, -3a, -3b and Mdh1) were imported into isolated YPH499 wt mitochondria. The import was terminated after 20 min at 25 °C and samples were further incubated at 25 °C for 30 min. Mitochondria were lysed, and proteins bound to Ssc1 were co-immunoprecipitated using antiserum against Ssc1. Precipitated proteins Zim17 proteins were assayed by SDS-PAGE and digital autoradiography. The co-precipitated amounts were quantified and the respective total amounts of imported proteins for each of the samples were set to 100%. The data represent the mean values and standard errors of three independent experiments.

teins were performed. [³⁵S]-Zim17-wt, -3a and -3b precursor proteins were generated by *in vitro* translation as described in section 2.6.1. Import into isolated mitochondria was performed 20 min at 25 °C. As Zim17 was reported to interact with Ssc1 in the absence of nucleotides (Sichting 2005), ATP was depleted by addition of apyrase and the uncoupler oligomycin after the import reaction was stopped. Mitochondria were lysed in a Triton-X100-containing buffer and immunoprecipitations with specific antibodies against Ssc1 were performed. To exclude that the signals were derived from an import-related interaction, radiolabelled Mdh1 (malat-dehydrogenase), a standard matrix-destined precursor that is transferred into the mitochondrial matrix via the Tim-PAM complex and does not interact with Ssc1 after import and folding has been completed, was used as a control. Precipitated proteins were analysed via SDS-PAGE and Western blot followed by digital autoradiography. Co-precipitated amounts of Zim17-wt, -3a and 3b and Mdh1 were quantified and total amounts of imported proteins were set to 100% for each of the samples. About 2% of Zim17-wt was co-precipitated with Ssc1 after 30 minute of post-import incubation while only 1.3% of Zim17-3a and 1.6% of Zim17-3b were associated with Ssc1 under the same conditions (figure 3.25). As less than 0.1% of Mdh1 was co-precipitated with Ssc1, the possibility that the imported proteins were bound to Ssc1 as substrates could be ruled out. In summary, Zim17-3a and Zim17-3a show a diminished, but not completely abolished interaction with Ssc1 in its native state.

3.5.4. Analysis of Ssq1-related processes in *zim17* conditional mutants

3.5.4.1. Expression levels of the Fe/S cluster protein aconitase in *zim17* mutants

The less abundant mitochondrial Hsp70 protein Ssq1 plays an important role in the biogenesis of mitochondrial Fe/S cluster-containing proteins. To monitor the effects of Zim17 on this process, the Fe/S cluster-containing citrate cycle component Aco1 was chosen as a model protein. It was shown previously, that the expression levels of Aco1 were strongly diminished in *zim17* Δ cells (Sichting 2005). Lysates of *zim17_{rc}* mitochondria were analysed via SDS-PAGE and Western blot. The aconitase levels in *zim17_{rc}-3a* and *zim17_{rc}-3b* mitochondria remained constant in mitochondria obtained from cells that were grown at permissive and non-permissive temperature (figure 3.26 A). In case of *zim17_{rc}-3b*, a slight enhancement of the aconitase levels could be observed after heat treatment.

As a shift to non-fermentable conditions resulted in a loss of respiratory competence of *zim17* mutants, the effect of a subjection to a fermentable carbon source on the expression levels of aconitase was examined. Respiratory competent *zim17* cells grown in non-fermentable medium were transferred to a fermentable carbon source for 48 h. The temperature was kept at 25 °C constantly and all cultures were maintained at an OD_{600} of 0.8-1.0 during the whole experiment. Whole cell yeast extracts were prepared and analysed via SDS-PAGE and Western blot. Aconitase was detected with specific antibodies. Tom40, a protein of the outer mitochondrial membrane translocase was used as a quantity control. After a 12h incubation on a fermentable carbon source the levels of aconitase were reduced to non-detectable amounts in *zim17* mutant cells (figure 3.26 B). The signals detected in wt mitochondria remained constant.

3.5.4.2. Expression levels of citrate cycle and respiratory chain proteins

Iron sulphur cluster proteins like Aconitase are involved in many essential metabolic pathways in the cell, including the electron transfer of the mitochondrial respiratory chain or, in case of aconitase, the citrate cycle. It has been shown that a number of genes encoding proteins of those metabolic pathways are substantially downregulated in *S. cerevisiae* with a defective mitochondrial Fe/S synthesis (Andrew 2008; Hausmann 2008; Lill 2012). Therefore, the levels of different proteins involved in respiratory metabolism in *Zim17_{rc}* and *Zim17_{ri}* mitochondria were measured. The proteins Rip1 (rieske protein of the cytochrome bc1 complex) and CoxIV (cytochrome

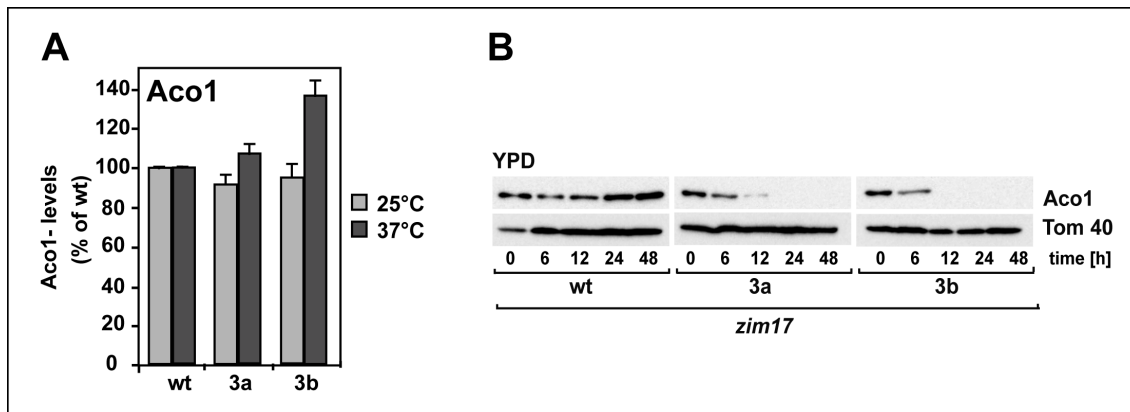


Figure 3.26.: Aconitase levels in *zim17_{rc}* mutant integrants. (A) Relative abundance of aconitase in *zim17_{rc}* mitochondria isolated from respiratory-competent yeast cells grown on YPG. Mitochondria were lysed and assayed by SDS-PAGE, Western blot and incubation with specific antisera against the indicated proteins as described in figure 3.23. (B) Loss of aconitase in respiratory-competent *zim17* mutants after growth on non-fermentable medium. Wt, *zim17-3a* and *zim17-3b* yeasts grown in YPG precultures were transferred to YPD medium 25°C. Whole cell yeast extracts taken at the indicated times were analysed via SDS-PAGE and immunoblotting with the indicated antisera.

c oxidase subunit IV) were decorated as examples of proteins of the respiratory chain. Rip1 carries an iron sulphur cluster itself and thus, like aconitase, was expected to be downregulated in respiratory-deficient *Zim17_{ri}* mutants. MDH1 (malat dehydrogenase) and Cit1 (citrate synthase), represent components of the citrate cycle. *Zim17_{ri}* integrants showed an almost complete loss of all decorated proteins while the protein levels of *zim17_{rc}* mutants were indistinguishable from wt (figure 3.27). The strong effect in the *zim17_{ri}* is not solely due to a loss of respiration as mitochondria from the comparable respiratory-deficient wt strain lacking mitochondrial DNA (ρ^-) showed a less severe downregulation of all examined proteins.

3.5.4.3. Diminishment of aconitase activity in respiratory-competent *zim17* mutants

While *zim17_{ri}* mutant integrants showed a strong reduction of aconitase and other proteins involved in respiratory metabolism, the levels of all measured proteins were constant in *zim17_{rc}* mutant mitochondria. However, it remained unclear if the aconitase of *zim17_{rc}* mutant mitochondria is still functional. To assess this question the enzymatic activity of aconitase was photometrically measured by following the increase in NADPH as described in section 2.6.8.

The activity of aconitase remained constant in *zim17_{rc}-wt*, *-3a* and *-3b* mitochondria obtained from yeast cells grown at permissive temperature (figure 3.28 A). Aconitase from heat-treated *zim17_{rc}-3a* only displayed an activity of 44% in comparison to the

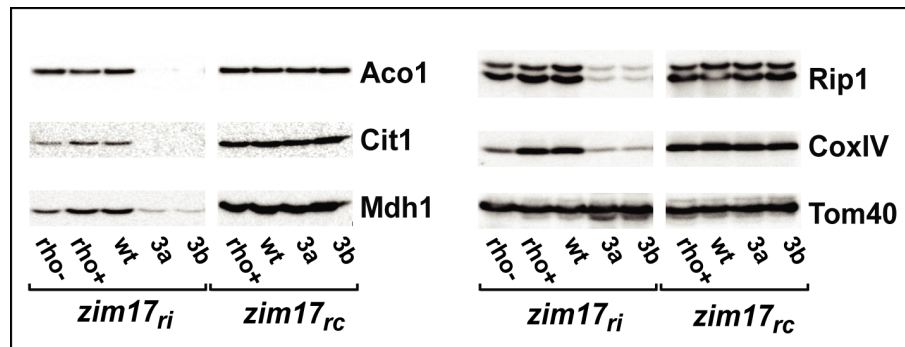


Figure 3.27.: Loss of enzymes of the citric acid cycle and respiratory chain in *zim17_{ri}* mitochondria. Isolated mitochondria of the indicated yeast strains grown on permissive temperature on YPD and YPG were analysed as described in figure 3.24. rho+, YPH499-wt, rho-, respiratory-deficient YPH499.

corresponding wt. In heat-treated *zim17-3b* mitochondria, the activity remained equal to wt levels. To confirm that the diminished enzymatic activity of Aco1 did not derive from an aggregation of the protein, *zim17_{rc}* mutant and wild type mitochondria were lysed and subjected to a high velocity centrifugation step. Isolated mitochondria from the temperature-sensitive mutant *ssc1-3* were heat-treated 15 min at 37 °C and used as an aggregation control (Bender 2011). Samples were analysed via SDS-PAGE and immunoblotting with specific antibodies. The soluble matrix proteins Sod2 and the ribosomal protein MrpL40 were decorated as loading controls for the supernatant and pellet fraction respectively (Bender 2011). While aconitase was detected in the pellet fraction of heat-treated *ssc1-2* mitochondria, no aggregation could be observed in mitochondria of heat-treated or untreated *zim17_{rc}* mutant cells (figure 3.28 B). In consistence with these results, Fe-incorporation assays into aconitase from *zim17_{rc}* mutants that were performed by N. Rietzschel in the laboratory of Prof. Dr. R. Lill in Marburg, Fe-incorporation into aconitase is diminished in respiratory *zim17-3a* mutant cells (Lewrenz et.al. 2013, submitted for publication).

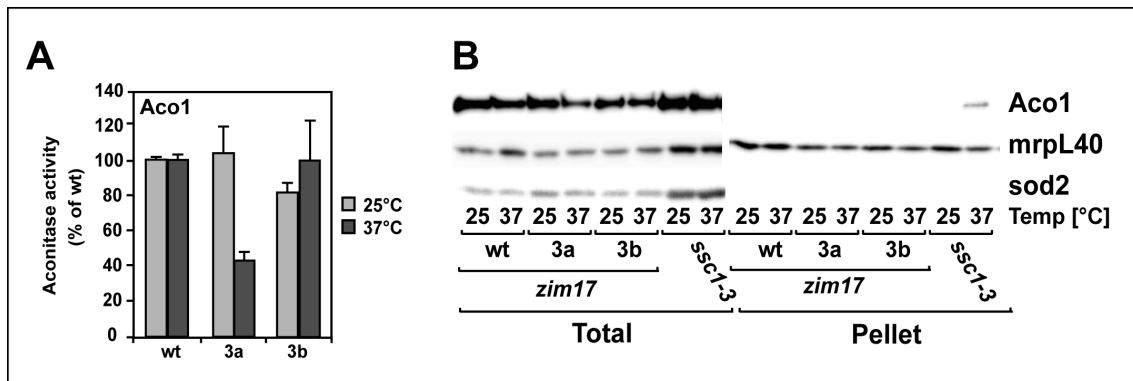


Figure 3.28.: Aconitase activity and aggregation in *zim17_{rc}* mitochondria. (A) Enzyme activity assay of aconitase in *zim17_{rc}* mitochondria isolated from *zim17* mutant cells grown on YPG at permissive and non-permissive temperature. **(B)** Aggregation of aconitase under non-fermentative conditions. Lysates of *zim17_{rc}* mitochondria isolated from yeast cells grown on YPG were centrifuged at high velocity (45 000 rpm, 30 min) and analysed via SDS-PAGE, Western blot and incubation with antisera against the indicated proteins.

3.5.5. Analysis of Ssc1-related processes in *zim17* conditional mutants

3.5.5.1. Preprotein import into respiratory-deficient *zim17* mitochondria

Zim17 Δ mitochondria display defects in the import of matrix-destined preproteins. Therefore the import phenotype of *zim17* mutant integrants was assessed *in organello*. Radiolabelled Su9(86)DHFR was denatured with 7M urea and imported into respiratory-deficient *zim17_{ri}* mitochondria at 25 °C for 30 min as described in section 2.6.2.2. For control purposes, one sample applying native preprotein and one sample where the membrane potential was interrupted using the uncoupler valinomycin were assayed for each mutant. YPH499 rho- mitochondria were used as a comparison. Samples were taken at the time points indicated in figure 3.29 A and analysed via digital autoradiography. Wt mitochondria showed a fast import of denatured and native preprotein (figure 3.29 A, lanes 6-9, 26-29). In comparison to the wt, less protein was imported to the matrix of respiratory-deficient YPH499 rho- mitochondria (figure 3.29 A, lanes 1-4, 21-24). The F_o subunit 9 of the *N.crassa* F_1F_o -ATPase has two MPP processing sites resulting in the formation of a transient intermediate form of Su9(86)DHFR (i) during the import reaction. In YPH499 rho- mitochondria both the pre-form and the intermediate form were detected in addition to the mature form of Su9(86)DHFR, showing the reduced import efficiency of respiratory-deficient mitochondria (figure 3.29 A, lanes 1-3, 21-23). *Zim17_{ri-3a}* and *-3b* mitochondria showed a very low, almost undetectable import when native preprotein was used (figure 3.29 A, lanes 14, 19, 34, 39). The import rates employing denatured preprotein were higher (figure 3.29 A, lanes 12-13, 16-18, 31-33, 36-39), however, in comparison to wt and YPH499 rho- mitochondria the import was still reduced.

A membrane potential measurement (section 2.6.9) showed that the electrochemical gradient at the inner membrane of *zim17_{ri}* mitochondrial was depleted (figure 3.29 B), indicating that the observed import deficiency of the mutant cells is probably a secondary effect due to the loss of respiratory competence of *zim17_{ri-3a}* and *-3b* mitochondria.

3.5.5.2. Preprotein import in respiratory-competent *zim17* mitochondria

To assess the import rates of respiratory-competent *zim17_{rc}* mitochondria, import reactions were carried out for 40 min as described in section 2.6.2.1 and analysed via SDS-PAGE and Western blot followed by digital autoradiography. Signals were

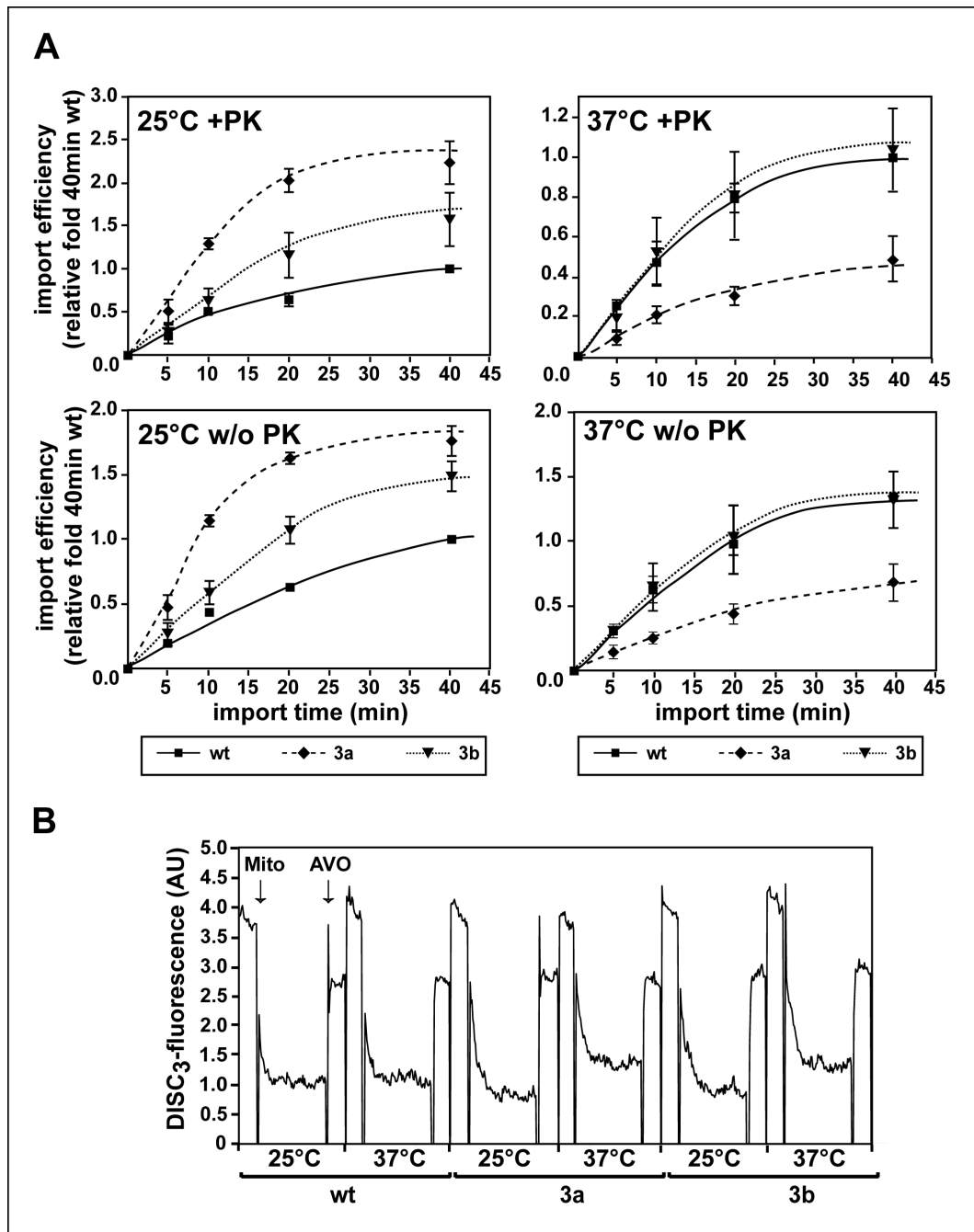


Figure 3.30.: Import phenotype of *zim17_{rc}* mitochondria. (A) Import of Su9(86)-DHFR. The [³⁵S]-labeled preprotein Su9(86)-DHFR was incubated with isolated *zim17_{rc}* mitochondria as described in section 2.6.2.1. Samples were taken at the indicated time-points, divided into halves and treated with proteinase K or water as a control and analysed as described in figure 3.29. Each data point shows the mean value of at least three independent experiments. **(B)** Membrane potential. The electric membrane potential ($\Delta\Psi$) of isolated *zim17_{rc}* mitochondria was assessed as described in figure 3.29.

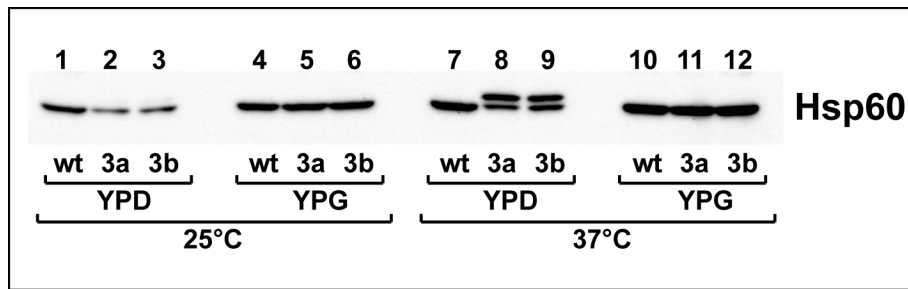


Figure 3.31.: *In-vivo* import phenotype of *zim17* mutant integrants. Respiratory competent *zim17* mutant integrants were grown to log phase in YPD and YPG medium at 25 °C and 37 °C. Protein extracts from equal amounts of cells were prepared and analysed via SDS-PAGE, Western blot and incubation with a GroEL/Hsp60 antibody.

grown on YPD at 37 °C, both *zim17-3a* and *zim17-3b* cells showed a second band slightly above the mature Hsp60 form, presumably representing an unimported pre-form of Hsp60 (figure 3.31, lanes 8+9). On YPG, even at elevated temperatures only the mature Hsp60 was visible, indicating that the observed *in organello* import defects of *zim17_{rc}-3a* mitochondria are less severe in the living cell.

3.5.5.4. Analysis of import-related functions of Ssc1 in respiratory-competent *zim17* mitochondria

3.5.5.4.1. ATP-binding properties of Ssc1

ATP-bound Ssc1 is recruited to the translocase via the scaffold protein Tim44. Hydrolysis of ATP occurs upon the binding of the incoming preprotein and is stimulated by Pam18, a class III J-protein located at the matrix surface of the inner mitochondrial membrane. The attachment of Ssc1 to the translocase during this process enables Ssc1 to exert an inward-directed force ('pulling') on the incoming protein. As *zim17_{rc}-3a* mitochondria showed a diminished import at elevated temperatures, the ability of Ssc1 to generate an inward-directed translocation force on preproteins in transit was tested in wt and mutant mitochondria. The activity of Ssc1 is dependent on its ability to interact with ATP. It was shown previously that Zim17 does not act as a nucleotide exchange factor and does not stimulate the ATPase activity of Ssc1. Therefore, its influence on the general ability of Ssc1 to bind to the nucleotide was assessed. *Zim17_{rc}* mitochondria were lysed in a Triton-X-100-containing buffer and subjected to immobilized ATP as described in section 2.6.6.1.2. The binding to ATP in *zim17_{rc}-3a* and *-3b* mitochondria was indistinguishable from the wt, revealing

that the general ability of Ssc1 to interact with ATP is not diminished in the *zim17* mutants (figure 3.32 A).

3.5.5.4.2. *Zim17* mutants show an intact inward directed translocation force

To measure the ability of Ssc1 to generate an inward directed translocation force in *zim17_{rc}* mitochondria, import reactions applying the preprotein b₂(167)_ΔDHFR were carried out in the presence of the DHFR-ligand MTX as described in section 2.6.3. The ts mutant *ssc1-2* is known to display a pulling defect due to a mutation in its substrate-binding domain (Voisine 1999) and was therefore used as a control. Import reactions were carried out for 20 min at 25 °C and subsequently treated with proteinase K. The amount of protease-resistant b₂(167)_ΔDHFR was determined in relation to the total amount of imported protein. As the general import efficiencies of wild type and mutant mitochondria differed, all signals were normalized to the total amount of imported protein that was trapped in the import channel. While *ssc1-2* mitochondria showed a reduction in the pulling activity after a 15 min heat treatment at 37 °C, accumulated translocation intermediates remained largely protease-resistant in all measured *zim17* mutants, implying that ATP-hydrolysis and the interaction of Ssc1 with the translocase complex of the inner mitochondrial membrane are still intact in the *zim17* mutants.

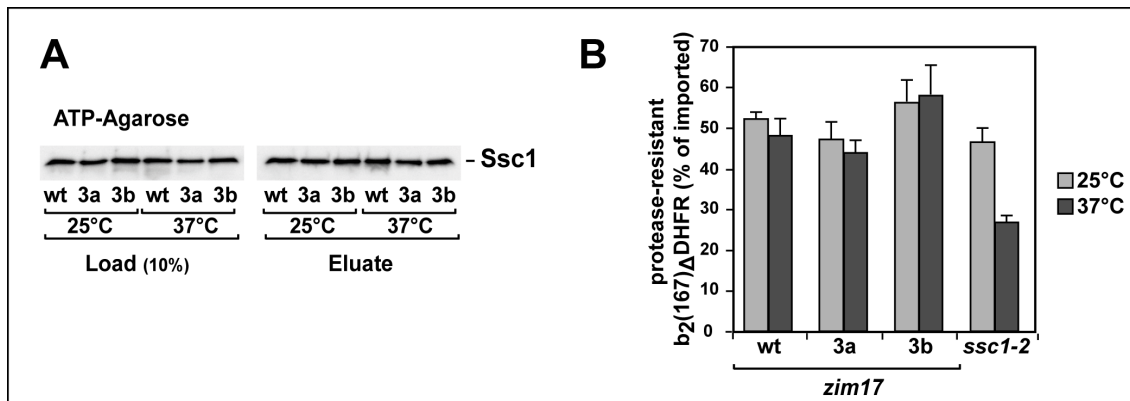


Figure 3.32.: Ssc1 nucleotide-binding and 'pulling' activity in *zim17_{rc}* mitochondria. (A) Binding of Ssc1 from *zim17_{rc}* mitochondria to ATP-agarose. Isolated mitochondria of wild-type and *zim17* mutants were lysed as described under 'experimental procedures' and subjected to ATP-agarose. Bound proteins were eluted with Laemmli-buffer and analysed via SDS-PAGE and immunoblotting with a Ssc1-specific antibody. **(B)** Ssc1-dependent pulling activity on preproteins in transit in *zim17_{rc}* mitochondria. Radiolabeled $b_2(167)\Delta$ DHFR with the prebound DHFR ligand MTX was incubated with isolated *zim17_{rc}*-wt, -3a -3b and *ssc1-2* mitochondria to accumulate translocation intermediates. The import was terminated after 20 min at 25 °C and samples were assayed as described in section 2.6.3. Protease-resistant $b_2(167)\Delta$ DHFR was assayed by SDS-PAGE and digital autoradiography. The graph represents the mean values of three independent experiments.

3.5.5.4.3. *Zim17* mutants show a diminished Ssc1-interaction with newly imported substrate proteins

To assess if the import defect in *zim17_{rc}*-3a mitochondria is due to a diminished substrate interaction of Ssc1, a co-immunoprecipitation experiment was performed. Radiolabelled Su9(86)DHFR was imported 20 min in *zim17_{rc}* mitochondria. After the import reaction was stopped, samples were divided into two halves. One half was further incubated at 25 °C for 15 min, the other half was directly subjected to immunoprecipitation. Mitochondria were lysed under native conditions and immunoprecipitations were carried out. Samples were assayed by SDS-PAGE and the signals obtained by digital autoradiography were quantified. Due to the differing import efficiencies, the amounts of co-precipitated Su9(86)DHFR were set in relation to the total amounts of imported protein for each mutant. As both mutants showed slightly differing levels of Ssc1 and a partial Ssc1 aggregation phenotype at non-permissive temperature, the amounts of precipitated Ssc1 differed between the samples. Therefore, the relative amounts of co-precipitated substrate were additionally normalized to the precipitation efficiency. At permissive temperature, 5% of newly imported Su9(86)DHFR could be co-precipitated with Ssc1 from wt mitochondria (figure 3.33). As the interaction of Ssc1 with substrate proteins is transient, the

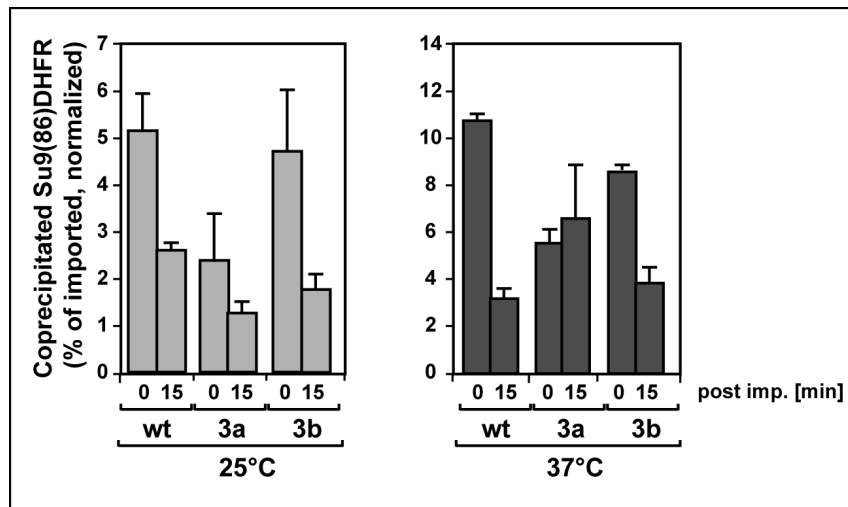


Figure 3.33.: Interaction of Ssc1 from *zim17_{rc}* mitochondria with newly imported substrate proteins. Radiolabeled Su9(86)-DHFR was imported into isolated *zim17_{rc}* mitochondria. The import was terminated after 20 min at 25 °C and samples were further incubated at 25 °C for 15 min. Mitochondria taken at the time-points indicated were lysed, and Su9(86)DHFR were co-immunoprecipitated using Ssc1 antiserum. Co-precipitated Su9(86)DHFR was assayed by SDS-PAGE, Western blot and digital autoradiography. Signals from at least three independent experiments were quantified and the substrate-binding efficiency of Ssc1 was calculated as described in the text. Error bars represent the standard errors of at least 3 independent experiments.

amounts of co-precipitated Su9(86)DHFR were reduced approximately 2-fold after 15 min of post-import incubation. At non-permissive temperature, the overall yield of co-precipitated substrate was higher than at 25 °C, probably due to higher metabolic rates at elevated temperatures. The association of Ssc1 with preprotein in *zim17_{rc}-3b* mitochondria was indistinguishable from wt under permissive conditions. After heat-treatment, *zim17_{rc}-3b* mitochondria displayed a slightly reduced association of Ssc1 with its substrate in heat shocked mitochondria, nevertheless, the substrate was released from Ssc1 after a 15 min post-import incubation in a wt-like manner. In contrast, a significant decrease in the amount of co-precipitated Su9(86)DHFR was measured in *zim17_{rc}-3a* mitochondria already under permissive conditions. After a 16 h heat treatment at 37 °C, only 6% of the total amount of imported Su9(86)DHFR could be co-precipitated with Ssc1. Taken together, *zim17_{rc}-3a* shows a temperature-independent defect in the interaction with newly imported substrate proteins at the translocation channel that might contribute to the import deficiency observed in the mutant.

3.5.5.5. Analysis of matrix functions of Ssc1 in respiratory-competent *zim17* mitochondria

3.5.5.5.1. Binding of Ssc1 to immobilized model substrates

To examine the interaction of Ssc1 with substrates in the mitochondrial matrix independently from the processes that take place at the import channel, an *in vitro* substrate interaction assay using the unfolded model substrate RCMLA was performed section 2.6.6.2. Mitochondrial lysates were prepared under native conditions. To exclude aggregated Ssc1 from the reaction, all lysates were subjected to a 30 min centrifugation step at 45 000 x g. Soluble fractions were incubated with immobilized RCMLA and analysed as described in figure 3.34. Surprisingly and in contrast to its diminished binding to newly imported substrate proteins in the *zim17-3a* mutant, the interaction of Ssc1 with RCMLA was stable in the *zim17_{rc}* mutants under permissive and non-permissive conditions (figure 3.34 A).

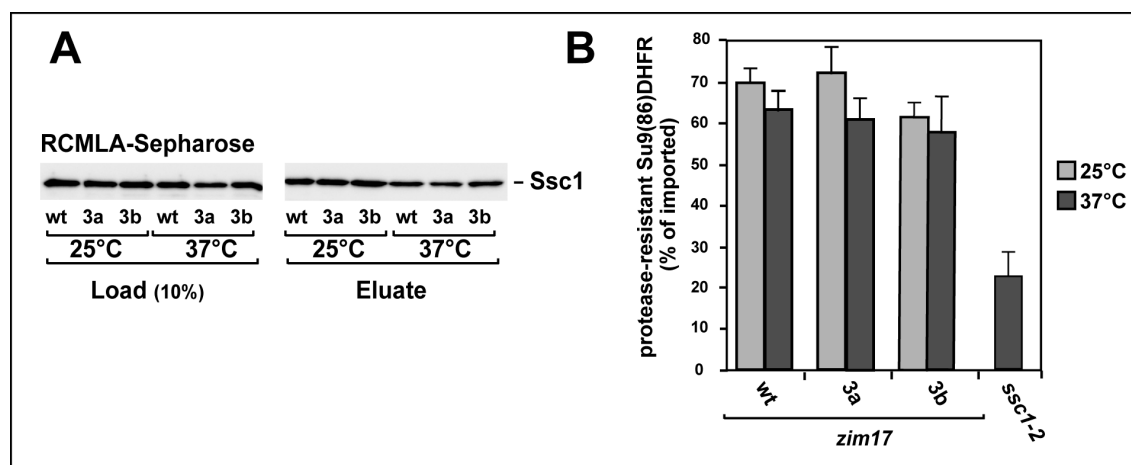


Figure 3.34.: Ssc1 substrate-binding and 'folding' activity in *zim17_{rc}* mitochondria. (A) Binding of Ssc1 from *zim17_{rc}* mitochondria to RCMLA-sepharose. Mitochondrial lysates were prepared as described in the text and subjected to RCMLA-Sepharose. Bound proteins were eluted with excess ATP and analysed via SDS-PAGE, Western blot and incubation with an antibody against Ssc1. **(B)** Folding activity of Ssc1 in wild-type and *zim17* mutants. Radiolabeled Su9(86)-DHFR was denatured with 7 M urea and imported into the indicated isolated mitochondria. The import was terminated after 5 min at 25 °C and mitochondria were lysed and treated with proteinase K. Samples were analysed via SDS-PAGE, autoradiography and quantification of seven independent experiments.

3.5.5.5.2. *Zim17* mutants show an intact folding activity of Ssc1

To further assess the folding capacity of Ssc1 in the *zim17_{rc}* mutants, a specific assay employing the protein Su9(86)DHFR was performed. Urea-denatured Su9(86)DHFR

was imported into isolated *zim17_{rc}* mitochondria for 5 min and the protease-resistance of imported DHFR was determined as described in section 2.6.4. As expected, *ssc1-2* mutant mitochondria, that were used as a control, displayed a strong folding defect (figure 3.34 B). In contrast to the Ssc1-deficiencies that were observed during the import reaction, the folding capacities of in *zim17_{rc}* mutant mitochondria were indistinguishable from the wt.

4. Discussion

4.1. Co-expression with Zim17 is a suitable method to purify functional recombinant Ssc1.

The interaction of Zim17 with the main mitochondrial Hsp70 protein Ssc1 has been characterized in several studies and most likely occurs under nucleotid-free conditions (Blamowska 2010; Sichting 2005). Zim17 is known to prevent the aggregation of Hsp70s in the mitochondrial matrix of *S.cerevisiae* (Sichting 2005) and in the cytosol of *E.coli* cells (Momose 2007). Recent studies using yeast deletion mutants (*zim17* Δ) showed that both mitochondrial Hsp70s, Ssc1 and Ssq1, had a high tendency to aggregate and that the ATPase domain of newly imported Ssc1 is unable to fold properly in the absence of Zim17 (Blamowska, Neupert and Hell 2012). In this work, the aggregation-protective character of Zim17 was utilized to study the interaction of Zim17 with Ssc1, the main yeast mitochondrial Hsp70 protein, in an *in vitro* approach. As Ssc1 is known to form insoluble aggregates when it is expressed in *E.coli* cells, its recombinant expression and purification for *in vitro* experiments is difficult and time-consuming. Co-expression with Zim17 could thus pave the way for a quick and easy purification of recombinant Ssc1 from *E.coli* cells under native conditions. Three different plasmids (pDB10, pIL1 and pIL2) that originate from the vector pETDuet (Novagen) were used for the co-expression of His-tagged Ssc1 and Strep-tagged Zim17 in *E.coli* cells. PETDuet contains two multiple cloning sites, each with its own T7-promotor and ribosome binding site. Expression from pDB10, that derives from the unmodified pETDuet vector, resulted in high levels of Zim17 compared to small quantities of Ssc, probably due to the largely differing lengths of the proteins. A modification of the plasmid by removing the T7 promotor in front of the second multiple cloning site (pIL1) resulted in transcription of both the *SSC1* and the *ZIM17* gene on a single mRNA and improved the ratio of Zim17 and Ssc1.

However, Zim17 was still overexpressed in comparison to the Hsp70 chaperone with a Zim17-Ssc1 ratio of approximately 3:1. Additional deletion of the second ribosome binding site upstream of the *ZIM17* insert (pIL2) yielded Zim17-levels that were lower than the amounts of Ssc1 with an approximate Zim17-Ssc1 ratio of 1:5. Thus, expression from pIL2 closer resembled the proportions of Zim17 and Ssc1 in the matrix of yeast mitochondria.

Expression from pIL2 resulted in a partial aggregation (approximately 50%) of Ssc1 in *E.coli* cells. Even when Zim17 was expressed in saturated amounts (pIL1), 50% of the co-expressed Ssc1 was found in the insoluble fraction of the *E.coli* lysates. However, the co-expression system allowed the purification of the remaining 50% of soluble Ssc1 under native conditions. Binding assays with immobilized ATP showed that the nucleotid-binding properties of the purified Ssc1 were preserved. It has to be noted that Ssc1 could not be eluted from the column with excess ATP, indicating a diminished ability to hydrolyse ATP or to release the bound ADP from its nucleotide-binding pocket after hydrolysis. These defects, however, are most likely derived from the lack of the nucleotide exchange factor Mge1 and the J-protein Mdj1 that stimulates the ATP hydrolysis of Ssc1 *in vivo*. When an elution with Lämmli buffer was performed, Ssc1 and Zim17 were eluted together from the ATP column. In summary, the experiments show that the expression of Ssc1 in the presence of Zim17 provides an efficient method to express and purify relatively large amounts of Ssc1 from *E.coli* under native conditions. The purified chaperone is still functional as its ability to interact with immobilized nucleotides is preserved. Nevertheless, it was not possible to purify Zim17-free Ssc1 as the binding of Zim17 to the chaperone seems to be relatively stable. This, however, may not be a problem in the presence of other components of the Ssc1 chaperone system that potentially exclude the binding of Zim17 (Goswami, Chittoor and D'Silva 2010). Furthermore, there is no hint that Zim17 functionally interferes with other Ssc1 cochaperones. The Ssc1-Zim17 co-expression system is thus a suitable method to purify soluble Ssc1 for *in vitro* experiments.

4.2. Recombinant Zim17 tends to form dimers in solution but interacts with Ssc1 as a monomer

The interaction behaviour of Zim17 and Ssc1 was studied via gel filtration analysis. Interestingly, Zim17 eluted at the size of a dimer but seemed to interact with Ssc1 in a monomeric form. Zim17 that was expressed in the absence of Ssc1 occurred almost completely in the dimeric form, confirming that the dimerization occurs independently of its interaction with Ssc1. The occurrence of dimeric forms has also been observed for the human Zim17-orthologue Hep1 (Zhai 2008) and the chloroplast Zim17 orthologue HEP2 (Willmund 2008), raising the question for their functional importance. Similarly, it was shown in a recent study (Dores-Silva 2013) that recombinant human Hep1 eluted mainly at the size of an apparent dimer (29.6 kDa) in FPLC experiments. However, it was pointed out that an asymmetric monomeric form of Hep1 would elute at the same size. Thus, the apparent dimeric form of Zim17 could just represent a different conformation of the monomeric protein in its unbound state. However, recombinant Hep1 showed the tendency to form concentration-dependent oligomers and the structural stability of the oligomers and the monomer was furthermore dependent on the presence of zinc (Dores-Silva 2013). The stabilising role of the zinc atom in yeast Zim17 has been directly demonstrated in other studies. Recombinant Zim17 mutants that were carrying a mutation in one of the zinc-chelating cysteines and thus were unable to bind their ligand, were aggregating in *E.coli* cells (Momose 2007). Furthermore, molecular dynamics (MD) simulations showed that the Zn^{2+} ion stabilised the whole Zim17 molecule through local and long range effects mediated by the coordinating cysteines C75 and C100 (Fraga 2012). Interestingly, these effects particularly affect the region around the residues R106, H107 and D111 that have been implicated to take part in the interaction with Hsp70 (Fraga 2012; Momose 2007; Zhai 2011). In accordance with these results, Zim17 zinc finger mutants that were generated in this work aggregated after recombinant expression in *E.coli* (section 3.2.2). However, upon import of their precursor forms into the mitochondrial matrix, the zinc finger mutants remained soluble (section 3.2.3), pointing towards a less severe and maybe more specific effect of the zinc ligand under *in vivo* conditions.

An example for the stabilising effect of a zinc ligand in mitochondrial proteins is represented by the small IMS-proteins Tim9 and Tim10 that assist in the import of mitochondrial membrane proteins. In the IMS, Tim9 and Tim10 proteins form

disulfide-bonds between their zinc-chelating cysteine residues and are found in hexameric heterocomplexes (Lu 2004; Webb 2006). Nevertheless, the binding of zinc seems to stabilise newly synthesised monomeric Tim10 in the cytosol to maintain it in a reduced, import-competent state (Lu and Woodburn 2005). However, import of Tim9 and Tim10 seems to occur preferential in their zinc free apo-form (Morgan 2009). A spontaneous cysteine oxidation in the absence of zinc, resulting in disulfide bonds between the cysteine residues, could not be detected in Zim17 (Fraga 2012). Moreover, while the intermembrane-space protein Mia40 assists in the folding and complex formation of newly imported Tim9 and Tim10 (Müller 2008), a comparable import pathway is not known to occur in the mitochondrial matrix. Thus, functional or structural similarities of Zim17 with the small Tim proteins are unlikely. It cannot be excluded that Zim17 is stabilised by binding to cytosolic zinc prior to its import. However, as zinc-binding induces a stably folded conformation, it is unlikely that Zim17 is imported in its zinc-chelated form. As the binding of zinc to Zim17 is fast and relatively stable (Fraga 2012), the zinc atom would have to be removed or zinc-binding would have to be prevented by a cytosolic factor prior to the import reaction. The presence of such an unknown cytosolic factor has already been suggested to facilitate the import of Tim9 and Tim10 (Morgan 2009) and might also be important for the import of other metal-chelating proteins.

Apart from the special role of the zinc atom during the biogenesis pathway of the small Tim proteins, a stabilising role of ligands has also been shown for a diversity of other metal chelating proteins (Cunningham, Mulkerrin and Wells 1991; Maret 2005; McCall, Huang and Fierke 2000; Namuswe and Berg 2012). For some of these proteins, the metal-binding region seems to be directly involved in dimerization events or even forms the dimerization site itself (Chantalat 1999; Cunningham, Mulkerrin and Wells 1991; Frankel, Bredt and Pabo 1988; Maret 2005; McIntyre 1993). However, none of those proteins shows structural or functional similarities with Zim17, potentially excluding a role the zinc binding domain in its dimerization. The N-terminal domain of Zim17 (amino acids 64-112, Vu 2012) involves its zinc-chelating residues and the conserved His107 and D111 that are believed to be part of the Ssc1-interaction site (Momose 2007; Zhai 2011). However, not much is known about the function of the C-terminal domain of Zim17 (amino acids 112-160). Fluorescence emission spectroscopy data of human Hep1 using the conserved W115 in its C-terminal region as an internal probe, indicated that W115 itself might be part of the oligomerization interface of human Hep1 (Dores-Silva 2013) raising the

question if this region might be involved in Zim17 oligomerization.

Taken together, the phenomenon of putative Zim17 oligomers and dimers and the precise role of the zinc ligand remain to be clarified. As oligomerization of Zim17 seems to take place in the absence of a Hsp70 binding partner, it could provide an inactive storage form of the protein. This would make sense when no zinc is available to stabilise the monomer and to render the protein into a functional state. However, not only the monomeric but also the oligomeric forms of Zim17 seem to display a higher stability in the presence of the zinc ligand, raising more questions about its functional significance. Further studies will be necessary to elucidate the relationship between zinc-binding, oligomerization and function of Zim17.

4.3. Dependence of the Zim17-interaction on the nucleotide-binding state of Ssc1

The interaction of Zim17 with mtHsp70s occurs most likely in the absence of nucleotides (Blamowska, Neupert and Hell 2012; Sichting 2005). Nevertheless, it has been demonstrated that the human Zim17 orthologue Hep1 can also interact with mtHsp70 in the presence of ATP or ADP, though with reduced efficiency (Goswami, Chittoor and D'Silva 2010; Zhai 2008). Furthermore, the human Hep1 is known to stimulate the ATP hydrolysis activity of mtHsp70 (Zhai 2008) and thus must be able to bind to the chaperone in the presence of ATP.

In ATP-binding experiments using FPLC-purified components, Zim17 was eluted together with Ssc1 from immobilized ATP, indicating a stable, nucleotide-independent interaction between the two proteins. However, as other components of the Hsp70 system were missing in the experiment, it is unclear if the Zim17 binding to Ssc1 is as stable under *in vitro* conditions. A study on human mitochondrial Hsp70 chaperones with an impaired J-protein interaction showed enhanced binding to the Zim17-orthologue Hep1. Moreover, the binding sites for the J-protein Tid1 and Hep1 at the ATPase-Domain of mtHsp70 are mutually exclusive (Goswami, Chittoor and D'Silva 2010). It is thus possible that binding of Zim17 to Ssc1 is weakened preferentially during a stage of the Hsp70 reaction cycle where other cochaperones displace Zim17.

To revise the nucleotide-dependency of the Zim17-Ssc1 interaction, a Ni-NTA pull-down experiment applying mitochondria from a yeast strain carrying a Ssc1-His gene was performed. Zim17, like the nucleotide-exchange factor Mge1, coeluted with

Ssc1-His under nucleotide-free conditions while the J-protein Mdj1 bound to Ssc1 in the presence of ATP. In a second approach, the binding of Ssc1 to immobilized Zim17 was examined. Ssc1 bound to Zim17 under both ATP and nucleotide-free conditions. However, the experiments were perturbed by a high background of Zim17 interacting with the crude column material was observed. Furthermore, it cannot be excluded that Ssc1 interacts with the immobilized Zim17 in a substrate-like manner. Taken together, the experiments confirm that Zim17 seems to bind to Ssc1 preferably in the absence of nucleotides. However, as observed under *in vitro* conditions in experiments with immobilized ATP, an interaction in the presence of nucleotides seems to be generally possible and might also occur *in vivo*, though to a much lower extent.

4.4. Expression of Zim17 conditional mutants in a *zim17* Δ genetic background is not suitable for the direct analysis of Zim17 functions

Previous studies applying yeast deletion mutants (*zim17* Δ) showed that both mitochondrial Hsp70s, Ssc1 and Ssq1, had a high tendency to aggregate and that the ATPase domain of newly imported Ssc1 is unable to fold properly in the absence of Zim17 (Blamowska, Neupert and Hell 2012; Blamowska 2010). However, a direct analysis of Zim17 functions under these conditions was difficult due to the accumulation of severe secondary defects caused by the aggregation of mtHsp70s. To overcome those difficulties, a set of temperature-sensitive mutations of the *ZIM17* gene of *S. cerevisiae* from a library generated by random mutagenesis was cloned into the yeast vector pFL39 and expressed in *zim17* Δ cells under the control of their own promotor (Sanjuán Szklarz 2005). Yeasts were screened for temperature-sensitive growth behaviour and the yeast strains *zim17-2* (L40S/ L59S/ H107P), *zim17-3* (D111G, N79S) and *zim17-4* (V31A, L113P, I115T) were chosen for further analysis. For control purposes, a corresponding wt (*zim17-corrWT*) strain carrying the *ZIM17* gene on the same plasmid as the mutants was generated. A subcellular fractionation experiment and a sequence analysis of the mutants revealed that *zim17-2*, that was previously analysed by Szklarz (2005), and *zim17-4* carried mutations in the predicted Zim17 pre-sequence. In case of *zim17-2* the exchange of leucine with a neutral serine at position 40 probably interferes with its import into the mitochondrial matrix, leading to virtually undetectable amounts in the mitochondrial matrix. Zim17-4 that carries an alanine instead of a valine at position 31 was found in the mitochondrial

fraction, though in much lower amounts than Zim17-corrWT and Zim17-3.

PFLzim17-ts3-CEN (*zim17-3*), pFLzim17-ts4-CEN (*zim17-4*) and the corresponding wt plasmid were transformed into a respiratory-deficient *zim17* Δ -strain. Expression of Zim17-corrWT in the *zim17* Δ background were able to rescue the temperature-sensitive phenotype. Furthermore, *zim17-3*, *zim17-4* and *zim17-corrWT* apparently had regained their respiratory competence as they were viable under non-fermentable (YPG) conditions. However, growth on YPD lead to a relapse of the respiratory-incompetent phenotype in the mutants as well as in *zim17-corrWT* cells. As expression of wild type Zim17 did not fully rescue the respiratory-deficient phenotype of the original *zim17* Δ cells, it has to be assumed that the loss of respiratory competence is not a direct effect of the lack of Zim17 but more likely derives from an accumulation of secondary effects due to the *ZIM17* deletion.

On the molecular level, the expression of *zim17-corrWT* and *zim17-3* lead to a high overexpression of both proteins, probably as a response to the lack of Zim17 in the Δ mutant. Moreover, Ssc1 showed a severe aggregation in the corresponding wild type as well as the *zim17-3* mutant even at a permissive temperature of 25 °C. The *zim17-4* mutant exhibited lower expression levels of Zim17 and a more temperature-sensitive aggregation-behaviour of Ssc1, nevertheless, also in this mutant a considerable aggregation of Hsp70 chaperone was already observed at 25 °C.

Zim17 Δ mutants tend to accumulate primary and secondary effects as a consequence of mtHsp70 loss of function. These include important processes like the import of pre-proteins and the biogenesis of Fe/S cluster proteins (Sanjuán Szklarz 2005; Sichtung 2005). As these deficiencies result in the formation of dysfunctional mitochondria, the inability of wt Zim17 to fully rescue the growth and aggregation phenotype of these cells could be explained. The recombinant expression of conditional *zim17* mutants in the *zim17* Δ genetic background consequently leads to a mixture of primary and secondary effects that are not fully distinguishable. Thus, the recombinant expression of *zim17*-mutants in *zim17* Δ cells is not suitable to study the direct consequences of a Zim17 loss-of-function.

4.5. Two novel genomic integrated *zim17* mutants show a temperature-sensitive phenotype combined with an instable respiratory deficiency

To obviate the described accumulation of secondary effects, two conditional *zim17* mutants were integrated into the genome of the *S.cerevisiae* YPH499 wt strain under the addition of the *LEU2* marker. The mutant *zim17-3a* derives from the recombinant mutant *zim17-3* and contains a mutation at residue D111 that belongs to the conserved DNL-motif of Zim17 and is believed to be part of the interface for the interaction with Ssc1 (Momose 2007). Similarly, the human Zim17 orthologue Hep1 showed a dependence on residue D111 in its interaction with the Hsp70 chaperone HSP9A (Zhai 2011). The random mutagenesis thus confirms the importance of the D111 site in Zim17. *Zim17-3a* carries a second mutation at the less conserved residue N79 that is in direct neighbourhood to one the zinc-chelating residues (C78) of Zim17. In order to distinguish the effects of the different point mutations, the strain *zim17-3b*, that contains only the D111G mutation, was constructed.

Zim17-3a and *-3b* were successfully integrated into the yeast genome while the integration of a third mutant, *zim17-4* (V31A, LI113/115PT), did not yield any viable positive clones. While the D111G mutation from *zim17-3* has been characterized previously (Momose 2007; Zhai 2011), the functional significance of the mutated residues in *zim17-4* is not known. It thus remains elusive if the integration of *zim17-4* failed because the respective mutations are probably lethal or due to technical problems.

While the original *zim17-3a* and *-3b* mutant integrants were not able to grow on non-fermentable carbon sources and thus showed a respiratory-deficient phenotype, a random spore analysis yielded a mixture of respiratory-competent (*zim17_{rc}*) and respiratory-incompetent (*zim17_{ri}*) mutant cells. The corresponding wt cells showed a 100% respiratory competence. For *zim17-3b*, the proportion of respiratory-competent cells was higher (74% of tetrades) than for *zim17-3a* (36.6% of tetrades). Further experiments revealed that the respiratory deficiency could be induced by growth on a fermentable carbon source as it was already observed for the recombinant mutants *zim17-3* and *zim17-4*. However, a high temperature treatment did not induce respiratory deficiency. In summary, both *zim17* mutant integrants showed a temperature-sensitive phenotype going along with an instable respiratory competence. Thus, this data confirms that the respiratory deficiency is not a direct effect of the

loss of functional Zim17 but derives from secondary effects that are most likely due to the concomitant loss of functional mtHsp70s. To characterize the direct and secondary effects of the Zim17 loss of function on yeast mtHsp70s *zim17_{rc}* and *zim17_{ri}* mutants were analysed separately.

4.6. The respiratory instable phenotype of conditional *zim17* mutants derives from a deficient mitochondrial Fe/S cluster biogenesis as a consequence of mtHsp70 loss of function

A biochemical analysis of *zim17_{ri}* mutant integrants revealed defects in mtHsp70-dependent processes. Zim17-3a and -3b were expressed in slightly higher amounts than Zim17-wt in the *zim17_{ri}* cells. Both *zim17-3a* and *-3b* showed a substantial aggregation of the two mtHsp70 chaperones Ssc1 and Ssq1 already at a permissive temperature of 25 °C. The second yeast mtHsp70 chaperone Ssq1 plays a role in the biogenesis of mitochondrial Fe/S proteins and is believed to promote the transfer of the Fe/S cluster from the scaffold protein Isu1 to its apo-protein in the biogenesis of mitochondrial Fe/S cluster proteins (Dutkiewicz 2006). In mitochondria, Fe/S clusters are found in proteins of the respiratory chain complexes and in aconitase, an enzyme of the citric acid cycle (Lill and Mühlenhoff 2008; Lill 2006). *S. cerevisiae* with defects in the Fe/S cluster biogenesis are known to display a decrease in proteins of respiratory metabolism (Hausmann 2007, Lill 2012 and references therein). Indeed, the levels of proteins of the respiratory chain and the citrate cycle were downregulated to almost non-detectable amounts in the *zim17_{ri}* mutant integrants. Furthermore, a complete loss of iron-sulfur cluster containing proteins like aconitase and Rip1 was observed. A decrease of aconitase has been shown previously in *zim17Δ* cells and was linked to the loss of function of Ssq1 in these cells (Sichting 2005). The loss of aconitase observed in this study was induced by growth of originally respiratory-competent cells on YPD. While aconitase levels were reduced to non-detectable amounts already after 6-12 h of incubation on YPD, cells became respiratory-deficient after 24 h on the fermentable carbon source, supporting the idea that the respiratory incompetence derives from ongoing damages in the Ssq1-mediated steps of Fe/S biogenesis.

Analyses of the levels of other proteins in *zim17_{ri}* mitochondria revealed no further abnormalities. The expression of Ssc1 and Ssq1 themselves along with their J-proteins Pam18, Mdj1 and Jac1 was stable in the respiratory-deficient mutants. The only

exception was the Ssq1 substrate Isu1 that showed a substantial upregulation in the mutants. Elevated levels of Isu1 have been observed previously in cells lacking components of the mitochondrial Fe/S cluster assembly machinery and are caused by an up-regulated protein expression both at a translational and posttranslational level (Andrew 2008). The Isu1-upregulation thus further indicates a defective Fe/S biogenesis in the *zim17_{ri}* mutants.

Zim17 mutant cells displayed a respiratory-competent phenotype (*zim17_{rc}*) as long as they were forced to grow under non-fermentable conditions. In contrast to its expression levels in *zim17_{ri}* cells, Zim17 itself was expressed in lower levels in both mutants. Similarly, the levels of Ssq1, the Fe/S biogenesis chaperone were strongly downregulated and showed an almost complete aggregation in the *zim17_{rc-3a}* mutant at elevated temperatures. This behaviour was reflected by significant alterations in the amounts of Isu1 and the Ssq J-domain partner Jac1 after a 37°C heat treatment. It has been shown that Jac1 is able to interact with Isu1 independently (Andrew 2006; Dutkiewicz 2006) and it is widely accepted that holo-Isu1 and Jac1 form a complex first and are together recruited to the Hsp70 chaperone by interaction of Jac1 and Ssq1. The Isu1-upregulation and the presence of Jac1 are critical for the survival of yeasts in the absence of Ssq1. Hence, it is likely that growth of the *zim17* mutant cells under non-fermentable conditions induces an adaptive process in the gene expression leading to an improved conservation of mitochondrial functions, in particular respiratory competence. The overexpression of Jac1 might be able to enhance the substrate affinity of mtHsp70s for Isu1. Since the levels of Ssq1 are reduced in the *zim17* mutants, it is also likely that the role of Ssq1 is partially taken over by Ssc1 under these conditions. This is corroborated by the observation that an artificial overexpression of Jac1 is able to shift the function of Ssq1 in Fe/S cluster biogenesis to Ssc1 and rescue the growth defects of *ssq1Δ* mutants (Schilke 2006). The high temperature-dependent overexpression of Ssc1 in both *zim17_{rc}* mutants further supports this hypothesis.

In support of these results, no significant reductions in the levels of respiratory enzymes or Fe/S proteins were observed in the respiratory-competent *zim17* mutants. However, a loss of activity of the Fe/S-protein aconitase that was going along with a defective Fe-incorporation into the enzyme was measurable in *zim17_{rc}* mitochondria (Lewrenz et.al, submitted). In conclusion, the initial damage of mitochondrial Fe/S biogenesis in the *zim17*-mutants over time could emerge in a respiratory-deficient phenotype on non-fermentable carbon sources where no protec-

tive mechanisms are induced in the mutants. Taken together, this data confirms that the respiratory instable phenotype of *zim17* mutants most likely displays a long-term effect deriving from a defective Fe/S biogenesis as a consequence of a Ssc1 loss of function. Hence, the temperature-sensitive lethal phenotype of our *zim17_{rc}* mutant cells most likely correlates with a functional defect of the main mtHsp70 Ssc1.

4.7. Zim17 exerts a direct supportive function on Hsp70 activities independent of its aggregation-protective role

Hsp70 chaperones showed a strong aggregation even at permissive temperature in respiratory-deficient *zim17_{ri}* mutant cells. *In vivo* import experiments with *zim17_{ri}* cells revealed a deficient import, at an elevated temperature of 37°C, favouring the theory of a direct influence of Zim17 on the matrix-destined preprotein import. A diminished matrix import has also been shown in *zim17Δ* cells. However, as both *zim17Δ* and *zim17_{ri}* mitochondria are known to be respiratory unstable, one has to take into consideration, that the membrane potential $\Delta\Psi$ of these mitochondria might be low.

As measurements confirmed that the *zim17_{ri}* mutants showed a disrupted inner membrane potential, *in organello* import experiments were carried out in the presence of excess ATP and denatured preproteins. The import into both *zim17_{ri}-3a* and *zim17_{ri}-3b* was diminished not only in comparison to the respiratory-competent *zim17-wt* cells but also in comparison to a respiratory-incompetent, $\Delta\Psi$ -deficient YPH499 strain (YPH499 rho⁻). Thus, the diminution of import seems to be a direct effect of the *zim17* mutations and is only partly deriving from the lack of $\Delta\Psi$. However, as large amounts of Ssc1 were aggregating in the mutants, it cannot be excluded that the observed import defect is solely deriving from a lack of soluble Ssc1 under these conditions.

The aggregation phenotype of *zim17_{rc}* cells was temperature-dependent and less severe than in the *zim17_{ri}* mutants. Interestingly, the import into both *zim17_{rc}-3a* and *-3b* was increased at a permissive temperature when no Ssc1 aggregation was detected. After a 16 h heat treatment at 37°C the import into *zim17_{rc}-3a* mitochondria was decreased in comparison to wild type mitochondria while the import into *zim17_{rc}-3b* was indistinguishable from wt. The *zim17_{rc}-3a* mutant showed a more severe aggregation of mtHsp70s than *zim17_{rc}-3b*. The import rates

of the mutants thus seemed to correlate with the aggregation behaviour of Ssc1. However, as only about 30% of the total amount of Ssc1 aggregated in the *zim17_{rc}-3a* mutant after the heat-treatment leaving 70% of Ssc1 in the soluble fraction, it is unlikely that the strong import defect solely derives from the aggregation of the chaperone. Moreover, the Ssc1 aggregation phenotype does not explain the elevated import into *zim17_{rc}* mitochondria at permissive temperature.

Unexpectedly, an *in vivo* import analysis of the *zim17* mutants only showed an import defect under fermentable conditions. The alterations in the import behaviour of isolated *zim17_{rc}* mitochondria thus mirror only a slight effect that is undetectable *in vivo*. Hence, the influence of Zim17 on the enzymatic cycle of Ssc1 must be only indirectly related to the import function of the chaperone. To this end, the behaviour of Ssc1 at different points of its enzymatic cycle that are relevant for the import reaction was examined. Ssc1 is recruited to the translocase via the scaffold protein Tim44. At this position, it is able to exert an inward-directed translocation force ('pulling') on the incoming protein that is driven by a conformational change induced by ATP-hydrolysis. The ability of Ssc1 to generate an import-driving force on preproteins in transit was not affected in the *zim17_{rc}* mutants. Since both mutants further showed a wild type-like interaction of Ssc1 with ATP, their import-motor functions in general did not seem to be affected as such. Nevertheless, co-immunoprecipitation experiments revealed a reduced interaction of Ssc1 with newly imported proteins after the import reaction in the *zim17-3a* mutant. In contrast, the interaction of Ssc1 with general Hsp70 substrates *in vitro* (RCMLA) was not altered. Thus, the substrate-interaction deficiency seemed to be restricted to import-related processes that are mediated by Ssc1.

During folding reactions in the matrix compartment, Ssc1 functionally interacts with the J-protein Mdj1, a homolog of the bacterial DnaJ. Mdj1 belongs to the class I J-proteins that contain a substrate-binding domain and two zinc-binding motifs at their C-terminus. Mitochondrial Hsp70s have two more specialised J-protein interaction partners in addition to Mdj1. Pam18, a small J-protein associated with the inner membrane protein translocase TIM23, interacts with Ssc1 during the import of matrix-targeted proteins. Jac1 interacts with the second mtHsp70 chaperone Ssq1 during Fe/S cluster assembly. Both proteins are class III J-proteins and lack the typical cysteine-rich C-terminal domain of Mdj1. It is generally assumed that Pam18 does not have an intrinsic substrate-binding activity. However, Jac1 seems to be able to interact with the Ssq1-substrate Isu1 through a motif in its C-terminal

region (Ciesielski 2012). Due to its zinc finger domain, it has been presumed earlier, that Zim17 might act as one polypeptide part of a 'fractured' J-protein providing a substrate-binding motif for class III J-proteins like Pam18 and Jac1 (Burri 2004). The observed direct effect of Zim17 on the import activity of Ssc1 supports an aspect of the 'fractured' J-protein hypothesis. The diminished co-immunoprecipitation of precursor proteins with soluble Ssc1 at the import channel in the *zim17-3a* mutant demonstrates that Zim17 may directly support the interaction of Ssc1 with imported substrate proteins. In the same process, the inner membrane J-protein Pam18, consisting virtually only of a membrane-tethered J-domain, would activate the ATPase activity of Ssc1. The combined activity of both proteins would contribute to the full activity of the import motor with its core enzyme Ssc1.

Since a direct physical interaction of Zim17 with mtHsp70 substrate polypeptides has not been reported so far, the question arises how Zim17 influences the substrate-binding activity of mtHsp70s. Ssc1 is recruited to the import channel by the scaffold protein Tim44 and thus is in close proximity to incoming substrate proteins. Hence, the substrate-delivering properties that have been described for other J-proteins are dispensable for Ssc1 at the import channel (Kampinga and Craig 2010). Moreover, Jac1, the J-protein of the second Zim17-interaction partner Ssq1 is able to bind the specific substrate Isu1 and delivers it to the chaperone. It is thus likely that Zim17 rather enhances the substrate affinity of mtHsp70s than to deliver unfolded substrates to the Hsp70 chaperone. The upregulation of the specific Ssq1 cochaperone Jac1 in the *zim17_{rc}* mutants further supports this conclusion. As mentioned earlier, the specific binding of Jac1 to Isu1, confers the substrate specificity (Knieszner 2005). It is therefore possible that the upregulation of Jac1 occurs as a reaction to the diminished substrate affinity of Ssq1 in the mutants.

The interaction of Zim17 with mtHsp70s occurs most likely in the absence of nucleotides. Nevertheless, it has been demonstrated that the human Zim17 orthologue Hep1 can also interact with mtHsp70 in the presence of ATP or ADP, though with reduced efficiency. Furthermore, the interaction of Hep1 and mtHsp70 remained stable after addition of a model-substrate protein under both nucleotide-free and ATP conditions (Goswami, Chittoor and D'Silva 2010). This, together with the results of this work, would favour a model in which Zim17-binding to Ssc1 occurs after or during the initial binding of substrate and stabilises the Hsp70-substrate complex after ATP-hydrolysis to allow a more efficient interaction with the client protein. A similar task has been suggested for zinc centerII in the C-terminal

substrate-binding domain of the class I J-protein DnaJ. While zinc centerI seems to be directly involved in the interaction with unfolded substrates, it has been proposed that zinc centerII contributes to the high-affinity interaction of Hsp70s with client proteins (Linke 2003). In support of this thesis Hep1 has been shown to enhance the ATPase activity of mtHsp70s, a feature that could not be observed for the yeast Zim17 protein and may have evolved to further support the stable binding of substrates to mtHsp70. In conclusion, Zim17 seems to specifically influence the function of mtHsp70 proteins in processes that involve class III J-proteins, most likely by a mechanism that regulates the interaction of the chaperone with substrate proteins. As class I J-protein partners contain domains for the regulation of the Hsp70 substrate-affinity themselves, the function of Zim17 is dispensable in those cases. Collectively, Zim17 exerts a direct effect on the import activity of Ssc1 that differs from a simple aggregation-preventive function.

The decreased Hsp70 affinity for substrate proteins in the *zim17* mutants may also explain the elevated import into *zim17_{rc}* mutant mitochondria at permissive temperature. The faster substrate release in the mutants would consequently lead to a faster import when the ATPase- and the pulling-activity of Ssc1 are intact. At elevated temperatures, the temperature-sensitive *zim17-3a* mutant shows an even more transient substrate-binding. This, together with a lower availability of Ssc1 at the import channel caused by temperature-induced aggregation would consequently lead to a decelerated import and jamming of the TIM23 translocase. One would expect that in this situation the inward directed translocation force that Ssc1 exerts on the incoming preprotein should be diminished. Unexpectedly, the Ssc1 pulling activity of the mutants *in organello* was indistinguishable from wt. However, as the pulling activity of Ssc1 was measured in relation to the total amount of imported protein, a decrease of the inward-directed translocation force was probably masked by normalization to the lower import efficiency in the *zim17-3a* mutant and thus could not be detected under these conditions. A recent study on the enzymatic cycle of Ssc1 using purified components revealed that the binding of Ssc1 to its matrix J-protein Mdj1 is relatively stable in comparison to the binding of other Hsp70 chaperones to their J-proteins (Mapa 2010). During the Ssc1-dependent import-reaction, a prolonged substrate-binding due to a stable J-protein interaction would lead to stagnation of the import process and to jamming of the translocase (Mapa 2010). Conversely, a rapid substrate release due to insufficient substrate affinity would lead to similar consequences, raising the question of a regulatory

mechanism for Ssc1 chaperone system during the import of preproteins (Mapa 2010, see above). According to the results presented in this work, it is possible that Zim17 is part of such a regulatory mechanism.

4.8. Does the zinc finger domain of Zim17 play a role in exerting its Hsp70-supporting function?

Zim17_{rc-3a} and *-3b* mutants showed a similar phenotype, however, most of the observed effects were stronger in the *3a* than in the *3b* mutant. While both mutants showed an enhanced import activity at 25 °C, only the import of *zim17_{rc-3a}* was decreased in comparison to the wt after a 16 h heat treatment at 37 °C. Furthermore, the diminishment in the substrate-interacting activity of Ssc1 and the decrease in the activity of the Fe/S protein aconitase were much stronger in *zim17_{rc-3a}* than in *zim17_{rc-3b}* mitochondria. The aspartic acid at position 111 that is mutated in both mutants belongs to the conserved DNL-motif of Zim17 and is believed to be part of the interface for the interaction with Ssc1 (Momose 2007). Accordingly, the human Zim17 orthologue Hep1 showed a dependence on residue D111 in its interaction with the chaperone HSP9A (Zhai 2011). The additional mutation in Zim17-3a at position 79 is in direct neighbourhood to one of the four zinc-chelating cysteines in Zim17. Furthermore, it is positioned at the end of one of the β -sheets that are flanking the zinc-binding site. Alteration of the aspartic acid to a neutral serine at this position could lead to changes in the secondary structure of Zim17 that probably prevent an efficient binding of the zinc atom. It was reported recently, that zinc-free Zim17 displays an unstructured conformation and folds independently to its native structure after the addition of Zn²⁺. In particular, the coordinating cysteines C75 and C100 transmit stabilising intramolecular effects to the residues at the Hsp70 binding site (Fraga 2012). Furthermore, it was proposed that the zinc centerII of DnaJ provides a second site for interaction with the Hsp70 chaperone (Linke 2003). It is thus likely that the enhanced thermolability of Zim17-3a due to a diminished binding of zinc could be the reason for a generally more severe phenotype of *zim17-3a* mutant cells that contain the additional N79S amino acid exchange.

However, the exact role of the zinc finger domain of Zim17 could not be resolved in this work and remains elusive. Furthermore, experimental evidence if alteration of the poorly conserved residue N79 indeed influences the zinc-binding properties of

Zim17 is missing. Alternatively, it could be possible that the domain containing the zinc-chelating residues of Zim17 provides an interaction site for class III J-proteins or Hsp70-bound substrates themselves. Further investigations will need to elucidate the importance of this site and the exact mechanism of the interplay between Zim17 and the different components of the mtHsp70 chaperone system.

4.9. Is the prevention of Hsp70 aggregation a primary Zim17 function?

Why are mtHsp70s aggregating in *zim17*-mutant and *zim17* Δ cells? In the ATP-bound state the substrate-binding domain (SBD) and nucleotide-binding domain (NBD) of Ssc1 are in close proximity to each other. As soon a substrate is bound and ATP-hydrolysis has occurred the two domains are undocked. It was therefore proposed that mitochondrial Hsp70s represent a class of 70kDa heat shock proteins that are particularly prone to aggregation, probably due to flexible conformers that occur as cycle intermediates or loosely folded, *de novo* imported proteins (Blamowska 2010). In addition, it was shown that Zim17 is able to assist in the *de novo* folding of newly imported Ssc1 to a trypsin-resistant conformation in the mitochondrial matrix (Blamowska, Neupert and Hell 2012). However, no *de novo* imported Ssc1 was detectable in the aggregate pellets of *zim17_{rc}* cells under both permissive and non-permissive conditions. Thus, though newly imported Ssc1 might be less resistant to protease-treatment in the absence of Zim17, it still seems to be able to fold into a soluble conformation. The results of this work do not exclude the possibility that Zim17 is able to interact with the ATPase-domain of nucleotide-free, newly imported mtHsp70s or stays attached to intermediates in the enzymatic cycle to prevent their misfolding and subsequent aggregation. In the *zim17_{rc}* mutants, 30 and 13% of total Ssc1 aggregated after subjection to a non-permissive temperature. Due to its reduced substrate-affinity, aggregation of Ssc1 in the *zim17*-mutant mitochondria could be caused by an accumulation of substrate-free intermediates of the enzymatic cycle. It thus seems to be reasonable to assume that an enhancement of substrate affinity and the prevention of aggregation through the binding of Zim17 might just represent aspects of the same overall function. As Zim17 seems to assist mtHsp70s during a reaction cycle that is mediated by class III J-proteins, it is conceivable that the binding of other cochaperones to aggregation-prone conformers also have stabilising effects (Momose 2007).

5. Bibliography

Abe, Y (2000), 'Structural basis of presequence recognition by the mitochondrial protein import receptor Tom20.' *Cell* **100**(5), pp. 551–60.

Adam, Alexander C (2006), 'The Nfs1 interacting protein Isd11 has an essential role in Fe/S cluster biogenesis in mitochondria.' *The EMBO journal* **25**(1), pp. 174–83.

Adams, Keith L and Jeffrey D Palmer (2003), 'Evolution of mitochondrial gene content: gene loss and transfer to the nucleus.' *Molecular phylogenetics and evolution* **29**(3), pp. 380–95.

Andrew, Amy J (2006), 'Characterization of the interaction between the J-protein Jac1p and the scaffold for Fe-S cluster biogenesis, Isu1p.' *The Journal of biological chemistry* **281**(21), pp. 14580–7.

Andrew, Amy J (2008), 'Posttranslational regulation of the scaffold for Fe-S cluster biogenesis, Isu.' *Molecular biology of the cell* **19**(12), pp. 5259–66.

Baudin, A (1993), 'A simple and efficient method for direct gene deletion in *Saccharomyces cerevisiae*.' *Nucleic acids research* **21**(14), pp. 3329–30.

Bender, Tom (2011), 'Mitochondrial enzymes are protected from stress-induced aggregation by mitochondrial chaperones and the Pim1/LON protease.' *Molecular biology of the cell* **22**(5), pp. 541–54.

Blamowska, Marta, Walter Neupert and Kai Hell (2012), 'Biogenesis of the mitochondrial Hsp70 chaperone.' *The Journal of cell biology* **199**(1), pp. 125–35.

Blamowska, Marta (2010), 'ATPase domain and interdomain linker play a key role in aggregation of mitochondrial Hsp70 chaperone Ssc1.' *The Journal of biological chemistry* **285**(7), pp. 4423–31.

Bonneaud, N (1991), 'A family of low and high copy replicative, integrative and single-stranded *S. cerevisiae*/*E. coli* shuttle vectors.' *Yeast (Chichester, England)* **7**(6), pp. 609–15.

- Brachmann, C B (1998), 'Designer deletion strains derived from *Saccharomyces cerevisiae* S288C: a useful set of strains and plasmids for PCR-mediated gene disruption and other applications.' *Yeast (Chichester, England)* **14**(2), pp. 115–32.
- Bukau, Bernd, Jonathan Weissman and Arthur Horwich (2006), 'Molecular chaperones and protein quality control.' *Cell* **125**(3), pp. 443–51.
- Burri, Lena (2004), 'Zim17, a novel zinc finger protein essential for protein import into mitochondria.' *The Journal of biological chemistry* **279**(48), pp. 50243–9.
- Chacinska, Agnieszka (2004), 'Essential role of Mia40 in import and assembly of mitochondrial intermembrane space proteins.' *The EMBO journal* **23**(19), pp. 3735–46.
- Chacinska, Agnieszka (2005), 'Mitochondrial presequence translocase: switching between TOM tethering and motor recruitment involves Tim21 and Tim17.' *Cell* **120**(6), pp. 817–29.
- Chacinska, Agnieszka (2010), 'Distinct forms of mitochondrial TOM-TIM supercomplexes define signal-dependent states of preprotein sorting.' *Molecular and cellular biology* **30**(1), pp. 307–18.
- Chantalat, L (1999), 'Crystal structure of the human protein kinase CK2 regulatory subunit reveals its zinc finger-mediated dimerization.' *The EMBO journal* **18**(11), pp. 2930–40.
- Cheng, M Y (1989), 'Mitochondrial heat-shock protein hsp60 is essential for assembly of proteins imported into yeast mitochondria.' *Nature* **337**(6208), pp. 620–5.
- Ciesielski, Szymon J (2012), 'Interaction of J-protein co-chaperone Jac1 with Fe-S scaffold Isu is indispensable in vivo and conserved in evolution.' *Journal of molecular biology* **417**(1-2), pp. 1–12.
- Cunningham, B C, M G Mulkerrin and J A Wells (1991), 'Dimerization of human growth hormone by zinc.' *Science (New York, N.Y.)* **253**(5019), pp. 545–8.
- Díaz de la Loza, María Del Carmen (2011), 'Zim17/Tim15 links mitochondrial iron-sulfur cluster biosynthesis to nuclear genome stability.' *Nucleic acids research* **39**(14), pp. 6002–15.
- Ding, Feng and Nikolay V Dokholyan (2008), 'Dynamical roles of metal ions and the disulfide bond in Cu, Zn superoxide dismutase folding and aggregation.' *Proceedings of the National Academy of Sciences of the United States of America* **105**(50), pp. 19696–701.
- Dores-Silva, P R (2013), 'Structural and stability studies of the human mtHsp70-escort protein 1: An essential mortalin co-chaperone.' *International journal of biological macromolecules*.

- D'Silva, Patrick D (2003), 'J protein cochaperone of the mitochondrial inner membrane required for protein import into the mitochondrial matrix.' *Proceedings of the National Academy of Sciences of the United States of America* **100**(24), pp. 13839–44.
- D'Silva, Patrick R (2005), 'Role of Pam16's degenerate J domain in protein import across the mitochondrial inner membrane.' *Proceedings of the National Academy of Sciences of the United States of America* **102**(35), pp. 12419–24.
- D'Silva, P.R. (2008), 'Interaction of the J-protein heterodimer Pam18/Pam16 of the mitochondrial import motor with the translocon of the inner membrane', *Molecular Biology of the Cell* **19**(1), p. 424.
- Duchniewicz, M (1999), 'Dual role of the mitochondrial chaperone Mdj1p in inheritance of mitochondrial DNA in yeast.' *Molecular and cellular biology* **19**(12), pp. 8201–10.
- Dutkiewicz, Rafal (2003), 'Ssq1, a mitochondrial Hsp70 involved in iron-sulfur (Fe/S) center biogenesis. Similarities to and differences from its bacterial counterpart.' *The Journal of biological chemistry* **278**(32), pp. 29719–27.
- Dutkiewicz, Rafal (2006), 'The Hsp70 chaperone Ssq1p is dispensable for iron-sulfur cluster formation on the scaffold protein Isu1p.' *The Journal of biological chemistry* **281**(12), pp. 7801–8.
- Dyall, Sabrina D, Mark T Brown and Patricia J Johnson (2004), 'Ancient invasions: from endosymbionts to organelles.' *Science (New York, N.Y.)* **304**(5668), pp. 253–7.
- Dyck, L van (1998), 'Mcx1p, a ClpX homologue in mitochondria of *Saccharomyces cerevisiae*.' *FEBS letters* **438**(3), pp. 250–4.
- Foury, F and D Talibi (2001), 'Mitochondrial control of iron homeostasis. A genome wide analysis of gene expression in a yeast frataxin-deficient strain.' *The Journal of biological chemistry* **276**(11), pp. 7762–8.
- Fraga, Hugo (2012), 'Zinc induced folding is essential for TIM15 activity as an mtHsp70 chaperone.' *Biochimica et biophysica acta* **1830**(1), pp. 2139–2149.
- Frankel, A D, D S Bredt and C O Pabo (1988), 'Tat protein from human immunodeficiency virus forms a metal-linked dimer.' *Science (New York, N.Y.)* **240**(4848), pp. 70–3.
- Frazier, Ann E (2004), 'Pam16 has an essential role in the mitochondrial protein import motor.' *Nature structural & molecular biology* **11**(3), pp. 226–33.

- Froschauer, Elisabeth M, Rudolf J Schweyen and Gerlinde Wiesenberger (2009), 'The yeast mitochondrial carrier proteins Mrs3p/Mrs4p mediate iron transport across the inner mitochondrial membrane.' *Biochimica et biophysica acta* **1788**(5), pp. 1044–50.
- Frydman, J (2001), 'Folding of newly translated proteins in vivo: the role of molecular chaperones.' *Annual review of biochemistry* **70**, pp. 603–47.
- Gabaldón, Toni and Martijn A Huynen (2004), 'Shaping the mitochondrial proteome.' *Biochimica et biophysica acta* **1659**(2-3), pp. 212–20.
- Gakh, Oleksandr, Patrizia Cavadini and Grazia Isaya (2002), 'Mitochondrial processing peptidases.' *Biochimica et biophysica acta* **1592**(1), pp. 63–77.
- Gamsjaeger, Roland (2007), 'Sticky fingers: zinc-fingers as protein-recognition motifs.' *Trends in biochemical sciences* **32**(2), pp. 63–70.
- Geissler, Andreas (2002), 'The mitochondrial presequence translocase: an essential role of Tim50 in directing preproteins to the import channel.' *Cell* **111**(4), pp. 507–18.
- Gerber, Jana, Ulrich Mühlenhoff and Roland Lill (2003), 'An interaction between frataxin and Isu1/Nfs1 that is crucial for Fe/S cluster synthesis on Isu1.' *EMBO reports* **4**(9), pp. 906–11.
- Germaniuk, Aleksandra, Krzysztof Liberek and Jaroslaw Marszalek (2002), 'A chaperone (Hsp70-Hsp78) system restores mitochondrial DNA synthesis following thermal inactivation of Mip1p polymerase.' *The Journal of biological chemistry* **277**(31), pp. 27801–8.
- Glick, B S (1993), 'Import of cytochrome b2 to the mitochondrial intermembrane space: the tightly folded heme-binding domain makes import dependent upon matrix ATP.' *Protein science : a publication of the Protein Society* **2**(11), pp. 1901–17.
- Goswami, Arvind Vittal, Balasubramanyam Chittoor and Patrick D'Silva (2010), 'Understanding the functional interplay between mammalian mitochondrial Hsp70 chaperone machine components.' *The Journal of biological chemistry* **285**(25), pp. 19472–82.
- Gray, M W, G Burger and B F Lang (2001), 'The origin and early evolution of mitochondria.' *Genome biology* **2**(6), REVIEWS1018.
- Hartl, F Ulrich, Andreas Bracher and Manajit Hayer-Hartl (2011), 'Molecular chaperones in protein folding and proteostasis.' *Nature* **475**(7356), pp. 324–32.
- Hausmann, Anja (2008), 'Cellular and mitochondrial remodeling upon defects in iron-sulfur protein biogenesis.' *The Journal of biological chemistry* **283**(13), pp. 8318–30.

- Hell, Kai (2008), 'The Erv1-Mia40 disulfide relay system in the intermembrane space of mitochondria.' *Biochimica et biophysica acta* **1783**(4), pp. 601–9.
- Heyrovská, N (1998), 'Directionality of polypeptide transfer in the mitochondrial pathway of chaperone-mediated protein folding.' *Biological chemistry* **379**(3), pp. 301–9.
- Higuchi, R, B Krummel and R K Saiki (1988), 'A general method of in vitro preparation and specific mutagenesis of DNA fragments: study of protein and DNA interactions.' *Nucleic acids research* **16**(15), pp. 7351–67.
- Ho, S N (1989), 'Site-directed mutagenesis by overlap extension using the polymerase chain reaction.' *Gene* **77**(1), pp. 51–9.
- Hoffman, C S and F Winston (1987), 'A ten-minute DNA preparation from yeast efficiently releases autonomous plasmids for transformation of Escherichia coli.' *Gene* **57**(2-3), pp. 267–72.
- Janowsky, Birgit von (2006), 'The disaggregation activity of the mitochondrial ClpB homolog Hsp78 maintains Hsp70 function during heat stress.' *Journal of molecular biology* **357**(3), pp. 793–807.
- Kampinga, Harm H and Elizabeth A Craig (2010), 'The HSP70 chaperone machinery: J proteins as drivers of functional specificity.' *Nature reviews. Molecular cell biology* **11**(8), pp. 579–92.
- Kang, P J (1990), 'Requirement for hsp70 in the mitochondrial matrix for translocation and folding of precursor proteins.' *Nature* **348**(6297), pp. 137–43.
- Kelley, W L (1999), 'Molecular chaperones: How J domains turn on Hsp70s.' *Current biology : CB* **9**(8), R305–8.
- Kluth, Jantjeline (2012), 'Arabidopsis Zinc Ribbon 3 is the ortholog of yeast mitochondrial HSP70 escort protein HEP1 and belongs to an ancient protein family in mitochondria and plastids.' *FEBS letters* **586**(19), pp. 3071–6.
- Knieszner, Helena (2005), 'Compensation for a defective interaction of the hsp70 ssq1 with the mitochondrial Fe-S cluster scaffold isu.' *The Journal of biological chemistry* **280**(32), pp. 28966–72.
- Knight, S A (1998), 'Mt-Hsp70 homolog, Ssc2p, required for maturation of yeast frataxin and mitochondrial iron homeostasis.' *The Journal of biological chemistry* **273**(29), pp. 18389–93.

- Krayl, Martin (2007), 'A cooperative action of the ATP-dependent import motor complex and the inner membrane potential drives mitochondrial preprotein import.' *Molecular and cellular biology* **27**(2), pp. 411–25.
- Krishna, S Sri, Indraneel Majumdar and Nick V Grishin (2003), 'Structural classification of zinc fingers: survey and summary.' *Nucleic acids research* **31**(2), pp. 532–50.
- Kutik, Stephan (2008), 'Dissecting membrane insertion of mitochondrial beta-barrel proteins.' *Cell* **132**(6), pp. 1011–24.
- Laan, Martin van der, Dana P Hutu and Peter Rehling (2010), 'On the mechanism of preprotein import by the mitochondrial presequence translocase.' *Biochimica et biophysica acta* **1803**(6), pp. 732–9.
- Laan, Martin van der (2006), 'A role for Tim21 in membrane-potential-dependent preprotein sorting in mitochondria.' *Current biology : CB* **16**(22), pp. 2271–6.
- Laan, Martin van der (2007), 'Motor-free mitochondrial presequence translocase drives membrane integration of preproteins.' *Nature cell biology* **9**(10), pp. 1152–9.
- Laemmli, U K (1970), 'Cleavage of structural proteins during the assembly of the head of bacteriophage T4.' *Nature* **227**(5259), pp. 680–5.
- Langer, T (1992), 'Successive action of DnaK, DnaJ and GroEL along the pathway of chaperone-mediated protein folding.' *Nature* **356**(6371), pp. 683–9.
- Leidhold, Claudia (2006), 'Structure and function of Hsp78, the mitochondrial ClpB homolog.' *Journal of structural biology* **156**(1), pp. 149–64.
- Li, Jingzhi, Xinguo Qian and Bingdong Sha (2003), 'The crystal structure of the yeast Hsp40 Ydj1 complexed with its peptide substrate.' *Structure (London, England : 1993)* **11**(12), pp. 1475–83.
- Li, Yanfeng (2004), 'The presequence translocase-associated protein import motor of mitochondria. Pam16 functions in an antagonistic manner to Pam18.' *The Journal of biological chemistry* **279**(36), pp. 38047–54.
- Lill, Roland and Ulrich Mühlenhoff (2008), 'Maturation of iron-sulfur proteins in eukaryotes: mechanisms, connected processes, and diseases.' en, *Annual review of biochemistry* **77**, pp. 669–700.

- Lill, Roland (2006), 'Mechanisms of iron-sulfur protein maturation in mitochondria, cytosol and nucleus of eukaryotes.' *Biochimica et biophysica acta* **1763**(7), pp. 652–67.
- Lill, Roland (2012), 'The role of mitochondria in cellular iron-sulfur protein biogenesis and iron metabolism.' *Biochimica et biophysica acta* **1823**(9), pp. 1491–508.
- Lim, J H (2001), 'The mitochondrial Hsp70-dependent import system actively unfolds preproteins and shortens the lag phase of translocation.' *The EMBO journal* **20**(5), pp. 941–50.
- Linke, Katrin (2003), 'The roles of the two zinc binding sites in DnaJ.' *The Journal of biological chemistry* **278**(45), pp. 44457–66.
- Longen, Sebastian (2009), 'Systematic analysis of the twin $\text{cx}(9)\text{c}$ protein family.' *Journal of molecular biology* **393**(2), pp. 356–68.
- Lorenz, M C (1995), 'Gene disruption with PCR products in *Saccharomyces cerevisiae*.' *Gene* **158**(1), pp. 113–7.
- Lu, Hui and Joanna Woodburn (2005), 'Zinc binding stabilizes mitochondrial Tim10 in a reduced and import-competent state kinetically.' *Journal of molecular biology* **353**(4), pp. 897–910.
- Lu, Hui (2004), 'Functional TIM10 chaperone assembly is redox-regulated in vivo.' *The Journal of biological chemistry* **279**(18), pp. 18952–8.
- Lu, Z and D M Cyr (1998), 'The conserved carboxyl terminus and zinc finger-like domain of the co-chaperone Ydj1 assist Hsp70 in protein folding.' *The Journal of biological chemistry* **273**(10), pp. 5970–8.
- Major, Tamara (2006), 'Proteomic analysis of mitochondrial protein turnover: identification of novel substrate proteins of the matrix protease pim1.' *Molecular and cellular biology* **26**(3), pp. 762–76.
- Mapa, Koyeli (2010), 'The conformational dynamics of the mitochondrial Hsp70 chaperone.' *Molecular cell* **38**(1), pp. 89–100.
- Maret, Wolfgang (2005), 'Zinc coordination environments in proteins determine zinc functions.' *Journal of trace elements in medicine and biology : organ of the Society for Minerals and Trace Elements (GMS)* **19**(1), pp. 7–12.
- Martin, J, K Mahlke and N Pfanner (1991), 'Role of an energized inner membrane in mitochondrial protein import. Delta psi drives the movement of presequences.' *The Journal of biological chemistry* **266**(27), pp. 18051–7.

- Mayer, M P and B Bukau (2005), 'Hsp70 chaperones: cellular functions and molecular mechanism.' *Cellular and molecular life sciences : CMLS* **62**(6), pp. 670–84.
- McCall, K A, C Huang and C A Fierke (2000), 'Function and mechanism of zinc metalloenzymes.' *The Journal of nutrition* **130**(5S Suppl), 1437S–46S.
- McIntyre, M C (1993), 'Human papillomavirus type 18 E7 protein requires intact Cys-X-X-Cys motifs for zinc binding, dimerization, and transformation but not for Rb binding.' *Journal of virology* **67**(6), pp. 3142–50.
- Meinecke, Michael (2006), 'Tim50 maintains the permeability barrier of the mitochondrial inner membrane.' *Science (New York, N.Y.)* **312**(5779), pp. 1523–6.
- Meisinger, Chris (2004), 'The mitochondrial morphology protein Mdm10 functions in assembly of the preprotein translocase of the outer membrane.' *Developmental cell* **7**(1), pp. 61–71.
- Mesecke, Nikola (2005), 'A disulfide relay system in the intermembrane space of mitochondria that mediates protein import.' *Cell* **121**(7), pp. 1059–69.
- Miao, B, J E Davis and E A Craig (1997), 'Mge1 functions as a nucleotide release factor for Ssc1, a mitochondrial Hsp70 of *Saccharomyces cerevisiae*.' *Journal of molecular biology* **265**(5), pp. 541–52.
- Miller, J, A D McLachlan and A Klug (1985), 'Repetitive zinc-binding domains in the protein transcription factor IIIA from *Xenopus oocytes*.' *The EMBO journal* **4**(6), pp. 1609–14.
- Mokranjac, Dejana and Walter Neupert (2010), 'The many faces of the mitochondrial TIM23 complex.' *Biochimica et biophysica acta* **1797**(6-7), pp. 1045–54.
- Mokranjac, Dejana (2005), 'Role of Tim21 in mitochondrial translocation contact sites.' *The Journal of biological chemistry* **280**(25), pp. 23437–40.
- Momose, Takaki (2007), 'Structural basis of functional cooperation of Tim15/Zim17 with yeast mitochondrial Hsp70.' *EMBO reports* **8**(7), pp. 664–70.
- Morgan, Bruce (2009), 'Zinc can play chaperone-like and inhibitor roles during import of mitochondrial small Tim proteins.' *The Journal of biological chemistry* **284**(11), pp. 6818–25.
- Mossmann, Dirk, Chris Meisinger and F-Nora Vögtle (2012), 'Processing of mitochondrial presequences.' *Biochimica et biophysica acta* **1819**(9-10), pp. 1098–106.

Mühlenhoff, Ulrich (2003), 'Components involved in assembly and dislocation of iron-sulfur clusters on the scaffold protein Isu1p.' *The EMBO journal* **22**(18), pp. 4815–25.

Mühlenhoff, Ulrich (2007), 'The ISC [corrected] proteins Isa1 and Isa2 are required for the function but not for the de novo synthesis of the Fe/S clusters of biotin synthase in *Saccharomyces cerevisiae*.' *Eukaryotic cell* **6**(3), pp. 495–504.

Mühlenhoff, Ulrich (2011), 'Specialized function of yeast Isa1 and Isa2 proteins in the maturation of mitochondrial [4Fe-4S] proteins.' *The Journal of biological chemistry* **286**(48), pp. 41205–16.

Müller, Judith M (2008), 'Precursor oxidation by Mia40 and Erv1 promotes vectorial transport of proteins into the mitochondrial intermembrane space.' *Molecular biology of the cell* **19**(1), pp. 226–36.

Namuswe, Frances and Jeremy M Berg (2012), 'Secondary interactions involving zinc-bound ligands: roles in structural stabilization and macromolecular interactions.' *Journal of inorganic biochemistry* **111**, pp. 146–9.

Navarro-Sastre, Aleix (2011), 'A fatal mitochondrial disease is associated with defective NFU1 function in the maturation of a subset of mitochondrial Fe-S proteins.' *American journal of human genetics* **89**(5), pp. 656–67.

Netz, Daili J A (2012), 'Eukaryotic DNA polymerases require an iron-sulfur cluster for the formation of active complexes.' *Nature chemical biology* **8**(1), pp. 125–32.

Neupert, Walter and Johannes M Herrmann (2007), 'Translocation of proteins into mitochondria.' *Annual review of biochemistry* **76**, pp. 723–49.

Pierrel, Fabien, Paul A Cobine and Dennis R Winge (2007), 'Metal Ion availability in mitochondria.' *Biometals : an international journal on the role of metal ions in biology, biochemistry, and medicine* **20**(3-4), pp. 675–82.

Popov-Celeketić, Dusan (2008), 'Active remodelling of the TIM23 complex during translocation of preproteins into mitochondria.' *The EMBO journal* **27**(10), pp. 1469–80.

Pukszta, Sebastian (2010), 'Co-evolution-driven switch of J-protein specificity towards an Hsp70 partner.' *EMBO reports* **11**(5), pp. 360–5.

Renart, J, J Reiser and G R Stark (1979), 'Transfer of proteins from gels to diazobenzyloxymethyl-paper and detection with antisera: a method for studying antibody specificity and antigen structure.' *Proceedings of the National Academy of Sciences of the United States of America* **76**(7), pp. 3116–20.

- Rodríguez-Manzanares, María Teresa (2002), 'Grx5 is a mitochondrial glutaredoxin required for the activity of iron/sulfur enzymes.' *Molecular biology of the cell* **13**(4), pp. 1109–21.
- Roise, D and G Schatz (1988), 'Mitochondrial presequences.' *The Journal of biological chemistry* **263**(10), pp. 4509–11.
- Rottgers, Karin (2002), 'The ClpB homolog Hsp78 is required for the efficient degradation of proteins in the mitochondrial matrix.' *The Journal of biological chemistry* **277**(48), pp. 45829–37.
- Rowley, N (1994), 'Mdj1p, a novel chaperone of the DnaJ family, is involved in mitochondrial biogenesis and protein folding.' *Cell* **77**(2), pp. 249–59.
- Saibil, Helen R (2008), 'Chaperone machines in action.' *Current opinion in structural biology* **18**(1), pp. 35–42.
- Saiki, R K (1985), 'Enzymatic amplification of beta-globin genomic sequences and restriction site analysis for diagnosis of sickle cell anemia.' *Science (New York, N.Y.)* **230**(4732), pp. 1350–4.
- Saitoh, Takashi (2007), 'Tom20 recognizes mitochondrial presequences through dynamic equilibrium among multiple bound states.' *The EMBO journal* **26**(22), pp. 4777–87.
- Sanjuán Szklarz, Luiza K (2005), 'Inactivation of the mitochondrial heat shock protein zim17 leads to aggregation of matrix hsp70s followed by pleiotropic effects on morphology and protein biogenesis.' *Journal of molecular biology* **351**(1), pp. 206–18.
- Schilke, Brenda (2006), 'Evolution of mitochondrial chaperones utilized in Fe-S cluster biogenesis.' *Current biology : CB* **16**(16), pp. 1660–5.
- Schmidt, Oliver, Nikolaus Pfanner and Chris Meisinger (2010), 'Mitochondrial protein import: from proteomics to functional mechanisms.' *Nature reviews. Molecular cell biology* **11**(9), pp. 655–67.
- Sha, B, S Lee and D M Cyr (2000), 'The crystal structure of the peptide-binding fragment from the yeast Hsp40 protein Sis1.' *Structure (London, England : 1993)* **8**(8), pp. 799–807.
- Sheftel, Alex, Oliver Stehling and Roland Lill (2010), 'Iron-sulfur proteins in health and disease.' *Trends in endocrinology and metabolism: TEM* **21**(5), pp. 302–14.
- Sichting, Martin (2005), 'Maintenance of structure and function of mitochondrial Hsp70 chaperones requires the chaperone Hep1.' *The EMBO journal* **24**(5), pp. 1046–56.

Sikorski, R S and P Hieter (1989), 'A system of shuttle vectors and yeast host strains designed for efficient manipulation of DNA in *Saccharomyces cerevisiae*.' *Genetics* **122**(1), pp. 19–27.

Stuart, Rosemary (2002), 'Insertion of proteins into the inner membrane of mitochondria: the role of the Oxa1 complex.' *Biochimica et biophysica acta* **1592**(1), pp. 79–87.

Szabo, a (1996), 'A zinc finger-like domain of the molecular chaperone DnaJ is involved in binding to denatured protein substrates.' *The EMBO journal* **15**(2), pp. 408–17.

Truscott, Kaye N (2003), 'A J-protein is an essential subunit of the presequence translocase-associated protein import motor of mitochondria.' *The Journal of cell biology* **163**(4), pp. 707–13.

Van Der Laan, M. (2005), 'Pam17 is required for architecture and translocation activity of the mitochondrial protein import motor', *Molecular and cellular biology* **25**(17), p. 7449.

Van Dyck, L, D A Pearce and F Sherman (1994), 'PIM1 encodes a mitochondrial ATP-dependent protease that is required for mitochondrial function in the yeast *Saccharomyces cerevisiae*.' *The Journal of biological chemistry* **269**(1), pp. 238–42.

Veatch, Joshua R (2009), 'Mitochondrial dysfunction leads to nuclear genome instability via an iron-sulfur cluster defect.' *Cell* **137**(7), pp. 1247–58.

Voisine, C (1999), 'The protein import motor of mitochondria: unfolding and trapping of preproteins are distinct and separable functions of matrix Hsp70.' *Cell* **97**(5), pp. 565–74.

Voos, W (1993), 'Presequence and mature part of preproteins strongly influence the dependence of mitochondrial protein import on heat shock protein 70 in the matrix.' *The Journal of cell biology* **123**(1), pp. 119–26.

Voos, W (1996), 'Differential requirement for the mitochondrial Hsp70-Tim44 complex in unfolding and translocation of preproteins.' *The EMBO journal* **15**(11), pp. 2668–77.

Voos, Wolfgang (2013), 'Chaperone-protease networks in mitochondrial protein homeostasis.' *Biochimica et biophysica acta* **1833**(2), pp. 388–99.

Voos, Wolfgang and Karin Röttgers (2002), 'Molecular chaperones as essential mediators of mitochondrial biogenesis.' *Biochimica et biophysica acta* **1592**(1), pp. 51–62.

Vu, Michael T (2012), 'The DNLZ/HEP zinc-binding subdomain is critical for regulation of the mitochondrial chaperone HSPA9.' *Protein science : a publication of the Protein Society* **21**(2), pp. 258–67.

- Waggoner, A (1976), 'Optical probes of membrane potential.' *The Journal of membrane biology* **27**(4), pp. 317–34.
- Wagner, Karina (2008), 'The assembly pathway of the mitochondrial carrier translocase involves four preprotein translocases.' *Molecular and cellular biology* **28**(13), pp. 4251–60.
- Walsh, Peter (2004), 'The J-protein family: modulating protein assembly, disassembly and translocation.' *EMBO reports* **5**(6), pp. 567–71.
- Walter, S (2002), 'Structure and function of the GroE chaperone.' *Cellular and molecular life sciences : CMLS* **59**(10), pp. 1589–97.
- Webb, Chaille T (2006), 'Crystal structure of the mitochondrial chaperone TIM9.10 reveals a six-bladed alpha-propeller.' *Molecular cell* **21**(1), pp. 123–33.
- Westermann, B (1996), 'Role of the mitochondrial DnaJ homolog Mdj1p as a chaperone for mitochondrially synthesized and imported proteins.' *Molecular and cellular biology* **16**(12), pp. 7063–71.
- Wiedemann, Nils (2006), 'Essential role of Isd11 in mitochondrial iron-sulfur cluster synthesis on Isu scaffold proteins.' *The EMBO journal* **25**(1), pp. 184–95.
- Wiedemann, Nils (2007), 'Sorting switch of mitochondrial presequence translocase involves coupling of motor module to respiratory chain.' *The Journal of cell biology* **179**(6), pp. 1115–22.
- Willmund, Felix (2008), 'Assistance for a chaperone: Chlamydomonas HEP2 activates plastidic HSP70B for cochaperone binding.' *The Journal of biological chemistry* **283**(24), pp. 16363–73.
- Wu, Yunkun (2005), 'The crystal structure of the C-terminal fragment of yeast Hsp40 Ydj1 reveals novel dimerization motif for Hsp40.' *Journal of molecular biology* **346**(4), pp. 1005–11.
- Yamamoto, Hayashi (2005), 'Identification of a novel member of yeast mitochondrial Hsp70-associated motor and chaperone proteins that facilitates protein translocation across the inner membrane.' *FEBS letters* **579**(2), pp. 507–11.
- Young, Jason C, Nicholas J Hoogenraad and F Ulrich Hartl (2003), 'Molecular chaperones Hsp90 and Hsp70 deliver preproteins to the mitochondrial import receptor Tom70.' *Cell* **112**(1), pp. 41–50.
- Young, Jason C (2004), 'Pathways of chaperone-mediated protein folding in the cytosol.' *Nature reviews. Molecular cell biology* **5**(10), pp. 781–91.

Zhai, Peng (2008), 'The human escort protein Hep binds to the ATPase domain of mitochondrial hsp70 and regulates ATP hydrolysis.' *The Journal of biological chemistry* **283**(38), pp. 26098–106.

Zhai, Peng (2011), 'A conserved histidine in human DNLZ/HEP is required for stimulation of HSPA9 ATPase activity.' *Biochemical and biophysical research communications* **408**(4), pp. 589–94.

Zhao, Xin-Qing and Feng-wu Bai (2012), 'Zinc and yeast stress tolerance: micronutrient plays a big role.' *Journal of biotechnology* **158**(4), pp. 176–83.

A. Appendix

A.1. Sequences

A.1.1. pIL1 and pIL2

= ribosome binding sites
 = annealing sites primer
 = ATG *ZIM17**-artefact and in frame ATGs *ZIM17*
 = restriction sites

```

10      20      30      40      50      60      70      80      90      100
pETDuet-Novagen  ggggaattgtgagcggataacaattcccctctagaaataatTTGTTAACTTTAAGAAGGAGATATAccatgg
pDB10             GGGGAATTGTGAGCGGATAACAATTCCCCTCTAGAAAATAATTTGTTAACTTTAAGAAGGAGATATAccatggCGTCAACCAAGGTTCAAGGTTCCGTC
pIL1 +rbs        GGGGAATTGTGAGCGGATAACAATTCCCCTCTAGAAAATAATTTGTTAACTTTAAGAAGGAGATATAccatggCGTCAACCAAGGTTCAAGGTTCCGTC
Zim17*-artefact-pIL1
pIL2 -rbs        GGGGAATTGTGAGCGGATAACAATTCCCCTCTAGAAAATAATTTGTTAACTTTAAGAAGGAGATATAccatggCGTCAACCAAGGTTCAAGGTTCCGTC
zim17*-artefact-pIL2
Ssc1*His10      -----M-A-S-T-K-V-Q-G-S-V-----
Zim17*Strep      -----NcoI-----

110     120     130     140     150     160     170     180     190     200
pETDuet-Novagen  ATCGGTATCGATTGGGTACCACCAACTCTGCGGTTGCCATTATGGAAGGTAAGTTCCAAAAATTTATGAAAACGCCGAGGTTCCAGAACTACTCCTT
pDB10             ATCGGTATCGATTGGGTACCACCAACTCTGCGGTTGCCATTATGGAAGGTAAGTTCCAAAAATTTATGAAAACGCCGAGGTTCCAGAACTACTCCTT
pIL1 +rbs        ATCGGTATCGATTGGGTACCACCAACTCTGCGGTTGCCATTATGGAAGGTAAGTTCCAAAAATTTATGAAAACGCCGAGGTTCCAGAACTACTCCTT
Zim17*-artefact-pIL1
pIL2 -rbs        ATCGGTATCGATTGGGTACCACCAACTCTGCGGTTGCCATTATGGAAGGTAAGTTCCAAAAATTTATGAAAACGCCGAGGTTCCAGAACTACTCCTT
zim17*-artefact-pIL2
Ssc1*His10      -I-G-I-D-L-G-T-T-N-S-A-V-A-I-M-E-G-K-V-P-K-I-I-E-N-A-E-G-S-R-R-T-T-P-
Zim17*Strep

210     220     230     240     250     260     270     280     290     300
pETDuet-Novagen  CTGTAGTAGCTTTCACTAAAGAGGGAGACGTTTGGTTGGTATTCCAGCCAAGCGTCAAGCCGTAGTGAACCCAGAAAACACCCCTATTGCTACCAAGCG
pDB10             CTGTAGTAGCTTTCACTAAAGAGGGAGACGTTTGGTTGGTATTCCAGCCAAGCGTCAAGCCGTAGTGAACCCAGAAAACACCCCTATTGCTACCAAGCG
pIL1 +rbs        CTGTAGTAGCTTTCACTAAAGAGGGAGACGTTTGGTTGGTATTCCAGCCAAGCGTCAAGCCGTAGTGAACCCAGAAAACACCCCTATTGCTACCAAGCG
Zim17*-artefact-pIL1
pIL2 -rbs        CTGTAGTAGCTTTCACTAAAGAGGGAGACGTTTGGTTGGTATTCCAGCCAAGCGTCAAGCCGTAGTGAACCCAGAAAACACCCCTATTGCTACCAAGCG
zim17*-artefact-pIL2
Ssc1*His10      S-V-V-A-F-T-K-E-G-E-R-L-V-G-I-P-A-K-R-Q-A-V-V-N-P-E-N-T-L-F-A-T-K-R
Zim17*Strep

310     320     330     340     350     360     370     380     390     400
pETDuet-Novagen  TTTGATTGGTCGCTGTTTCAAGACGCTGAAAGTGAAGAGATATCAAGCAAGTTCCATACAAGATCGTCAAGCACTCCAACGGGGATGCTTGGGTTGAG
pDB10             TTTGATTGGTCGCTGTTTCAAGACGCTGAAAGTGAAGAGATATCAAGCAAGTTCCATACAAGATCGTCAAGCACTCCAACGGGGATGCTTGGGTTGAG
pIL1 +rbs        TTTGATTGGTCGCTGTTTCAAGACGCTGAAAGTGAAGAGATATCAAGCAAGTTCCATACAAGATCGTCAAGCACTCCAACGGGGATGCTTGGGTTGAG
Zim17*-artefact-pIL1
pIL2 -rbs        TTTGATTGGTCGCTGTTTCAAGACGCTGAAAGTGAAGAGATATCAAGCAAGTTCCATACAAGATCGTCAAGCACTCCAACGGGGATGCTTGGGTTGAG
zim17*-artefact-pIL2
Ssc1*His10      -L-I-G-R-R-F-E-D-A-E-V-Q-R-D-I-K-Q-V-P-Y-K-I-V-K-H-S-N-G-D-A-W-V-E-
Zim17*Strep

410     420     430     440     450     460     470     480     490     500
pETDuet-Novagen  GCCAGAGTCAAACCTTACTCACCAGCCCAAATCGTGGGTTCTGCTTGAACAAGATGAAGGAAACAGCTGAGGCCCTACTTGGGTAAGCCAGTTAAGAATG
pDB10             GCCAGAGTCAAACCTTACTCACCAGCCCAAATCGTGGGTTCTGCTTGAACAAGATGAAGGAAACAGCTGAGGCCCTACTTGGGTAAGCCAGTTAAGAATG
pIL1 +rbs        GCCAGAGTCAAACCTTACTCACCAGCCCAAATCGTGGGTTCTGCTTGAACAAGATGAAGGAAACAGCTGAGGCCCTACTTGGGTAAGCCAGTTAAGAATG
Zim17*-artefact-pIL1
pIL2 -rbs        GCCAGAGTCAAACCTTACTCACCAGCCCAAATCGTGGGTTCTGCTTGAACAAGATGAAGGAAACAGCTGAGGCCCTACTTGGGTAAGCCAGTTAAGAATG
zim17*-artefact-pIL2
Ssc1*His10      -A-R-G-Q-T-Y-S-P-A-Q-I-G-G-F-V-L-N-K-M-K-E-T-A-E-A-Y-L-G-K-P-V-K-N-
Zim17*Strep

510     520     530     540     550     560     570     580     590     600
pETDuet-Novagen  CTGTGTGCTGCTCCAGCTTATTTCAAGCACTCTCAAAGACAAGTACTAAAGACGCGAGCCAAATGTTGGTTTGAACGTTTACGTGCTGCTCAATGA
pDB10             CTGTGTGCTGCTCCAGCTTATTTCAAGCACTCTCAAAGACAAGTACTAAAGACGCGAGCCAAATGTTGGTTTGAACGTTTACGTGCTGCTCAATGA
pIL1 +rbs        CTGTGTGCTGCTCCAGCTTATTTCAAGCACTCTCAAAGACAAGTACTAAAGACGCGAGCCAAATGTTGGTTTGAACGTTTACGTGCTGCTCAATGA
Zim17*-artefact-pIL1
pIL2 -rbs        CTGTGTGCTGCTCCAGCTTATTTCAAGCACTCTCAAAGACAAGTACTAAAGACGCGAGCCAAATGTTGGTTTGAACGTTTACGTGCTGCTCAATGA
zim17*-artefact-pIL2
Ssc1*His10      A-V-V-T-V-P-A-Y-F-N-D-S-Q-R-Q-A-T-K-D-A-G-Q-I-V-G-L-N-V-L-R-V-V-N-E-
Zim17*Strep
    
```

```
        610      620      630      640      650      660      670      680      690      700
.....|.....|.....|.....|.....|.....|.....|.....|.....|.....|.....|
pETDuet-Novagen
pDB10      ACCAACCCGCGTGCCTTAGCTTACGGTTTGGAAAAATCCGACTCTAAAGTTGTTGCCGTTTTTCGATTTGGGTGGTGGTACTTTCGATATCTCCATCTTA
pIL1 +rbs  ACCAACCCGCGTGCCTTAGCTTACGGTTTGGAAAAATCCGACTCTAAAGTTGTTGCCGTTTTTCGATTTGGGTGGTGGTACTTTCGATATCTCCATCTTA
Zim17*-artefact-pIL1
pIL2 -rbs  ACCAACCCGCGTGCCTTAGCTTACGGTTTGGAAAAATCCGACTCTAAAGTTGTTGCCGTTTTTCGATTTGGGTGGTGGTACTTTCGATATCTCCATCTTA
zim17*-artefact-pIL2
Ssc1*His10 --P--T--A--A--A--L--A--Y--G--L--E--K--S--D--S--K--V--V--A--V--F--D--L--G--G--G--T--F--D--I--S--I--L--
Zim17*Strep -----|-----|-----|-----|-----|-----|-----|-----|-----|-----|-----|

        710      720      730      740      750      760      770      780      790      800
.....|.....|.....|.....|.....|.....|.....|.....|.....|.....|.....|
pETDuet-Novagen
pDB10      GATATTGACAACGGTGTTTTGAAGTTAAGTCCACTAACGGTGACACTCATTGGGTGGTGAAGATTTCGACATCTATTGTTGAGAGAGATTGTTTCTC
pIL1 +rbs  GATATTGACAACGGTGTTTTGAAGTTAAGTCCACTAACGGTGACACTCATTGGGTGGTGAAGATTTCGACATCTATTGTTGAGAGAGATTGTTTCTC
Zim17*-artefact-pIL1
pIL2 -rbs  GATATTGACAACGGTGTTTTGAAGTTAAGTCCACTAACGGTGACACTCATTGGGTGGTGAAGATTTCGACATCTATTGTTGAGAGAGATTGTTTCTC
zim17*-artefact-pIL2
Ssc1*His10 -D--I--D--N--G--V--F--E--V--K--S--T--N--G--D--T--H--L--G--G--E--D--F--D--I--Y--L--L--R--E--I--V--S--
Zim17*Strep -----|-----|-----|-----|-----|-----|-----|-----|-----|-----|-----|

        810      820      830      840      850      860      870      880      890      900
.....|.....|.....|.....|.....|.....|.....|.....|.....|.....|.....|
pETDuet-Novagen
pDB10      GTTTCAGACCGAAACTGGTATTGATTGGAAAAATGACCGTATGGCTATCCAAAGAATTAGAGAAGCTGCTGAAAAGGCTAAGATTGAGCTATCTTCTAC
pIL1 +rbs  GTTTCAGACCGAAACTGGTATTGATTGGAAAAATGACCGTATGGCTATCCAAAGAATTAGAGAAGCTGCTGAAAAGGCTAAGATTGAGCTATCTTCTAC
Zim17*-artefact-pIL1
pIL2 -rbs  GTTTCAGACCGAAACTGGTATTGATTGGAAAAATGACCGTATGGCTATCCAAAGAATTAGAGAAGCTGCTGAAAAGGCTAAGATTGAGCTATCTTCTAC
zim17*-artefact-pIL2
Ssc1*His10 R--F--K--T--E--T--G--I--D--L--E--N--D--R--M--A--I--Q--R--I--R--E--A--A--E--K--A--K--I--E--L--S--S--T
Zim17*Strep -----|-----|-----|-----|-----|-----|-----|-----|-----|-----|-----|

        910      920      930      940      950      960      970      980      990      1000
.....|.....|.....|.....|.....|.....|.....|.....|.....|.....|.....|
pETDuet-Novagen
pDB10      CGTTTCCACTGAAATCAACCTGCCATTTATCACTGCTGATGCCCTCAGGTCCAAGCATATCAACATGAAGTTCTCCAGGGCTCAATTCGAGACTTTGACA
pIL1 +rbs  CGTTTCCACTGAAATCAACCTGCCATTTATCACTGCTGATGCCCTCAGGTCCAAGCATATCAACATGAAGTTCTCCAGGGCTCAATTCGAGACTTTGACA
Zim17*-artefact-pIL1
pIL2 -rbs  CGTTTCCACTGAAATCAACCTGCCATTTATCACTGCTGATGCCCTCAGGTCCAAGCATATCAACATGAAGTTCTCCAGGGCTCAATTCGAGACTTTGACA
zim17*-artefact-pIL2
Ssc1*His10 --V--S--T--E--I--N--L--P--F--I--T--A--D--A--S--G--P--K--H--I--N--M--K--F--S--R--A--Q--F--E--T--L--T--
Zim17*Strep -----|-----|-----|-----|-----|-----|-----|-----|-----|-----|-----|

        1010     1020     1030     1040     1050     1060     1070     1080     1090     1100
.....|.....|.....|.....|.....|.....|.....|.....|.....|.....|.....|
pETDuet-Novagen
pDB10      GCCCCACTAGTTAAGAGAAGTGTGACCCAGTCAAGAAGGCTTTGAAAGACGCCGGTTTGTCTACTTACAGACATATCTGAAGTCTTATTGGTCGGTGGTA
pIL1 +rbs  GCCCCACTAGTTAAGAGAAGTGTGACCCAGTCAAGAAGGCTTTGAAAGACGCCGGTTTGTCTACTTACAGACATATCTGAAGTCTTATTGGTCGGTGGTA
Zim17*-artefact-pIL1
pIL2 -rbs  GCCCCACTAGTTAAGAGAAGTGTGACCCAGTCAAGAAGGCTTTGAAAGACGCCGGTTTGTCTACTTACAGACATATCTGAAGTCTTATTGGTCGGTGGTA
zim17*-artefact-pIL2
Ssc1*His10 -A--P--L--V--K--R--T--V--D--P--V--K--K--A--L--K--D--A--G--L--S--T--S--D--I--S--E--V--L--L--V--G--G--
Zim17*Strep -----|-----|-----|-----|-----|-----|-----|-----|-----|-----|-----|

        1110     1120     1130     1140     1150     1160     1170     1180     1190     1200
.....|.....|.....|.....|.....|.....|.....|.....|.....|.....|.....|
pETDuet-Novagen
pDB10      TGTCCAGATGCCTAAGGTTGTCGAAACCGTTAAATCTTTGTTGGTAAGGACCCATCTAAGCCGCTCAACCCAGATGAAGCTGTTGCCATTGGTCTGC
pIL1 +rbs  TGTCCAGATGCCTAAGGTTGTCGAAACCGTTAAATCTTTGTTGGTAAGGACCCATCTAAGCCGCTCAACCCAGATGAAGCTGTTGCCATTGGTCTGC
Zim17*-artefact-pIL1
pIL2 -rbs  TGTCCAGATGCCTAAGGTTGTCGAAACCGTTAAATCTTTGTTGGTAAGGACCCATCTAAGCCGCTCAACCCAGATGAAGCTGTTGCCATTGGTCTGC
zim17*-artefact-pIL2
Ssc1*His10 M--S--R--M--P--K--V--V--E--T--V--K--S--L--F--G--K--D--P--S--K--A--V--N--P--D--E--A--V--A--I--G--A--A
Zim17*Strep -----|-----|-----|-----|-----|-----|-----|-----|-----|-----|-----|

        1210     1220     1230     1240     1250     1260     1270     1280     1290     1300
.....|.....|.....|.....|.....|.....|.....|.....|.....|.....|.....|
pETDuet-Novagen
pDB10      TGTGCAAGGTGCTGTCTTGTCCGGTGAGGTTACTGACGCTTATTATTAGATGTTACCCCATTTGCTCTAGGTATCGAAACTTTAGTGGTGTTTTCACA
pIL1 +rbs  TGTGCAAGGTGCTGTCTTGTCCGGTGAGGTTACTGACGCTTATTATTAGATGTTACCCCATTTGCTCTAGGTATCGAAACTTTAGTGGTGTTTTCACA
Zim17*-artefact-pIL1
pIL2 -rbs  TGTGCAAGGTGCTGTCTTGTCCGGTGAGGTTACTGACGCTTATTATTAGATGTTACCCCATTTGCTCTAGGTATCGAAACTTTAGTGGTGTTTTCACA
zim17*-artefact-pIL2
Ssc1*His10 --V--Q--G--A--V--L--S--G--E--V--T--D--V--L--L--L--D--V--T--P--L--S--L--G--I--E--T--L--G--G--V--F--T--
Zim17*Strep -----|-----|-----|-----|-----|-----|-----|-----|-----|-----|-----|

        1310     1320     1330     1340     1350     1360     1370     1380     1390     1400
.....|.....|.....|.....|.....|.....|.....|.....|.....|.....|.....|
pETDuet-Novagen
pDB10      AGATTGATTCGAAGAACTACTATTCCAAACAAAGAAATCTCAAACTTCTCCACTGCCGCTGCTGGTCAAACCTCTGTTGAAATCAGAGTTTCCAAAG
pIL1 +rbs  AGATTGATTCGAAGAACTACTATTCCAAACAAAGAAATCTCAAACTTCTCCACTGCCGCTGCTGGTCAAACCTCTGTTGAAATCAGAGTTTCCAAAG
Zim17*-artefact-pIL1
pIL2 -rbs  AGATTGATTCGAAGAACTACTATTCCAAACAAAGAAATCTCAAACTTCTCCACTGCCGCTGCTGGTCAAACCTCTGTTGAAATCAGAGTTTCCAAAG
zim17*-artefact-pIL2
Ssc1*His10 -R--L--I--P--R--N--T--T--I--P--T--K--K--S--Q--I--F--S--T--A--A--A--G--Q--T--S--V--E--I--R--V--F--Q--
Zim17*Strep -----|-----|-----|-----|-----|-----|-----|-----|-----|-----|-----|
```

1410 1420 1430 1440 1450 1460 1470 1480 1490 1500
 pETDuet-Novagen
 pDB10 GTGAAAGAGAATTGGTTAGAGACAACAAATGATGGTAACTTCACCTTTAGCCGGTATCCACCTGCTCCAAGGGGTGCCACAAATCGAAGTCACCTT
 pIL1 +rbs GTGAAAGAGAATTGGTTAGAGACAACAAATGATGGTAACTTCACCTTTAGCCGGTATCCACCTGCTCCAAGGGGTGCCACAAATCGAAGTCACCTT
 Zim17*-artefact-pIL1
 pIL2 -rbs GTGAAAGAGAATTGGTTAGAGACAACAAATGATGGTAACTTCACCTTTAGCCGGTATCCACCTGCTCCAAGGGGTGCCACAAATCGAAGTCACCTT
 zim17*-artefact-pIL2
 Ssc1*His10 G-E-R-E-L-V-R-D-N-K-L-I-G-N-F-T-L-A-G-I-P-P-A-P-K-G-V-P-Q-I-E-V-T-F
 Zim17*Strep

1510 1520 1530 1540 1550 1560 1570 1580 1590 1600
 pETDuet-Novagen
 pDB10 TGACATCGATGCCGATGGTATTATTAACGTTTCTGCTAGAGACAAAGCTACAACAAGATTCCTTCTATTA~~CTGTTGCCGGTCTCTG~~GGTTTGTCCGAA
 pIL1 +rbs TGACATCGATGCCGATGGTATTATTAACGTTTCTGCTAGAGACAAAGCTACAACAAGATTCCTTCTATTA~~CTGTTGCCGGTCTCTG~~GGTTTGTCCGAA
 Zim17*-artefact-pIL1
 pIL2 -rbs TGACATCGATGCCGATGGTATTATTAACGTTTCTGCTAGAGACAAAGCTACAACAAGATTCCTTCTATTA~~CTGTTGCCGGTCTCTG~~GGTTTGTCCGAA
 zim17*-artefact-pIL2
 Ssc1*His10 -D-I-D-A-D-G-I-I-N-V-S-A-R-D-K-A-T-N-K-D-S-S-I-T-V-A-G-S-S-G-L-S-E
 Zim17*Strep

pDB20-IL1-f

1610 1620 1630 1640 1650 1660 1670 1680 1690 1700
 pETDuet-Novagen
 pDB10 AACGAAATTGAACAAATGGTTAACGACGCTGAAAATTCAGTCTCAAGATGAAGCTAGAAAAACAGCCATCGAAACTGCCAACAGGCTGACCAATTGG
 pIL1 +rbs AACGAAATTGAACAAATGGTTAACGACGCTGAAAATTCAGTCTCAAGATGAAGCTAGAAAAACAGCCATCGAAACTGCCAACAGGCTGACCAATTGG
 Zim17*-artefact-pIL1
 pIL2 -rbs AACGAAATTGAACAAATGGTTAACGACGCTGAAAATTCAGTCTCAAGATGAAGCTAGAAAAACAGCCATCGAAACTGCCAACAGGCTGACCAATTGG
 zim17*-artefact-pIL2
 Ssc1*His10 -N-E-I-E-Q-M-V-N-D-A-E-K-F-K-S-Q-D-E-A-R-K-Q-A-I-E-T-A-N-K-A-D-Q-L-
 Zim17*Strep

MfeI

1710 1720 1730 1740 1750 1760 1770 1780 1790 1800
 pETDuet-Novagen
 pDB10 CCAACGATACGAAAACCTCCTTGAAGAATTTGAAGGTAAGGTTGACAAGGCTGAAGCCCAAAGGTTAGGGATCAAACTCCTTGAAGGAGTTGGT
 pIL1 +rbs CCAACGATACGAAAACCTCCTTGAAGAATTTGAAGGTAAGGTTGACAAGGCTGAAGCCCAAAGGTTAGGGATCAAACTCCTTGAAGGAGTTGGT
 Zim17*-artefact-pIL1
 pIL2 -rbs CCAACGATACGAAAACCTCCTTGAAGAATTTGAAGGTAAGGTTGACAAGGCTGAAGCCCAAAGGTTAGGGATCAAACTCCTTGAAGGAGTTGGT
 zim17*-artefact-pIL2
 Ssc1*His10 A-N-N-D-T-E-N-S-L-K-E-F-E-G-K-V-D-K-A-E-A-Q-K-V-R-D-Q-I-I-T-S-L-K-E-L-V
 Zim17*Strep

1810 1820 1830 1840 1850 1860 1870 1880 1890 1900
 pETDuet-Novagen
 pDB10 TGCTAGAGTACAAGGTGGCGAAGAGGTTAACGCTGAGGAGTTAAGACCAAGACCGAAGAAATGCAAACTTCCCTCGATGAAATTGTTGAACAATTATAC
 pIL1 +rbs TGCTAGAGTACAAGGTGGCGAAGAGGTTAACGCTGAGGAGTTAAGACCAAGACCGAAGAAATGCAAACTTCCCTCGATGAAATTGTTGAACAATTATAC
 Zim17*-artefact-pIL1
 pIL2 -rbs TGCTAGAGTACAAGGTGGCGAAGAGGTTAACGCTGAGGAGTTAAGACCAAGACCGAAGAAATGCAAACTTCCCTCGATGAAATTGTTGAACAATTATAC
 zim17*-artefact-pIL2
 Ssc1*His10 -A-R-V-Q-G-G-E-E-V-N-A-E-E-L-K-T-K-T-E-E-L-Q-T-S-S-M-K-L-F-E-Q-L-Y
 Zim17*Strep

1910 1920 1930 1940 1950 1960 1970 1980 1990 2000
 pETDuet-Novagen
 pDB10 AAGAAGACTCTAACAAACAACAACAACAACCGCAACA~~ATG~~CCGAATCTGGTGAAGTAAAGCAGCCAGGAGCTCACCACCACCACCAcCATCATCATC
 pIL1 +rbs AAGAAGACTCTAACAAACAACAACAACAACAACCGCAACA~~ATG~~CCGAATCTGGTGAAGTAAAGCAGCCAGGAGCTCACCACCACCACCAcCATCATCATC
 Zim17*-artefact-pIL1
 pIL2 -rbs AAGAAGACTCTAACAAACAACAACAACAACAACCGCAACA~~ATG~~CCGAATCTGGTGAAGTAAAGCAGCCAGGAGCTCACCACCACCACCAcCATCATCATC
 zim17*-artefact-pIL2
 Ssc1*His10 -M-P-N-L-V-K-L-S-S-Q-E-L-T-T-T-T-T-I-I-I-
 Zim17*Strep

2010 2020 2030 2040 2050 2060 2070 2080 2090 2100
 pETDuet-Novagen
 pDB10 ----aagcttgcggccgcataatgcttaagtgcgaacagaaagtaatcgta~~ttgtacacggccgcataa~~cgaaattaatcagactcactataggggaa
 pIL1 +rbs AtcActaAGCTTTCGGCCGCATAATGCTTAAAGTCGAACAGAAAGTAAATCGTATTGTACACGGCCGCATAATCGAAATTAATACGACTCACTATAGGGGAA
 Zim17*-artefact-pIL1
 pIL2 -rbs AtcActaAGCTTTCGGCCGCATAATGCTTAAAGTCGAACAGAAAGTAAATCGTATTGTACACGGCCGCATAATCGAAATTAATACGACTCACTATAGGGGAA
 zim17*-artefact-pIL2
 Ssc1*His10 -I-T-K-L-A-A-A-*
 Zim17*Strep

HindIII pDB20-IL1+rbs-r/ pDB20-IL1-r


```

                2110      2120      2130      2140      2150      2160      2170      2180      2190      2200
pETDuet-Novagen .....|.....|.....|.....|.....|.....|.....|.....|.....|.....|.....|
pDB10      ttgtgagcggataacaattcccacatcttagtatattagtttaagtataagaagggagatacatatg
pIL1 +rbs  -----|-----|-----|-----|-----|-----|-----|-----|-----|-----|
Zim17*-artefact-pIL1 -----|-----|-----|-----|-----|-----|-----|-----|-----|-----|
pIL2 -rbs  -----|-----|-----|-----|-----|-----|-----|-----|-----|-----|
zim17*-artefact-pIL2 -----|-----|-----|-----|-----|-----|-----|-----|-----|-----|
Ssc1*His10 -----|-----|-----|-----|-----|-----|-----|-----|-----|-----|
Zim17*Strep -----|-----|-----|-----|-----|-----|-----|-----|-----|-----|
                rbs MCS2      NdeI
                Shine dalgarno

```

```

                2210      2220      2230      2240      2250      2260      2270      2280      2290      2300
pETDuet-Novagen .....|.....|.....|.....|.....|.....|.....|.....|.....|.....|.....|
pDB10      ATAAGAAGGTTTCATTTGGGGTCTTTTAAAGGTAGACAAGCCTAAGATGATGATAGCTTTCACCTGCAAGAAATGTAACACCCGATCTTCACACACATCTC
pIL1 +rbs  -----|-----|-----|-----|-----|-----|-----|-----|-----|-----|
Zim17*-artefact-pIL1 -----|-----|-----|-----|-----|-----|-----|-----|-----|-----|
pIL2 -rbs  -----|-----|-----|-----|-----|-----|-----|-----|-----|-----|
zim17*-artefact-pIL2 -----|-----|-----|-----|-----|-----|-----|-----|-----|-----|
Ssc1*His10 -----|-----|-----|-----|-----|-----|-----|-----|-----|-----|
Zim17*Strep D--K--K--V--H--L--G--S--F--K--V--D--K--P--K--M--M--I--A--F--T--C--K--K--C--N--T--R--S--S--H--T--M--S

```

```

                2310      2320      2330      2340      2350      2360      2370      2380      2390      2400
pETDuet-Novagen .....|.....|.....|.....|.....|.....|.....|.....|.....|.....|.....|
pDB10      CAAGCAGCGGTACGAGAAAGTACTGCTCTTGTCTCTTGTCCGCACTGCAAGTGAAGACATTTGATAGCAGACCATCTGAAAATATTCATGATCATCAT
pIL1 +rbs  -----|-----|-----|-----|-----|-----|-----|-----|-----|-----|
Zim17*-artefact-pIL1 -----|-----|-----|-----|-----|-----|-----|-----|-----|-----|
pIL2 -rbs  -----|-----|-----|-----|-----|-----|-----|-----|-----|-----|
zim17*-artefact-pIL2 -----|-----|-----|-----|-----|-----|-----|-----|-----|-----|
Ssc1*His10 --K--Q--A--Y--E--K--G--T--V--L--I--S--C--P--H--C--K--V--R--H--L--I--A--D--H--L--K--I--F--H--D--H--H
Zim17*Strep --K--Q--A--Y--E--K--G--T--V--L--I--S--C--P--H--C--K--V--R--H--L--I--A--D--H--L--K--I--F--H--D--H--H

```

```

                2410      2420      2430      2440      2450      2460      2470      2480      2490      2500
pETDuet-Novagen .....|.....|.....|.....|.....|.....|.....|.....|.....|.....|.....|
pDB10      GTTACCCTGGAACAGTTAATCAAGCTAACGGAGAACAAGTTAGCCAAGACGTTGGCGCACTTGGAGTTTGAAGACATCCAGATTTCGTAAGGACGCTCC
pIL1 +rbs  -----|-----|-----|-----|-----|-----|-----|-----|-----|-----|
Zim17*-artefact-pIL1 -----|-----|-----|-----|-----|-----|-----|-----|-----|-----|
pIL2 -rbs  -----|-----|-----|-----|-----|-----|-----|-----|-----|-----|
zim17*-artefact-pIL2 -----|-----|-----|-----|-----|-----|-----|-----|-----|-----|
Ssc1*His10 -V--T--V--E--Q--L--M--K--A--N--G--E--Q--V--S--Q--D--V--G--D--L--E--F--E--D--I--P--D--S--L--K--D--V--
Zim17*Strep -V--T--V--E--Q--L--M--K--A--N--G--E--Q--V--S--Q--D--V--G--D--L--E--F--E--D--I--P--D--S--L--K--D--V--

```

```

                2510      2520      2530      2540      2550      2560      2570      2580      2590      2600
pETDuet-Novagen .....|.....|.....|.....|.....|.....|.....|.....|.....|.....|.....|
pDB10      TGGGAAAATATGCCAAGAACAACCTCAGAAAATGCATCCAGCTCCCTCACCCCTCCAGAAAAGGTAGCGCTTGGAGCCACCCGAGTTCGAAAAATAACT
pIL1 +rbs  -----|-----|-----|-----|-----|-----|-----|-----|-----|-----|
Zim17*-artefact-pIL1 -----|-----|-----|-----|-----|-----|-----|-----|-----|-----|
pIL2 -rbs  -----|-----|-----|-----|-----|-----|-----|-----|-----|-----|
zim17*-artefact-pIL2 -----|-----|-----|-----|-----|-----|-----|-----|-----|-----|
Ssc1*His10 L--G--K--Y--A--K--N--N--S--E--N--A--S--Q--L--P--H--P--S--Q--K--G--S--A--W--S--H--P--Q--F--E--K--*
Zim17*Strep L--G--K--Y--A--K--N--N--S--E--N--A--S--Q--L--P--H--P--S--Q--K--G--S--A--W--S--H--P--Q--F--E--K--*

```

```

                2610      2620      2630      2640      2650      2660      2670      2680      2690      2700
pETDuet-Novagen .....|.....|.....|.....|.....|.....|.....|.....|.....|.....|.....|
pDB10      cgagctctggttaaagaaccgctgctggaattgaagccagcacatggactcgtctactagcgcagcttaataacctaggctgctgccaccgctgag
pIL1 +rbs  -----|-----|-----|-----|-----|-----|-----|-----|-----|-----|
pIL2 -rbs  CGAGTCTGGTAAAGAAACCGCTGCTGCGAAATTTGAACGCCAGCACATGGACTCGTCTACTAGCCGAGCTTAATTAACCTAGGCTGCTGCCACCGCTGAG
CGAGTCTGGTAAAGAAACCGCTGCTGCGAAATTTGAACGCCAGCACATGGACTCGTCTACTAGCCGAGCTTAATTAACCTAGGCTGCTGCCACCGCTGAG

```

XhoI

```

                2710      2720      2730      2740      2750      2760      2770      2780      2790      2800
pETDuet-Novagen .....|.....|.....|.....|.....|.....|.....|.....|.....|.....|.....|
pDB10      caataactagcataaacccttggggcctctaaacgggtcttgagggttttttgcgtaaaggaggaactatataccgattggcgaatgggacgcccctg
pIL1 +rbs  -----|-----|-----|-----|-----|-----|-----|-----|-----|-----|
pIL2 -rbs  CAATAACTAGCATAAACCCTTGGGGCCTCTAAACGGGTCTTGAGGGTCTTTTGTCTGAAAGGAGGAACCTATATCCGGATTGGCGAATGGGACGCGCCCTG
CAATAACTAGCATAAACCCTTGGGGCCTCTAAACGGGTCTTGAGGGTCTTTTGTCTGAAAGGAGGAACCTATATCCGGATTGGCGAATGGGACGCGCCCTG

```

```

                2810      2820      2830      2840      2850      2860      2870      2880      2890      2900
pETDuet-Novagen .....|.....|.....|.....|.....|.....|.....|.....|.....|.....|.....|
pDB10      tagcggcgcatatgaagcggcgggtgtgtgtgttacggcgcagctgacogctacactgocagcgccttagcggcgcctcttctgctttcttcccttcc
pIL1 +rbs  -----|-----|-----|-----|-----|-----|-----|-----|-----|-----|
pIL2 -rbs  TAGCGGCGCATTAAGCGCGCGGGTGTGTGTGTACGCGCAGCGTGACCGCTACACTTGCCAGCGCCCTAGCGCCGCTCTTTTCGCTTTCTCCCTTCC
TAGCGGCGCATTAAGCGCGCGGGTGTGTGTGTACGCGCAGCGTGACCGCTACACTTGCCAGCGCCCTAGCGCCGCTCTTTTCGCTTTCTCCCTTCC

```

```

                2910      2920      2930      2940      2950      2960      2970      2980      2990      3000
pETDuet-Novagen .....|.....|.....|.....|.....|.....|.....|.....|.....|.....|.....|
pDB10      tttctcggcagcttcgcccgtttcccgcgtaagctcctaaatcgggggtccctttagggttccgatttagtgccttaaggcaacctgacccccaaaaaac
pIL1 +rbs  -----|-----|-----|-----|-----|-----|-----|-----|-----|-----|
pIL2 -rbs  TTTCTCGCCAGCTTCGCCGCTTTCCCCTCAAGCTCTAAATCGGGGCTCCCTTAGGGTTCGATTAGTGTCTTACGGCACCTCGACCCCAAAAAAC
TTTCTCGCCAGCTTCGCCGCTTTCCCCTCAAGCTCTAAATCGGGGCTCCCTTAGGGTTCGATTAGTGTCTTACGGCACCTCGACCCCAAAAAAC
TTTCTCGCCAGCTTCGCCGCTTTCCCCTCAAGCTCTAAATCGGGGCTCCCTTAGGGTTCGATTAGTGTCTTACGGCACCTCGACCCCAAAAAAC

```

```

3010      3020      3030      3040      3050      3060      3070      3080      3090      3100
pETDuet-Novagen      . . . . .
pDB10      ttgattagggtgatggttcaactgagtgaggccatcgccctgatagacgggtttttcgccctttgacgttggagtcacagcttctttaaagtgagctctgtt
pIL1 +rbs      TTGATTAGGGTGATGGTTCACGTAGTGGGCCATCGCCCTGATAGACGGTTTTTCGCCCTTTGACGTTGGAGTCCACGTTCTTTAATAGTGGACTCTTGT
pIL2 -rbs      TTGATTAGGGTGATGGTTCACGTAGTGGGCCATCGCCCTGATAGACGGTTTTTCGCCCTTTGACGTTGGAGTCCACGTTCTTTAATAGTGGACTCTTGT

3110      3120      3130      3140      3150      3160      3170      3180      3190      3200
pETDuet-Novagen      . . . . .
pDB10      ccaaaactggaacaacactcaacctatctcggtctattcttttgattataaggattttgcccatttggccctattgggttaaaaaatgagctgatttaa
pIL1 +rbs      CCAAACCTGGAACAACACTCAACCTATCTCGGTCTATTCTTTTGATTATAAGGGATTTTGCCGATTTGCGCCTATTGGTTAAAAAATGAGCTGATTAA
pIL2 -rbs      CCAAACCTGGAACAACACTCAACCTATCTCGGTCTATTCTTTTGATTATAAGGGATTTTGCCGATTTGCGCCTATTGGTTAAAAAATGAGCTGATTAA

3210      3220      3230      3240      3250      3260      3270      3280      3290      3300
pETDuet-Novagen      . . . . .
pDB10      caaaaatttaacgcgaattttaacaaaataataaagtttaacattcttggcggcagcagtgccatgagattatcaaaaaggattcttaccctagatcccttt
pIL1 +rbs      CAAAAATTTAACGCGAATTTTAAACAAAATATAACGTTTACAATTTCTGGCGGCACGATGGCATGAGATTATCAAAAAGGATCTTACCCTAGATCCTTTT
pIL2 -rbs      CAAAAATTTAACGCGAATTTTAAACAAAATATAACGTTTACAATTTCTGGCGGCACGATGGCATGAGATTATCAAAAAGGATCTTACCCTAGATCCTTTT

3310      3320      3330      3340      3350      3360      3370      3380      3390      3400
pETDuet-Novagen      . . . . .
pDB10      aaataaaaaatgaagttttaaatcaatctaaagtaataatgagtaaaacttggtctgacagttaccaatgcttaacagtgaggcacctatctcagcagtc
pIL1 +rbs      AAATTAATAATGAAGTTTTAAATCAATCTAAAGTATATATGAGTAAACTTGGTCTGACAGTTACCAATGCTTAATCAGTGAGGCACCTATCTCAGCGATC
pIL2 -rbs      AAATTAATAATGAAGTTTTAAATCAATCTAAAGTATATATGAGTAAACTTGGTCTGACAGTTACCAATGCTTAATCAGTGAGGCACCTATCTCAGCGATC

3410      3420      3430      3440      3450      3460      3470      3480      3490      3500
pETDuet-Novagen      . . . . .
pDB10      tctctatttcggtcaatccatagttgctgactcccctgctgttagataactacgatacgggagggttaccatctggcccagtgctgcaatgataccgc
pIL1 +rbs      TGCTATTTCGTTTCATCCATAGTTGCTGACTCCCCTGCTGTAGATAACTACGATACGGGAGGGCTTACCATCTGGCCCCAGTCTGCAATGATACCGC
pIL2 -rbs      TGCTATTTCGTTTCATCCATAGTTGCTGACTCCCCTGCTGTAGATAACTACGATACGGGAGGGCTTACCATCTGGCCCCAGTCTGCAATGATACCGC

3510      3520      3530      3540      3550      3560      3570      3580      3590      3600
pETDuet-Novagen      . . . . .
pDB10      gagaaccagctcaccggctccagatttatcagcaataaaaccagcagccggaaggccgagcgcagaaagtggtctgcaactttatccgctccatcca
pIL1 +rbs      GAGACCCAGCTCACCAGCTCCAGATTTATCAGCAATAAACAGCCAGCCGGAAGGCCGAGCGCAAGTGGTCTGCAACTTTATCCGCTCCATCCA
pIL2 -rbs      GAGACCCAGCTCACCAGCTCCAGATTTATCAGCAATAAACAGCCAGCCGGAAGGCCGAGCGCAAGTGGTCTGCAACTTTATCCGCTCCATCCA

3610      3620      3630      3640      3650      3660      3670      3680      3690      3700
pETDuet-Novagen      . . . . .
pDB10      gtcctataattggtgcccgggaagctagagtaagtagttcgccagtttaagtttgcccaactggttgcacaggtcaggtggtgcaactgctc
pIL1 +rbs      GTCTATTAATGTTGCCGGGAAGCTAGAGTAAGTAGTTTCGCCAGTTAAAGTTTGGCGAACGTTGTTGCCATTGCTACAGGCATCGTGGTGTACGCTCG
pIL2 -rbs      GTCTATTAATGTTGCCGGGAAGCTAGAGTAAGTAGTTTCGCCAGTTAAAGTTTGGCGAACGTTGTTGCCATTGCTACAGGCATCGTGGTGTACGCTCG

3710      3720      3730      3740      3750      3760      3770      3780      3790      3800
pETDuet-Novagen      . . . . .
pDB10      tegtgttgatggcttcaatcagctccggttcccaacgatacaaggcgagttacatgatccccatggtgtgcaaaaaagcggttagctctcgtgctc
pIL1 +rbs      TCGTTTGGTATGGCTTCATTCAGCTCCGGTTCCTCAACGATCAAGCGAGTTACATGATCCCCATGTTGTGCAAAAAGCGGTTAGCTCCTCGGTCTC
pIL2 -rbs      TCGTTTGGTATGGCTTCATTCAGCTCCGGTTCCTCAACGATCAAGCGAGTTACATGATCCCCATGTTGTGCAAAAAGCGGTTAGCTCCTCGGTCTC

3810      3820      3830      3840      3850      3860      3870      3880      3890      3900
pETDuet-Novagen      . . . . .
pDB10      cgaatggtgacagaagtaagttgcccagctggttatcactcatggttatggcagcactgcataaattctctactgctcagccatccgtaagatgctttc
pIL1 +rbs      CGATCGTTGTCAGAAGTAAGTTGGCCGAGTGTATCACTCATGTTATGGCAGCAGTGCATAAATCTCTTACTGTCATGCCATCCGTAAGATGCTTTTC
pIL2 -rbs      CGATCGTTGTCAGAAGTAAGTTGGCCGAGTGTATCACTCATGTTATGGCAGCAGTGCATAAATCTCTTACTGTCATGCCATCCGTAAGATGCTTTTC

3910      3920      3930      3940      3950      3960      3970      3980      3990      4000
pETDuet-Novagen      . . . . .
pDB10      tgtgactggtgagtaactcaaccaagtcattctgagaatagtgatgcccggcaccgagttgctcttggccggcgtcaatacgggataaacggcgccaat
pIL1 +rbs      TGTGACTGGTGAAGTACTCAACCAAGTCTCTGAGAATAGTGTATGCGGCGACCGAGTTGCTCTTGGCCGGCCTCAATACGGGATAAATACCGCGCCACAT
pIL2 -rbs      TGTGACTGGTGAAGTACTCAACCAAGTCTCTGAGAATAGTGTATGCGGCGACCGAGTTGCTCTTGGCCGGCCTCAATACGGGATAAATACCGCGCCACAT

4010      4020      4030      4040      4050      4060      4070      4080      4090      4100
pETDuet-Novagen      . . . . .
pDB10      agcagaactttaaagtgcctcaatcattgaaaacggttcttggggcgaaaactctcaagatcttaccgctggtgagatccagttcgatgtaacccaactc
pIL1 +rbs      AGCAGAACTTTAAAAGTGCCTCATCTTGGAAAACGTTCTTGGGGCGAAAACCTCTCAAGGATCTTACCCTGTTGAGATCCAGTTCGATTAACCCATCTC
pIL2 -rbs      AGCAGAACTTTAAAAGTGCCTCATCTTGGAAAACGTTCTTGGGGCGAAAACCTCTCAAGGATCTTACCCTGTTGAGATCCAGTTCGATTAACCCATCTC

4110      4120      4130      4140      4150      4160      4170      4180      4190      4200
pETDuet-Novagen      . . . . .
pDB10      gtgcaccaactgatcttcagatcttcttactttaccaggtttctgggtgagcaaaaacaggaaggcaaaatgcccgaataaaggcgac
pIL1 +rbs      GTGCACCAACTGATCTTCAGACTCTTTTACTTTTACCAGCGTTTCTGGGTGAGCAAAAACAGGAAGGCAAAATGCCGCAAAAAGGGAATAAGGGCGAC
pIL2 -rbs      GTGCACCAACTGATCTTCAGACTCTTTTACTTTTACCAGCGTTTCTGGGTGAGCAAAAACAGGAAGGCAAAATGCCGCAAAAAGGGAATAAGGGCGAC

```


5410 5420 5430 5440 5450 5460 5470 5480 5490 5500
pETDuet-Novagen
pDB10
pIL1 +rbs
pIL2 -rbs

5510 5520 5530 5540 5550 5560 5570 5580 5590 5600
pETDuet-Novagen
pDB10
pIL1 +rbs
pIL2 -rbs

5610 5620 5630 5640 5650 5660 5670 5680 5690 5700
pETDuet-Novagen
pDB10
pIL1 +rbs
pIL2 -rbs

5710 5720 5730 5740 5750 5760 5770 5780 5790 5800
pETDuet-Novagen
pDB10
pIL1 +rbs
pIL2 -rbs

5810 5820 5830 5840 5850 5860 5870 5880 5890 5900
pETDuet-Novagen
pDB10
pIL1 +rbs
pIL2 -rbs

5910 5920 5930 5940 5950 5960 5970 5980 5990 6000
pETDuet-Novagen
pDB10
pIL1 +rbs
pIL2 -rbs

6010 6020 6030 6040 6050 6060 6070 6080 6090 6100
pETDuet-Novagen
pDB10
pIL1 +rbs
pIL2 -rbs

6110 6120 6130 6140 6150 6160 6170 6180 6190 6200
pETDuet-Novagen
pDB10
pIL1 +rbs
pIL2 -rbs

6210 6220 6230 6240 6250 6260 6270 6280 6290 6300
pETDuet-Novagen
pDB10
pIL1 +rbs
pIL2 -rbs

6310 6320 6330 6340 6350 6360 6370 6380 6390 6400
pETDuet-Novagen
pDB10
pIL1 +rbs
pIL2 -rbs

6410 6420 6430 6440 6450 6460 6470 6480 6490 6500
pETDuet-Novagen
pDB10
pIL1 +rbs
pIL2 -rbs

6510 6520 6530 6540 6550 6560 6570 6580 6590 6600
pETDuet-Novagen
pDB10
pIL1 +rbs
pIL2 -rbs

810 820 830 840 850 860 870 880 890 900
pFL39
pFL-Zim17-ts2-CEN
pFL-Zim17-ts3-CEN
pFL-Zim17-ts4-CEN
pFL-Zim17-corrWT-CEN

910 920 930 940 950 960 970 980 990 1000
pFL39
pFL-Zim17-ts2-CEN
pFL-Zim17-ts3-CEN
pFL-Zim17-ts4-CEN
pFL-Zim17-corrWT-CEN
Zim17-coding

1010 1020 1030 1040 1050 1060 1070 1080 1090 1100
pFL39
pFL-Zim17-ts2-CEN
pFL-Zim17-ts3-CEN
pFL-Zim17-ts4-CEN
pFL-Zim17-corrWT-CEN
Zim17-coding

1110 1120 1130 1140 1150 1160 1170 1180 1190 1200
pFL39
pFL-Zim17-ts2-CEN
pFL-Zim17-ts3-CEN
pFL-Zim17-ts4-CEN
pFL-Zim17-corrWT-CEN
Zim17-coding

1210 1220 1230 1240 1250 1260 1270 1280 1290 1300
pFL39
pFL-Zim17-ts2-CEN
pFL-Zim17-ts3-CEN
pFL-Zim17-ts4-CEN
pFL-Zim17-corrWT-CEN
Zim17-coding

1310 1320 1330 1340 1350 1360 1370 1380 1390 1400
pFL39
pFL-Zim17-ts2-CEN
pFL-Zim17-ts3-CEN
pFL-Zim17-ts4-CEN
pFL-Zim17-corrWT-CEN
Zim17-coding

1410 1420 1430 1440 1450 1460 1470 1480 1490 1500
pFL39
pFL-Zim17-ts2-CEN
pFL-Zim17-ts3-CEN
pFL-Zim17-ts4-CEN
pFL-Zim17-corrWT-CEN
Zim17-coding

1510 1520 1530 1540 1550 1560 1570 1580 1590 1600
pFL39
pFL-Zim17-ts2-CEN
pFL-Zim17-ts3-CEN
pFL-Zim17-ts4-CEN
pFL-Zim17-corrWT-CEN
Zim17-coding

1610 1620 1630 1640 1650 1660 1670 1680 1690 1700
pFL39
pFL-Zim17-ts2-CEN
pFL-Zim17-ts3-CEN
pFL-Zim17-ts4-CEN
pFL-Zim17-corrWT-CEN

predicted ZIM17-presequence (Yamamoto 2005)
V31A
L40S L59S
N79S
H107P D111G L114P I115T
CAGAAATGA
frame shift

1710 1720 1730 1740 1750 1760 1770 1780 1790 1800

pFL39
pFL-Zim17-ts2-CEN TTTTCAAACGTTCAAACCAACCGAATCATGAAACGGTTGCAATTGTTGGTAGGTCAAATAATTTCTCGCTGGTCTCCAGTCTCGGAAGGAGGAAGAAG
pFL-Zim17-ts3-CEN TTTTCAAACGTTCAAACCAACCGAATCATGAAACGGTTGCAATTGTTGGTAGATCAAATAATTTCTCGCTGGTCTCCAGTCTCGGAAGGAGGAAGAAG
pFL-Zim17-ts4-CEN TTTTCAAACGTTCAAACCAACCGAATCATGAAACGGTTGCAATTGTTGGTAGATCAAATAATTTCTCGCTGGTCTCCAGTCTCGGAAGGAGGAAGAAG
pFL-Zim17-corrWT-CEN TTTTCAAACGTTCAAACCAACCGAATCATGAAACGGTTGCAATTGTTGGTAGATCAAATAATTTCTCGCTGGTCTCCAGTCTCGGAAGGAGGAAGAAG

1810 1820 1830 1840 1850 1860 1870 1880 1890 1900

pFL39
pFL-Zim17-ts2-CEN AAGAGGAAGAGcnnnnnnngcgttaactatggtcagctgtttccctgtgtgaaattggtatcccgctcaacaattccacacacaacacagcgcgggaagca
pFL-Zim17-ts3-CEN AAGAGGAAGAGGnnnaaGcTtggcgttaactatggtcagctgtttccctgtgtgaaattggtatcccgctcaacaattccacacacaacacagcgcgggaagca
pFL-Zim17-ts4-CEN AAGAGGAAGAGGnnnaagcttggcgttaactatggtcagctgtttccctgtgtgaaattggtatcccgctcaacaattccacacacaacacagcgcgggaagca
pFL-Zim17-corrWT-CEN AAGAGGAAGAGGnnnaagcttggcgttaactatggtcagctgtttccctgtgtgaaattggtatcccgctcaacaattccacacacaacacagcgcgggaagca

HindIII

1910 1920 1930 1940 1950 1960 1970 1980 1990 2000

pFL39
pFL-Zim17-ts2-CEN taaagtgtaaagcctggggtgcctaatgagtgagtaactcaacataattgogtggcgtcaactgcccgtttccagtcgggaaacctgtcgtgccaagca
pFL-Zim17-ts3-CEN taaagtgtaaagcctggggtgcctaatgagtgagtaactcaacataattgogtggcgtcaactgcccgtttccagtcgggaaacctgtcgtgccaagca
pFL-Zim17-ts4-CEN taaagtgtaaagcctggggtgcctaatgagtgagtaactcaacataattgogtggcgtcaactgcccgtttccagtcgggaaacctgtcgtgccaagca
pFL-Zim17-corrWT-CEN taaagtgtaaagcctggggtgcctaatgagtgagtaactcaacataattgogtggcgtcaactgcccgtttccagtcgggaaacctgtcgtgccaagca

2010 2020 2030 2040 2050 2060 2070 2080 2090 2100

pFL39
pFL-Zim17-ts2-CEN gatctgggcaagtgcacaaacaactacttaataaataactactcagtaataaactattcttagcattttgacgaaattgctattttgttagagctctt
pFL-Zim17-ts3-CEN gatctgggcaagtgcacaaacaactacttaataaataactactcagtaataaactattcttagcattttgacgaaattgctattttgttagagctctt
pFL-Zim17-ts4-CEN gatctgggcaagtgcacaaacaactacttaataaataactactcagtaataaactattcttagcattttgacgaaattgctattttgttagagctctt
pFL-Zim17-corrWT-CEN gatctgggcaagtgcacaaacaactacttaataaataactactcagtaataaactattcttagcattttgacgaaattgctattttgttagagctctt

2110 2120 2130 2140 2150 2160 2170 2180 2190 2200

pFL39
pFL-Zim17-ts2-CEN tacaccatttgtctccacacctccgcttacatcaaaccaataaacgccatttaactaaagcgcatacacaacattttctggcgtcagtcaccagcgtaac
pFL-Zim17-ts3-CEN tacaccatttgtctccacacctccgcttacatcaaaccaataaacgccatttaactaaagcgcatacacaacattttctggcgtcagtcaccagcgtaac
pFL-Zim17-ts4-CEN tacaccatttgtctccacacctccgcttacatcaaaccaataaacgccatttaactaaagcgcatacacaacattttctggcgtcagtcaccagcgtaac
pFL-Zim17-corrWT-CEN tacaccatttgtctccacacctccgcttacatcaaaccaataaacgccatttaactaaagcgcatacacaacattttctggcgtcagtcaccagcgtaac

2210 2220 2230 2240 2250 2260 2270 2280 2290 2300

pFL39
pFL-Zim17-ts2-CEN ataaaaatgtaaaactttcggggctctcttgccctccaaccagtcagaaatcgagttccaaatccaaaagttccactgtccacactgtcttgaatcaaaaca
pFL-Zim17-ts3-CEN ataaaaatgtaaaactttcggggctctcttgccctccaaccagtcagaaatcgagttccaaatccaaaagttccactgtccacactgtcttgaatcaaaaca
pFL-Zim17-ts4-CEN ataaaaatgtaaaactttcggggctctcttgccctccaaccagtcagaaatcgagttccaaatccaaaagttccactgtccacactgtcttgaatcaaaaca
pFL-Zim17-corrWT-CEN ataaaaatgtaaaactttcggggctctcttgccctccaaccagtcagaaatcgagttccaaatccaaaagttccactgtccacactgtcttgaatcaaaaca

2310 2320 2330 2340 2350 2360 2370 2380 2390 2400

pFL39
pFL-Zim17-ts2-CEN agggaaataacgaaatgaggtttctgtgaagctgcaactgagtagtagtggcagctctttggaaatacagagctctttaaatactggcaaacccgaggaactc
pFL-Zim17-ts3-CEN agggaaataacgaaatgaggtttctgtgaagctgcaactgagtagtagtggcagctctttggaaatacagagctctttaaatactggcaaacccgaggaactc
pFL-Zim17-ts4-CEN agggaaataacgaaatgaggtttctgtgaagctgcaactgagtagtagtggcagctctttggaaatacagagctctttaaatactggcaaacccgaggaactc
pFL-Zim17-corrWT-CEN agggaaataacgaaatgaggtttctgtgaagctgcaactgagtagtagtggcagctctttggaaatacagagctctttaaatactggcaaacccgaggaactc

2410 2420 2430 2440 2450 2460 2470 2480 2490 2500

pFL39
pFL-Zim17-ts2-CEN ttggtattcttgccaagcactcaatccatgcaactggaagcagatacaatgcccgttaactatgaccagagccaaaacatctctcttaggttgattacgaaac
pFL-Zim17-ts3-CEN ttggtattcttgccaagcactcaatccatgcaactggaagcagatacaatgcccgttaactatgaccagagccaaaacatctctcttaggttgattacgaaac
pFL-Zim17-ts4-CEN ttggtattcttgccaagcactcaatccatgcaactggaagcagatacaatgcccgttaactatgaccagagccaaaacatctctcttaggttgattacgaaac
pFL-Zim17-corrWT-CEN ttggtattcttgccaagcactcaatccatgcaactggaagcagatacaatgcccgttaactatgaccagagccaaaacatctctcttaggttgattacgaaac

2510 2520 2530 2540 2550 2560 2570 2580 2590 2600

pFL39
pFL-Zim17-ts2-CEN acgcaacaagaattttcggagtgccctgaactattttatagcttttacaagactgaaattttccttgcaataaccggggtcaattgttctctttctat
pFL-Zim17-ts3-CEN acgcaacaagaattttcggagtgccctgaactattttatagcttttacaagactgaaattttccttgcaataaccggggtcaattgttctctttctat
pFL-Zim17-ts4-CEN acgcaacaagaattttcggagtgccctgaactattttatagcttttacaagactgaaattttccttgcaataaccggggtcaattgttctctttctat
pFL-Zim17-corrWT-CEN acgcaacaagaattttcggagtgccctgaactattttatagcttttacaagactgaaattttccttgcaataaccggggtcaattgttctctttctat

2610 2620 2630 2640 2650 2660 2670 2680 2690 2700

pFL39
pFL-Zim17-ts2-CEN tgggcacacataataaccagcaagtcagcactcggaaatctagagcacaattctcggcctctgtgctctgcaagcgcgcaaaccttccacaaatggaccaga
pFL-Zim17-ts3-CEN tgggcacacataataaccagcaagtcagcactcggaaatctagagcacaattctcggcctctgtgctctgcaagcgcgcaaaccttccacaaatggaccaga
pFL-Zim17-ts4-CEN tgggcacacataataaccagcaagtcagcactcggaaatctagagcacaattctcggcctctgtgctctgcaagcgcgcaaaccttccacaaatggaccaga
pFL-Zim17-corrWT-CEN tgggcacacataataaccagcaagtcagcactcggaaatctagagcacaattctcggcctctgtgctctgcaagcgcgcaaaccttccacaaatggaccaga

2710 2720 2730 2740 2750 2760 2770 2780 2790 2800

pFL39
pFL-Zim17-ts2-CEN actaactgtgaaatataaacagacatactccaagctgccccttgggtgtgcttaatacaggtatataactcaactgctcaatagtcaacaaatgcccctcct
pFL-Zim17-ts3-CEN actaactgtgaaatataaacagacatactccaagctgccccttgggtgtgcttaatacaggtatataactcaactgctcaatagtcaacaaatgcccctcct
pFL-Zim17-ts4-CEN actaactgtgaaatataaacagacatactccaagctgccccttgggtgtgcttaatacaggtatataactcaactgctcaatagtcaacaaatgcccctcct
pFL-Zim17-corrWT-CEN actaactgtgaaatataaacagacatactccaagctgccccttgggtgtgcttaatacaggtatataactcaactgctcaatagtcaacaaatgcccctcct

A.1.3. *ZIM17::LEU2*-insert for *in vitro* mutagenesis at the example of wild type *ZIM17*

■ =annealing sites forward primers ■ =annealing sites reverse primers

```

10      20      30      40      50      60      70      80      90
.....|.....|.....|.....|.....|.....|.....|.....|.....|.....|
ZIM17-LEU2-Insert
LEU2-Marker
LEU2-coding (rev.compl.)
Zim17 coding sequence
ATGATTCCGAGGACTAGAACACTACTGCAAAGTAAAATACCAATTACCAGGTACTTTGCCAGATGTTGGGCGCCTCGCGTACGCTACAAC

100     110     120     130     140     150     160     170     180
.....|.....|.....|.....|.....|.....|.....|.....|.....|.....|
ZIM17-LEU2-Insert
LEU2-Marker
LEU2-coding (rev.compl.)
Zim17 coding sequence
GTGTGCCGTACTCTACCCGCAGCAGCGTTGCATACCAATATCATCGCACATAATGAAGTGAAAAGGACGATAAGAAGGTTTCATTTGGGG
Al-fw

190     200     210     220     230     240     250     260     270
.....|.....|.....|.....|.....|.....|.....|.....|.....|.....|
ZIM17-LEU2-Insert
LEU2-Marker
LEU2-coding (rev.compl.)
Zim17 coding sequence
TCTTTTAAGGTAGACAAGCCTAAGATGATGATAGCTTTCACCTGCAAGAAATGTAACACCCGATCTTCACACACAATGCCAAGCAGGGC
Alb-fw

280     290     300     310     320     330     340     350     360
.....|.....|.....|.....|.....|.....|.....|.....|.....|.....|
ZIM17-LEU2-Insert
LEU2-Marker
LEU2-coding (rev.compl.)
Zim17 coding sequence
TACGAGAAAGGTACTGTCTTGATCTCTTGTCCGCACTGCAAAGTGAGACATTTGATAGCAGACCATCTGAAAATATTCATGATCATCAT

370     380     390     400     410     420     430     440     450
.....|.....|.....|.....|.....|.....|.....|.....|.....|.....|
ZIM17-LEU2-Insert
LEU2-Marker
LEU2-coding (rev.compl.)
Zim17 coding sequence
GTTACCGTGGAACAGTTAATGAAAGCTAACGGAGAACAAGTTAGCCAAGACGTTGGGCGACTTGGAGTTTGAAGACATCCAGATTCGCTA

460     470     480     490     500     510     520     530     540
.....|.....|.....|.....|.....|.....|.....|.....|.....|.....|
ZIM17-LEU2-Insert
LEU2-Marker
LEU2-coding (rev.compl.)
Zim17 coding sequence
AAGGACGTCCTGGGAAAATATGCCAAGAACAACCTCAGAAAATGCATCCAGCTCCCTCACCTTCCCAGAAATGA-----

550     560     570     580     590     600     610     620     630
.....|.....|.....|.....|.....|.....|.....|.....|.....|.....|
ZIM17-LEU2-Insert
LEU2-Marker
LEU2-coding (rev.compl.)
Zim17 coding sequence
ACAGGCATGTACATAGATAGATATATAACCGTTAAATAGCACGTTTTTCCAGAGACTGAGTCATGATTACTGCCAAAACCCGCACATCA

640     650     660     670     680     690     700     710     720
.....|.....|.....|.....|.....|.....|.....|.....|.....|.....|
ZIM17-LEU2-Insert
LEU2-Marker
LEU2-coding (rev.compl.)
Zim17 coding sequence
CATATTTTTTCCGATAACCAGCAGAAAGATTAGATTGTACTGAGAGTGCACCATATCGACTACGTCGTAAGGCCGTTTTCTGACAGAGTAA
AGATTGTACTGAGAGTGCACCATATCGACTACGTCGTAAGGCCGTTTTCTGACAGAGTAA
Bl-fw
A2-rev

730     740     750     760     770     780     790     800     810
.....|.....|.....|.....|.....|.....|.....|.....|.....|.....|
ZIM17-LEU2-Insert
LEU2-Marker
LEU2-coding (rev.compl.)
Zim17 coding sequence
AATCTTGAGGGAACTTTCACCATTTATGGGAAATGGTTCAAGAAGGTATTGACTTAAACTCCATCAAATGGTCAGGTCATTGAGTGTTTT
AATCTTGAGGGAACTTTCACCATTTATGGGAAATGGTTCAAGAAGGTATTGACTTAAACTCCATCAAATGGTCAGGTCATTGAGTGTTTT

```

```

      820      830      840      850      860      870      880      890      900
ZIM17-LEU2-Insert .....|.....|.....|.....|.....|.....|.....|.....|.....|
LEU2-Marker TTATTGTGTATTTTTTTTTTTTAGAGAAAAATCCCAATATCAAATAGGAATCGTAGTTTCATGATTTTCGTTACACCTAACTTT
LEU2-coding (rev.compl.) -----
Zim17 coding sequence -----

      910      920      930      940      950      960      970      980      990
ZIM17-LEU2-Insert .....|.....|.....|.....|.....|.....|.....|.....|.....|
LEU2-Marker TTGTGTGGTGCCTCCTCCTTGTCATATTAATGTTAAAGTCAATTTCTTTCCCTTATCACGTTGAGCCATAGTATCAATTTGCTTAC
LEU2-coding (rev.compl.) -----
Zim17 coding sequence -----

     1000     1010     1020     1030     1040     1050     1060     1070     1080
ZIM17-LEU2-Insert .....|.....|.....|.....|.....|.....|.....|.....|.....|
LEU2-Marker CTGTATTCCCTTACATATCCCTTTTCTCCTTCTTGATAAATGTATGTAGATTGCGTATATAGTTTCGCTACCCATGAACATATCC
LEU2-coding (rev.compl.) -----
Zim17 coding sequence -----

     1090     1100     1110     1120     1130     1140     1150     1160     1170
ZIM17-LEU2-Insert .....|.....|.....|.....|.....|.....|.....|.....|.....|
LEU2-Marker ATTTTGTAAATTCGTGTCGTTCTATTATGAATTCATTATAAAGTTTATGTACAAATATCAAAAAAAGAGAATCTTTTAAGCAAG
LEU2-coding (rev.compl.) -----
Zim17 coding sequence -----

     1180     1190     1200     1210     1220     1230     1240     1250     1260
ZIM17-LEU2-Insert .....|.....|.....|.....|.....|.....|.....|.....|.....|
LEU2-Marker GATTTTCTTAACTTCTTCGGCGACAGCATCACCGACTTCGGTGGTACTGTTGGAAACCCTAAATCACCAGTTCGTATACCTGCATCCAA
LEU2-coding (rev.compl.) -----
Zim17 coding sequence -----

     1270     1280     1290     1300     1310     1320     1330     1340     1350
ZIM17-LEU2-Insert .....|.....|.....|.....|.....|.....|.....|.....|.....|
LEU2-Marker AACCTTTTAACTGCATCTCAATGGCCTTACCCTTTCAGGCAAGTCAATGACAATTTCAACATCATTGCAGCAGACAAGATAGTGGC
LEU2-coding (rev.compl.) -----
Zim17 coding sequence -----

     1360     1370     1380     1390     1400     1410     1420     1430     1440
ZIM17-LEU2-Insert .....|.....|.....|.....|.....|.....|.....|.....|.....|
LEU2-Marker GATAGGGTCAACCTTATCTTTGGCAAAATCTGGAGCAGAACCCTGGCATGGTTCGTACAACCAAAATGCGGTGTTCTTGTCTGGCAAAAG
LEU2-coding (rev.compl.) -----
Zim17 coding sequence -----

     1450     1460     1470     1480     1490     1500     1510     1520     1530
ZIM17-LEU2-Insert .....|.....|.....|.....|.....|.....|.....|.....|.....|
LEU2-Marker GGCCAAGGACGCAGATGGCAACAAACCAAGGAACCTGGGATAACGGAGGCTTCATCGGAGATGATATCACCAAACATGTTGCTGGTGTAT
LEU2-coding (rev.compl.) -----
Zim17 coding sequence -----

     1540     1550     1560     1570     1580     1590     1600     1610     1620
ZIM17-LEU2-Insert .....|.....|.....|.....|.....|.....|.....|.....|.....|
LEU2-Marker TATAATACCATTAGGTGGGTTGGGTTCTTAACTAGGATCATGGCGGCAGAATCAATCAATGATGTTGAACCTTCAATGTAGGGAATTC
LEU2-coding (rev.compl.) -----
Zim17 coding sequence -----

     1630     1640     1650     1660     1670     1680     1690     1700     1710
ZIM17-LEU2-Insert .....|.....|.....|.....|.....|.....|.....|.....|.....|
LEU2-Marker GTTCTTGATGGTTTCTCCACAGTTTTTCTCCATAATCTTGAAGAGGCCAAAACATTAGCTTTATCCAAGGACCAAAATAGGCAATGGTGG
LEU2-coding (rev.compl.) -----
Zim17 coding sequence -----

     1720     1730     1740     1750     1760     1770     1780     1790     1800
ZIM17-LEU2-Insert .....|.....|.....|.....|.....|.....|.....|.....|.....|
LEU2-Marker CTCATGTTGTAGGGCCATGAAAGCGGCATTCTTGTGATCTTTGCACCTTCTGGAACGGTGTATTGTTCACTATCCCAAGCGACACCATC
LEU2-coding (rev.compl.) -----
Zim17 coding sequence -----

     1810     1820     1830     1840     1850     1860     1870     1880     1890
ZIM17-LEU2-Insert .....|.....|.....|.....|.....|.....|.....|.....|.....|
LEU2-Marker ACCATCGTCTTCTTCTTACCAAGTAAATACCTCCCACTAATCTCTGACAACAACGAAGTCAGTACCTTTAGCAAAATGTGGCTT
LEU2-coding (rev.compl.) -----
Zim17 coding sequence -----

```

```

1900      1910      1920      1930      1940      1950      1960      1970      1980
.....|.....|.....|.....|.....|.....|.....|.....|.....|.....|
ZIM17-LEU2-Insert  GATTGGAGATAAGTCTAAAAGAGAGTCGGATGCAAAGTTACATGGTCTTAAGTTGGCGTACAATTGAAGTTCTTTACGGATTTTGTAGTAA
LEU2-Marker        GATTGGAGATAAGTCTAAAAGAGAGTCGGATGCAAAGTTACATGGTCTTAAGTTGGCGTACAATTGAAGTTCTTTACGGATTTTGTAGTAA
LEU2-coding (rev.compl.) GATTGGAGATAAGTCTAAAAGAGAGTCGGATGCAAAGTTACATGGTCTTAAGTTGGCGTACAATTGAAGTTCTTTACGGATTTTGTAGTAA
Zim17 coding sequence -----

1990      2000      2010      2020      2030      2040      2050      2060      2070
.....|.....|.....|.....|.....|.....|.....|.....|.....|.....|
ZIM17-LEU2-Insert  ACCTTGTTCAGGTCTAACACTACCGGTACCCCAATTTAGGACCACCCACAGCACCTAACAAAACGGCATCAACCTTCTTGGAGGCTTCCAG
LEU2-Marker        ACCTTGTTCAGGTCTAACACTACCGGTACCCCAATTTAGGACCACCCACAGCACCTAACAAAACGGCATCAACCTTCTTGGAGGCTTCCAG
LEU2-coding (rev.compl.) ACCTTGTTCAGGTCTAACACTACCGGTACCCCAATTTAGGACCACCCACAGCACCTAACAAAACGGCATCAACCTTCTTGGAGGCTTCCAG
Zim17 coding sequence -----

2080      2090      2100      2110      2120      2130      2140      2150      2160
.....|.....|.....|.....|.....|.....|.....|.....|.....|.....|
ZIM17-LEU2-Insert  CGCCTCATCTGGAAGTGGGACACCTGTAGCATCGATAGCAGCACCAATTAATGATTTTCGAAATCGAACTTGACATTGGAACGAAC
LEU2-Marker        CGCCTCATCTGGAAGTGGGACACCTGTAGCATCGATAGCAGCACCAATTAATGATTTTCGAAATCGAACTTGACATTGGAACGAAC
LEU2-coding (rev.compl.) CGCCTCATCTGGAAGTGGGACACCTGTAGCATCGATAGCAGCACCAATTAATGATTTTCGAAATCGAACTTGACATTGGAACGAAC
Zim17 coding sequence -----

2170      2180      2190      2200      2210      2220      2230      2240      2250
.....|.....|.....|.....|.....|.....|.....|.....|.....|.....|
ZIM17-LEU2-Insert  ATCAGAAATAGCTTTAAGAACCCTTAATGGCTTCGGCTGTGATTTCTTGACCAACGTGGTCACCTGGCAAACGACGATCTTCTTAGGGGC
LEU2-Marker        ATCAGAAATAGCTTTAAGAACCCTTAATGGCTTCGGCTGTGATTTCTTGACCAACGTGGTCACCTGGCAAACGACGATCTTCTTAGGGGC
LEU2-coding (rev.compl.) ATCAGAAATAGCTTTAAGAACCCTTAATGGCTTCGGCTGTGATTTCTTGACCAACGTGGTCACCTGGCAAACGACGATCTTCTTAGGGGC
Zim17 coding sequence -----

2260      2270      2280      2290      2300      2310      2320      2330      2340
.....|.....|.....|.....|.....|.....|.....|.....|.....|.....|
ZIM17-LEU2-Insert  AGACATAGGGGAGACATAGAAATGGTATATCCTTGAATATATATATATATATGCTGAAATGTAAGGTAAGAAAGTTAGAAAGTAAG
LEU2-Marker        AGACATAGGGGAGACATAGAAATGGTATATCCTTGAATATATATATATATATATGCTGAAATGTAAGGTAAGAAAGTTAGAAAGTAAG
LEU2-coding (rev.compl.) AGACATAGGGGAGACATAGAAATGGTATATCCTTGAATATATATATATATATATGCTGAAATGTAAGGTAAGAAAGTTAGAAAGTAAG
Zim17 coding sequence -----

2350      2360      2370      2380      2390      2400      2410      2420      2430
.....|.....|.....|.....|.....|.....|.....|.....|.....|.....|
ZIM17-LEU2-Insert  ACGATTGCTAACACCTATTGGAAAAACAATAGGTCCTTAAATAATATGTCACCTCAAGTATTGTGATGCAAGCATTTAGTCATGAA
LEU2-Marker        ACGATTGCTAACACCTATTGGAAAAACAATAGGTCCTTAAATAATATGTCACCTCAAGTATTGTGATGCAAGCATTTAGTCATGAA
LEU2-coding (rev.compl.) ACGATTGCTAACACCTATTGGAAAAACAATAGGTCCTTAAATAATATGTCACCTCAAGTATTGTGATGCAAGCATTTAGTCATGAA
Zim17 coding sequence -----

2440      2450      2460      2470      2480      2490      2500      2510      2520
.....|.....|.....|.....|.....|.....|.....|.....|.....|.....|
ZIM17-LEU2-Insert  CGCTTCTTATCTATATGAAAAGCCGGTCCGGCCTCTCACCTTTCCTTTTCTCCCAATTTTCAGTTGAAAAGGTATATGCGCTCAG
LEU2-Marker        CGCTTCTTATCTATATGAAAAGCCGGTCCGGCCTCTCACCTTTCCTTTTCTCCCAATTTTTCAGTTGAAAAGGTATATGCGCTCAG
LEU2-coding (rev.compl.) CGCTTCTTATCTATATGAAAAGCCGGTCCGGCCTCTCACCTTTCCTTTTCTCCCAATTTTTCAGTTGAAAAGGTATATGCGCTCAG
Zim17 coding sequence -----

2530      2540      2550      2560      2570      2580      2590      2600      2610
.....|.....|.....|.....|.....|.....|.....|.....|.....|.....|
ZIM17-LEU2-Insert  GCGACCTCTGAAATTAACAAAAAATTTCCAGTCATCGAATTTGATTCGTGCGGATAGCGCCCTGTGTGTTCTCCTTATGTTGAGGAAAA
LEU2-Marker        GCGACCTCTGAAATTAACAAAAAATTTCCAGTCATCGAATTTGATTCGTGCGGATAGCGCCCTGTGTGTTCTCCTTATGTTGAGGAAAA
LEU2-coding (rev.compl.) GCGACCTCTGAAATTAACAAAAAATTTCCAGTCATCGAATTTGATTCGTGCGGATAGCGCCCTGTGTGTTCTCCTTATGTTGAGGAAAA
Zim17 coding sequence -----

2620      2630      2640      2650      2660      2670      2680      2690      2700
.....|.....|.....|.....|.....|.....|.....|.....|.....|.....|
ZIM17-LEU2-Insert  AAATAATGGTTGCTAAGAGATTGCAACTCTTGCATCTTACGATACCTGAGTATCCACAGTTAACTGCGGTCAAGATATTTCTTGAATC
LEU2-Marker        AAATAATGGTTGCTAAGAGATTGCAACTCTTGCATCTTACGATACCTGAGTATCCACAGTTAACTGCGGTCAAGATATTTCTTGAATC
LEU2-coding (rev.compl.) AAATAATGGTTGCTAAGAGATTGCAACTCTTGCATCTTACGATACCTGAGTATCCACAGTTAACTGCGGTCAAGATATTTCTTGAATC
Zim17 coding sequence -----

2710      2720      2730      2740      2750      2760      2770      2780      2790
.....|.....|.....|.....|.....|.....|.....|.....|.....|.....|
ZIM17-LEU2-Insert  AGGGCCCTTAGACCGCTCGGCCAAACAACCAATTACTTGTGAGAAAATAGAGTATAAATATCCCTATAAATAAAGCTTTTGAACACACA
LEU2-Marker        AGGGCCCTTAGACCGCTCGGCCAAACAACCAATTACTTGTGAGAAAATAGAGTATAAATATCCCTATAAATAAAGCTTTTGAACACACA
LEU2-coding (rev.compl.) AGGGCCCTTAGACCGCTCGGCCAAACAACCAATTACTTGTGAGAAAATAGAGTATAAATATCCCTATAAATAAAGCTTTTGAACACACA
Zim17 coding sequence -----

2800      2810      2820      2830      2840      2850      2860      2870      2880
.....|.....|.....|.....|.....|.....|.....|.....|.....|.....|
ZIM17-LEU2-Insert  TGAACAAGGAAGTACAGGACAATTGATTTGAAGAGAATGTGGATTTGATGTAATTGTTGGGATTCATTTTAAATAAGGCAATAATAT
LEU2-Marker        TGAACAAGGAAGTACAGGACAATTGATTTGAAGAGAATGTGGATTTGATGTAATTGTTGGGATTCATTTTAAATAAGGCAATAATAT
LEU2-coding (rev.compl.) TGAACAAGGAAGTACAGGACAATTGATTTGAAGAGAATGTGGATTTGATGTAATTGTTGGGATTCATTTTAAATAAGGCAATAATAT
Zim17 coding sequence -----

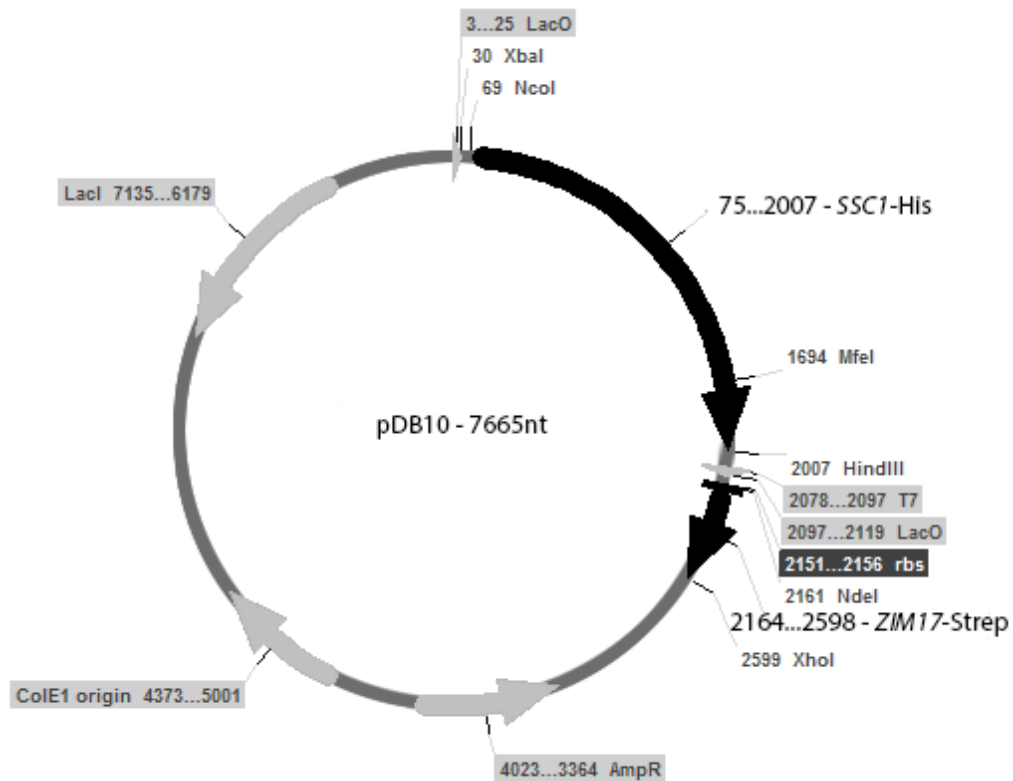
2890      2900      2910      2920      2930      2940      2950      2960      2970
.....|.....|.....|.....|.....|.....|.....|.....|.....|.....|
ZIM17-LEU2-Insert  TAGGTATGTGGATATACTAGAAGTTCTCCTCGACCGTCGATATGCGGTGTGAAATACCGCACAGTAGGACTAGACTACATAAAGATGAGC
LEU2-Marker        TAGGTATGTGGATATACTAGAAGTTCTCCTCGACCGTCGATATGCGGTGTGAAATACCGCACAGTAGGACTAGACTACATAAAGATGAGC
LEU2-coding (rev.compl.) TAGGTATGTGGATATACTAGAAGTTCTCCTCGACCGTCGATATGCGGTGTGAAATACCGCACAGTAGGACTAGACTACATAAAGATGAGC
Zim17 coding sequence -----

```

B2-rev
C-rev

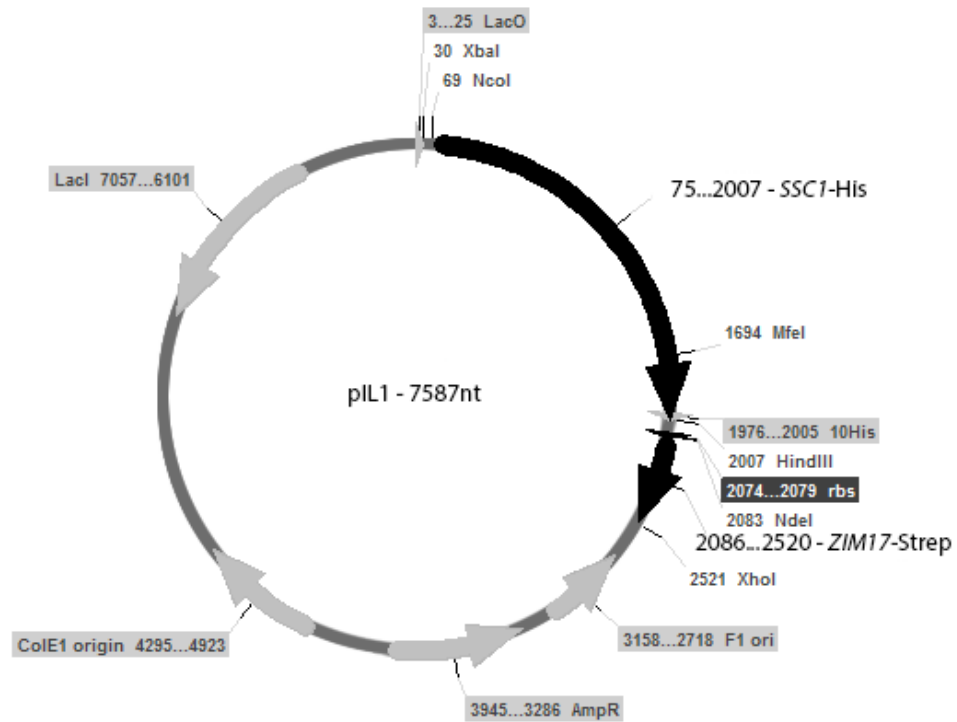
A.2. Vector maps

A.2.1. pDB10



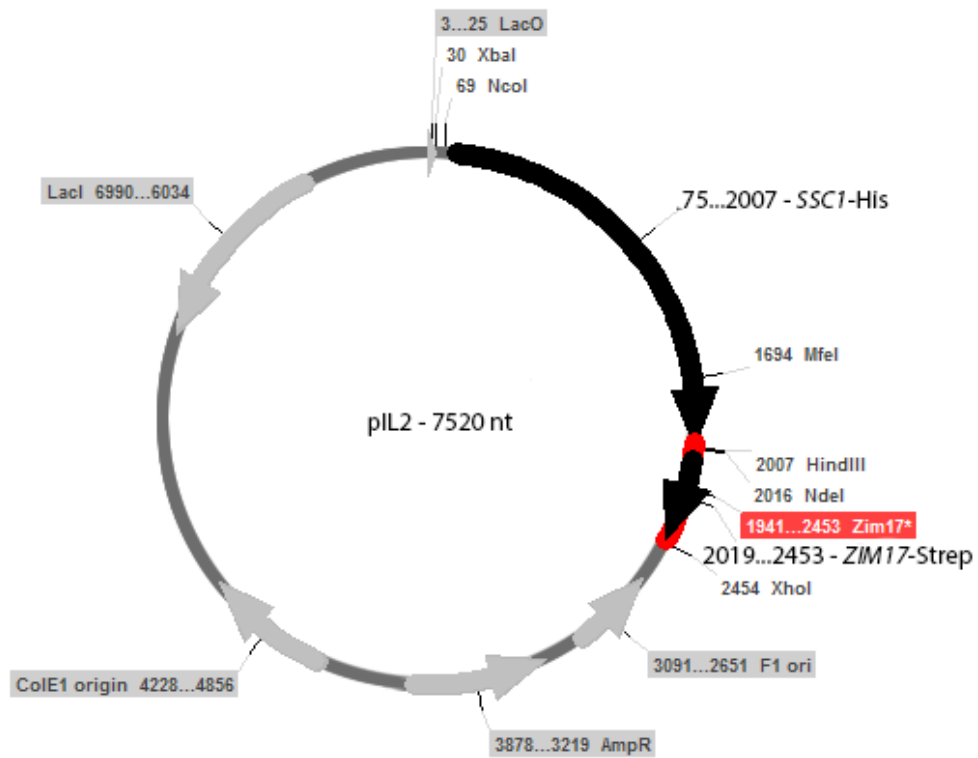
Plasmid map of pDB10. *SSC1-His* and *ZIM17-Strep* were cloned into multiple cloning sites (MCS) I and II of the pETDuet Vector (Novagen) via the NcoI/HindIII and NdeI/XhoI restriction sites. The restriction enzymes MfeI and NdeI were used to remove the T7-promotor and ribosome binding site (rbs) of MCS II to create the vectors pIL1 and pIL2.

A.2.2. pIL1



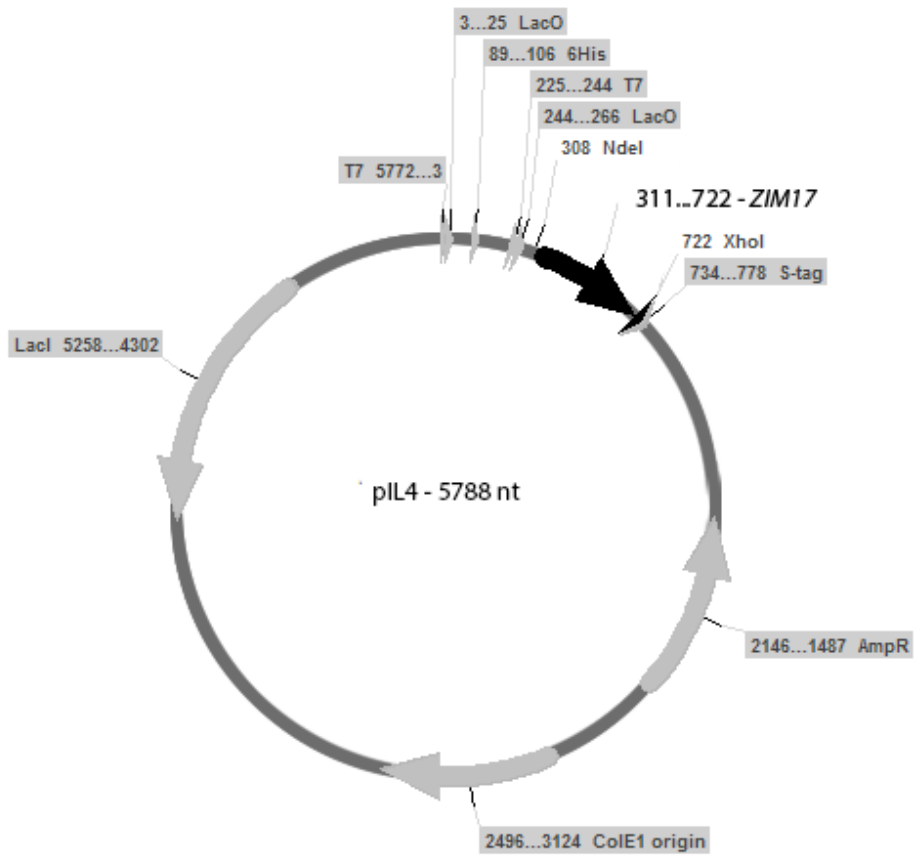
Plasmid map of pIL1. The T7-promotor and ribosome-binding site (rbs) in front of the *ZIM17*-insert of pDB10 were removed via an MfeI/NdeI restriction digest. The 3'end of *SSC1* and the ribosome binding site were amplified using the primer pair pDB10-IL1-f and pDB10-IL1+rbs-r table 2.8 and re-inserted into the plasmid.

A.2.3. pIL2



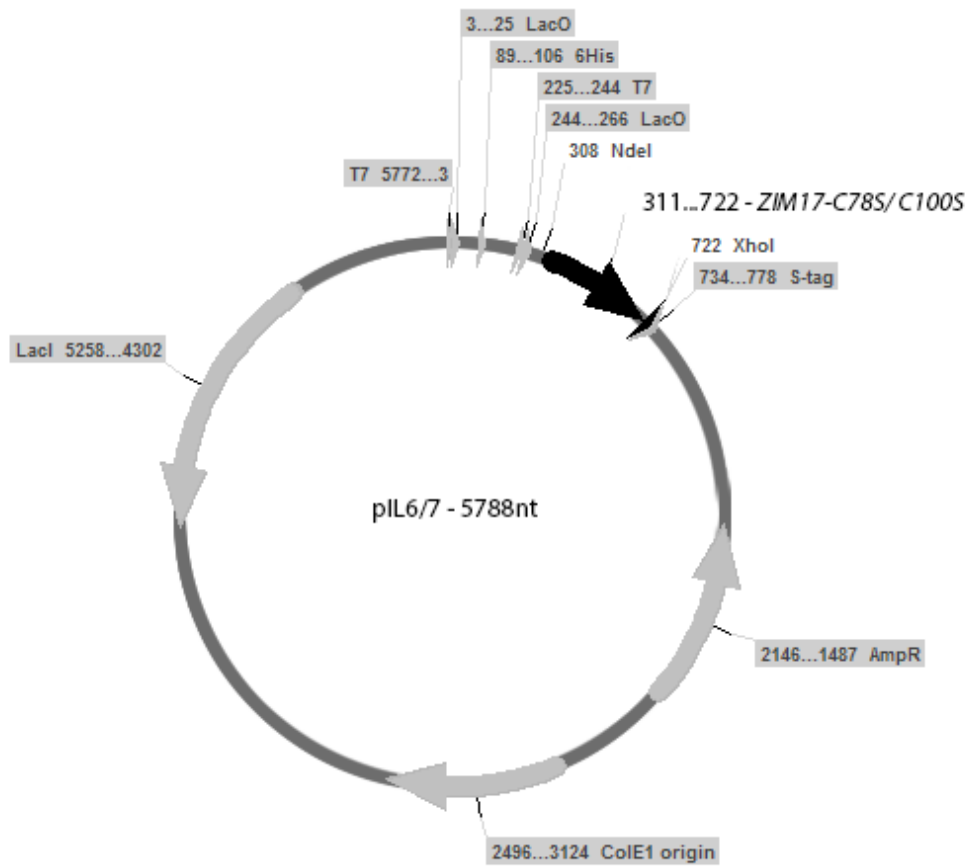
Plasmid map of pIL2. The T7-promotor and ribosome-binding site (**rbs**) in front of the *ZIM17*-insert of pDB10 were removed via an MfeI/NdeI restriction digest. The 3'end of *SSC1* site was amplified using the primer pair pDB10-IL1-f and pDB10-IL2-r table 2.8 and re-inserted into the plasmid. **Zim17*** = Zim17-artefact derived from an additional ATG in the *SSC1*-His gene

A.2.4. pIL4



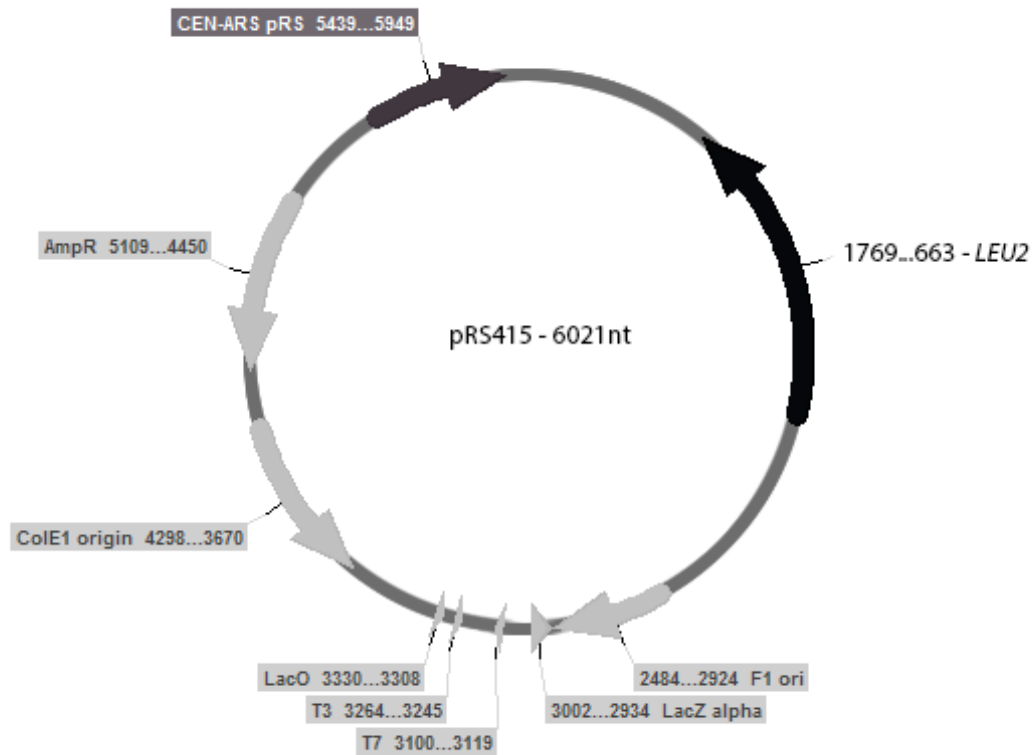
Plasmid map of pIL4. *ZIM17* was cloned into MCSII of the pETDuet vector (Novagen) via the NdeI/XhoI restriction sites.

A.2.5. pIL6/ pIL7



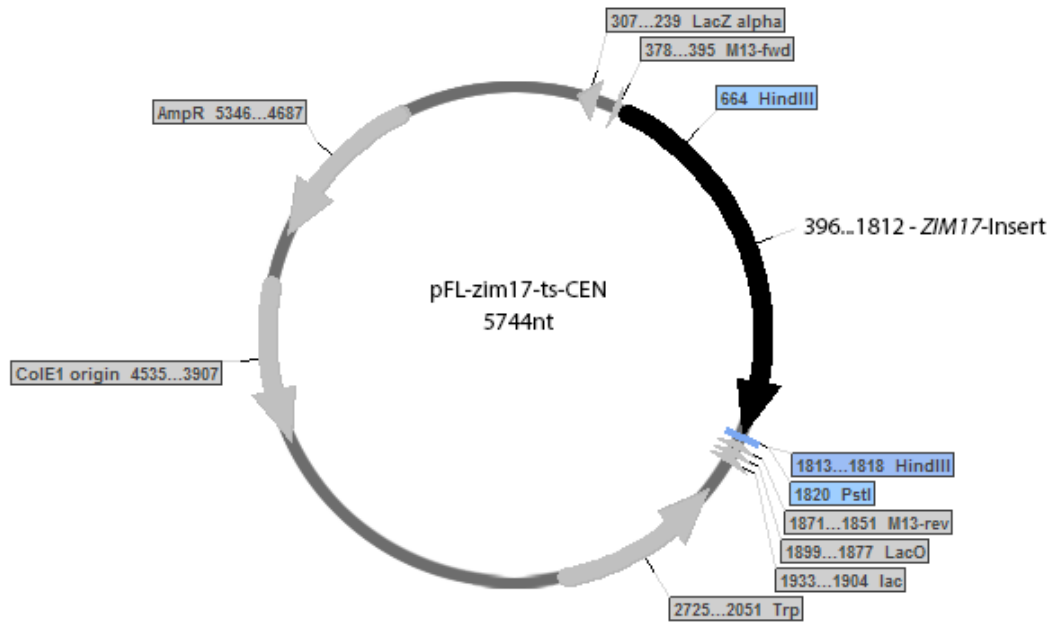
Plasmid map of pIL6 and pIL7. The zinc finger mutants *zim17-C78S* and *-C100S* were cloned into MCS II of the pETDuet vector (Novagen) via the NdeI/XhoI restriction sites.

A.2.6. pRS415



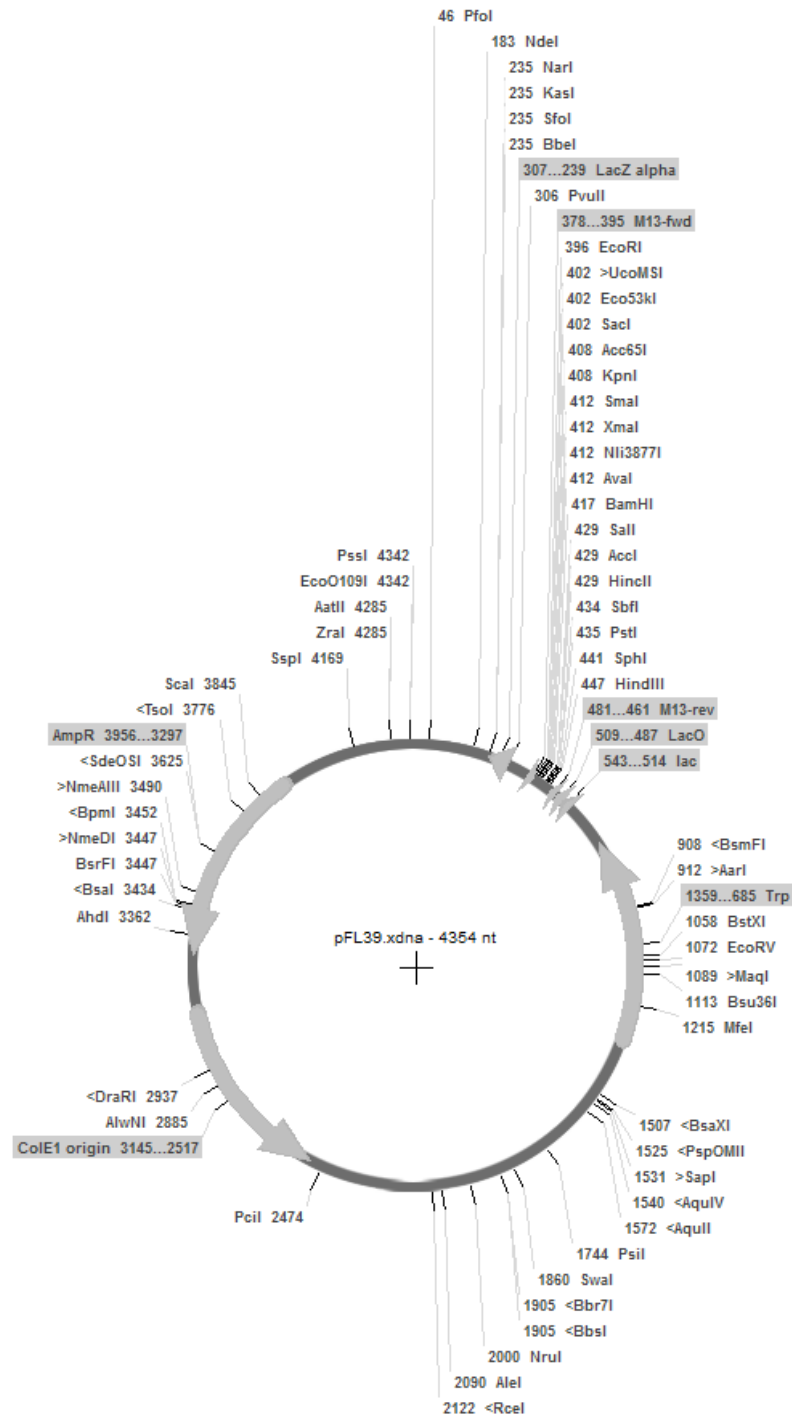
Plasmid map of pRS415. pRS415 (Sikorski and Hieter 1989) was used for the amplification of the *Leu2* marker via the primer pair B1-fw and B2-rev (table 2.8). The *LEU2* gene was used as a selection marker for genomic integration of *zim17-3a*, *-3b* and *-4*.

A.2.7. pFL-zim17-ts-CEN



Plasmid map of pFL-Zim17-ts-CEN at the example of Zim17-corrWT. The vector pFL39 was used for cloning and expression of *zim17-2*, *-3*, and *-4* in yeast. The HindIII restriction sites were used for the cloning of the corresponding wild type.

A.2.8. pFL39



Plasmid map of pFL39 (Bonneaud 1991). pFL39 that was used to create the pFL-zim17-ts-CEN plasmids (Sanjuán Szklarz 2005).

Erklärung

Hiermit erkläre ich, Ilka Lewrenz, dass ich die vorliegende Arbeit weder bei der Universität Bonn noch bei anderen wissenschaftlichen Einrichtungen als Dissertation eingereicht habe.

Weiterhin versichere ich, dass ich die vorliegende Arbeit selbständig und ohne andere Hilfsmittel und Quellen als die angegebenen verfasst habe.

Bonn, Mai 2013

Ilka Lewrenz